Doctoral theses at NTNU, 2022:115

Jan Sandstad Næss

Advancing sustainable land and water management strategies for deployment of bioenergy production systems

Doctoral thesis

NTNU
Norwegian University of Science and Technology
Thesis for the Degree of
Philosophiae Doctor
Faculty of Engineering
Department of Energy and Process Engineering

NTNU
Norwegian University of
Science and Technology

Jan Sandstad Næss

Advancing sustainable land and water management strategies for deployment of bioenergy production systems

Thesis for the Degree of Philosophiae Doctor

Trondheim, April 2022

Norwegian University of Science and Technology
Faculty of Engineering
Department of Energy and Process Engineering

NTNU
Norwegian University of
Science and Technology

NTNU
Norwegian University of Science and Technology

Thesis for the Degree of Philosophiae Doctor

Faculty of Engineering
Department of Energy and Process Engineering

ISBN 978-82-326-6277-7 (printed ver.)
ISBN 978-82-326-5378-2 (electronic ver.)
ISSN 1503-8181 (printed ver.)
ISSN 2703-8084 (online ver.)

Doctoral theses at NTNU, 2022:115

Printed by NTNU Grafisk senter

Preface

The thesis has been submitted to the Faculty of Engineering Science (IV) at the Norwegian University of Science and Technology (NTNU) in partial fulfilment of the degree of Philosophiae Doctor. This work was carried out at the Industrial Ecology Programme (IndEcol) and the Department of Energy and Process Engineering (EPT), in the period 2018-2021.

Jan Sandstad Næss,
Trondheim, December 2021

Abstract

Bioenergy is a necessity in most climate change mitigation scenario limiting global warming to below 2°C at the end of century relative to pre-industrial times. The large land-requirements associated with large-scale production of dedicated bioenergy crops has led to concerns of how sustainability trade-offs with food security and biodiversity can be avoided. Irrigated bioenergy production can ramp-up bioenergy crop yields relative to rain-fed conditions and contribute to alleviate pressure on land resources, but risks increased water stress. Promising opportunities include targeting abandoned cropland or degraded cropland where a switch to bioenergy crops can co-deliver environmental benefits. These areas are not yet sufficiently mapped, sustainable irrigation expansion opportunities are unclear, and bioenergy and climate change mitigation potentials are still poorly understood.

In this thesis, I integrate multiple models and approaches to determine sustainable bioenergy potentials, including satellite-based land cover data, a crop yield model, and datasets of water scarcity and availability. The thesis provides a first-of-its-kind spatially explicit and high-resolution global assessment of cropland abandonment and associated management dependent bioenergy potentials. It contributes to unravel the complex interactions between bioenergy production and land and water use, considering opportunities for nature conservation and irrigation constraints induced by water scarcity. The likelihood of abandoned cropland to be developed is assessed by integrating suitable land with development potential indices. I also produced refined estimates of suitable abandoned areas for bioenergy production in the former Soviet Union, which is a region with major historical abandonment and irrigation expansion opportunities. Beyond abandoned cropland, the opportunity to deploy perennial bioenergy crops on areas threatened from soil erosion by wind and water is explored in a Nordic case study. Finally, I investigate the climate change mitigation potential of liquid biofuel production with and without carbon capture and storage (CCS) in Nordic countries and compare with achievable carbon dioxide removal through natural regrowth.

I find 83 million hectares of abandoned cropland globally between 1992 and 2015. Global bioenergy potentials from recultivating abandoned cropland are 6-39 exajoules per year, or 11-68% of today's bioenergy demand, depending on agricultural management, water use for irrigation, and land sparing efforts for nature conservation. A total of 20 exajoules per year is achievable by increasing global cropland extent with 3% and global agricultural blue water withdrawals by 8%, whilst avoiding production in biodiversity hotspots and irrigation in water scarce areas. Regions with both high bioenergy potentials from abandoned cropland and high development potentials are mainly found in Central America, southeastern parts of South America, Southeast Asia and in the southern parts of North America. Furthermore, the former Soviet Union is highlighted as a region with high land availability, high marginal energy gains of irrigation, and with opportunities for irrigation expansion. Refined bioenergy potentials on abandoned land in the former Soviet Union are 3.5 to 23 exajoules per year, with high-end estimates requiring complete irrigation. An upper potential of 9 exajoules per year is achievable through sustainable irrigation expansion. This would require recultivating 35 million hectares of land combined with 67 billion cubic meters per year of blue water withdrawals.

Bioenergy production deployed on abandoned cropland and cropland threatened by soil erosion in Nordic countries can provide -7.4 to -18 megatons of carbon dioxide equivalents per year of climate change mitigation, depending on biorefinery technology and CCS

availability. Natural regrowth on the same areas can provide -10 megatons of carbon dioxide equivalents per year of negative emissions. High bioenergy yields are key to ensure larger climate benefits than natural regrowth without gains in biorefinery energy conversion efficiency or CCS. Biofuel production outperforms natural regrowth in 61% of abandoned croplands with a current biorefinery technology, and nearly everywhere with technological gain. For willow deployed as windbreaks, improved biorefinery technology or CCS is typically required to outperform natural regrowth. Biofuel production delivers larger climate benefits on 17% of cropland threatened by soil erosion with current technologies, and on 95% of the land with improved energy conversion efficiencies and CCS.

This work shows that current opportunities to sustainably deploy bioenergy crops exists at a scale which is meaningful for future climate change mitigation pathways. It is vital to simultaneously consider land and water use sustainability when designing bioenergy deployment strategies. Lack of proper governance risks increased land-use competition with trade-offs on food security and biodiversity, and to increase water stress due to unsustainable blue water withdrawals. With sustainable governance, bioenergy and BECCS will contribute to decarbonize the energy sector and deliver climate change mitigation, whilst co-delivering other environmental benefits and enhancing ecosystem services. The findings presented here helps enlighten the importance of sustainable land and water management strategies in bioenergy production systems and can essentially contribute to achieve global sustainability targets.

Sammendrag

Bioenergi er en nøkkel i scenarioer som begrenser global oppvarming til under 2°C i 2100. De store arealkravene til dedikerte bioenergivekster i slike scenarioer har ledet til en debatt om hvordan utplassering av bioenergiproduksjon kan unngå å negativt påvirke matsikkerhet og biologisk manfold. Vanning kan bidra til økte avlinger og å lette trykket på landressurser, men risikerer også å skape økt vannmangel. Lovende muligheter for en bærekraftig ekspansjon av bioenergiproduksjon inkluderer å rekultivere tidligere dyrkamark, eller å konvertere forringet dyrkemark til bioenergiproduksjon hvor bioenergivekster kan bidra til å redusere degraderingsprosesser og gi miljøgevinster. Slike områder er til nå ikke tilstrekkelig kartlagt, ekspanderingspotensialet for bærekraftig vanning er uklart, og bioenergi- og klimavernpotensialer er ikke godt nok forstått.

Her integrerer jeg flere modeller og datasett for å fastslå bærekraftige bioenergipotensialer, inkudert satellitbaserte landdata, vekstmodeller, og datasett på vanningsmuligheter. Avhandlingen presenterer den første høyoppløselige globale kartleggingen av tidligere dyrkamark og bioenergipotensialer på disse områdene. Den bidrar til å nøste opp de komplekse interaksjonene mellom bioenergipotensialer, arealbruk og vannbruk, tatt i betraktining muligheter for naturvern og tilgjengelige vannressurser. Gjennomførbarheten for å rekultiverere tidligere dyrkamark blir vurdert ved hjelp av indikatorer på lokalt utviklingspotensiale for bioenergiproduksjon. Forbedrede anslag av bioenergipotensialer blir produsert for den tidligere Sovietunionen, en region med mye historisk nedleggelse av dyrkamark over de siste tre tiårene og med store vanningsmulighter. Videre blir fokus også satt på mulgiheten for å introdusere bioenergivekster på dyrkamark som er truet av jorderosjon i et Nordisk case studie. Tilslutt kvantifiseres potensielle klimagevinster av å produsere biodrivstoff fra tidligere dyrkamark og på dyrkamark truet av jorderosjon, tatt i betraktning ulike bioraffineriteknologier og muligheten for karbonfangst og lagring (CCS).

Jeg identifiserte 83 millioner hektar tidligere dyrkamark som ble nedlagt mellom 1992 og 2015. Bioenergipotensialer er 6-39 exajoule per år, eller 11-68% av dagens globale bioenergibruk, avhengig av landbruksdrift, naturvernstiltak og vanningsbruk. Det er et potensiale for å produsere 20 exajoule per år ved å øke globale landbruksarealer med 3% og globalt vannuttak for jordbruk med 8%, uten produksjon i hotspots for biologisk mangfold og uten vannuttak i områder med vannmangel. Regioner med både høye bioenergipotensialer og høy gjennomførbarhet for rekultivering inkluderer Mellom-Amerika, Sørøst-Asia, sørvestlige deler av Sør-Amerika, og sørøstlige deler av Nord-Amerika. Den tidligere Sovietunionen fremheves som en region med mye tidligere dyrkamark, høy marginal gevinst av vanning, og stort potensiale for vanningsekspansjon. Forbedrede estimater av bioenergipotensialer i den tidligere Sovietunionen er 3.5 til 23 exajoule per år, med høye potensialer avhengig av storstilt og ikke bærekraftig bruk av vanning. Et øvre potensial på 9 exajoule per år kan oppnås med bærekraftig vanning og innebærer å rekultivere 35 millioner hektar kombinert med 67 milliarder kubikkmeter blått vannuttak i den tidligere Sovietunionen.

Produksjon av biodrivstoff på tidligere dyrkamark og på dyrkamark truet av jorderosjon i Norden kan oppnå en klimagevinst lik -7.4 til -18 megatonn karbondioksid-ekvivalenter per år, avhengig av bioraffineriteknologi og CCS bruk. Naturlig gjengroing kan gi negative utslipp lik -10 megatonn karbondioksid-ekvivalenter per år på de samme områdene. Høye avlinger er nøvendig for å sikre større klimagevinst ved produksjon av biodrivstoff enn naturlig gjengroing uten forbedringer i energikonverteringseffektivitet ved bioraffineriet eller CCS. Biodrivstoffproduksjon utkonkurrerer naturlig gjengroing på 61% av tidligere

dyrkamark med dagens bioraffineriteknologi, og nesten overalt med CCS. For vindfang etablert med seljeproduksjon er forbedret energikonverteringseffektivitet eller CCS typisk nødvendig for å levere større klimagevinst enn naturlig gjengroing. Biodrivstoffsproduksjon er bedre enn naturlig gjengroing på 17% av jordbruksarealer truet av jorderosjon med dagens tilgjengelige bioraffineriteknologi, og på 95% av arealene med forbedret teknologi og CCS.

Dette arbeidet viser at det finnes nåværende muligheter for en bærekraftig ekspansjon av bioenergiproduksjonssystemer på en stor nok skala til at det kan gi et meningsfult bidrag til globalt klimavern. Det må vurderes hvordan tilgjengelige land og vannressurser best kan forvaltes fra et bærekraftsperspektiv når gode strategier for bioenergiekspansjon skal designes. Uten tilstrekkelig forvaltning risikerer bioenergiproduksjon å negativt påvirke matsikkerhet og biologisk mangfold. Med god forvaltning vil bioenergiproduksjon bidra til å avkarbonisere energisystemet og levere ytterligere miljøgevinster gjennom reduserte degraderingsprosesser og forbedrede økosystemtjenester. Denne avhandlingen opplyser viktighten av bærekraftige arealbruksstrategier og vannforvaltning ved utplassering av storskala bioenergiproduksjon, og bidrar med nødvendig kunnskap i jakten på å nå globale bærekraftsmål.

Acknowledgements

First, thanks to my supervisor Francesco Cherubini for giving me the chance to do a PhD, pushing me to continuously improve, and for all the helpful inputs and guidance. Huge thanks also to my co-supervisors Otavio Cavalett and Bo Huang for the support and fruitful discussions. Thanks to everyone I have been working with throughout the PhD, including Cristina, Alex, Xiangping, Maren, Malene, Johana, and Priscilla.

A special thanks to Nina for putting me on the path which led me to do a PhD. If it was not for you, I don't think I would be in academia. Also, thanks to Magnus and Helge for awaking my initial interest in science.

I've gained many friends during my time at Indecol. An honorable mention goes to the ones brave enough to join me at Lerkendal in support of Rosenborg BK, especially Kjernen season-ticket holders Otavio (again) and Koen. Thanks to Martin for all the common runs, cross country skiing, terrain races, and generally keeping me fit. I am also grateful to Eivind for the late-night pizza parties and for making Sonic give Colin a run for his money. Thanks to Carine, John, Dan, Helen, Romain, Maren L, Philomena, Lorenzo, Christine, Linda, Fernando, Diogo, Ruslan, Konstantin, Radek, and all others that contributed to make this PhD a pleasure.

Thanks to my parents Torunn and Anbjørn for all the support you have shown me. Thanks also to my sisters Kristine and Marita for making me laugh when needed. Thanks to my grandparents for being there for me, always. You have all been a great inspiration.

Finally, the biggest thank you to Helene for all the love and backing given. You are the best, and I look forward to the next life-stage with you and our new family member.

List of publications

Peer-reviewed publications included in the thesis

Næss, J.S., Cavalett, O. & Cherubini, F. The land–energy–water nexus of global bioenergy potentials from abandoned cropland. *Nature Sustainability* **4,** 525–536 (2021). https://doi.org/10.1038/s41893-020-00680-5
Author contribution: Research co-design, data collection, code development, visualization, analysis, and writing.

Leirpoll, M. E., **Næss, J. S.**, Cavalett, O., Dorber, M., Hu, X., & Cherubini, F. (2021). Optimal combination of bioenergy and solar photovoltaic for renewable energy production on abandoned cropland. *Renewable Energy*, *168*, 45-56. https://doi.org/10.1016/j.renene.2020.11.159
Author contribution: Research co-design, data collection, visualization, analysis, writing, and co-supervision.

Næss, J. S., Iordan, C. M., Muri, H. & Cherubini, F. Energy potentials and water requirements from perennial grasses on abandoned land in the former Soviet Union. Environ. Res. Lett. 17, 45017 (2022). https://doi.org/10.1088/1748-9326/ac5e67
Author contribution: Research design, data collection, visualization, analysis, and writing.

Næss, J. S., Hu, X., Gvein, M. H., Iordan, C., Cavalett, O., Dorber, M., & Cherubini, F. (Under review). Negative emission potentials of biofuels produced from perennial crops and nature-based solutions on abandoned and degraded cropland in Nordic countries. Under review: *Journal of Environmental Management.* Submitted: December 23rd.
Author contribution: Research co-design, data collection, visualization, analysis, and writing.

Other peer-reviewed publications

Hu, X., **Næss, J. S.**, Iordan, C. M., Huang, B., Zhao, W., & Cherubini, F. (2021). Recent global land cover dynamics and implications for soil erosion and carbon losses from deforestation. *Anthropocene*, *34*, 100291. https://doi.org/10.1016/j.ancene.2021.100291
Author contribution: Research co-design, analysis, and writing.

Zhou, N., Hu, X., Byskov, I., **Næss, J. S.**, Wu, Q., Zhao, W., & Cherubini, F. (2021). Overview of recent land cover changes, forest harvest areas, and soil erosion trends in Nordic countries. *Geography and Sustainability*, *2*(3), 163-174.
https://doi.org/10.1016/j.geosus.2021.07.001
Author contribution: Analysis and writing.

Urrego, J. P. F., Huang, B., **Næss, J. S.**, Hu, X., & Cherubini, F. (2021). Meta-analysis of leaf area index, canopy height and root depth of three bioenergy crops and their effects on land surface modeling. *Agricultural and Forest Meteorology*, *306*, 108444.
https://doi.org/10.1016/j.agrformet.2021.108444
Author contribution: Research co-design and writing.

Sandberg, N. H., **Næss, J. S.**, Brattebø, H., Andresen, I., & Gustavsen, A. (2021). Large potentials for energy saving and greenhouse gas emission reductions from large-scale

deployment of zero emission building technologies in a national building stock. *Energy Policy*, *152*, 112114. https://doi.org/10.1016/j.enpol.2020.112114
Author contribution: Research co-design, data collection, analysis, visualization, and writing.

Nord, N., Sandberg, N. H., Ngo, H., Nesgård, E., Woszczek, A., Tereshchenko, T., **Næss, J. S.,** & Brattebø, H. (2019). Future energy pathways for a university campus considering possibilities for energy efficiency improvements. *IOP Conference Series: Earth and Environmental Science* (Vol. 352, No. 1, p. 012037). IOP Publishing. https://doi.org/10.1088/1755-1315/352/1/012037
Author contribution: Research co-design and writing.

Contents

Chapter 1: Introduction

Bioenergy is energy derived from biomass. Bioenergy is supplied to the energy system through a variety of energy carriers, ranging from traditional sources such as firewood and animal dung, to more modern alternatives such as liquid biofuels, biogas, or electricity. Traditional biomass has historically been vital for human civilizations, as biomass combustion has provided energy used for cooking and heating. It was the dominant energy carrier worldwide up until the 19th century, before being overtaken by fossil energy carriers[1]. Today's global primary bioenergy supply is 57 exajoules (EJ) per year, which corresponds to about 10% of global energy use[2]. The projected future bioenergy supply is dominated by modern bioenergy[3,4].

Modern bioenergy (hereafter, bioenergy) is typically grouped into first, second and third generation bioenergy[5]. First generation bioenergy is produced from biomass originating from food crops such as oil crops, sugar crops or grains. It is thus in direct competition with food production. Second generation bioenergy is based on biomass from lignocellulosic bioenergy crops (non-food) such as fast-growing woody crops and grasses, residues, and wastes. Third generation biofuels refer to production which avoids land use change such as microalgae[6,7], but is still not commercially ready due to high production and energy costs[5]. This work focuses on second generation bioenergy produced from perennial grasses and woody crops.

Bioenergy crop productivity depends on a variety of factors, such as local climatic conditions, soil characteristics, agricultural management and water supply systems[8,9]. Achieving optimal yields at a farm level may require the use of fertilizers, pesticides, mechanization, improved varieties, and irrigation[10,11]. After biomass has been produced, it can take different conversion routes into the energy system and be used to produce heat, electricity, or gasified and liquid fuels[12]. As bioenergy can take a variety of energy carriers, it can be used in a range of existing infrastructure such as in thermal power stations or combustion engines, offering potential climate change mitigation benefits through decarbonization of grid electricity or transportation systems[4,13].

The environmental performance of bioenergy production systems depends on the previous land use, their management, and water use[14,15]. A switch from cropland to perennial grasses

for bioenergy production can also improve a range of ecosystem services[16]. Perennial grasses have deep root systems which increase soil carbon, with benefits to climate change mitigation and the restoration of degraded lands[17–20]. They can contribute to mitigate soil erosion, reduce nutrient leaching, and improve indicators related to biodiversity species richness[16,21]. Woody bioenergy crops can also help mitigate soil erosion by wind when deployed as windbreaks[22,23]. Relative to food crops, bioenergy crops have been shown to provide a regional biophysical cooling effect which favors climate change adaptation[24–26].

On the other hand, the cultivation of bioenergy crops requires land and freshwater resources. The land availability of bioenergy crops is limited due to competition with food production and nature conservation[15,27,28]. Likewise, freshwater availability for irrigated bioenergy production is constrained due to environmental flow protection, urban water usage, and other agricultural water usage for food production[29,30]. An uncontrolled large-scale bioenergy deployment can cause environmental impacts and have adverse effects on food and water security[29,30]. Therefore, sustainable bioenergy deployment strategies must carefully balance potential environmental benefits and trade-offs to identify opportunities which generates synergies across multiple environmental dimensions.

In the next sections, I go more specifically into the value of bioenergy in climate change mitigation (1.1), sustainable bioenergy land use (1.2), and sustainable bioenergy water use (1.3). I identify research gaps in section 1.4 and define research aims in section 1.5.

1.1 Bioenergy in climate change mitigation scenarios

The Paris Agreement sets a target to limit global warming to below 2°C and to further pursue a 1.5°C temperature target relative to pre-industrial levels[31]. Major scientific efforts have been invested to explore and identify which scenarios and emission pathways makes it possible to achieve these ambitious targets[32–35]. A rapid reduction of greenhouse gas emissions and a decarbonization of the energy sector are among the necessary ingredients to meet these targets[36,37].

Bioenergy is attractive in climate change mitigation because biomass growth accumulates atmospheric CO_2 over time through photosynthesis. Bioenergy typically offers lower net life cycle greenhouse gas emissions when sustainably produced than fossil energy sources which only emits carbon[38]. Previous land use, bioenergy yields, and the lifetime of a bioenergy

plantation are important factors to determine net GHG emissions[14]. New cultivation of bioenergy crops on a location which previously had large natural stocks of aboveground carbon such as forested areas will cause an initial carbon penalty which needs to be paid back over time[13]. The initial carbon penalty occurs as a pulse emission, while other carbon flows such as supply chain emissions, the accumulation of aboveground carbon in bioenergy crops, soil carbon accumulation, or the release of biogenic carbon through combustion typically occurs continuously over time[13]. Carbon payback can occur through avoided emissions when bioenergy is used to replace fossil fuels, soil carbon sequestration, or carbon capture and storage (CCS)[14,15,39]. When assessing the climate change mitigation potential of bioenergy deployment, both time and spatial location is essential as carbon fluxes are unevenly distributed across the years after land use conversion, and land-surface characteristic and crop productivity varies with local conditions[14].

Coupling bioenergy production systems with carbon capture and storage (BECCS) has the unique ability that it both ramps-up renewable energy supply and can provide negative carbon emissions. This means capturing the carbon dioxide (CO_2) that is produced during biomass conversion and sequestering it in geological reservoirs for long-term storage[40]. Large-scale BECCS can contribute to climate stabilization or even help bring temperature levels back down after an initial overshoot of temperature targets[32,41,42].

Bioenergy plays a key role in climate change mitigation scenarios limiting global warming below 2°C or lower[33]. The median projected bioenergy supply in 2050 is between 83-249 EJ per year across the different Shared Socio-economic Pathways[43] (SSPs) for 1.5°C scenarios in Integrated Assessment Models (IAMs)[32,34] (Figure 1). Out of this, a median of 36-197 EJ per year is coupled to CCS across SSPs[32,34].

IAMs are tools which attempts to project how human activities and environmental impacts will evolve into the future through cost-optimization and simulation techniques, and they vary in assumptions, complexity and structure[44]. They have played an important role in assessing climate change, identifying options for climate action through scenario analysis, and the design of climate policies[33,34,45]. The five SSPs are based on narratives for socioeconomic development that reflect different futures where challenges to climate mitigation and adaptation vary from low to high[34]. For example, SSP1[46] assumes a change towards sustainable practices, SSP5[47] represents a fossil fuel based economy, whilst SSP2[48] is

a middle of the road scenario which considers a continuation of historical patterns. Together with the Representative Concentration Pathways[49] (RCPs) that sets trajectories of atmospheric GHG concentrations and climate forcing, SSP-RCP combinations represents a framework that allows assessing global environmental change[50,51].

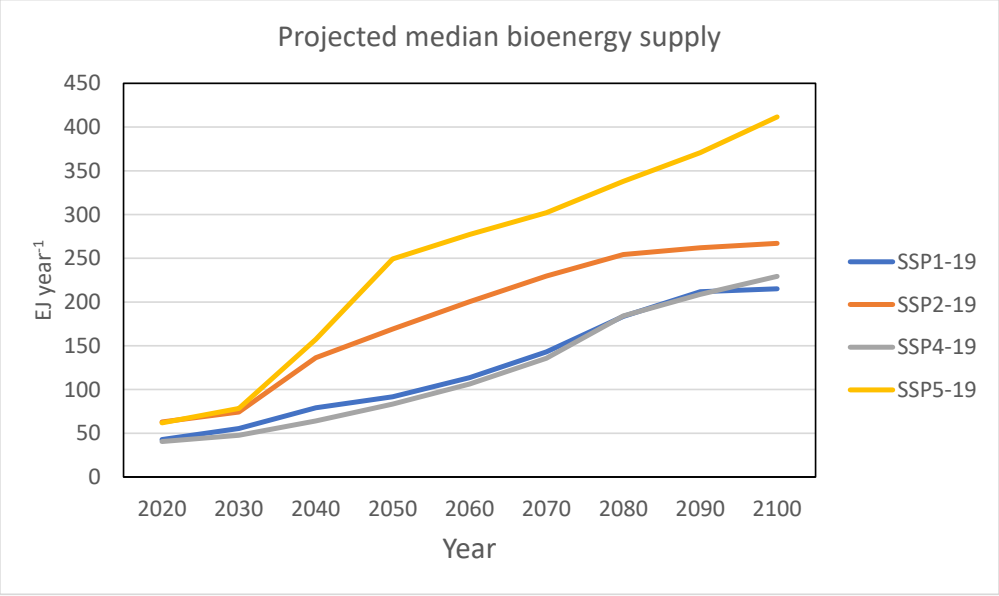

Figure 1: Median bioenergy supply in 1.5°C scenarios across the different SSPs[32,34]. Medians are based on multiple IAM projections using combinations of the different SSPs and RCP1.9[32]. SSP3[52] is not shown because no models could meet the temperature target.

The projected bioenergy increase is mainly supplied by agricultural and forestry residues and dedicated bioenergy crops, with bioenergy crops becoming increasingly dominant as bioenergy supply increases[3,4]. Median associated land requirements across SSPs for dedicated bioenergy crops are 210-670 million hectares (Mha) in 2050[28]. This is equal to 13-42% of the current global cropland area extent[53] and would require major near-term land use change, thereby creating pressure on land resources. By the end of the century, bioenergy supply and land requirements for bioenergy crops in 1.5°C scenarios increase further to medians of 222-412 EJ per year[32,34] and 430-760 Mha of land[28] across the different SSPs, respectively.

Bioenergy land requirements are high in scenarios that delays decarbonization with emission pathways that lead to an overshoot of the temperature target, before returning to below 2°C through the deployment of biomass based negative emission technologies later in the century[36]. Bioenergy land-use is also high in scenarios that avoids the use of negative

emission technologies, mainly due to bioenergy's flexibility as an energy carrier[54,55], thereby providing a vital contribution to decarbonize transportation sectors that are hard to electrify such as aviation and shipping[56]. Future scenarios thus show an extensive dependence on bioenergy in most scenarios that align with the Paris Agreement's temperature goals.

1.2 Sustainable bioenergy land use

The large land-requirements for bioenergy production in 1.5°C scenarios have led to concerns about how such vast areas can be sustainably supplied without causing severe environmental impacts or affecting food security[15,27,57]. The potential adverse impacts on biodiversity from bioenergy crop deployment on areas covered by primary vegetation is well established in the literature[58,59]. Deployment on areas with large natural aboveground carbon stocks to bioenergy production can also create substantial carbon debts[13]. By limiting bioenergy deployment to areas which are already heavily affected by human activities such as croplands and managed grasslands, environmental trade-offs on natural ecosystems can be reduced. However, converting in-use agricultural land to bioenergy crops reduces local food production due to the direct land use change. Consequentially, food prices may increase, and the need to replace the initial loss of agricultural production can drive indirect land use change, thereby causing deforestation due to cropland expansion elsewhere[60].

Sustainable bioenergy land management strategies should target areas where a switch to bioenergy crops can co-deliver multiple environmental benefits and minimize sustainability trade-offs[23,61]. Whilst land use change for bioenergy is often portrayed as something negative (for example, deforestation or loss of food production), a partial strategic integration of bioenergy production into agricultural landscapes can in fact improve a variety of environmental indicators, such as indicators related to biodiversity, pollination, soil erosion, sediment and nutrient retention and flood regulation[16,62,63]. Such "beneficial land use change" can contribute to mitigate environmental impacts caused by intensive agriculture and reduce, stop, or even reverse ongoing land degradation processes[21]. The possibility to target marginal, abandoned, or degraded land is an option which is receiving increasing attention as a win-win strategy for bioenergy deployment[15,64]. In this work, I go into depth on two bioenergy deployment strategies that show promise for a sustainable ramp-up of biomass production. These are abandoned cropland and cropland threatened by soil erosion.

Recultivating abandoned cropland for bioenergy production represents an opportunity for bioenergy deployment with reduced environmental and societal impacts[65,66]. Abandoned cropland typically lays unproductive, and competition with food production can be avoided. Biodiversity impacts and carbon penalties from recultivation of abandoned cropland is typically lower relative to cultivating areas of primary vegetation because they had limited time to regrow natural vegetation and to restore ecosystem functionality[13,65,67]. Abandoned croplands are also usually located near existing farming infrastructure and roads as they were previously used to produce food[68,69]. Most land abandonment processes have historically been driven by socio-economic change, and not necessarily because lands turned uncultivable[70]. For example, the former Soviet Union became a global hotspot of land abandonment after its dissolution due to access to open markets and a restructuring of the economy[71–73]. Other abandonment drivers include ecological factors and agricultural mismanagement[70]. Recultivation can bring economic benefits to rural areas[74,75]. Bioenergy crop deployment can help restore degraded soils and potentially allow future food production on areas which would otherwise in the future lay barren[28,63].

Sustainable land management strategies should also consider cases where continued natural regrowth can be preferable to agricultural recultivation, for example if negative emissions from regrowth outperforms the climate change mitigation performance of bioenergy production[13]. Abandoned cropland in areas where biodiversity may benefit extra from nature conservation should also be considered for continued regrowth, such as inside protected areas, inside biodiversity hotspots, or if the land can contribute to connect fragmented habitats[76–78].

Targeting croplands threatened by soil erosion for bioenergy production is an example of a strategy which can co-deliver both reduced land degradation and increased energy production[22,23,63]. Unsustainably high soil-erosion rates risks compromising agricultural productivity over time[79–81]. Perennial grasses can be deployed to limit soil erosion by water by trapping eroded sediments by providing continuous soil cover, even with annual harvest[82–84]. Woody bioenergy crops can also prevent soil erosion by water as they physically stabilize soil with their roots, intercept rain and snow, and improve water infiltration[83]. Woody bioenergy crops can also be deployed as windbreaks to shelter surrounding areas from wind, thereby reducing wind erosion rates and providing additional benefits to food crop productivity in sheltered areas[83,85,86].

1.3 Sustainable bioenergy water use

Water availability is essential for crop productivity. Rain-fed agriculture relies completely on water from local precipitation stored in soils, or so-called "green water"[87,88]. Crop yields are often limited by water deficits throughout the growth cycle, which occurs when crop water losses from evapotranspiration exceeds water availability.

Irrigation can increase crop yields in areas where green water is not sufficient to sustain optimal crop growth, alleviate pressure on land resources, and may even make arid areas which are uncultivable under rain-fed conditions turn productive. Irrigation requires water withdrawals from surface water, artificially created reservoirs, or groundwater. Human-induced water withdrawals which are either moved from one body to another, returned at a different time or evaporates is termed "blue water"[88]. Currently, global anthropogenic blue water withdrawals in the agricultural sector are about 2700 billion m^3 $year^{-1}$, equal to about half a year of cumulative water flow from the Amazon River[53]. Human modification of the global water cycle is thus substantial, and it has led to increased environmental flow depletion and water scarcity in parts of the world[89].

Water scarcity means that water demand is not sufficiently met by water supply. It has been estimated that about 2 billion people live in areas threatened by water scarcity[89]. In extreme cases, this can mean that water supply is not even sufficient to meet domestic water use and basic human needs such as sanitation. Different indicators exist to assess water scarcity, and it can be both due to physical and economical constraints[89–91]. Physical water scarcity refers to cases where renewable water resources are not sufficient to meet water demand[89]. Economic water scarcity refers to situations where renewable blue water is available to meet demand, but societal and economical constraints and a lack of existing infrastructure hinders water withdrawals[89]. In agriculture, green water scarcity refers to situations where soil moisture available for uptake by plants through roots are not sufficient to sustain unstressed crop growth, and irrigation would provide yield benefits[89,92]. Blue water scarcity means renewable blue water resources cannot sustainably meet the irrigation water requirements needed to avoid crop water deficits[89]. Opportunities for new deployment of sustainable irrigation arise when green water scarcity occurs simultaneously with economical water scarcity, or so-called agricultural economic water scarcity[93]. In these situations, blue water

resources are available, but there is no existing infrastructure or institutional capacity there to use it.

Global bioenergy potentials are limited by possibilities for sustainable irrigation[29,30]. Sustainable water use in bioenergy production systems means avoiding modifications of the water cycle to produce biomass which depletes environmental flows and avoids inducing environmental or societal trade-offs. Production in physical water-scarce areas should primarily be rain-fed to avoid further water depletion. Irrigated bioenergy deployment strategies should target areas with agricultural economic water scarcity[93], thereby limiting sustainability trade-offs. Furthermore, deployment strategies should target areas where the relative bioenergy yield gains of irrigation are high per unit of applied blue water, thereby providing increased benefits with lower impacts.

1.4 Research gaps

Sustainable bioenergy deployment strategies are an important area of research. Bioenergy production and BECCS can make a vital contribution in the global quest to achieve the climate mitigation targets of the Paris Agreement and limit global warming to below 2°C at the end of century relative to pre-industrial levels. The projected future bioenergy expansion found in mitigation pathways from IAMs gives valuable insights into bioenergy's role to cost-efficiently mitigate climate change[54]. However, IAMs have limitations due to their coarse spatial resolution and many assumptions[57,61,94], which means that their analysis should be complemented with more detailed bottom-up analysis of bioenergy land and water availability and bioenergy productivity. The improved and integrated design of sustainable land and water management strategies for bioenergy production requires taking a high-resolution approach.

The global extent and locations of abandoned cropland is currently unclear and there is limited knowledge on how their recultivation for bioenergy production could contribute to increase bioenergy supply in line with mitigation pathways. Previous studies have shown large-scale global abandonment and potentials (up to 472 Mha and 45 EJ $year^{-1}$), but they assessed very long time periods (up to 300 years), used coarse land cover datasets, and lacked site-specific assessments of bioenergy productivity[65,95]. These estimates thus included large areas which have had many decades or even centuries to regrow and to restore both natural carbon pools and ecosystem functionality.

The Food and Agricultural Organization of the United Nations has highlighted the need for increased cropland monitoring through remote sensing, as 40% of member countries do not perform agricultural censuses[96]. Recent progress in remote-sensing techniques and the availability of high-resolution land cover datasets means there is an opportunity to improve our knowledge of historical cropland abandonment patterns and potential bioenergy land availability.

Previous area-limited studies of cropland abandonment have also shown that abandonment estimates using regional data can differ from those obtained through global assessments. Studies assessing bioenergy deployment on abandoned cropland with a regional scope has so far been limited to the United States[66,97,98]. What value regional land cover datasets covering other parts of the world can bring to the table is still unclear.

It is unknown how bioenergy land availability is limited by nature conservation policies promoting continued regrowth on abandoned cropland in key areas. Additionally, it is poorly understood how competition for land with other land-intensive renewable energy production technologies such as photovoltaics might affect deployment patterns. Integrating abandonment maps with technology-specific indicators of development potentials for renewable energy production offers an opportunity to obtain insights on the bioenergy deployment feasibility on abandoned cropland across the world and potential deployment competition with photovoltaic solar energy parks. The use of development potential indices seems particularly attractive as it allows to account for resource yield, market accessibility, and land supply elasticity[99].

There is a need to assess bioenergy crop productivity and potentials on abandoned cropland, whilst accounting for local climatic conditions and the effect of different agricultural management. Recent calls have been made to pursue new ideas in water research and develop new methods to assess water use sustainability[100]. Increasing attention is given to the nexus between energy potentials and their land and water requirements[101]. It is unclear how irrigation can contribute to increased bioenergy crop productivity, and to what extent blue water withdrawals for increased production can be deployed on abandoned cropland without causing sustainability trade-offs. No attempts have been made to map the overlap between abandoned croplands and areas with sustainable potentials for irrigation expansion.

The climate change mitigation potential of producing liquid biofuels on abandoned cropland is unclear. Previous research warns about the large carbon penalties that occurs if long-standing secondary vegetation is replaced with bioenergy production[13]. Historical carbon accumulation on abandoned cropland has not been determined, and it is unclear how it may affect the mitigation benefits of future biofuel production in these areas. Furthermore, it is not well established how liquid biofuel production performs relative to continued natural regrowth on abandoned cropland, and how spatial variations in productivity and temporal abandonment patterns affects achieved mitigation. Technological gains in energy conversion efficiencies and deployment of BECCS may also affect optimal land management strategies. These effects are not yet properly addressed in the literature.

Beyond abandoned cropland, increasing attention is given to target croplands where beneficial land-use change to perennial crops can bring additional environmental co-benefits[21–23,61]. Degraded croplands suitable for bioenergy production and associated potentials are still not fully understood[61]. More research is required to quantify biofuel production and climate mitigation potentials of deploying bioenergy crops on areas threatened by soil erosion, as commonly found in Nordic countries[102,103]. Limited knowledge is currently available comparing how achievable mitigation from biofuel production systems perform versus nature-based solutions for soil erosion control through natural regrowth.

1.5 Research aims

The aim with this thesis is to advance sustainable land and water management strategies for large-scale bioenergy deployment. I hence investigated the following research questions:

1. Where can bioenergy plantations be deployed in the near-term to increase sustainable bioenergy supply, what is the extent of suitable areas, and what are the energy potentials?
2. How can the nexus between sustainable bioenergy potentials and their land and water requirements be unraveled, and what is the importance of the following factors: agricultural management, climatic conditions, resource constraints arising from water scarcity for irrigation, and potential land-sparing strategies for nature conservation?
3. Where does bioenergy show both high energy potentials and high development potentials, and how does bioenergy spatially compare against solar photovoltaics?

4. What is the climate change mitigation potential of liquid biofuel production with and without CCS, and how does the achieved mitigation spatially compare to negative emissions from natural regrowth?

Research questions are addressed in chapters 2-5 (Table 1). The first research question is a common thread throughout the thesis, while the others are addressed by individual chapters.

Table 1: Research questions addressed by the different chapters in the thesis.

Chapter	Research question adressed			
	1	2	3	4
2	X	X		
3	X		X	
4	X	X		
5	X			X

I first assess a potential bioenergy deployment on abandoned cropland. In chapter 2, I spatially quantify global cropland abandonment, assess the potential to deploy bioenergy crops on these areas and unravel the nexus between bioenergy potentials and land and water use. I consider the effect of agricultural management, rain-fed and irrigated water supply, present and future climatic conditions on bioenergy productivity, and examine land and water availability limitations arising from potential nature conservation policies and physical water scarcity. Chapter 3 addresses the development potential of abandoned croplands for bioenergy, and additionally compares with solar photovoltaics which represents another land-intensive renewable energy option.

Departing from the assessment of global bioenergy potentials on abandoned cropland, I continue with two lines of research. In Chapter 4, I target the former Soviet Union to refine estimates of suitable areas, bioenergy potentials and water requirements. The former Soviet Union is a region which has experienced intensive land abandonment over the last three decades, shows high bioenergy potentials and where sustainable irrigation expansion is possible. I refine estimates of suitable areas under different irrigation schemes using an extensively validated regional land cover dataset with relatively high accuracy of land abandonment. In chapter 5, I focus on the Nordic region. I expand the Nordic land

availability assessment to also include croplands threatened by soil erosion by wind and water, as deploying bioenergy production in these areas can be a win-win strategy co-delivering energy production, climate change mitigation and decreased soil erosion rates. I assess the climate change mitigation potential of producing liquid biofuels with and without BECCS and compare with the negative emissions achievable by natural regrowth.

In chapter 6, I synthesize the work and provide answers to research questions. Chapter 6 further discusses policy implications, addresses study limitations, and provides concluding remarks.

1.6 References

1. Guo, M., Song, W. & Buhain, J. Bioenergy and biofuels: History, status, and perspective. *Renew. Sustain. Energy Rev.* **42**, 712–725 (2015).
2. IEA. Energy technology perspectives 2017. *Catal. Energy Technol. Transform.* (2017).
3. Hanssen, S. V *et al.* Biomass residues as twenty-first century bioenergy feedstock—a comparison of eight integrated assessment models. *Clim. Change* **163**, 1569–1586 (2020).
4. Daioglou, V., Doelman, J. C., Wicke, B., Faaij, A. & Vuuren, D. P. Van. Integrated assessment of biomass supply and demand in climate change mitigation scenarios. *Glob. Environ. Chang.* **54**, 88–101 (2019).
5. Dalena, F., Senatore, A., Tursi, A. & Basile, A. 17 - Bioenergy production from second- and third-generation feedstocks. in (eds. Dalena, F., Basile, A. & Rossi, C. B. T.-B. S. for the F.) 559–599 (Woodhead Publishing, 2017). doi:https://doi.org/10.1016/B978-0-08-101031-0.00017-X
6. Alam, F., Mobin, S. & Chowdhury, H. Third Generation Biofuel from Algae. *Procedia Eng.* **105**, 763–768 (2015).
7. Singh, A., Olsen, S. I. & Nigam, P. S. A viable technology to generate third-generation biofuel. *J. Chem. Technol. Biotechnol.* **86**, 1349–1353 (2011).
8. Li, W., Ciais, P., Makowski, D. & Peng, S. A global yield dataset for major lignocellulosic bioenergy crops based on field measurements. *Sci. Data* **5**, 180169 (2018).
9. Zegada-Lizarazu, W. *et al.* Agronomic aspects of future energy crops in Europe. *Biofuels, Bioprod. Biorefining* **4**, 674–691 (2010).
10. Lewandowski, I., Clifton-Brown, J. C., Scurlock, J. M. O. & Huisman, W. Miscanthus: European experience with a novel energy crop. *Biomass and Bioenergy* **19**, 209–227 (2000).

11. Casler, M. D., Mitchell, R. B. & Vogel, K. P. Switchgrass. in *Handbook of Bioenergy Crop Plants.* 563–590 (2012).
12. Faaij, A. Modern Biomass Conversion Technologies. *Mitig. Adapt. Strateg. Glob. Chang.* **11**, 343–375 (2006).
13. Field, J. L. *et al.* Robust paths to net greenhouse gas mitigation and negative emissions via advanced biofuels. *Proc. Natl. Acad. Sci.* **117**, 21968 LP – 21977 (2020).
14. Creutzig, F. *et al.* Bioenergy and climate change mitigation: an assessment. *GCB Bioenergy* **7**, 916–944 (2015).
15. Calvin, K. *et al.* Bioenergy for climate change mitigation: scale and sustainability. *GCB Bioenergy* **n/a**, (2021).
16. Robertson, G. P. *et al.* Cellulosic biofuel contributions to a sustainable energy future: Choices and outcomes. *Science (80-.).* **356**, (2017).
17. Qin, Z., Dunn, J. B., Kwon, H., Mueller, S. & Wander, M. M. Soil carbon sequestration and land use change associated with biofuel production: empirical evidence. *GCB Bioenergy* **8**, 66–80 (2016).
18. Dou, F. G. *et al.* Soil Organic Carbon Pools Under Switchgrass Grown as a Bioenergy Crop Compared to Other Conventional Crops. *Pedosphere* **23**, 409–416 (2013).
19. Liu, W., Yan, J., Li, J. & Sang, T. Yield potential of Miscanthus energy crops in the Loess Plateau of China. *GCB Bioenergy* **4**, 545–554 (2012).
20. Don, A. *et al.* Land-use change to bioenergy production in Europe: implications for the greenhouse gas balance and soil carbon. *GCB Bioenergy* **4**, 372–391 (2012).
21. Englund, O. *et al.* Beneficial land use change: Strategic expansion of new biomass plantations can reduce environmental impacts from EU agriculture. *Glob. Environ. Chang.* **60**, 101990 (2020).
22. Englund, O. *et al.* Strategic deployment of riparian buffers and windbreaks in Europe can co-deliver biomass and environmental benefits. *Commun. Earth Environ.* **2**, 176 (2021).
23. Englund, O. *et al.* Beneficial land-use change in Europe: deployment scenarios for multifunctional riparian buffers and windbreaks. (2021).
24. Georgescu, M., Lobell, D. B. & Field, C. B. Direct climate effects of perennial bioenergy crops in the United States. *Proc. Natl. Acad. Sci.* **108**, 4307–4312 (2011).
25. Harding, K. J., Twine, T. E., VanLoocke, A., Bagley, J. E. & Hill, J. Impacts of second-generation biofuel feedstock production in the central U.S. on the hydrologic cycle and global warming mitigation potential. *Geophys. Res. Lett.* **43**, 10,710-773,781 (2016).
26. Wang, J. *et al.* Global cooling induced by biophysical effects of bioenergy crop cultivation. *Nat. Commun.* **12**, 7255 (2021).
27. Anderson, K. & Peters, G. The trouble with negative emissions. *Science (80-.).* **354**, 182 LP – 183 (2016).

28. IPCC. Summary for Policymakers. in *Climate Change and Land: an IPCC Special Report on climate change, desertification, land degradation, sustainable land management, food security, and greenhouse gas fluxes in terrestrial ecosystems* (2019).
29. Stenzel, F. *et al.* Irrigation of biomass plantations may globally increase water stress more than climate change. *Nat. Commun.* **12**, 1512 (2021).
30. Ai, Z., Hanasaki, N., Heck, V., Hasegawa, T. & Fujimori, S. Global bioenergy with carbon capture and storage potential is largely constrained by sustainable irrigation. *Nat. Sustain.* (2021). doi:10.1038/s41893-021-00740-4
31. UNFCC. Adoption of the Paris Agreement. Report No. FCC/CP/2015/L.9/Rev.1. Available at: http://unfccc.int/resource/docs/2015/cop21/eng/l09r01.pdf.
32. Rogelj, J. *et al.* Scenarios towards limiting global mean temperature increase below 1.5 °C. *Nat. Clim. Chang.* **8**, 325–332 (2018).
33. Rogelj, J. *et al.* Chapter 2: Mitigation pathways compatible with 1.5°C in the context of sustainable development. in *Global Warming of 1.5 °C an IPCC special report on the impacts of global warming of 1.5 °C above pre-industrial levels and related global greenhouse gas emission pathways, in the context of strengthening the global response to the threat of climate change* (Intergovernmental Panel on Climate Change, 2018).
34. Riahi, K. *et al.* The Shared Socioeconomic Pathways and their energy, land use, and greenhouse gas emissions implications: An overview. *Glob. Environ. Chang.* **42**, 153–168 (2017).
35. Bauer, N. *et al.* Global energy sector emission reductions and bioenergy use: overview of the bioenergy demand phase of the EMF-33 model comparison. *Clim. Change* (2018). doi:10.1007/s10584-018-2226-y
36. Bauer, N. *et al.* Shared Socio-Economic Pathways of the Energy Sector – Quantifying the Narratives. *Glob. Environ. Chang.* **42**, 316–330 (2017).
37. Rogelj, J. *et al.* Energy system transformations for limiting end-of-century warming to below 1.5 C. *Nat. Clim. Chang.* **5**, 519 (2015).
38. Cherubini, F. *et al.* Energy- and greenhouse gas-based LCA of biofuel and bioenergy systems: Key issues, ranges and recommendations. *Resour. Conserv. Recycl.* **53**, 434–447 (2009).
39. Ledo, A. *et al.* Changes in soil organic carbon under perennial crops. *Glob. Chang. Biol.* **26**, 4158–4168 (2020).
40. Shahbaz, M. *et al.* A comprehensive review of biomass based thermochemical conversion technologies integrated with CO2 capture and utilisation within BECCS networks. *Resour. Conserv. Recycl.* **173**, 105734 (2021).
41. Muri, H. The role of large-scale BECCS in the pursuit of the 1.5°C target: an Earth system model perspective. *Environ. Res. Lett.* **13**, 44010 (2018).
42. Hanssen, S. V *et al.* The climate change mitigation potential of bioenergy with carbon capture

and storage. *Nat. Clim. Chang.* **10**, 1023–1029 (2020).

43. Popp, A. *et al.* Land-use futures in the shared socio-economic pathways. *Glob. Environ. Chang.* **42**, 331–345 (2017).
44. Weyant, J. Some Contributions of Integrated Assessment Models of Global Climate Change. *Rev. Environ. Econ. Policy* **11**, 115–137 (2017).
45. IPCC. *Climate Change 2014: Synthesis Report. Contribution of Working Groups I, II and III to the Fifth Assessment Report of the Intergovernmental Panel on Climate Change [Core Writing Team, R.K. Pachauri and L.A. Meyer (eds.)]*. (2014).
46. van Vuuren, D. P. *et al.* Energy, land-use and greenhouse gas emissions trajectories under a green growth paradigm. *Glob. Environ. Chang.* **42**, 237–250 (2017).
47. Kriegler, E. *et al.* Fossil-fueled development (SSP5): An energy and resource intensive scenario for the 21st century. *Glob. Environ. Chang.* **42**, 297–315 (2017).
48. Fricko, O. *et al.* The marker quantification of the Shared Socioeconomic Pathway 2: A middle-of-the-road scenario for the 21st century. *Glob. Environ. Chang.* **42**, 251–267 (2017).
49. van Vuuren, D. P. *et al.* The representative concentration pathways: an overview. *Clim. Change* **109**, 5 (2011).
50. O'Neill, B. C. *et al.* Achievements and needs for the climate change scenario framework. *Nat. Clim. Chang.* **10**, 1074–1084 (2020).
51. Kriegler, E. *et al.* A new scenario framework for climate change research: the concept of shared climate policy assumptions. *Clim. Change* **122**, 401–414 (2014).
52. Doelman, J. C. *et al.* Exploring SSP land-use dynamics using the IMAGE model: Regional and gridded scenarios of land-use change and land-based climate change mitigation. *Glob. Environ. Chang.* **48**, 119–135 (2018).
53. FAO. *The state of the world's land and water resources for food and agriculture: Managing systems at risk.* (Earthscan, 2011).
54. Köberle, A. C. The Value of BECCS in IAMs: a Review. *Curr. Sustain. Energy Reports* **6**, 107–115 (2019).
55. Hasegawa, T. *et al.* Land-based implications of early climate actions without global net-negative emissions. *Nat. Sustain.* (2021). doi:10.1038/s41893-021-00772-w
56. Klein, D. *et al.* The value of bioenergy in low stabilization scenarios: an assessment using REMIND-MAgPIE. *Clim. Change* **123**, 705–718 (2014).
57. Vaughan, N. E. & Gough, C. Expert assessment concludes negative emissions scenarios may not deliver. *Environ. Res. Lett.* **11**, 95003 (2016).
58. Fitzherbert, E. B. *et al.* How will oil palm expansion affect biodiversity? *Trends Ecol. Evol.* **23**, 538–545 (2008).
59. Immerzeel, D. J., Verweij, P. A., van der Hilst, F. & Faaij, A. P. C. Biodiversity impacts of bioenergy crop production: a state-of-the-art review. *GCB Bioenergy* **6**, 183–209 (2014).

60. Berndes, G., Ahlgren, S., Börjesson, P. & Cowie, A. L. Bioenergy and land use change—state of the art. *WIREs Energy Environ.* **2**, 282–303 (2013).
61. Berndes, G. & Cowie, A. Land sector impacts of early climate action. *Nat. Sustain.* (2021). doi:10.1038/s41893-021-00777-5
62. Donnison, C., Holland, R. A., Harris, Z. M., Eigenbrod, F. & Taylor, G. Land-use change from food to energy: meta-analysis unravels effects of bioenergy on biodiversity and cultural ecosystem services. *Environ. Res. Lett.* **16**, 113005 (2021).
63. Englund, O. *et al.* Multifunctional perennial production systems for bioenergy: performance and progress. *WIREs Energy Environ.* **9**, e375 (2020).
64. Fritsche, U. R., Sims, R. E. H. & Monti, A. Direct and indirect land-use competition issues for energy crops and their sustainable production – an overview. *Biofuels, Bioprod. Biorefining* **4**, 692–704 (2010).
65. Campbell, J. E., Lobell, D. B., Genova, R. C. & Field, C. B. The global potential of bioenergy on abandonded agricultural lands. *Environ. Sci. Technol.* **42**, 5791–5794 (2008).
66. Zumkehr, A. & Campbell, J. E. Historical U.S. Cropland Areas and the Potential for Bioenergy Production on Abandoned Croplands. *Environ. Sci. Technol.* **47**, 3840–3847 (2013).
67. Hanssen, S. V *et al.* Global implications of lignocellulosic crop-based BECCS for terrestrial vertebrate biodiversity. *GCB Bioenergy* **n/a**, (2021).
68. Benayas, J. M. R., Martins, A., Nicolau, J. M. & Schulz, J. J. Abandonment of agricultural land: an overview of drivers and consequences. *CAB Rev. Perspect. Agric. Vet. Sci. Nutr. Nat. Resour.* **2**, 1–14 (2007).
69. Lasanta, T. *et al.* Space–time process and drivers of land abandonment in Europe. *CATENA* **149**, 810–823 (2017).
70. Li, S. & Li, X. Global understanding of farmland abandonment: A review and prospects. *J. Geogr. Sci.* **27**, 1123–1150 (2017).
71. Jepsen, M. R. *et al.* Transitions in European land-management regimes between 1800 and 2010. *Land use policy* **49**, 53–64 (2015).
72. Lesiv, M. *et al.* Spatial distribution of arable and abandoned land across former Soviet Union countries. *Sci. Data* **5**, 180056 (2018).
73. Schierhorn, F. *et al.* Post-Soviet cropland abandonment and carbon sequestration in European Russia, Ukraine, and Belarus. *Global Biogeochem. Cycles* **27**, 1175–1185 (2013).
74. Meyfroidt, P., Schierhorn, F., Prishchepov, A. V, Müller, D. & Kuemmerle, T. Drivers, constraints and trade-offs associated with recultivating abandoned cropland in Russia, Ukraine and Kazakhstan. *Glob. Environ. Chang.* **37**, 1–15 (2016).
75. Prishchepov, A. V, Ponkina, E. V, Sun, Z., Bavorova, M. & Yekimovskaja, O. A. Revealing the intentions of farmers to recultivate abandoned farmland: A case study of the Buryat Republic in Russia. *Land use policy* **107**, 105513 (2021).

76. Hu, X., Huang, B., Verones, F., Cavalett, O. & Cherubini, F. Overview of recent land-cover changes in biodiversity hotspots. *Front. Ecol. Environ.* (2020). doi:10.1002/fee.2276
77. Kuipers, K. J. J., May, R. F., Graae, B. J. & Verones, F. Reviewing the potential for including habitat fragmentation to improve life cycle impact assessments for land use impacts on biodiversity. *Int. J. Life Cycle Assess.* **24**, 2206–2219 (2019).
78. Myers, N., Mittermeier, R. A., Mittermeier, C. G., Fonseca, G. A. B. & Kent, J. Biodiversity hotspots for conservation priorities. *Nature* **403**, 853–858 (2000).
79. Borrelli, P. *et al.* An assessment of the global impact of 21st century land use change on soil erosion. *Nat. Commun.* **8**, 1–13 (2017).
80. Borrelli, P. *et al.* Land use and climate change impacts on global soil erosion by water (2015-2070). *Proc. Natl. Acad. Sci.* **117**, 21994 LP – 22001 (2020).
81. Kaiser, J. Wounding Earth's Fragile Skin. *Science (80-.).* **304**, 1616 LP – 1618 (2004).
82. Ferrarini, A., Serra, P., Almagro, M., Trevisan, M. & Amaducci, S. Multiple ecosystem services provision and biomass logistics management in bioenergy buffers: A state-of-the-art review. *Renew. Sustain. Energy Rev.* **73**, 277–290 (2017).
83. Kort, J., Collins, M. & Ditsch, D. A review of soil erosion potential associated with biomass crops. *Biomass and Bioenergy* **14**, 351–359 (1998).
84. Wang, E. *et al.* Strategic switchgrass (Panicum virgatum) production within row cropping systems: Regional-scale assessment of soil erosion loss and water runoff impacts. *GCB Bioenergy* **12**, 955–967 (2020).
85. Osorio, R. J., Barden, C. J. & Ciampitti, I. A. GIS approach to estimate windbreak crop yield effects in Kansas–Nebraska. *Agrofor. Syst.* **93**, 1567–1576 (2019).
86. Smith, M. M. *et al.* Windbreaks in the United States: A systematic review of producer-reported benefits, challenges, management activities and drivers of adoption. *Agric. Syst.* **187**, 103032 (2021).
87. Rockström, J. *et al.* Future water availability for global food production: The potential of green water for increasing resilience to global change. *Water Resour. Res.* **45**, (2009).
88. M., F. & J., R. The New Blue and Green Water Paradigm: Breaking New Ground for Water Resources Planning and Management. *J. Water Resour. Plan. Manag.* **132**, 129–132 (2006).
89. Liu, J. *et al.* Water scarcity assessments in the past, present, and future. *Earth's Futur.* **5**, 545–559 (2017).
90. Brown, A. & Matlock, M. D. A review of water scarcity indices and methodologies. *White Pap.* **106**, 19 (2011).
91. Rijsberman, F. R. Water scarcity: Fact or fiction? *Agric. Water Manag.* **80**, 5–22 (2006).
92. Schyns, J. F., Hoekstra, A. Y. & Booij, M. J. Review and classification of indicators of green water availability and scarcity. *Hydrol. Earth Syst. Sci.* **19**, 4581–4608 (2015).
93. Rosa, L., Chiarelli, D. D., Rulli, M. C., Dell'Angelo, J. & D'Odorico, P. Global agricultural

economic water scarcity. *Sci. Adv.* **6**, eaaz6031 (2020).

94. Forster, J., Vaughan, N. E., Gough, C., Lorenzoni, I. & Chilvers, J. Mapping feasibilities of greenhouse gas removal: Key issues, gaps and opening up assessments. *Glob. Environ. Chang.* **63**, 102073 (2020).
95. Field, C. B., Campbell, J. E. & Lobell, D. B. Biomass energy: the scale of the potential resource. *Trends Ecol. Evol.* 65–72 (2008). doi:10.1016/j.tree.2007.12.001
96. Gennari, P., Rosero-Moncayo, J. & Tubiello, F. N. The FAO contribution to monitoring SDGs for food and agriculture. *Nat. Plants* **5**, 1196–1197 (2019).
97. Baxter, R. E. & Calvert, K. E. Estimating Available Abandoned Cropland in the United States: Possibilities for Energy Crop Production. *Ann. Am. Assoc. Geogr.* **107**, 1162–1178 (2017).
98. Lark, T. J., Meghan Salmon, J. & Gibbs, H. K. Cropland expansion outpaces agricultural and biofuel policies in the United States. *Environ. Res. Lett.* **10**, 44003 (2015).
99. Oakleaf, J. R. *et al.* Mapping global development potential for renewable energy, fossil fuels, mining and agriculture sectors. *Sci. Data* 1–17 (2019). doi:10.1038/s41597-019-0084-8
100. Too much and not enough. *Nat. Sustain.* **4**, 659 (2021).
101. Johnson, N. *et al.* Integrated Solutions for the Water-Energy-Land Nexus: Are Global Models Rising to the Challenge? *Water* **11**, (2019).
102. Zhou, N. *et al.* Overview of recent land cover changes, forest harvest areas, and soil erosion trends in Nordic countries. *Geogr. Sustain.* **2**, 163–174 (2021).
103. Borrelli, P. *et al.* Towards a Pan-European Assessment of Land Susceptibility to Wind Erosion. *L. Degrad. Dev.* **27**, 1093–1105 (2016).

Chapter 2: The land-energy-water nexus of global bioenergy potentials from abandoned cropland

Material from: Næss, J.S., Cavalett, O. & Cherubini, F. The land–energy–water nexus of global bioenergy potentials from abandoned cropland. Nat Sustain 4, 525–536 (2021). https://doi.org/10.1038/s41893-020-00680-5

nature sustainability

ANALYSIS

https://doi.org/10.1038/s41893-020-00680-5

The land–energy–water nexus of global bioenergy potentials from abandoned cropland

Jan Sandstad Næss ✉, Otavio Cavalett and Francesco Cherubini

Bioenergy is a key option in climate change mitigation scenarios. Growing perennial grasses on recently abandoned cropland is a near-term strategy for gradual bioenergy deployment with reduced risks for food security and the environment. However, the extent of global abandoned cropland, bioenergy potentials and management requirements are unclear. Here we integrate satellite-derived land cover maps with a yield model to investigate the land–energy–water nexus of global bioenergy potentials. We identified 83 million hectares of abandoned cropland between 1992 and 2015, corresponding to 5% of today's cropland area. Bioenergy potentials are 6–39 exajoules per year (11–68% of today's bioenergy demand), depending on multiple local and management factors. About 20 exajoules per year can be achieved by increasing today's global cropland area and water use by 3% and 8%, respectively, and without production inside biodiversity hotspots or irrigation in water-scarce areas. The consideration of context-specific practices and multiple environmental dimensions can mitigate trade-offs of bioenergy deployment.

Future emission scenarios limiting global temperature increase to relatively low levels are associated with sharp increases in bioenergy production[1]. Top-down economic models project a median increase in bioenergy supply from today's 57 exajoules (EJ) per year[2] to 222–412 EJ per year in 2100 across different Shared Socio-economic Pathways (SSPs) aligning with 1.5 °C warming[3,4]. This corresponds to median projected land requirements for bioenergy crops of 430–760 million hectares (Mha)[5].

The environmental benefits of bioenergy crops largely depend on biomass production systems and land availability[6]. Growing perennial grasses as bioenergy crops on abandoned cropland is typically considered a near-term opportunity for gradual large-scale deployment while minimizing trade-offs with food security and biodiversity as well as revitalizing rural areas[7–10]. Abandoned cropland is typically located in proximity to farms and road networks, and it is usually abandoned due to socio-economic, ecological or political factors[11–13]. Relative to cropland, perennial grasses improve a variety of ecosystem services[8]. Thanks to their deep root system, these grasses increase soil carbon with positive effects for both climate change mitigation by sequestering atmospheric carbon dioxide[14,15] and restoration of degraded land by improving soil quality[16,17]. Perennial bioenergy crops contribute to higher plant diversity, reduce leaching of nutrients and improve a variety of indicators related to biodiversity and species richness[8,18]. The switch from cropland to perennial grasses is also associated with a regional cooling effect, mainly during the growing season, which can provide additional local benefits and favour climate change adaptation[19,20].

The current area of abandoned cropland and the corresponding global bioenergy potentials are still unclear. Previous analyses provide a wide range of estimates (up to 472 Mha of abandoned cropland and 45 EJ yr^{-1})[7,21–23], which reflects the use of different land cover datasets, abandonment criteria and time periods, and to what extent site-specific growing conditions are factored in. One major limitation is the quality of land cover datasets, which typically have relatively coarse resolution and little consistency in terms of period of observation and temporal evolution of land cover change[24,25]. Additionally, bioenergy crop yields are frequently based on simplified assumptions and not explicitly linked to key factors such as local soil fertility, water supply, management intensity, local climate conditions or ecological constraints[6,26–29]. For example, high yields usually require irrigation and can potentially exacerbate water scarcity[29], or bioenergy crops that grow in today's semi-arid areas may become unfeasible under future drier and warmer conditions.

These complex interlinkages can be jointly assessed using a nexus approach, a rapidly expanding new concept to investigate interdependencies, trade-offs and synergies across multiple dimensions (physical resources, environmental impacts or economic sectors) and guide the development of sustainable strategies[30–32]. A nexus analysis based on local physical resource constraints and agricultural management of bioenergy systems helps to identify context-specific solutions and implications[31]. Coupling accurate estimates of available land with parametric crop yield models for different climatic conditions and datasets of water resources can offer new estimates of bioenergy potentials and unravel their interconnections with local factors. However, these aspects have often been studied separately, thereby hindering an overview of their interdependencies and masking the local environmental and management conditions on which global estimates of bioenergy potentials rely.

Here we performed a bottom-up analysis integrating a recently developed high-resolution temporal land cover dataset (European Space Agency (ESA) Climate Change Initiative Land Cover (CCI-LC)) [25,33] with a spatially explicit agro-ecological crop yield model (Global Agro-Ecological Zones (GAEZ) v.3.0)[34] to estimate global bioenergy potentials on recently abandoned cropland under the land–energy–water nexus (Methods). Bioenergy potentials are computed using local soil and climatic characteristics for a variety of combinations (296 individual estimates) that consider multiple management factors and constraints (Table 1): land availability (for example, exclusion of land within biodiversity hotspots to allow targeted nature conservation and restoration measures for endangered native vascular plants[35]), bioenergy crop types (miscanthus, switchgrass, reed canary grass or grid-specific energy-based crop optimization), intensity of agricultural management (low, medium, high or a mix of these based on today's yield gaps) and water

Industrial Ecology Programme, Department of Energy and Process Engineering, Norwegian University of Science and Technology, Trondheim, Norway. ✉e-mail: jan.s.nass@ntnu.no

Table 1 | Overview of the possible combinations of global bioenergy potentials investigated in this study

Land availability	Perennial grass type	Agricultural management intensity	Water supply	Climatic conditions
All abandoned cropland (1992–2015)	Miscanthus	High	Rain-fed	Present day
	Reed canary grass	Medium	Irrigated	RCP 4.5 in 2050 and 2080
Exclusion of biodiversity hotspots	Switchgrass	Low	Mixed	RCP 8.5 in 2050 and 2080
	Optimal energy-based crop allocation	Mixed		

A total of 296 individual estimates of bioenergy potentials are produced, excluding unlikely combinations (for example, those that include irrigation with low agricultural management intensity, or mixed management with future climate). For water supply, 'mixed' refers to irrigation in areas under medium or high management intensity that are not affected by water scarcity. For agricultural management intensity, 'mixed' refers to a combination of intensity levels based on today's yield gaps. RCP, Representative Concentration Pathway.

supply system (irrigated, rain-fed or a mixed approach where irrigation occurs only at medium and high management intensity in areas not affected by water scarcity). Changes in bioenergy potentials under future climatic conditions are also explored. The land–energy–water nexus approach, assessed in terms of total and marginal energy gains from irrigation, blue water footprint and total water withdrawals, is used to identify which regions can benefit most from irrigated bioenergy production. We thereby unravel the interdependencies between bioenergy potentials, land availability and water supply for different management intensities and water scarcity levels.

Results

In this section, we present key findings related to land availability, bioenergy productivity and irrigation water use.

Global abandoned cropland. We identified 83 Mha of abandoned cropland from 1992 to 2015 (Fig. 1a), out of which 50 Mha is located outside biodiversity hotspots (Fig. 1b) and 13 Mha in areas threatened by physical water scarcity. About 30% of the global abandoned cropland is in Asia, especially Southeast Asia. Africa accounts for about 22%, mainly just south of the Equator, followed by Europe with about 20%. In South America, abandoned cropland is mostly located near the southeastern coastline (13%). Smaller fractions of abandoned cropland are found in North America, Oceania and Central America, with about 5% each.

Socio-economic growth and exposure to open agricultural markets are historically the main drivers of cropland abandonment, as it has often occurred in regions without significant constraints to crop production[36,37]. For example, the large extent of abandoned cropland in Eastern Europe largely followed the dissolution of the Soviet Union, resulting in lower agricultural investments, connection to global markets and rural–urban migration[36,38,39].

Previous studies that mapped abandoned cropland confirm widespread abandonment across the world (Supplementary Table 1). A direct comparison of our global findings with other studies is not possible because they considered a different time period and/or different criteria to identify cropland abandonment[7,21,22]. Estimates of abandoned cropland can be better compared at a regional scale (Supplementary Text 1). The main trends identified here are broadly consistent with those from regional studies, despite some discrepancies between estimates, mostly due to unharmonized land cover classification systems, spatial resolution and temporal mismatches[40]. For example, our estimated 16 Mha of abandoned cropland in Europe between 1992 and 2015 is higher than a previous estimate (7.6 Mha)[38] that used a more recent time period (2001–2012), and thus did not include the well-documented cropland abandonment of the post-Soviet Union era.

For additional validation purposes, we compared country-level cropland inventories from the Food and Agriculture Organization (FAO)[41] with total national cropland extent from the ESA CCI-LC product for the years 1992 and 2015 (Supplementary Fig. 1). The datasets are largely consistent for both years, with a few countries as outliers (mainly developing countries). While ESA CCI-LC data show some regional differences in accuracy[33], outliers are probably due to FAO data based on official national statistics of varying reliability. For example, around 40% of FAO member countries did not perform an agricultural census between 2005 and 2015[42]. This recently led the FAO to start promoting remote-sensing techniques (such as those applied here) as a cost-efficient way to improve future agricultural statistics[42].

Global bioenergy potentials. Global bioenergy potentials from the cultivation of miscanthus, switchgrass and reed canary grass on recently abandoned cropland are 19 EJ yr^{-1}, 5.4 EJ yr^{-1} and 4.3 EJ yr^{-1}, respectively (Fig. 2a,b,c). These potentials are based on present-day climatic conditions, high agricultural management intensity, rain-fed water supply and with no land restrictions for nature conservation. An optimal distribution of bioenergy crops based on their local growing conditions (Fig. 2d) achieves a potential of 25 EJ yr^{-1} (Fig. 2f), with an average global bioenergy yield of 298 GJ ha^{-1} yr^{-1} (Fig. 2e).

Bioenergy potentials of different perennial grasses show a clear latitudinal pattern. The potential of miscanthus is larger in the tropical band (Fig. 2a), switchgrass at mid-latitudes (Fig. 2c) and reed canary grass at higher latitudes and in mountainous areas (Fig. 2b). This latitudinal pattern is reflected in the optimal crop allocation (Fig. 2d), which maximizes the bioenergy yields per grid cell (Fig. 2e). In general, bioenergy yields are higher in the tropics and subtropics, where they can exceed 600 GJ ha^{-1} yr^{-1}, and wetter regions of temperate zones. In Europe, bioenergy yields mainly range between 200 GJ ha^{-1} yr^{-1} and 400 GJ ha^{-1} yr^{-1}. About 20% of the identified global abandoned cropland (17 Mha) is not suitable for growing bioenergy crops under rain-fed conditions and today's climate (mostly located in arid areas and mountainous regions).

Global bioenergy potentials range from 5.5–39 EJ yr^{-1} (Supplementary Table 2) as a result of different conditions of land availability, management intensity and water supply (Fig. 3). The lowest potential (5.5 EJ yr^{-1}) occurs when considering rain-fed conditions, low agricultural management intensity and exclusion of land within biodiversity hotspots. At high agricultural management intensity and rain-fed conditions, excluding 33 Mha of abandoned cropland inside biodiversity hotspots reduces the potential from 25 EJ yr^{-1} to about 13 EJ yr^{-1}. Losing 40% of the land available for nature conservation thus reduces bioenergy potentials by 48%. On average, the exclusion of areas within biodiversity hotspots reduces potentials by 45% across management intensities and water supply systems. This shows an important trade-off between energy supply and nature conservation. Large hotspots are in the tropics, where bioenergy crop yields are relatively high. The highest potential (39 EJ yr^{-1}) is achieved with complete irrigation under high agricultural management intensity. The consideration of a mixed approach where the use of irrigation is limited to areas that are not affected by physical water scarcity results in a bioenergy potential under optimal crop distribution of 35 EJ yr^{-1} (or 20 EJ yr^{-1} if areas within biodiversity hotspots are excluded), where irrigated areas contribute 95% to this potential. The global bioenergy potential based on today's common agricultural intensity levels in different

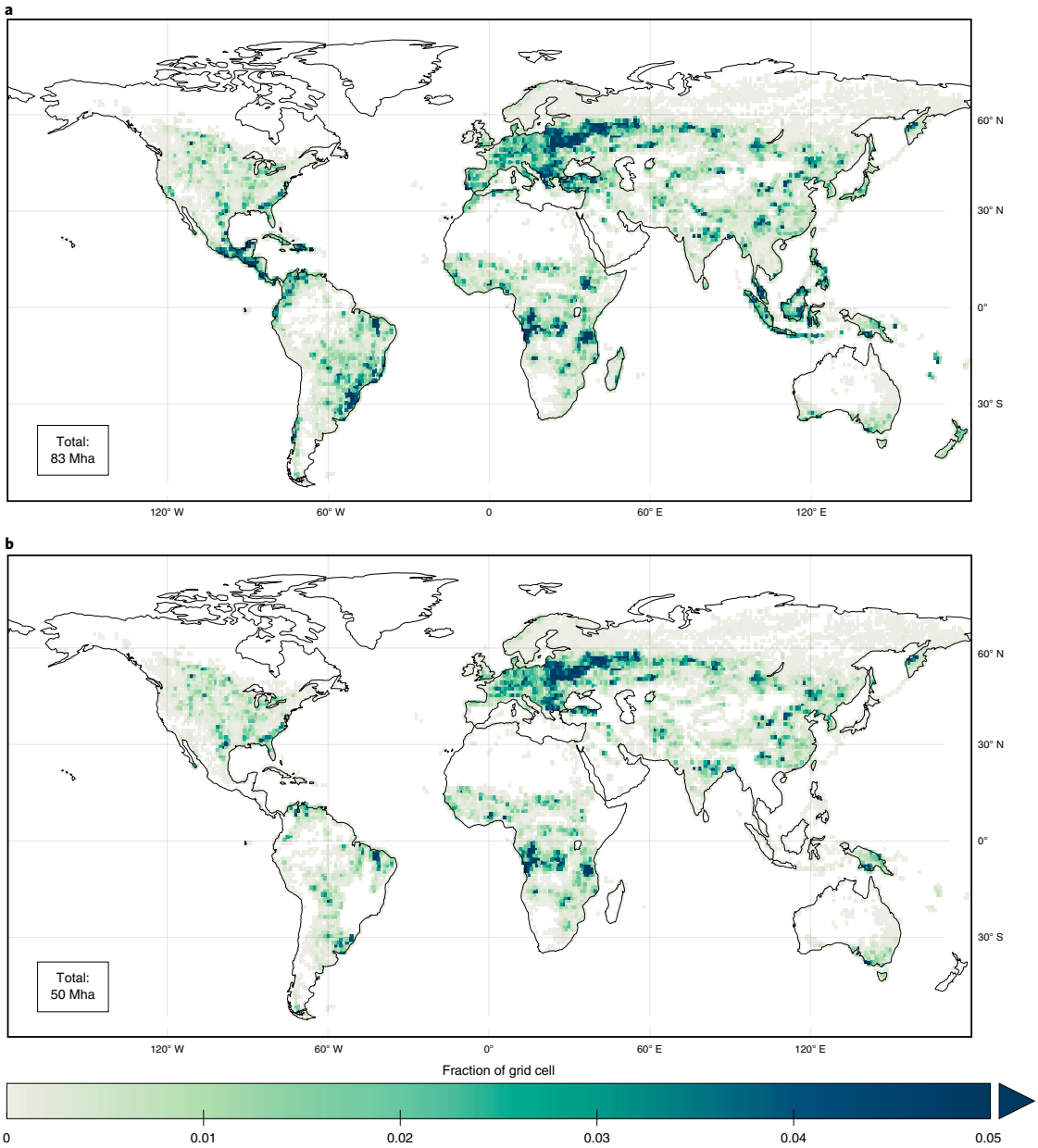

Fig. 1 | Global abandoned cropland between 1992 and 2015 as fraction of grid cell. a,**b**, Maps showing all abandoned cropland (**a**) and abandoned cropland located outside biodiversity hotspots (**b**). The maps are aggregated to 1 degree resolution for improved visualization.

locations, estimated according to existing yield gaps[34], is 25 EJ yr^{-1} under the mixed approach of water supply (Extended Data Fig. 1). Areas managed at low, medium or high management intensities are 15 Mha, 49 Mha and 19 Mha, respectively, and contribute 1.9 EJ yr^{-1}, 15 EJ yr^{-1} and 8.6 EJ yr^{-1}, respectively.

In general, miscanthus contributes the most to total bioenergy potentials. Switchgrass contributes about 10% of the potential under rain-fed conditions and low agricultural management intensity. Switchgrass becomes increasingly important at increased irrigation and higher management intensities, as these are favourable conditions for switchgrass growth at mid-latitudes. Reed canary grass has the smallest contributions across the range of combinations considered in our study.

Bioenergy potentials show nonlinear responses and trade-offs between land availability, agriculture management intensity and water requirements (Supplementary Fig. 2). At irrigated conditions

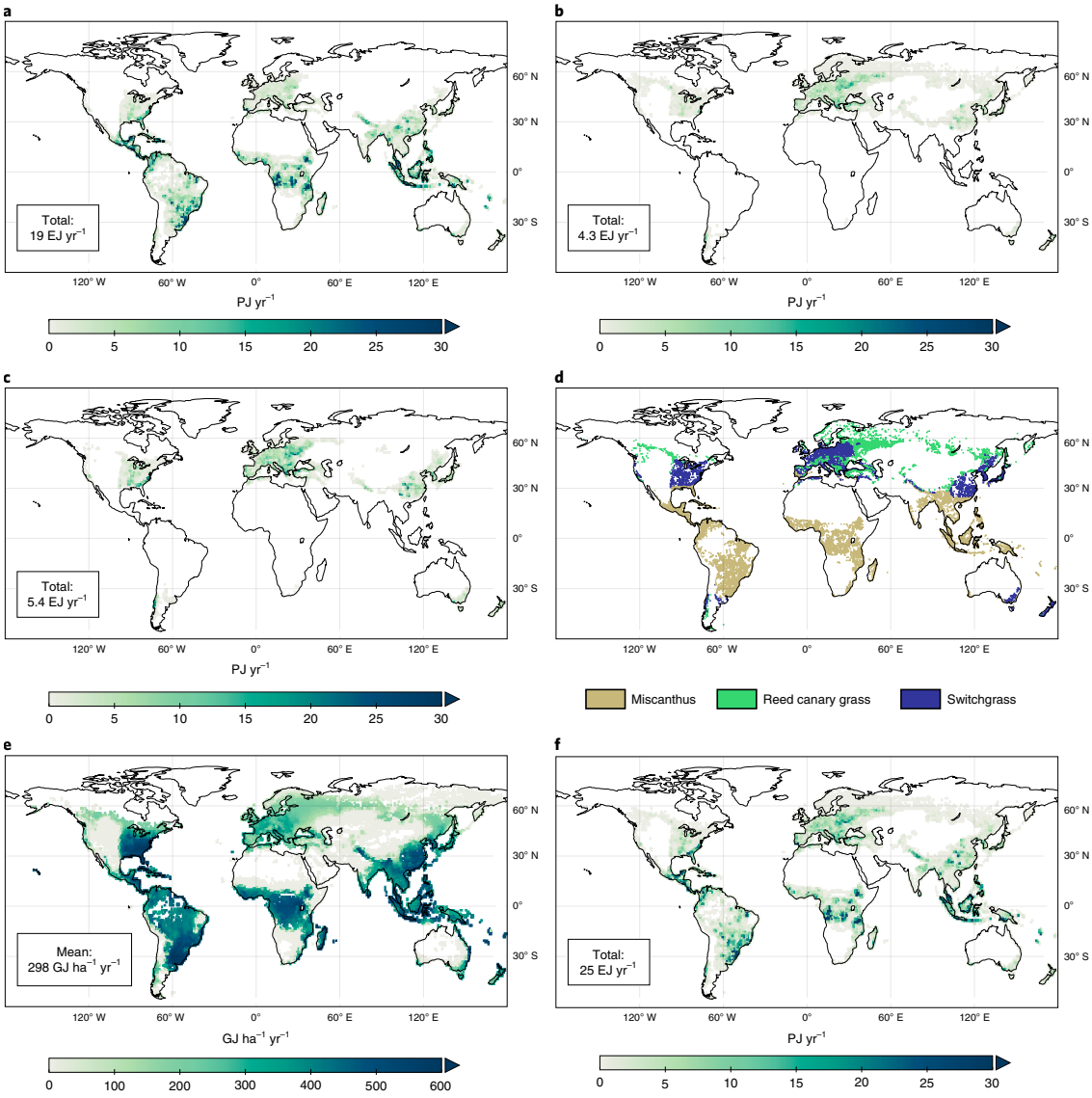

Fig. 2 | Global bioenergy potentials on abandoned cropland. a–c, Spatially explicit estimates of bioenergy potentials (PJ yr^{-1}) for miscanthus (**a**), reed canary grass (**b**) and switchgrass (**c**). **d**, Optimal global crop distribution based on local growing conditions to maximize biomass energy output per grid cell. **e**, Global bioenergy yields (GJ ha^{-1} yr^{-1}) with optimal crop allocation. **f**, Global bioenergy potential (PJ yr^{-1}) on abandoned cropland with optimal crop allocation. These results refer to present-day climatic conditions, high agricultural management intensity, rain-fed water supply and no nature conservation measures (that is, abandoned cropland within biodiversity hotspots is included). Maps **a–c** and **e**,**f** are aggregated to 1 degree resolution for improved visualization, while map **d** is shown at 5 arc minutes.

and high agricultural management intensity, the first 10 EJ yr^{-1} of bioenergy potential is reached with 16 Mha of abandoned cropland (ranked by productivity). In comparison, 10 EJ yr^{-1} requires 20 Mha with rain-fed water supply and 17 Mha with the mixed approach. Relying on rain-fed water supply reduces risks for water depletion but increases land requirements for a given bioenergy potential. Nonlinear effects are more severe in the biodiversity hotspots, where (irrigated) bioenergy potentials of 5 EJ yr^{-1}, 10 EJ yr^{-1} and 15 EJ yr^{-1} require 8.3 Mha, 18 Mha and 28 Mha, respectively.

Climate change affects bioenergy potentials, here examined using two future projections: RCP 4.5 (ref. [43]) and RCP 8.5 (ref. [44]) (Extended Data Fig. 2). In general, potentials decrease at low latitudes and increase at high latitudes. In subarctic and continental climates, significant gains in potentials are expected, because areas that are currently unsuitable for bioenergy production will become

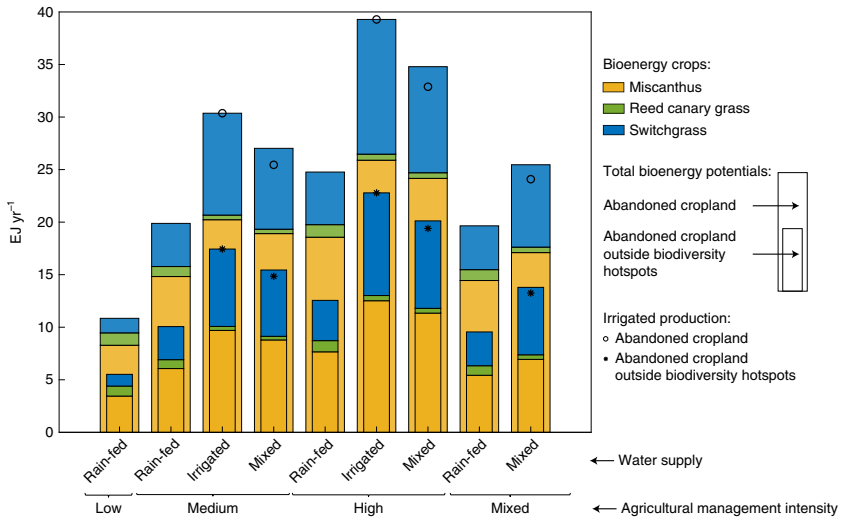

Fig. 3 | Bioenergy potentials (EJ yr^{-1}) on abandoned cropland for present-day climatic conditions and a set of different assumptions regarding water supply, agricultural management intensity level and land availability. Bioenergy potentials from all abandoned cropland are shown with wide bars and those from abandoned cropland located outside biodiversity hotspots with thin bars. Four agricultural management intensities (low, medium, high and mixed) and three water supply levels (rain-fed, irrigated and mixed) are considered. Specific contributions from irrigated areas and individual crops to total potentials are shown. Estimates are based on an energy-based optimal crop allocation per grid cell.

productive with climate change (up to about 3 Mha). In the tropics, bioenergy potentials consistently decrease. Yield declines are relatively large in areas affected by physical water scarcity, and different future climatic conditions will affect the energy-based optimal crop distribution (Supplementary Text 2).

Bioenergy crop productivity. Bioenergy yields generally range between 100 and 600 GJ ha^{-1} yr^{-1} and are higher than 600 GJ ha^{-1} yr^{-1} with high agricultural management intensity only (Fig. 4). Reducing agricultural management intensity from high to medium or low levels decreases annual average bioenergy yields with rain-fed water supply on all abandoned cropland from 298 GJ ha^{-1} yr^{-1} to 239 GJ ha^{-1} yr^{-1} and 130 GJ ha^{-1} yr^{-1}, respectively (Supplementary Table 2). Complete irrigation deployment, together with high management intensity and no nature conservation measures, achieves a global average bioenergy yield of 472 GJ ha^{-1} yr^{-1}.

Without irrigation, 13–17 Mha of abandoned cropland have no potential; these are mainly located in dry and polar climates or in mountainous areas (Supplementary Fig. 3). We find that 70 Mha, 68 Mha and 66 Mha are productive without irrigation at low, medium and high management intensities, respectively. Lower management levels show slightly higher productive area extent due to the unfeasibility of higher management levels under poor soil conditions that cap potential yields, as well as to the impracticalities of mechanization on steep slopes[34]. With irrigation deployment on all abandoned cropland, less than 2 Mha of land are left unavailable for bioenergy production irrespective of management intensity. The mixed approach, where irrigation is applied only to areas that are not affected by water scarcity, has average global bioenergy yields of 418 GJ ha^{-1} yr^{-1} at high agricultural management intensity, with 7.9 Mha of abandoned cropland left unproductive.

The energy-based optimization of bioenergy crop per grid cell depends on agricultural management levels and water supply systems. At low agricultural management intensity and rain-fed conditions, 45 Mha are allocated to miscanthus, 15 Mha to reed canary grass and 10 Mha to switchgrass. Increasing the agricultural management intensity to high changes the crop distribution to 43 Mha, 7.6 Mha and 16 Mha, respectively. Irrigation will further expand the areas allocated to miscanthus (50 Mha) and switchgrass (29 Mha), and reduce those for reed canary grass (2.9 Mha). Typically, miscanthus is the preferred crop in tropical areas threatened by physical water scarcity due to its relatively high water-use efficiency, while switchgrass is favoured by irrigation and high agricultural management intensity outside the tropics. Reed canary grass yields are larger than those of other bioenergy crops at high latitudes only. They are outcompeted by switchgrass in many locations at high agricultural management intensity and with irrigation, which expand the switchgrass domain towards higher latitudes. Similarly, with irrigation miscanthus expands into the lower latitudes compared with its initial domain.

The joint effects on bioenergy potentials of agricultural management intensity, water supply and exclusion of biodiversity hotspots under future climatic conditions are discussed in Supplementary Text 3. Declines in global bioenergy potentials in RCP 8.5 can partially be reduced through large-scale irrigation, which can achieve 38 EJ yr^{-1} in 2080 (4% less than present-day conditions) (Extended Data Fig. 3). A partial deployment of irrigation on areas unthreatened by water scarcity can provide a potential of 33 EJ yr^{-1}. These two irrigation options would bring 21 Mha and 15 Mha of abandoned cropland under production, respectively, which would be otherwise unproductive under future climatic conditions.

The land–energy–water nexus. The land–energy–water nexus is assessed by combining the variables of the nexus into four indicators: total and marginal energy gains from irrigation, blue water footprint and total water withdrawals. Relative to rain-fed conditions, irrigation can increase global bioenergy potentials by 10 or 15 EJ yr^{-1} under medium or high agricultural management intensity, respectively (Fig. 5a,b). There are important gains from irrigation across humid continental climate zones with warm summers across Eastern Europe, Eastern Asia and North America. For example, complete irrigation deployment can increase potentials on abandoned

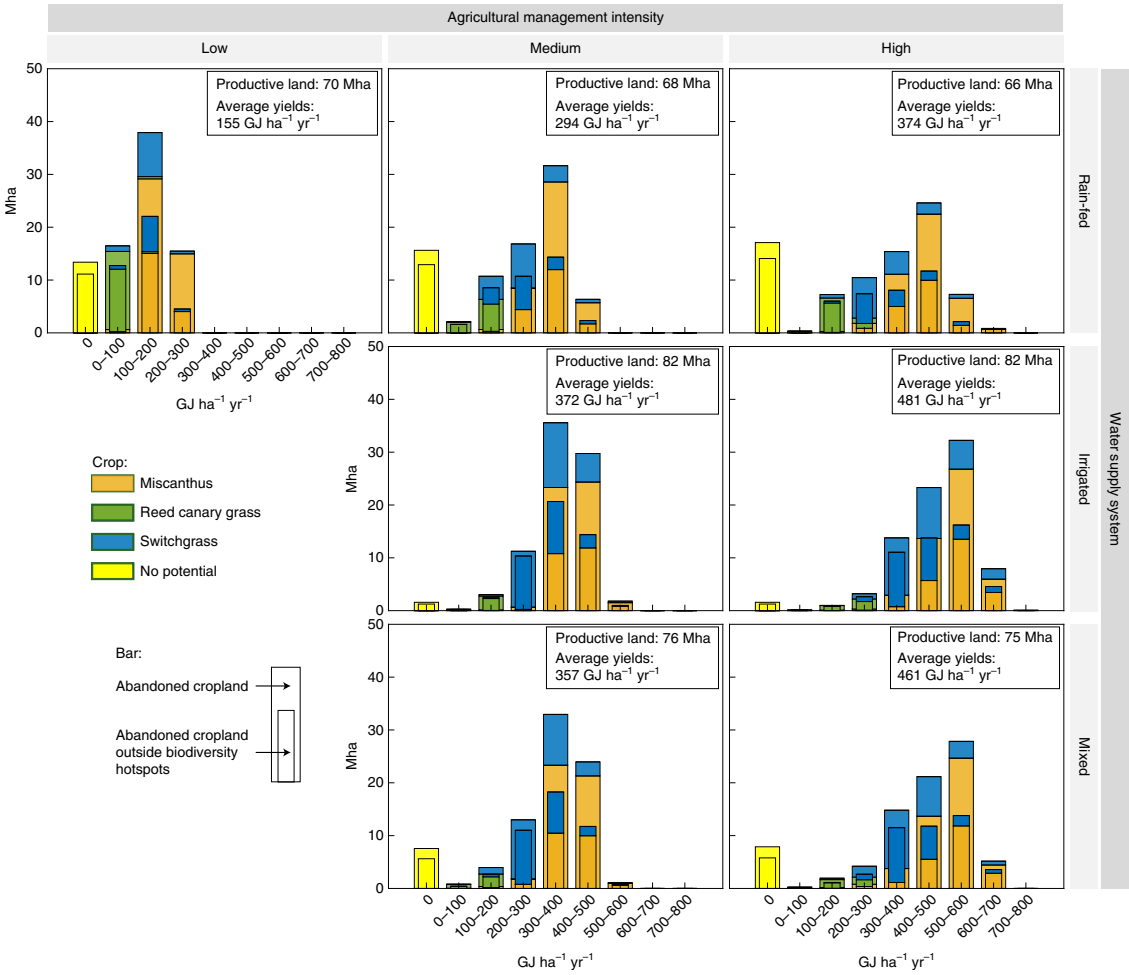

Fig. 4 | Present-day productivity distribution of global abandoned cropland (Mha) and optimal crop allocation as a function of bioenergy yields (GJ ha^{-1} yr^{-1}) for different management intensities and water supply systems. Bioenergy potentials from all abandoned cropland are shown with wide bars and those from abandoned cropland located outside biodiversity hotspots with thin bars. Three agricultural management intensities (low, medium and high) and three water supply levels (rain-fed, irrigated and mixed) are considered for different bioenergy crops. The average yields shown refer only to productive areas.

cropland in North America from 1.3 EJ yr^{-1} to 2.3 EJ yr^{-1}, mainly due to improved growing conditions for switchgrass in the western regions.

The global average marginal energy gain from supplying one extra unit of energy with irrigation is 0.26 GJ ha^{-1} mm^{-1} for medium agricultural management intensity and 0.32 GJ ha^{-1} mm^{-1} for high (Fig. 5c,d). The highest marginal energy gains (above 0.60 GJ ha^{-1} mm^{-1}) are in humid continental and subarctic climate zones. Lower marginal energy gains are in semi-arid and oceanic climatic zones (0.20–0.40 GJ ha^{-1} mm^{-1}). In tropical and fully humid subtropical climates crop water deficit is not a limitation for bioenergy (marginal energy gains are below 0.20 GJ ha^{-1} mm^{-1}).

Simultaneous consideration of combined total and marginal energy gains indicators allows the identification of priority areas for irrigation and trade-offs. For example, while tropical savannah and hot semi-arid climates (such as northern Africa, northeastern Brazil and parts of Central America) show high energy gains from irrigation, the marginal gains are low. This indicates that higher amounts of water relative to the global average are needed to increase bioenergy production. In Mediterranean climate zones, such as in Southern Europe and western North America, energy gains are high and less water is needed relative to the global average to increase bioenergy potentials. However, large parts of the Mediterranean basin are biodiversity hotspots and parts of western North America are subject to physical water scarcity, with potential trade-offs on either nature conservation or water depletion. The most promising locations for irrigated bioenergy production have both high total and marginal energy gains. These include humid continental climates across Eastern Europe, Northeastern Asia and in northern parts of North America.

There is large spatial variability in the blue water footprint and total water withdrawals of irrigated bioenergy production (Extended

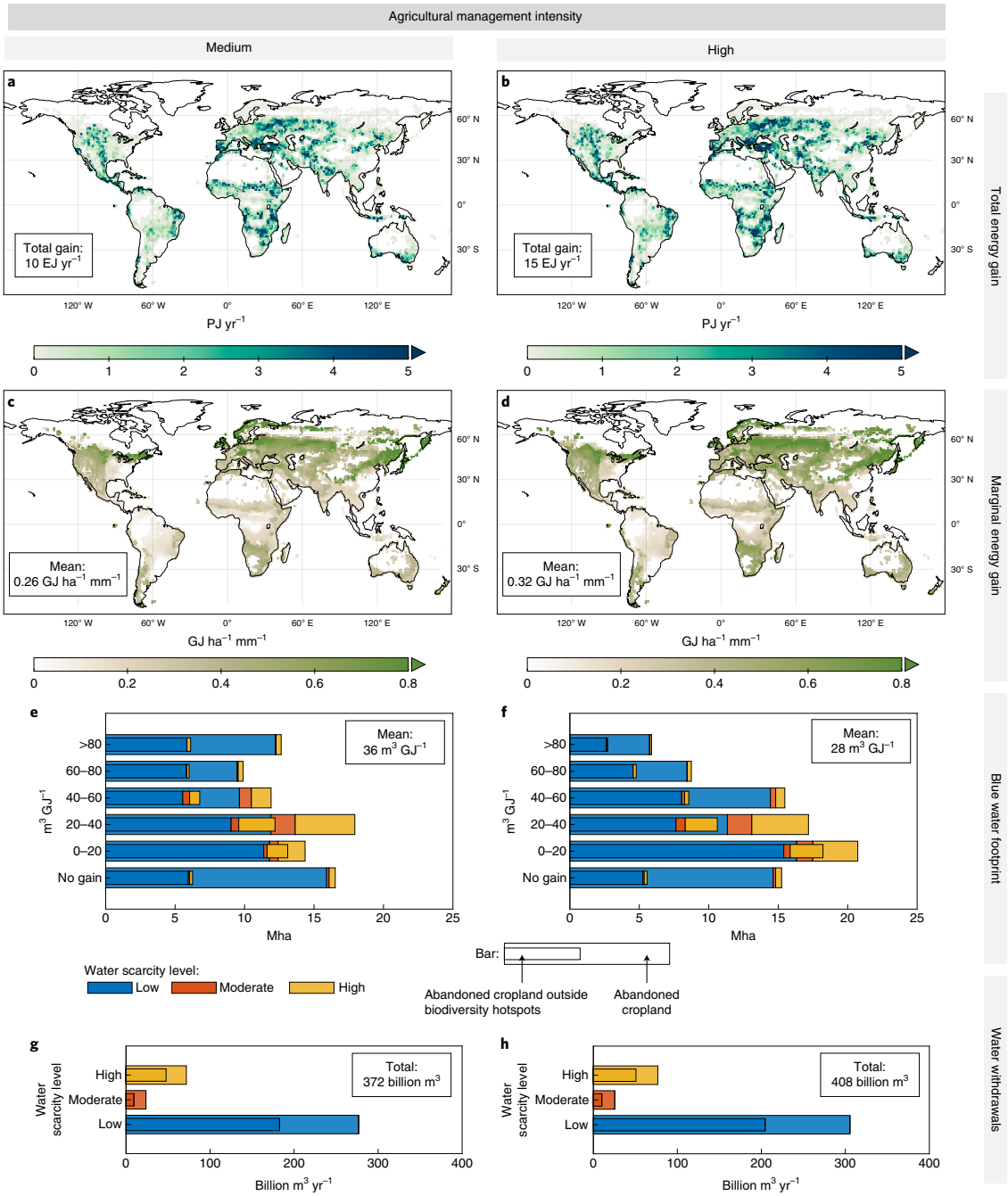

Fig. 5 | Irrigation effects on bioenergy potentials and key water requirement indicators under two alternative agricultural management intensities and water scarcity levels. a–h, Total energy gains from irrigation are shown in **a** and **b**, marginal energy gains for each additional unit of water supplied via irrigation in **c** and **d**, blue water footprints in **e** and **f** and water withdrawals in **g** and **h**. Agricultural management intensity: medium (**a**,**c**,**e**,**g**); high (**b**,**d**,**f**,**h**). Spatial explicit variabilities of blue water footprints and water withdrawals are shown in Extended Data Fig. 4. In **e**–**h**, the wide bars refer to values from all abandoned cropland and the thin bars exclude land in the biodiversity hotspots. These results refer to bioenergy potentials under today's climatic conditions and optimal energy-based allocation of crop types per grid cell. Maps are aggregated to 1 degree resolution for improved visualization.

Data Fig. 4). Blue water footprint values are almost evenly distributed across abandoned cropland areas, with a general decrease of the mean footprint with more efficient high management intensity from 36 $m^3 GJ^{-1}$ to 28 $m^3 GJ^{-1}$ (Fig. 5e,f). In general, blue water footprints are high around the Equator and across humid subtropical climates, such as western North America. In areas with high water scarcity, the mean blue water footprint is usually lower than the global average (23 $m^3 GJ^{-1}$), meaning that less water is required per additional energy unit. However, these areas have higher risks of water depletion.

Total water withdrawals for irrigated bioenergy production under high management intensity are 408 billion $m^3 yr^{-1}$, equivalent to 15% of today's annual global water withdrawals for agriculture[45] (Fig. 5g,h). Of this, 102 billion $m^3 yr^{-1}$ (or 25%) come from areas affected by physical water scarcity and can deliver 4.4 EJ yr^{-1} (or 30%) of additional bioenergy relative to rain-fed conditions. About 75% of total withdrawals come from areas with low water scarcity, and they can supply 10 EJ yr^{-1} of bioenergy. Excluding land within biodiversity hotspots reduces the global water requirements to 265 billion m^3. A bioenergy potential that reduces trade-offs with biodiversity and water depletion, by excluding land within biodiversity hotspots and avoiding irrigation in physical water-scarce areas, requires 204 billion m^3 of water (8% of today's global withdrawals for agriculture[45]) to produce 20 EJ yr^{-1} of bioenergy. There are non-linear relationships between bioenergy potentials and water withdrawals that vary per water scarcity level (Supplementary Fig. 4). Relative to rain-fed, the first 100 billion $m^3 yr^{-1}$ of global water withdrawals lead to 6.5 EJ yr^{-1} of bioenergy gains and the next 100 billion $m^3 yr^{-1}$ to an additional 4.0 EJ yr^{-1}, assuming irrigation is prioritized in areas with higher marginal energy gains. As the most suitable areas become irrigated, 208 billion $m^3 yr^{-1}$ of further water withdrawals will lead to an additional energy gain of 4.0 EJ yr^{-1}.

Discussion

As land is a limited resource, its management should address global challenges by prioritizing options that co-deliver multiple benefits while minimizing trade-offs. Abandoned cropland is a promising near-term option to increase land availability for bioenergy crops whilst minimizing risks for food security and other environmental aspects. The interplay of multiple environmental factors and conditions, here assessed with a land–energy–water nexus, influence estimates of possible bioenergy potentials. Our highest estimate is about 68% of today's global primary bioenergy demand[2] and 16–47% of median projected primary bioenergy demand in 2050 for 1.5 °C scenarios across different SSPs[3,4] (Extended Data Fig. 5). The associated land and water requirements are 5% and 15% of present-day agricultural cropland extent and water use, respectively[45]. Acknowledging site-specific trade-offs with water scarcity and nature conservation reduces global bioenergy potentials to 35% of today's demand, and land and water requirements to 3% and 8% of current cropland extent and agricultural water use, respectively[45]. Achieving high yields usually requires modern agricultural management systems, irrigation and use of land within biodiversity hotspots. Context-specific information can be used to improve management practices and reduce side-effects, such as using irrigation where it has high marginal energy gains and no risks of water depletion. Our approach integrated different datasets and approaches, and hence embeds the inherent uncertainties associated with them (Methods).

Meeting the projected bioenergy demand in 1.5 °C scenarios would require extensive land-use changes[5,10] and probably cause competition for land resources[46–48]. Today's available abandoned cropland is limited, and a further expansion of bioenergy crops on present cropland and pastureland is needed to meet future bioenergy requirements (Supplementary Table 3). Additional bioenergy can be produced from perennial grass cultivation as a restoration measure on land prone to degradation, but potentials are probably limited[17]. Reducing the demand for land-based food and feed products is essential to alleviate pressure on land resources and make them available to bioenergy crops[5]. Linking historical cropland abandonment patterns and site-specific bioenergy potentials to local socio-economic drivers might assist more accurate spatial and temporal projections of bioenergy estimates and management requirements.

Converting abandoned croplands to perennial grasses can provide a range of ecological and environmental benefits. However, forest restoration or reforestation for climate, environmental and ecological benefits are alternative options for abandoned cropland[49]. The use of nexus approaches that integrate various environmental factors are instrumental in addressing the complex interconnections of different land-based mitigation strategies and identifying their trade-offs and synergies, such as those connected to land availability, water scarcity and nature conservation. Context-specific analysis should identify which option can better address one (or more) global challenge in each given regional context. Likewise, including regional biomass density factors, spatial infrastructure requirements and other socio-economic indicators of local development potentials[50] are necessary ingredients to ultimately guide the design of sustainable land management strategies in the light of global challenges and regional contexts.

Methods

This section describes the multiple datasets and approaches we integrated in our analysis, including associated uncertainties and limitations.

Mapping abandoned cropland. ESA CCI-LC maps provide a dynamic description of the Earth's terrestrial surface at 300-m spatial resolution from 1992 to 2015[33]. This product was specifically developed to remedy limitations of previous datasets and to advance more realistic representations of land cover dynamics[25,51]. It provides annual identification of 37 land cover classes through a mix of satellite images and ground data. The ESA CCI-LC dataset is increasingly used to characterize temporal dynamics and spatial patterns of land cover changes at a landscape and global level[52–54] and for analysis of climate feedbacks related to land cover changes[55,56].

We performed a literature review to assess recent validation efforts of the ESA CCI-LC product (Supplementary Table 4). Global overall accuracies are 71–80%, with a 72% median across multiple global studies[33,57–59], and some regional variations[40,60–65]. Global producer and user accuracies of cropland classes are 66–92% and 79–94%, with medians of 79% and 89%, respectively[33,57–59]. The relatively high accuracies found for cropland classes make the product especially suitable for cropland monitoring.

There are six different land cover classes representing different types of croplands, of which two are cropland mosaics that include a mix of managed and non-managed land[33]. We identified global abandoned cropland using the difference in cropland extent (all six classes) between the ESA CCI-LC datasets in 1992 and 2015 (that is, a pixel that was classified as cropland in 1992 but not in 2015). The identification of global abandoned cropland includes all the transitions from cropland or mosaic cropland classes to any other land cover class except settlements, as urban areas cannot be available for bioenergy crops. For visualization purposes, we reduced all map resolutions from the one at which the land cover analysis was performed (10 arc seconds) to either 5 arc minutes or 1 degree (see figure captions). All maps are produced with Panoply 4 using the Earth.cno overlay[66].

Cropland extents are compared with land-use inventories from FAO data[41,45] (Supplementary Fig. 1) by applying country masks[67] to quantify country-level cropland extent in 1992 and 2015. In addition, we linked our cropland abandonment findings for different countries and regions to existing literature, and discussed their comparability and potential implications of methodological differences (Supplementary Table 1 and Supplementary Text 1).

Land and water availability. The land–energy–water nexus is investigated by assessing the interconnections between bioenergy yields and alternative options for land availability and suitability, and water supply.

From the identified abandoned cropland, a more restrictive option of land availability filters out areas that are within the so-called biodiversity hotspots. Biodiversity hotspots are classified as areas containing at least 1,500 endemic vascular plant species where at least 70% of the natural vegetation is lost[68]. Biodiversity hotspots host an enormous concentration of small-ranged species in places where most natural habitats have been cleared[69], and they were introduced to identify priority areas for nature conservation and restoration. Over the past decades, forest losses in biodiversity hotspots due to agricultural expansion have led to increased pressure on threatened ecosystems[54]. Sparing abandoned cropland inside

biodiversity hotspots for natural vegetation restoration can benefit conservation of vascular plants[35]. Maps of biodiversity hotspots[70] were used as overlapping masks to the maps of identified abandoned cropland (Supplementary Fig. 5).

Our study considers the relationships between bioenergy potentials and three possible options of water supply: rain-fed, irrigation and a mixed approach where only areas not affected by water scarcity are irrigated. Irrigated conditions assume no crop water deficits during the growth cycle (for example, crop water losses from evapotranspiration do not exceed absorption), thereby avoiding yield losses from water stress. Multiple methods and indicators exist to assess water scarcity, building on factors such as population densities, water availability and water use[71,72]. Here we adopted the concept of physical water scarcity, that is, when the available renewable water resources do not meet water demands[73,74]. This indicator is used mainly to address local potential for additional water infrastructure development and corresponding water-use efficiency measures[71]. Within physical water-scarce areas, further water withdrawals for new activities have high potential risks of water depletion. Datasets describing physical water scarcity at a river basin level were taken from the Aquamaps database[75]. Areas where annual agricultural water use (evapotranspiration) is below 10%, between 10–20% or exceeds 20% of total renewable freshwater resources are classified as low, moderate and high levels of water scarcity, respectively[45]. In addition to rain-fed and irrigation, we estimate bioenergy potentials including a constraint where irrigation does not occur in areas with moderate and high levels of physical water scarcity (mixed approach).

Bioenergy crops and yield model. Three different perennial grasses are considered as bioenergy crops: miscanthus, reed canary grass and switchgrass. All three species show promising characteristics as future bioenergy feedstocks, as they are adaptive to different climatic zones[76].

Miscanthus (*Miscanthus* × *giganteus*) is a C4 grass, occurring naturally at a wide climatic range, from tropical to subarctic regions[77]. Miscanthus has an optimal photosynthetic temperature between 30 °C and 35 °C[78], but maintains efficient productivity in temperatures higher than 10 °C[79]. However, miscanthus yields decrease with increasing latitudes, and longer periods of frost increase crop mortality[80,81]. Typically, miscanthus is harvested in late winter or early spring[82,83] and it has a relatively high water-use efficiency compared with other C4 crops[84].

Reed canary grass (*Phalaris arundinacea*) is a C3 grass growing in temperate climates across Eurasia and North America, thriving under cool and moist conditions[85,86]. It is able to grow under a range of water regimes and is resilient to temporary disturbances such as floods and droughts[87,88]. Photosynthetic rates of reed canary grass peak between 20 °C and 25 °C, with optimal temperatures decreasing with increased water stress[89]. Reed canary grass is normally harvested in late winter or spring[85,90].

Switchgrass (*Panicum virgatum*) is a C4 grass native to Northern America, typically found in the western United States from 55°N down to Mexico, known for its flexibility to grow in a variety of environments[76,91]. It has an optimal growth temperature range between 25 °C and 30 °C[92]. Severe drought events significantly impact switchgrass yields and potential yield losses can be decreased by increasing water supply through irrigation during droughts[93–95]. Switchgrass is usually harvested during autumn[20,91].

The GAEZ model v.3.0 (ref. [34]) is used to quantify local bioenergy crop yields (dry mass) for the three bioenergy crops. GAEZ is a widely used crop yield model that has been applied and validated in a variety of studies modelling agricultural productivity of different crops[96–98]. It has also been used for estimating water requirements of irrigated crops[99,100]. Some studies also used GAEZ specifically for bioenergy crops[101–103], but it has never before been coupled to high-resolution global land cover datasets, and a thorough analysis of the implications of different land and water availability is missing.

GAEZ considers site-specific parameters such as climatic conditions (for example, surface irradiation, precipitation and temperature), soil quality, and terrain to estimate crop yields and water use. It accounts for yearly variability in soil moisture, possible yield losses due to pests, soil workability constraints and frosts. GAEZ models yield responses to the use of fertilizer, pesticides and agricultural conservation measures. Based on the optimal crop calendar for growth at rain-fed conditions, it also estimates crop water balances, evapotranspiration and water deficits.

Crop yields are produced for three different levels of agricultural management intensities: low, medium and high[34]. Low management intensity refers to labour-intense subsistence-based farming with production based on traditional cultivars and without mechanization, pesticides, fertilizers or agricultural conservation measures. At medium intensity, production targets both subsistence and commercial sale. Production can still be based on manual labour using a mix of hand tools, animal traction and some mechanization. Technologies added include the application of some fertilizers and chemical pesticides, better varieties and some soil conservation measures. High management intensity refers to a modern and market-oriented commercial production system, with full mechanization, high-yielding varieties and optimal application of fertilizers and pesticides. Additionally, crop yields at irrigated conditions are estimated for medium and high management intensities (that is, no water deficit during crop growth cycle). Our analysis also considered a non-uniform agricultural management system based on spatially explicit data of current agricultural yield gaps[34] to allocate abandoned cropland to different management intensities (Extended Data Fig. 1a). Yield gaps of less than 45%, between 45–75% and above 75% are allocated to high, medium and low management intensities, respectively. Our map of agricultural management intensities is spatially consistent with global maps of nitrogen and phosphorus fertilizer application[104] and pesticide use[105]. Maximum attainable dry mass yields are converted to energy yields using lower heating values of 18.55 MJ kg^{-1} for miscanthus, 18.06 MJ kg^{-1} for reed canary grass and 17.82 MJ kg^{-1} for switchgrass[106].

In addition to present-day climatic conditions, we investigated how bioenergy potentials vary under future climatic conditions in 2050 and 2080 according to two alternative scenarios, RCP 4.5 and RCP 8.5. RCP 4.5 is typically associated with a global annual mean temperature increase of 2.4 ± 0.5 °C by 2100 relative to pre-industrial times[43,107]. RCP 8.5 is an unlikely high carbon emission scenario[108] associated with an increase of 4.3 ± 0.7 °C in global annual mean temperature and an increase in global annual mean precipitation of 5% by the end of the century[44,109–111]. We used future climatic conditions taken from the HadCM3 model projections (two 30-year period ensemble means, 2041–2069 and 2071–2100, indicated as 2050 and 2080) to explore the response of bioenergy yields to different background conditions of the climate system[112,113].

A total of 296 combinations of bioenergy potentials are assessed in our analysis, considering a variety of constraints and conditions: land availability (with or without abandoned cropland within the biodiversity hotspots), type of bioenergy crop (miscanthus, reed canary grass, switchgrass or an energy-based optimal crop allocation per grid cell), agricultural management intensity (low, medium, high or a mix), water supply (rain-fed, irrigation or a mixed approach where irrigation occurs only at medium and high management intensity in areas not threatened by water scarcity), climatic conditions (present-day or future conditions in line with RCP 4.5 and RCP 8.5) and three different points in time (present day, 2050 and 2080). Bioenergy potentials were computed for each individual combination, excluding the unlikely option that combines irrigation with low agricultural management intensity. Results are mainly shown for the energy-based optimal crop allocation.

Indicators for nexus approach. A nexus approach has been frequently advocated to assess the interlinkages of agricultural and bioenergy systems[31,114,115]. Application and implementation of nexus approaches are still in their infancy. We followed the five major steps that were proposed to standardize implementation of nexus approaches in the scoping of our analysis[31]. A quantitative understanding of the potentials and limitations of bioenergy crops on global recently abandoned cropland is our main research goal and system definition, the land–energy–water interactions are in the core of our nexus framework (describing dependencies of bioenergy yields on land and water factors) and a set of quantitative spatially explicit indicators are selected to simulate nexus dynamics. Different indicators are typically used for quantitative nexus analyses, and cross-resource intensities and indices that combine the main nexus variables into a single number are those commonly used in nexus research[31].

In our study, we consider four spatially explicit indicators of bioenergy potentials relative to irrigation efficiency, land availability and management intensity to visualize the land–energy–water nexus. The first is based on the total energy gains from irrigation given as the difference in bioenergy production between rain-fed and irrigated water supply (GJ yr^{-1}). This indicator informs about the absolute potential of increasing bioenergy production through irrigation per grid cell. The second is based on the marginal energy gains from supplying additional water assuming optimal water use for irrigation during the whole growth cycle, thereby avoiding water deficits. This indicator is expressed as the increase in bioenergy yields per unit supplied with water in a given area (GJ ha^{-1} mm^{-1}) and it embeds all the physical units of the land–energy–water nexus. The marginal energy gains describe how sensitive increases in bioenergy production are to additional water supply. The third indicator is the spatial blue water footprint per energy gain (m^3 GJ^{-1}), describing water withdrawals for irrigation from surface water or groundwater which either evaporates, is moved from one water body to another or is returned at another time[116]. This indicator assesses the trade-offs between increased energy production and water depletion from irrigation deployment on abandoned cropland. Then we estimated the total water withdrawals (m^3 yr^{-1}) of irrigation deployment at different physical water scarcity levels on abandoned cropland. Each indicator is calculated per grid cell and in average/total terms, and for different management intensities, land availability and water supply systems.

Uncertainties and limitations. Although the ESA CCI-LC dataset has the highest accuracy for cropland cover compared with the other land cover classes[33], it is likely that identification of abandoned cropland is affected by the limitations of the dataset regarding mosaic classes. Relative to other products, the ESA CCI-LC dataset is highly suitable for cropland monitoring in America[40], largely consistent at a global level with the FAO country-based inventory of cropland areas[53], but with potential risks of underestimating the amount of arable and abandoned land in the former Soviet Union[117]. More accurate and refined estimates of effective availability of abandoned cropland should rely on site-specific evaluations and controlling procedures because the land might already be (at least partially) committed to other uses or the presence of trees for agroforestry or fruits can mimic revegetation of areas that are still under crop production[118].

Despite being widely tested and used, GAEZ relies on assumptions and uncertainties such as yield losses caused by moisture stress, excess air humidity and risk of frost[34]. Expanding the analysis to include a multi-model intercomparison of effects of climate variability on crop growth could reveal how individual variables and climate model characteristics influence results. Similarly, changes in frequency and intensity of extreme events, such as droughts, floods and wildfires, are likely to affect crop yields in the future[119,120]. Our high estimates of bioenergy production are dependent on water availability for irrigation. We apply the physical water scarcity indicator to exclude areas from further water withdrawal for irrigation, but this indicator can change with future climate conditions and due to lack of a consistent global dataset we do not attempt to estimate remaining water budgets until physical water scarcity is reached. An approach integrating renewable water resources and future climate change patterns at a basin level can improve our understanding of the actual irrigation potential on abandoned land[121]. There is a potential for species invasiveness related to introducing non-native bioenergy species to new areas[8,122]. By including spatial crop-specific risk factors and constraints, management options to mitigate an invasive spread of bioenergy crops can be identified.

Future bioenergy potentials are heavily dependent on the spatially projected temperature and precipitation changes, which are sensitive to the type of climate model used. For instance, we find a reduction in bioenergy potentials in 2080 for RCP 8.5 in large parts of the Amazon region, with crop yields reduced by more than 50%. For high emission scenarios, several climate models consistently project a significant drying and warming in the Amazon region that can lead to a vegetation dieback[123–128], and a tipping point for the Amazon forest is estimated at around 3–4 °C of global warming[129,130]. Relative to other climate models, the Hadley projections used here show a stronger drying effect in the Amazon region than those from other models[123,131]. While there is a consensus across climate models projecting a drying effect in the Amazon[132], bioenergy yield changes are dependent on the individual model used for climate projections. However, we can expect that the use of different climate projections would affect the absolute changes of bioenergy potentials, but not the direction of their trends, because the projected temperature and precipitation patterns are generally consistent across models[132]. They generally find that: (1) the projected annual mean warming varies between 3 °C and 10 °C depending on location, with the strongest warming over Arctic regions (>8 °C), moderate warming over mid-latitudes between 40–60°N and the Tibetan plateau (5–7 °C) and weaker warming in other regions (<5 °C); (2) a reduction in precipitation rates is projected in the Mediterranean, southwestern North America, southern tropical South America, Central America, Southern Africa and Australia, while areas at higher latitudes (above 55°N), tropical Africa and South and East Asia become wetter. Other studies are consistent with our findings, also indicating that C3 and C4 crop yield changes in RCP 8.5 are twice those in RCP 4.5 in some locations of the world[133].

Further work is needed to map the actual socio-economic bioenergy deployment potential in the available abandoned cropland. Biomass is a low-density and low-value feedstock, so considering the regional critical production density is essential for planning future developments, especially if logistics costs prohibit moving biomass over long distances. Additionally, access to local infrastructure, distance to markets and local policies will also affect bioenergy deployment potentials[50].

The nexus concept is still evolving and difficult to univocally define with a default approach and standardized indicators[31,32]. Despite being sometimes criticized as a buzzword[134], framing research analysis across multiple sectors or dimensions within this terminology is a way to constantly highlight their strong interlinkages and stimulate critical thinking in terms of potential trade-offs and synergies when addressing environmental and societal challenges. We followed a transparent and traceable quantitative approach to link local factors of land conditions and water resources to bioenergy potentials under current and future climate scenarios. To better visualize and compare the possible synergies and trade-offs, we produced indicators that encapsulate all the nexus components (land, energy and water) in one score. Future efforts in developing and consolidating indicators more specifically tailored to address interlinkages of environmental systems with a nexus approach, ideally established through international multidisciplinary flagship initiatives, will be instrumental in optimizing the deployment of sustainable bioenergy potentials.

Reporting Summary. Further information on research design is available in the Nature Research Reporting Summary linked to this article.

Data availability

Datasets used in this analysis are publicly available from the references provided within the paper. Other data supporting the findings of this study are available from the corresponding author on reasonable request. Source data are provided with this paper.

Code availability

Custom code used in this analyses is available at https://github.com/janjsn/lew_nexus_ac_bioenergy.

Received: 7 May 2020; Accepted: 17 December 2020;
Published online: 18 January 2021

References

1. Rogelj, J. et al. in *Special Report on Global Warming of 1.5 °C* (eds Masson-Delmotte, V. et al.) Ch. 2 (WMO, 2018).
2. *Energy Technology Perspectives 2017: Catalysing Energy Technology Transformations* (IEA, 2017).
3. Riahi, K. et al. The Shared Socioeconomic Pathways and their energy, land use, and greenhouse gas emissions implications: an overview. *Glob. Environ. Change* **42**, 153–168 (2017).
4. Rogelj, J. et al. Scenarios towards limiting global mean temperature increase below 1.5 °C. *Nat. Clim. Change* **8**, 325–332 (2018).
5. IPCC: Summary for Policymakers. In *Special Report on Climate Change and Land* (eds Shukla, P. R. et al.) (IPCC, 2019).
6. Creutzig, F. et al. Bioenergy and climate change mitigation: an assessment. *GCB Bioenergy* **7**, 916–944 (2015).
7. Campbell, J. E., Lobell, D. B., Genova, R. C. & Field, C. B. The global potential of bioenergy on abandonded agricultural lands. *Environ. Sci. Technol.* **42**, 5791–5794 (2008).
8. Robertson, G. P. et al. Cellulosic biofuel contributions to a sustainable energy future: choices and outcomes. *Science* **356**, eaal2324 (2017).
9. Muri, H. The role of large-scale BECCS in the pursuit of the 1.5 °C target: an Earth system model perspective. *Environ. Res. Lett.* **13**, 44010 (2018).
10. Daioglou, V., Doelman, J. C., Wicke, B., Faaij, A. & van Vuuren, D. P. Integrated assessment of biomass supply and demand in climate change mitigation scenarios. *Glob. Environ. Change* **54**, 88–101 (2019).
11. Lasanta, T. et al. Space–time process and drivers of land abandonment in Europe. *CATENA* **149**, 810–823 (2017).
12. Li, S. & Li, X. Global understanding of farmland abandonment: a review and prospects. *J. Geogr. Sci.* **27**, 1123–1150 (2017).
13. Jepsen, M. R. et al. Transitions in European land-management regimes between 1800 and 2010. *Land Use Policy* **49**, 53–64 (2015).
14. Qin, Z., Dunn, J. B., Kwon, H., Mueller, S. & Wander, M. M. Soil carbon sequestration and land use change associated with biofuel production: empirical evidence. *GCB Bioenergy* **8**, 66–80 (2016).
15. Dou, F. G. et al. Soil organic carbon pools under switchgrass grown as a bioenergy crop compared to other conventional crops. *Pedosphere* **23**, 409–416 (2013).
16. Liu, W., Yan, J., Li, J. & Sang, T. Yield potential of Miscanthus energy crops in the Loess Plateau of China. *GCB Bioenergy* **4**, 545–554 (2012).
17. Englund, O. et al. Beneficial land use change: strategic expansion of new biomass plantations can reduce environmental impacts from EU agriculture. *Glob. Environ. Change* **60**, 101990 (2020).
18. Yang, Y., Tilman, D., Lehman, C. & Trost, J. J. Sustainable intensification of high-diversity biomass production for optimal biofuel benefits. *Nat. Sustain.* **1**, 686–692 (2018).
19. Georgescu, M., Lobell, D. B. & Field, C. B. Direct climate effects of perennial bioenergy crops in the United States. *Proc. Natl Acad. Sci. USA* **108**, 4307–4312 (2011).
20. Harding, K. J., Twine, T. E., VanLoocke, A., Bagley, J. E. & Hill, J. Impacts of second-generation biofuel feedstock production in the central US on the hydrologic cycle and global warming mitigation potential. *Geophys. Res. Lett.* **43**, 10,773–10,781 (2016).
21. Ramankutty, N. & Foley, J. A. Estimating historical changes in global land cover: croplands from 1700 to 1992. *Glob. Biogeochem. Cycles* **13**, 997–1027 (1999).
22. Field, C. B., Campbell, J. E. & Lobell, D. B. Biomass energy: the scale of the potential resource. *Trends Ecol. Evol.* **23**, 65–72 (2008).
23. Cai, X., Zhang, X. & Wang, D. Land availability analysis for biofuel production. *Environ. Sci. Technol.* **45**, 334–339 (2011).
24. Li, S. et al. An estimation of the extent of cropland abandonment in mountainous regions of China. *Land Degrad. Dev.* **29**, 1327–1342 (2018).
25. Poulter, B. et al. Plant functional type classification for Earth system models: results from the European Space Agency's Land Cover Climate Change Initiative. *Geosci. Model Dev.* **8**, 2315–2328 (2015).
26. Boysen, L. R., Lucht, W. & Gerten, D. Trade-offs for food production, nature conservation and climate limit the terrestrial carbon dioxide removal potential. *Glob. Change Biol.* **23**, 4303–4317 (2017).
27. Slade, R., Bauen, A. & Gross, R. Global bioenergy resources. *Nat. Clim. Change* **4**, 99–105 (2014).
28. Beringer, T., Lucht, W. & Schaphoff, S. Bioenergy production potential of global biomass plantations under environmental and agricultural constraints. *GCB Bioenergy* **3**, 299–312 (2011).
29. Jans, Y., Berndes, G., Heinke, J., Lucht, W. & Gerten, D. Biomass production in plantations: land constraints increase dependency on irrigation water. *GCB Bioenergy* **10**, 628–644 (2018).

30. Liu, J. et al. Systems integration for global sustainability. *Science* **347**, 1258832 (2015).
31. Liu, J. et al. Nexus approaches to global sustainable development. *Nat. Sustain.* **1**, 466–476 (2018).
32. Bleischwitz, R. et al. Resource nexus perspectives towards the United Nations Sustainable Development Goals. *Nat. Sustain.* **1**, 737–743 (2018).
33. Defourny, P. et al. *Land Cover CCI Product User Guide v.2.0* (ESA, 2017).
34. Fischer, G. et al. *Global Agro-ecological Zones (GAEZ v.3. 0) – Model Documentation* (IIASA/FAO, 2012).
35. Folberth, C. et al. The global cropland-sparing potential of high-yield farming. *Nat. Sustain.* **3**, 281–289 (2020).
36. Alcantara, C. et al. Mapping the extent of abandoned farmland in Central and Eastern Europe using MODIS time series satellite data. *Environ. Res. Lett.* **8**, 35035 (2013).
37. Ustaoglu, E. & Collier, M. J. Farmland abandonment in Europe: an overview of drivers, consequences, and assessment of the sustainability implications. *Environ. Rev.* **26**, 396–416 (2018).
38. Estel, S. et al. Mapping farmland abandonment and recultivation across Europe using MODIS NDVI time series. *Remote Sens. Environ.* **163**, 312–325 (2015).
39. Schierhorn, F. et al. Post-Soviet cropland abandonment and carbon sequestration in European Russia, Ukraine, and Belarus. *Glob. Biogeochem. Cycles* **27**, 1175–1185 (2013).
40. Pérez-Hoyos, A., Rembold, F., Kerdiles, H. & Gallego, J. Comparison of global land cover datasets for cropland monitoring. *Remote Sens.* **9**, 1118 (2017).
41. *FAOSTAT Database* (FAO, 2020); http://www.fao.org/faostat/en
42. Gennari, P., Rosero-Moncayo, J. & Tubiello, F. N. The FAO contribution to monitoring SDGs for food and agriculture. *Nat. Plants* **5**, 1196–1197 (2019).
43. Thomson, A. M. et al. RCP 4.5: a pathway for stabilization of radiative forcing by 2100. *Clim. Change* **109**, 77–94 (2011).
44. Riahi, K. et al. RCP 8.5—a scenario of comparatively high greenhouse gas emissions. *Clim. Change* **109**, 33–57 (2011).
45. FAO *The State of the World's Land and Water Resources for Food and Agriculture: Managing Systems at Risk* (Earthscan, 2011).
46. Peters, G. P. The 'best available science' to inform 1.5 °C policy choices. *Nat. Clim. Change* **6**, 646–649 (2016).
47. Anderson, K. & Peters, G. The trouble with negative emissions. *Science* **354**, 182–183 (2016).
48. Vaughan, N. E. & Gough, C. Expert assessment concludes negative emissions scenarios may not deliver. *Environ. Res. Lett.* **11**, 95003 (2016).
49. Field, J. L. et al. Robust paths to net greenhouse gas mitigation and negative emissions via advanced biofuels. *Proc. Natl Acad. Sci. USA* **117**, 21968–21977 (2020).
50. Oakleaf, J. R. et al. Mapping global development potential for renewable energy, fossil fuels, mining and agriculture sectors. *Sci. Data* **6**, 101 (2019).
51. Li, W. et al. Gross and net land cover changes in the main plant functional types derived from the annual ESA CCI land cover maps (1992–2015). *Earth Syst. Sci. Data* **10**, 219–234 (2018).
52. Liu, X. et al. Identifying patterns and hotspots of global land cover transitions using the ESA CCI Land Cover dataset. *Remote Sens. Lett.* **7058**, 972–981 (2018).
53. Liu, X. et al. Comparison of country-level cropland areas between ESA-CCI land cover maps and FAOSTAT data. *Int. J. Remote Sens.* **1161**, 1–15 (2018).
54. Hu, X., Huang, B., Verones, F., Cavalett, O. & Cherubini, F. Overview of recent land-cover changes in biodiversity hotspots. *Front. Ecol. Environ.* https://doi.org/10.1002/fee.2276 (2020).
55. Duveiller, G., Hooker, J. & Cescatti, A. The mark of vegetation change on Earth's surface energy balance. *Nat. Commun.* **9**, 679 (2018).
56. Huang, B. et al. Predominant regional biophysical cooling from recent land cover changes in Europe. *Nat. Commun.* **11**, 1066 (2020).
57. *Product Quality Assessment Report IDCR Land Cover 2016 and 2017* (UCLouvain, 2019).
58. Tsendbazar, N. E., de Bruin, S., Mora, B., Schouten, L. & Herold, M. Comparative assessment of thematic accuracy of GLC maps for specific applications using existing reference data. *Int. J. Appl. Earth Obs. Geoinf.* **44**, 124–135 (2016).
59. Liu, H. et al. Annual dynamics of global land cover and its long-term changes from 1982 to 2015. *Earth Syst. Sci. Data* **12**, 1217–1243 (2020).
60. Liang, L., Liu, Q., Liu, G., Li, H. & Huang, C. Accuracy evaluation and consistency analysis of four global land cover products in the Arctic region. *Remote Sens.* **11**, 1396 (2019).
61. Yang, Y., Xiao, P., Feng, X. & Li, H. Accuracy assessment of seven global land cover datasets over China. *ISPRS J. Photogramm. Remote Sens.* **125**, 156–173 (2017).
62. Hou, W. & Hou, X. Data fusion and accuracy analysis of multi-source land use/land cover datasets along coastal areas of the Maritime Silk Road. *ISPRS Int. J. Geoinf.* **8**, 557 (2019).
63. Madhusoodhanan, C. G., Sreeja, K. G. & Eldho, T. I. Assessment of uncertainties in global land cover products for hydro-climate modeling in India. *Water Resour. Res.* **53**, 1713–1734 (2017).
64. Karvonen, V., Ribard, C., Sädekoski, N., Tyystjärvi, V. & Muukkonen, P. in *Creating, Managing, and Analysing Geospatial Data and Databases in Geographical Themes* (eds Tyystjärvi, V. & Muukkonen, P.) 26–45 (Univ. of Helsinki, 2018).
65. Fonte, C. C., See, L., Lesiv, M. & Fritz, S. A preliminary quality analysis of the climate change initiative land cover products for continental Portugal. *ISPRS - Int. Arch. Photogramm. Remote Sens. Spat. Inf. Sci.* **42**, 1213–1220 (2019).
66. Schmunk, R. Panoply netCDF Visualization Software v.1.5.1 (NASA, 2020).
67. *Gridded Population of the World, Version 4 (GPWv4): National Identifier Grid* (Center for International Earth Science Information Network – CIESIN, Columbia University & Centro Internacional de Agricultura Tropical – CIAT, 2016); https://doi.org/10.7927/H4TD9VDP
68. Myers, N., Mittermeier, R. A., Mittermeier, C. G., Fonseca, G. A. B. & Kent, J. Biodiversity hotspots for conservation priorities. *Nature* **403**, 853–858 (2000).
69. Tracewski, Ł. et al. Toward quantification of the impact of 21st-century deforestation on the extinction risk of terrestrial vertebrates. *Conserv. Biol.* **30**, 1070–1079 (2016).
70. Hoffman, M., Koenig, K., Bunting, G., Costanza, J. & Williams, K. J. *Biodiversity Hotspots (v.2016.1)* (2016); https://doi.org/10.5281/zenodo.3261807
71. Liu, J. et al. Water scarcity assessments in the past, present, and future. *Earth's Future* **5**, 545–559 (2017).
72. Brown, A. & Matlock, M. D. *A Review of Water Scarcity Indices and Methodologies* (Sustainability Consortium, 2011).
73. Seckler, D. W., Amarasinghe, U., Molden, D., de Silva, R. & Barker, R. *World Water Demand and Supply, 1990 to 2025: Scenarios and Issues* (International Water Management Institute, 1998).
74. Rijsberman, F. R. Water scarcity: fact or fiction? *Agric. Water Manag.* **80**, 5–22 (2006).
75. *Aquamaps. Global Spatial Database on Water and Agriculture* (FAO, 2010); https://data.apps.fao.org/aquamaps/
76. Lewandowski, I., Scurlock, J. M. O., Lindvall, E. & Christou, M. The development and current status of perennial rhizomatous grasses as energy crops in the US and Europe. *Biomass Bioenergy* **25**, 335–361 (2003).
77. Lewandowski, I., Clifton-Brown, J. C., Scurlock, J. M. O. & Huisman, W. Miscanthus: European experience with a novel energy crop. *Biomass Bioenergy* **19**, 209–227 (2000).
78. Naidu, S. L., Moose, S. P., AL-Shoaibi, A. K., Raines, C. A. & Long, S. P. Cold tolerance of C4 photosynthesis in *Miscanthus* × *giganteus*: adaptation in amounts and sequence of C4 photosynthetic enzymes. *Plant Physiol.* **132**, 1688–1697 (2003).
79. Farage, P. K., Blowers, D., Long, S. P. & Baker, N. R. Low growth temperatures modify the efficiency of light use by photosystem II for CO_2 assimilation in leaves of two chilling-tolerant C4 species, *Cyperus longus* L. and *Miscanthus* × *giganteus*. *Plant. Cell Environ.* **29**, 720–728 (2006).
80. Chung, J. & Kim, D. Miscanthus as a potential bioenergy crop in East Asia. *J. Crop Sci. Biotechnol.* **2012**, 65–77 (2012).
81. Clifton-Brown, J. et al. Thermal requirements for seed germination in Miscanthus compared with switchgrass (*Panicum virgatum*), reed canary grass (*Phalaris arundinaceae*), maize (*Zea mays*) and perennial ryegrass (*Lolium perenne*). *GCB Bioenergy* **3**, 375–386 (2011).
82. Heaton, E. A., Dohleman, F. G. & Long, S. P. Seasonal nitrogen dynamics of *Miscanthus* × *giganteus* and *Panicum virgatum*. *GCB Bioenergy* **1**, 297–307 (2009).
83. Dopazo, R., Vega-Nieva, D. & Ortiz, L. *Herbaceous Energy Crops: Reviewing Their Productivity for Bioenergy Production* (2010).
84. VanLoocke, A., Twine, T. E., Zeri, M. & Bernacchi, C. J. A regional comparison of water use efficiency for miscanthus, switchgrass and maize. *Agric. For. Meteorol.* **164**, 82–95 (2012).
85. Usťak, S., Šinko, J. & Muňoz, J. Reed canary grass (*Phalaris arundinacea* L.) as a promising energy crop. *J. Cent. Eur. Agric.* **20**, 1143–1168 (2019).
86. Laurent, A., Pelzer, E., Loyce, C. & Makowski, D. Ranking yields of energy crops: a meta-analysis using direct and indirect comparisons. *Renew. Sust. Energ. Rev.* **46**, 41–50 (2015).
87. Miller, R. C. & Zedler, J. B. Responses of native and invasive wetland plants to hydroperiod and water depth. *Plant Ecol.* **167**, 57–69 (2003).
88. Mohapatra, S., Mishra, C., Behera, S. S. & Thatoi, H. Application of pretreatment, fermentation and molecular techniques for enhancing bioethanol production from grass biomass – a review. *Renew. Sust. Energ. Rev.* **78**, 1007–1032 (2017).
89. Ge, Z. M. et al. Acclimation of photosynthesis in a boreal grass (*Phalaris arundinacea* L.) under different temperature, CO_2, and soil water regimes. *Photosynthetica* **50**, 141–151 (2012).
90. Lind, S. E. et al. Carbon dioxide exchange of a perennial bioenergy crop cultivation on a mineral soil. *Biogeosciences* **12**, 16673–16708 (2016).

91. Cooney, D. et al. Switchgrass as a bioenergy crop in the Loess Plateau, China: potential lignocellulosic feedstock production and environmental conservation. *J. Integr. Agric.* **16**, 1211–1226 (2017).
92. Casler, M. D., Mitchell, R. B. & Vogel, K. P. in *Handbook of Bioenergy Crop Plants* (eds Kole, C. et al.) 563–590 (Routledge, 2012).
93. Hui, D. et al. Effects of precipitation changes on switchgrass photosynthesis, growth, and biomass: a mesocosm experiment. *PLoS ONE* **13**, e0192555 (2018).
94. Deng, Q. et al. Effects of precipitation changes on aboveground net primary production and soil respiration in a switchgrass field. *Agric. Ecosyst. Environ.* **248**, 29–37 (2017).
95. Barney, J. N. & DiTomaso, J. M. Bioclimatic predictions of habitat suitability for the biofuel switchgrass in North America under current and future climate scenarios. *Biomass Bioenergy* **34**, 124–133 (2010).
96. Deng, N. et al. Closing yield gaps for rice self-sufficiency in China. *Nat. Commun.* **10**, 1725 (2019).
97. Mauser, W. et al. Global biomass production potentials exceed expected future demand without the need for cropland expansion. *Nat. Commun.* **6**, 8946 (2015).
98. Davis, K. F., Rulli, M. C., Seveso, A. & D'Odorico, P. Increased food production and reduced water use through optimized crop distribution. *Nat. Geosci.* **10**, 919–924 (2017).
99. Staples, M. D. et al. Water consumption footprint and land requirements of large-scale alternative diesel and jet fuel production. *Environ. Sci. Technol.* **47**, 12557–12565 (2013).
100. Hayashi, A., Akimoto, K., Homma, T., Wada, K. & Tomoda, T. Change in the annual water withdrawal-to-availability ratio and its major causes: an evaluation for Asian river basins under socioeconomic development and climate change scenarios. *Energy Environ. Res.* **4**, 34 (2014).
101. Kang, S., Selosse, S. & Maïzi, N. Contribution of global GHG reduction pledges to bioenergy expansion. *Biomass Bioenergy* **111**, 142–153 (2018).
102. Staples, M. D., Malina, R. & Barrett, S. R. H. The limits of bioenergy for mitigating global life-cycle greenhouse gas emissions from fossil fuels. *Nat. Energy* **2**, 16202 (2017).
103. Staples, M. D., Malina, R., Suresh, P., Hileman, J. I. & Barrett, S. R. H. Aviation CO_2 emissions reductions from the use of alternative jet fuels. *Energy Policy* **114**, 342–354 (2018).
104. Potter, P., Ramankutty, N., Bennett, E. M. & Donner, S. D. Characterizing the spatial patterns of global fertilizer application and manure production. *Earth Interact.* **14**, 1–22 (2010).
105. Maggi, F., Tang, F. H. M., la Cecilia, D. & McBratney, A. PEST-CHEMGRIDS, global gridded maps of the top 20 crop-specific pesticide application rates from 2015 to 2025. *Sci. Data* **6**, 170 (2019).
106. *Phyllis2 Database for (treated) Biomass, Algae, Feedstocks for Biogas Production and Biochar* (ECN.TNO, 2019); https://phyllis.nl/
107. Collins, M. et al. in *Climate Change 2013: The Physical Science Basis* (eds Stocker, T. F. et al.) 1029–1136 (Cambridge Univ. Press, 2013).
108. Hausfather, Z. & Peters, G. Emissions – the 'business as usual' story is misleading. *Nature* **577**, 618–620 (2020).
109. van Vuuren, D. P. et al. The representative concentration pathways: an overview. *Clim. Change* **109**, 5–31 (2011).
110. Kharin, V. V., Zwiers, F. W., Zhang, X. & Wehner, M. Changes in temperature and precipitation extremes in the CMIP5 ensemble. *Clim. Change* **119**, 345–357 (2013).
111. IPCC *Climate Change 2014: Synthesis Report* (eds Core Writing Team, Pachauri, R. K. and Meyer, L. A.) (IPCC, 2014).
112. Pope, V. D., Gallani, M. L., Rowntree, P. R. & Stratton, R. A. The impact of new physical parametrizations in the Hadley Centre climate model: HadAM3. *Clim. Dyn.* **16**, 123–146 (2000).
113. Cox, P. M. et al. The impact of new land surface physics on the GCM simulation of climate and climate sensitivity. *Clim. Dyn.* **15**, 183–203 (1999).
114. Rulli, M. C., Bellomi, D., Cazzoli, A., De Carolis, G. & D'Odorico, P. The water–land–food nexus of first-generation biofuels. *Sci. Rep.* **6**, 22521 (2016).
115. Albrecht, T. R., Crootof, A. & Scott, C. A. The water–energy–food nexus: a systematic review of methods for nexus assessment. *Environ. Res. Lett.* **13**, 43002 (2018).
116. Hoekstra, A. Y., Chapagain, A. K., Mekonnen, M. M. & Aldaya, M. M. *The Water Footprint Assessment Manual: Setting the Global Standard* (Routledge, 2011).
117. Lesiv, M. et al. Spatial distribution of arable and abandoned land across former Soviet Union countries. *Sci. Data* **5**, 180056 (2018).
118. Tschora, H. & Cherubini, F. Co-benefits and trade-offs of agroforestry for climate change mitigation and other sustainability goals in West Africa. *Glob. Ecol. Conserv.* **22**, e00919 (2020).
119. Dowdy, A. J. et al. Future changes in extreme weather and pyroconvection risk factors for Australian wildfires. *Sci. Rep.* **9**, 10073 (2019).
120. Lesk, C., Rowhani, P. & Ramankutty, N. Influence of extreme weather disasters on global crop production. *Nature* **529**, 84–87 (2016).
121. Haddeland, I. et al. Global water resources affected by human interventions and climate change. *Proc. Natl Acad. Sci. USA* **111**, 3251–3256 (2014).
122. Pittman, S. E. et al. Mitigating the potential for invasive spread of the exotic biofuel crop, *Miscanthus* × *giganteus*. *Biol. Invasions* **17**, 3247–3261 (2015).
123. Chou, S. C. et al. Assessment of climate change over South America under RCP 4.5 and 8.5 downscaling scenarios. *Am. J. Clim. Change* **3**, 512–527 (2014).
124. Cox, P. M., Betts, R. A., Collins, M. & Harris, P. P. Amazonian forest dieback under climate–carbon cycle projections for the 21st century. *Theor. Appl. Climatol.* **156**, 137–156 (2004).
125. Cox, P. M., Betts, R. A., Jones, C. D. & Spall, S. A. Acceleration of global warming due to carbon-cycle feedbacks in a coupled climate model. *Nature* **408**, 184–187 (2000).
126. Gomes, V. H. F., Vieira, I. C. G., Salomão, R. P. & Steege, H. Amazonian tree species threatened by deforestation and climate change. *Nat. Clim. Change* **9**, 547–553 (2019).
127. Lyra, A. D. A., Chou, S. C. & Sampaio, G. D. O. Sensitivity of the Amazon biome to high resolution climate change projections. *Acta Amazon.* **46**, 175–188 (2016).
128. Rammig, A. et al. Estimating the risk of Amazonian forest dieback. *New Phytol.* **187**, 694–706 (2010).
129. Lenton, T. M. et al. Tipping elements in the Earth's climate system. *Proc. Natl Acad. Sci. USA* **105**, 1786–1793 (2008).
130. Lenton, T. M. et al. Climate tipping points—too risky to bet against. *Nature* **575**, 592–595 (2019).
131. Sorribas, M. V. et al. Projections of climate change effects on discharge and inundation in the Amazon basin. *Climatic Change* **136**, 555–570 (2016).
132. Feng, S. et al. Projected climate regime shift under future global warming from multi-model, multi-scenario CMIP5 simulations. *Glob. Planet. Change* **112**, 41–52 (2014).
133. Levis, S., Badger, A., Drewniak, B., Nevison, C. & Ren, X. CLMcrop yields and water requirements: avoided impacts by choosing RCP 4.5 over 8.5. *Clim. Change* **146**, 501–515 (2018).
134. Cairns, R. & Krzywoszynska, A. Anatomy of a buzzword: the emergence of 'the water–energy–food nexus' in UK natural resource debates. *Environ. Sci. Policy* **64**, 164–170 (2016).

Acknowledgements

The support of the Norwegian Research Council is acknowledged through the projects Bio4Fuels (project no. 257622), BioPath (project no. 293434) and MitiStress (project no. 286773). We thank B. Huang, X. Hu, H. Muri, D. Moran and C. Iordan for discussions regarding spatial data analysis. Additionally, we thank P. Chu for language editing. We gratefully acknowledge the provision of land cover data by ESA CCI-LC, GAEZ and SSP data by IIASA, lower heating values by Phyllis2, physical water scarcity data and cropland inventories by FAO, GPWv4 data and Panoply 4 by NASA and biodiversity hotspots data[70].

Author contributions

All authors designed the study, collected the data and analysed the results. J.S.N. developed custom code and generated all results and figures. J.S.N. wrote the manuscript with contributions from O.C. and F.C.

Competing interests

The authors declare no competing interests.

Additional information

Extended data is available for this paper at https://doi.org/10.1038/s41893-020-00680-5.

Supplementary information The online version contains supplementary material available at https://doi.org/10.1038/s41893-020-00680-5.

Correspondence and requests for materials should be addressed to J.S.N.

Peer review information *Nature Sustainability* thanks John Campbell, Katherine Zipp and the other, anonymous, reviewer(s) for their contribution to the peer review of this work.

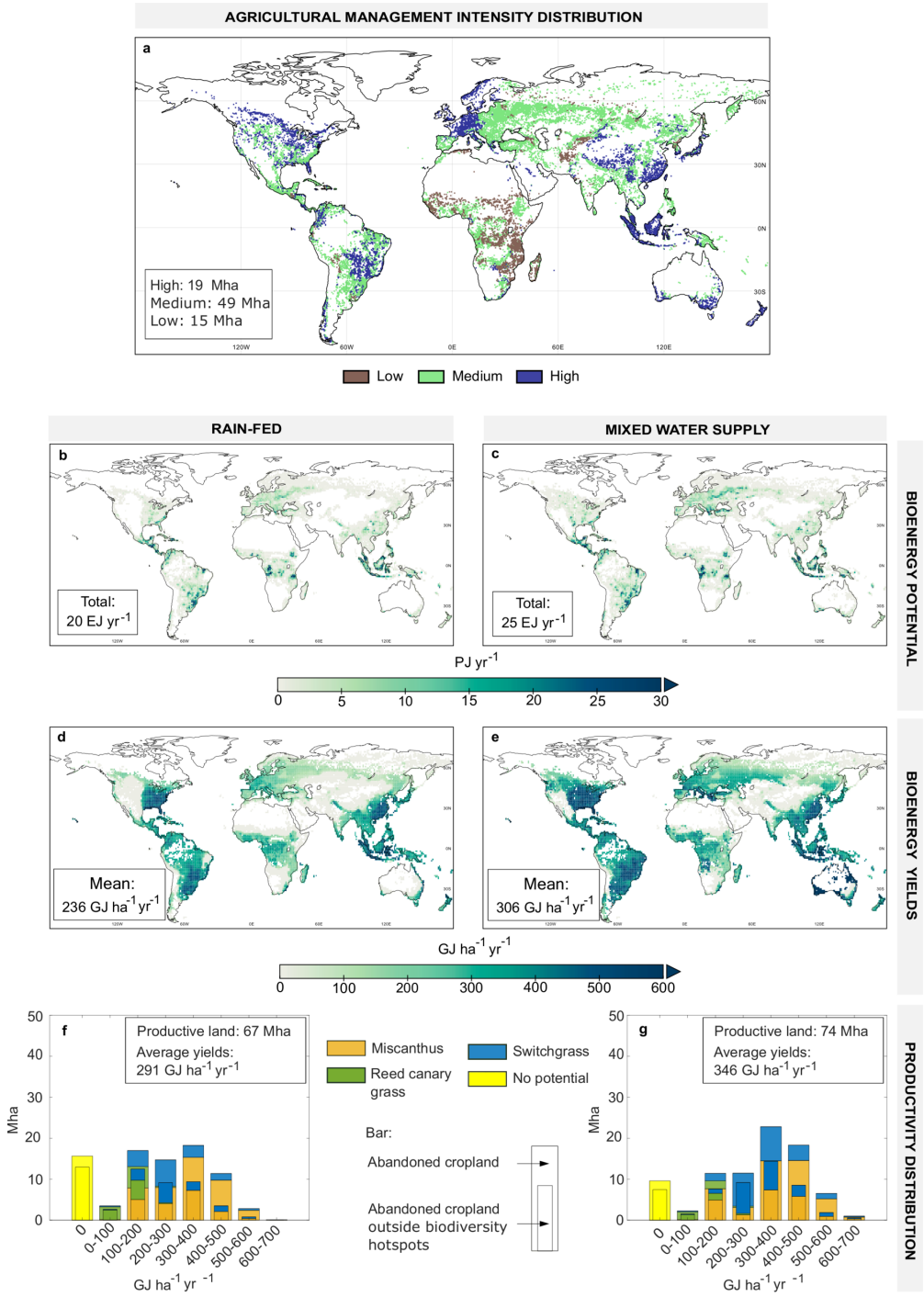

Extended Data Fig. 1 | See next page for caption.

Extended Data Fig. 1 | Bioenergy potentials on abandoned cropland with a mixed management distribution based on existing yield gaps. Results refer to present day climate with optimal crop allocation. Figures describe the agricultural management intensity distribution (**a**), global bioenergy potentials (**b**-**c**), bioenergy yields (**d**-**e**), and productivity distributions (**f**-**g**) for abandoned cropland (wide bars) and abandoned cropland outside biodiversity hotspots (thin bars). Figures (**b**, **d**, **f**), and (**c**, **e**, **g**) refer to rain-fed and mixed water supply, respectively. Average yields in (**f**) and (**g**) refer to only productive areas. Maps are shown at **5** arc minutes and 1 degree for (**a**) and (**b**-**e**), respectively (for improved visualization).

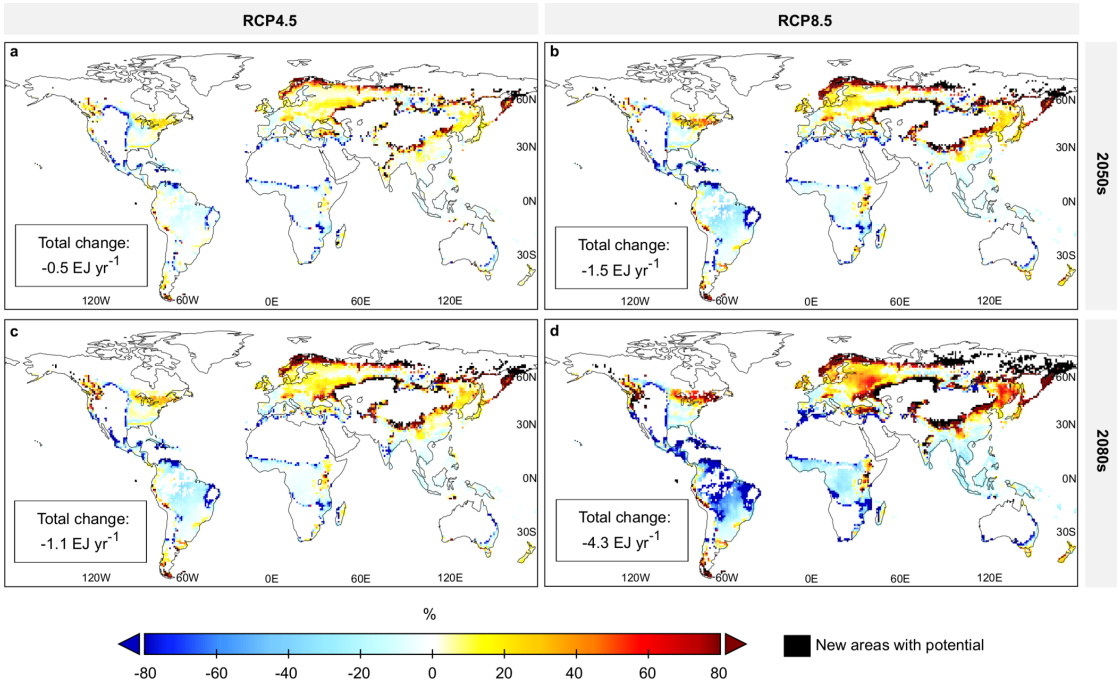

Extended Data Fig. 2 | Spatial explicit changes in bioenergy potentials under future climatic conditions relative to present day. Maps describe changes (%) in 2050 for RCP4.5 (**a**) and RCP8.5 (**b**), and in 2080 for RCP4.5 (**c**) and RCP8.5 (**d**). Results refer to optimal crop allocation, high management intensity, and rain-fed water supply. Crop allocation is re-optimized under each future climate projection. Maps are shown at one-degree resolution (aggregated for visualization purposes).

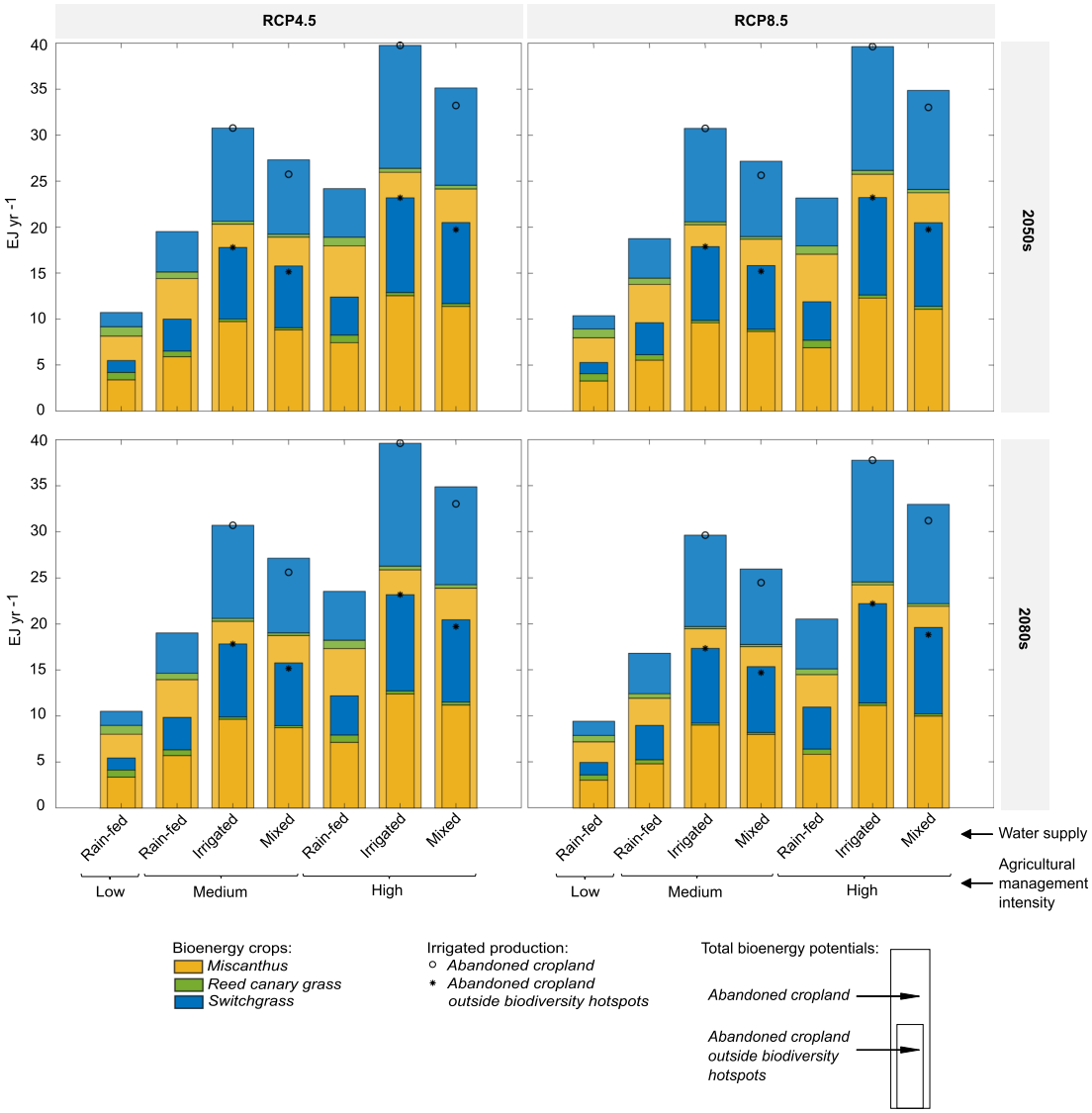

Extended Data Fig. 3 | Global bioenergy potentials under climate change. Bioenergy potentials (EJ year^{-1}) on abandoned cropland are shown for 2050 and 2080 under RCP4.5 and RCP8.5 for a set of different constraints. Land availability is constrained by consideration of abandoned cropland with or without (thinner bars) biodiversity hotspots. Three agricultural management intensity levels (low, medium and high) and three water supply levels (rain-fed, irrigated and mixed) are considered. Specific contributions from irrigated areas and individual crops to total potentials are shown.

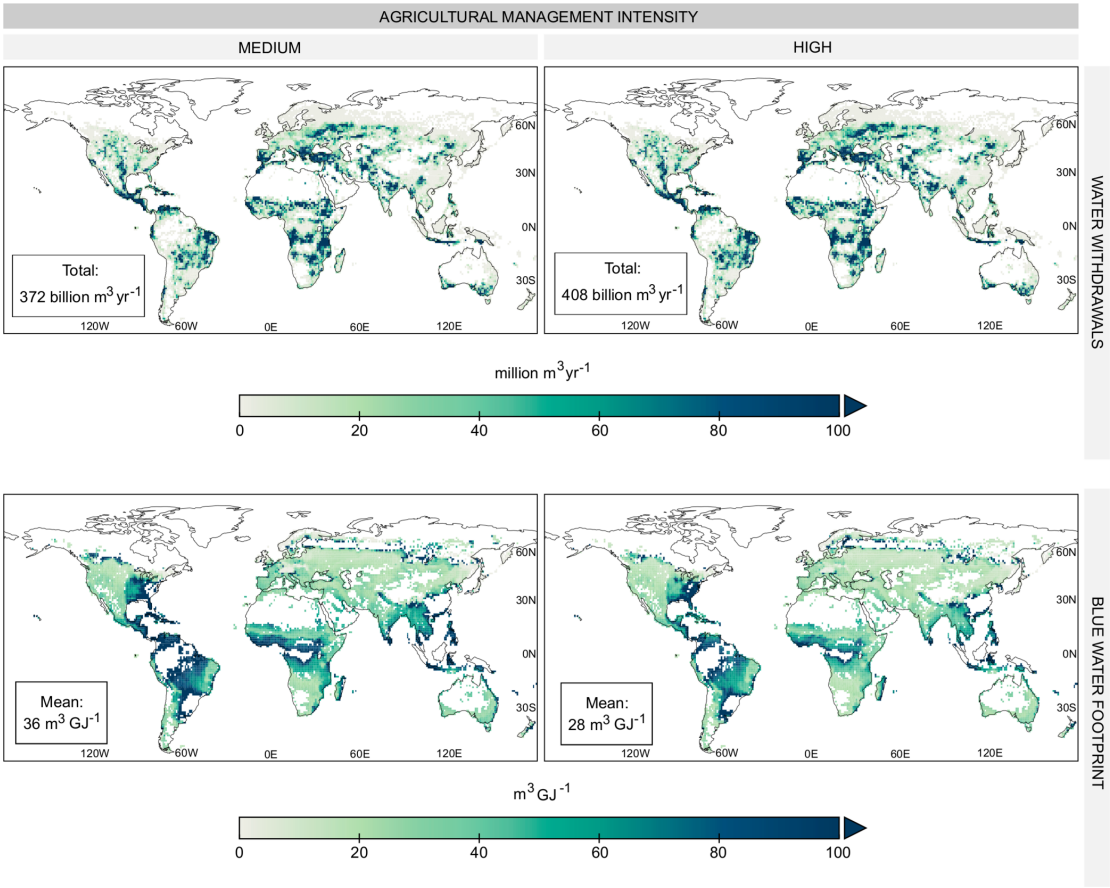

Extended Data Fig. 4 | Spatially explicit water withdrawals and blue water footprint of irrigated bioenergy potentials on abandoned cropland. Maps describe present day characteristics for two agricultural management intensities (medium, high), with optimal energy-based crop allocation per grid cell. Water withdrawals are given as million m^3 $year^{-1}$, and blue water footprint as m^3 GJ^{-1}. Maps are shown at one-degree resolution (aggregated for visualization purposes).

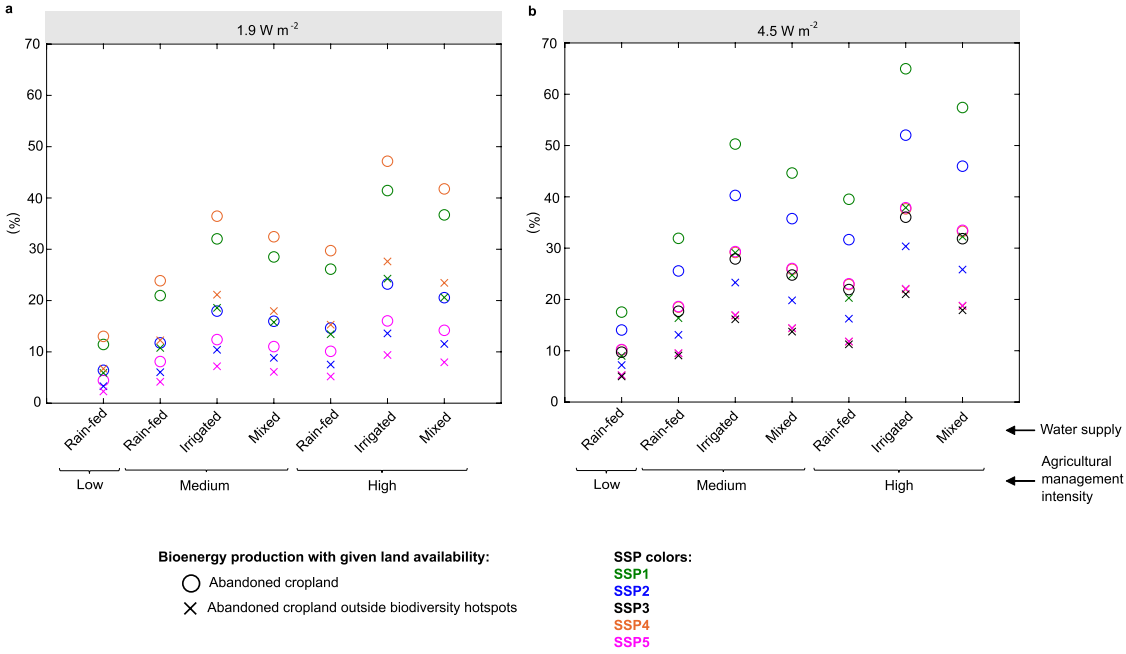

Extended Data Fig. 5 | Comparison of bioenergy potentials with future projections. Bioenergy potentials on abandoned cropland (optimal crop allocation), relative to median projected primary bioenergy demand in 2050 across different SSPs in top-down Integrated Assessment Models (%). Land availability for bioenergy production is constrained by consideration of abandoned cropland with or without biodiversity hotspots. Three agricultural management intensity levels (low, medium and high) and three water supply levels (rain-fed, irrigated and mixed) are considered. Individual figures refer to (**a**) bioenergy potentials at present day relative to median projected demand in 1.9 W m^{-2} scenarios, and (**b**) bioenergy potentials in 2050 for RCP4.5 relative to median projected demand in 4.5 W m^{-2} scenarios. SSP3 is not shown in **a**, as no models could reach the 1.5 °C climate target.

nature research

Corresponding author(s): DBPR NATSUSTAIN-20056162

Last updated by author(s): Dec 8, 2020

Reporting Summary

Nature Research wishes to improve the reproducibility of the work that we publish. This form provides structure for consistency and transparency in reporting. For further information on Nature Research policies, see our Editorial Policies and the Editorial Policy Checklist.

Statistics

For all statistical analyses, confirm that the following items are present in the figure legend, table legend, main text, or Methods section.

n/a	Confirmed
☒	☐ The exact sample size (*n*) for each experimental group/condition, given as a discrete number and unit of measurement
☒	☐ A statement on whether measurements were taken from distinct samples or whether the same sample was measured repeatedly
☒	☐ The statistical test(s) used AND whether they are one- or two-sided *Only common tests should be described solely by name; describe more complex techniques in the Methods section.*
☒	☐ A description of all covariates tested
☒	☐ A description of any assumptions or corrections, such as tests of normality and adjustment for multiple comparisons
☒	☐ A full description of the statistical parameters including central tendency (e.g. means) or other basic estimates (e.g. regression coefficient) AND variation (e.g. standard deviation) or associated estimates of uncertainty (e.g. confidence intervals)
☒	☐ For null hypothesis testing, the test statistic (e.g. *F*, *t*, *r*) with confidence intervals, effect sizes, degrees of freedom and *P* value noted *Give P values as exact values whenever suitable.*
☒	☐ For Bayesian analysis, information on the choice of priors and Markov chain Monte Carlo settings
☒	☐ For hierarchical and complex designs, identification of the appropriate level for tests and full reporting of outcomes
☒	☐ Estimates of effect sizes (e.g. Cohen's *d*, Pearson's *r*), indicating how they were calculated

Our web collection on statistics for biologists contains articles on many of the points above.

Software and code

Policy information about availability of computer code

Data collection	No software was used to collect data.
Data analysis	Custom Matlab code was developed to analyze the data applied in this study.

For manuscripts utilizing custom algorithms or software that are central to the research but not yet described in published literature, software must be made available to editors and reviewers. We strongly encourage code deposition in a community repository (e.g. GitHub). See the Nature Research guidelines for submitting code & software for further information.

Data

Policy information about availability of data

All manuscripts must include a data availability statement. This statement should provide the following information, where applicable:

- Accession codes, unique identifiers, or web links for publicly available datasets
- A list of figures that have associated raw data
- A description of any restrictions on data availability

Datasets used in this analysis are publicly available from the references provided within the paper. Source data is provided with this article. Other data supporting the findings of this study are available from the corresponding author upon reasonable request.

Field-specific reporting

Please select the one below that is the best fit for your research. If you are not sure, read the appropriate sections before making your selection.

☐ Life sciences ☐ Behavioural & social sciences ☒ Ecological, evolutionary & environmental sciences

For a reference copy of the document with all sections, see nature.com/documents/nr-reporting-summary-flat.pdf

Ecological, evolutionary & environmental sciences study design

All studies must disclose on these points even when the disclosure is negative.

Study description	This study quantifies spatially explicit global bioenergy potentials on recently abandoned cropland under the land-energy-water nexus. We integrated high resolution satellite-derived land cover data (European Space Agency's Climate Change Initiative Land Cover product) with a parameterized crop yield model (Global Agro-Ecological Zones 3.0 (GAEZ)) to estimate abandoned cropland between 1992 and 2015 and its corresponding bioenergy potentials. We assess and extensively discuss 296 different variants of primary bioenergy potentials, land requirements and water use dependent on multiple local and management factors. We consider the use of three bioenergy crops (miscanthus, switchgrass, reed canary grass, and an energy based optimal crop allocation), four agricultural management intensities (high, medium, low, and a mixed based on present day yield gaps), three water supply systems (rain-fed, irrigated and a mixed approach avoiding irrigation in physical water-scarce areas), and two sets of land availability (abandoned cropland, and abandoned cropland located outside biodiversity hotspots). Bioenergy potentials are computed at present day, and at future climatic conditions in 2050 and 2080 for RCP4.5 and RCP8.5. A nexus approach is taken to assess interactions between energy, land and water systems. We quantify four spatially explicit indicators related to irrigation efficiency across variants and water scarcity levels, thereby revealing sustainability trade-offs of different levels of irrigated bioenergy deployment. Regions which can benefit the most from irrigation are identified. Findings are compared with previous cropland abandonment studies, and with long-term projections of bioenergy supply from top-down models.
Research sample	We use the European Space Agency's Climate Change Initiative Land Cover product to quantify abandoned cropland (https://www.esa-landcover-cci.org/?q=webfm_send/84). The Global Agro-Ecological Zones 3.0 model is used to estimate dry mass bioenergy crop yields (http://www.gaez.iiasa.ac.at/docs/GAEZ_Model_Documentation.pdf). Lower heating values are obtained from the Phylis2 database (https://phyllis.nl/). Bioenergy hotspots data are obtainable from (https://zenodo.org/record/3261807#.XsUCXDozZPZ). Data on physical water scarcity is available from FAO (http://www.fao.org/nr/water/aquamaps/). National identifier grid is used to quantify country level cropland extent and abandonment (https://doi.org/10.7927/H4TD9VDP). Yield gaps of main crops are taken from http://www.gaez.iiasa.ac.at. FAO cropland inventories are available at http://www.fao.org/faostat/en/#data.
Sampling strategy	For information about data sampling, see previous relevant publications for specific datasets.
Data collection	We collected and integrated data from a variety of sources, which are needed to reproduce results presented in this work. Temporal land cover data from European Space Agency's Climate Change Initiative Land Cover product (https://www.esa-landcover-cci.org/?q=webfm_send/84). The Global Agro-Ecological Zones 3.0 model is used to quantify dry mass yields and water deficits (http://www.gaez.iiasa.ac.at/docs/GAEZ_Model_Documentation.pdf). Lower heating values are obtained from the Phylis2 database (https://phyllis.nl/). Bioenergy hotspots data are obtainable from Hoffman et al. (2016) (https://zenodo.org/record/3261807#.XsUCXDozZPZ). Data on physical water scarcity is available from FAO (http://www.fao.org/nr/water/aquamaps/). Data on projected bioenergy supply in future 1.5 degree scenarios was taken from the SSP data base (https://tntcat.iiasa.ac.at/SspDb/), and land requirements from the IPCC special report on climate change and land (https://www.ipcc.ch/srccl/). National identifier grid were obtained from (https://doi.org/10.7927/H4TD9VDP). Yield gaps of main crops are taken from (http://www.gaez.iiasa.ac.at). FAO cropland inventories were obtained at (http://www.fao.org/faostat/en/#data).
Timing and spatial scale	The global land cover product covers the period between 1992-2015 and has a resolution of 10 arc seconds (300m). Present day physical water scarcity data and yield gap data were obtained for present day at a resolution of 5 arc minutes. Biodiversity hotpots data at present day were obtained as shapefiles and used as land masks at 10 arc seconds. The yield model provided results at 5 arc minutes. Country masks were applied at 30 arc seconds.
Data exclusions	No data were excluded.
Reproducibility	The study is fully reproducible by acquiring necessary datasets and applying the same methodology, or by re-running developed custom code.
Randomization	Randomization is not relevant for this study.
Blinding	Blinding is not relevant for this study.

Did the study involve field work? ☐ Yes ☒ No

Reporting for specific materials, systems and methods

We require information from authors about some types of materials, experimental systems and methods used in many studies. Here, indicate whether each material, system or method listed is relevant to your study. If you are not sure if a list item applies to your research, read the appropriate section before selecting a response.

Materials & experimental systems

n/a	Involved in the study
☒	☐ Antibodies
☒	☐ Eukaryotic cell lines
☒	☐ Palaeontology and archaeology
☒	☐ Animals and other organisms
☒	☐ Human research participants
☒	☐ Clinical data
☒	☐ Dual use research of concern

Methods

n/a	Involved in the study
☒	☐ ChIP-seq
☒	☐ Flow cytometry
☒	☐ MRI-based neuroimaging

Chapter 3: Optimal combination of bioenergy and solar photovoltaic for renewable energy production on abandoned cropland

Material from: Leirpoll, M. E., Næss, J. S., Cavalett, O., Dorber, M., Hu, X., & Cherubini, F. (2021). Optimal combination of bioenergy and solar photovoltaic for renewable energy production on abandoned cropland. *Renewable Energy*, *168*, 45–56. https://doi.org/https://doi.org/10.1016/j.renene.2020.11.159

Renewable Energy 168 (2021) 45–56

Contents lists available at ScienceDirect

Renewable Energy

journal homepage: www.elsevier.com/locate/renene

Optimal combination of bioenergy and solar photovoltaic for renewable energy production on abandoned cropland

Malene Eldegard Leirpoll *, Jan Sandstad Næss , Otavio Cavalett , Martin Dorber , Xiangping Hu , Francesco Cherubini

Department of Energy and Process Engineering, Industrial Ecology Programme, Norwegian University of Science and Technology (NTNU), Høgskoleringen 1, 7491, Trondheim, Norway

ARTICLE INFO

Article history:
Received 6 September 2020
Received in revised form
9 November 2020
Accepted 30 November 2020
Available online 4 December 2020

Keywords:
Bioenergy
Solar energy
Land use
Renewable energy
Abandoned cropland

ABSTRACT

Ambitious climate change mitigation scenarios require large-scale deployment of bioenergy and solar photovoltaics. Utilizing recently abandoned cropland for renewable energy production is a promising option for energy supply while reducing competition for land and food security. However, the magnitude of abandoned cropland and its potential for renewable energy production is still unclear. Here, we mapped recently abandoned croplands at a global level and assessed the site-specific primary energy potentials for bioenergy and solar photovoltaics considering local climatic conditions, energy yields, and socio-economic feasibility constraints to identify optimal land use for renewable energy production. Of the 83 Mha of the identified abandoned cropland between 1992 and 2015, 68% of the area presented higher development potentials for the establishment of solar photovoltaic compared to dedicated bioenergy crops. In total, 125 EJ/year of primary energy can be produced with this optimal land management, of which 114 EJ/year is from solar photovoltaic and 11 EJ/year is from bioenergy. This figure corresponds to 33–50% of the projected median renewable energy demand in 2050 across the 1.5 °C stabilization scenarios. Mapping the suitability of renewable energy sources across different local, environmental, and socio-economic constraints will help identify the best implementation options for future energy systems transformation.

1. Introduction

The continuing rise in greenhouse gases (GHG) emissions presents a significant challenge for limiting warming to well below 2 °C relative to the pre-industrial era [1]. According to the International Energy Agency (IEA), the energy production by renewable energy sources experienced a record-high increase in 2019, both in terms of the fastest rate of growth and the largest absolute growth [2]. Despite these positive developments in the renewable energy sector, the transformation of global energy systems is still far from the levels required to meet the objectives of the Paris Agreement and deployment of renewable energy solutions must accelerate substantially [3].

The different Shared Socio-economic Pathways (SSP) expect higher future demands for second-generation bioenergy crops and increased energy production from renewable energy sources, especially solar photovoltaic (PV) [4,5]. Of those projections that can reach the 1.5 °C target by 2100, the annual primary energy needed from biomass and PV is in the range of 87–453 EJ and 54–396 EJ, respectively [5,6]. For providing such large amounts of primary energy from bioenergy and PV, different extents of land resources are required, which may conflict with other land uses, such as biodiversity conservation, and food security [7,8]. In order to distinguish the most appropriate solutions across different locations and socio-economic contexts, robust land and energy management planning is vital [9,10]. Mapping land that would be suitable for establishing renewable energy infrastructure under a range of environmental and socio-economic criteria is an essential tool for a sustainable energy transition [11,12]. Utilizing areas of recently abandoned cropland for the establishment of renewable energy infrastructure is a promising option for energy supply while reducing potential competition for land and its potential impacts on biodiversity and food security [13–15]. Conversion of abandoned cropland to active forms of energy supply is usually considered a near-term no-regrets opportunity to gradually achieve

* Corresponding author. Tromsøgata 17, 0565, OSLO, Norway.
E-mail address: malene@villenergi.no (M.E. Leirpoll).

https://doi.org/10.1016/j.renene.2020.11.159

large-scale renewable energy supply while, at the same time, stimulating socio-economic development in rural areas [16,17].

Re-cultivating abandoned cropland by bioenergy crops like perennial grasses may reduce atmospheric carbon concentrations from enhanced soil carbon sequestration and fossil fuel substitution [18,19]. In addition to climate mitigation, the conversion of former croplands to perennial grasses can also provide a range of ecological and environmental benefits such as enhanced biodiversity and ecosystem services [16,20], reduced losses of nutrients and soils [21], and local cooling effect due to increased evapotranspiration rates during the growing season [22,23]. At the same time, ground-mounted PV is well suited for deployment on abandoned cropland [24,25]. Utility-scale PV is predicted to play a key role in the sustainable transformation of the global energy systems, and the main reason is the rapid decline in the cost and the technological advancement [26]. However, it is reported that approximately one-third of the total PV farm surface can be covered with solar panels [27–29], as the rest of the area is required for its infrastructure. Covering the land with solar panels may lead to a decline in bio-productivity [30].

Based on the urgent need to transition towards less carbon-intense energy systems [31], spatially-explicit mapping energy potentials of bioenergy and PV is key to understand the future land and energy developments and ultimately stimulate renewable energy production on these areas. In this paper, we address the spatially explicit production of bioenergy and solar photovoltaic for recently abandoned cropland at a global level considering a set of local climate variables, resource yield, and socio-economic feasibility constraints. Global recently abandoned croplands are identified through time series of remotely-sensed land cover maps provided by the European Space Agency (ESA) Climate Change Initiative Land Cover (CCI-LC) [32]. Global primary energy potentials for bioenergy are derived from grid-specific yields of perennial grasses under modern agricultural management practices and site-specific agro-climatic, soil, and terrain conditions using the Global Agro-Ecological Zones (GAEZ) model [33]. For PV, the Centro Euro-Mediterraneo sui Cambiamenti Climatici Climate Model (CMCC-CM) products [34] provide site-specific meteorological data that are used to estimate the primary energy potential [35]. By integrating the gridded primary energy potentials for these renewable energy production options with a spatially explicit Development Potential Index (DPI) [36], we accounted for a range of socio-economic feasibility constraints to provide a more realistic quantification of renewable energy alternatives and identify the optimal use (bioenergy crop or solar PV) per grid cell. The global primary energy potential from an optimal land management at a global level is determined by combining all contributions from bioenergy and PV on the abandoned cropland areas as determined by the DPI. Numerous studies have assessed the resource and land suitability for bioenergy [13,15,30,37–40] or PV [12,14,30,41–43]. These studies focused on specific regions, characteristics and constraints of the different renewable energy production options and identified their contributions to the energy transition. However, to the best of our knowledge, this is the first study that systematically compares with high-resolution data the primary energy potentials from bioenergy crops and PV on abandoned cropland at a global level, and that considers a comprehensive set of local factors and socio-economic constraints to identify the optimal land management for renewable energy production.

2. Methods

2.1. Identification of recently abandoned cropland

The European Space Agency (ESA) Climate Change Initiative Land Cover (CCI-LC) provides global annual data of land cover classes from 1992 to 2015 at a spatial resolution of 10 arc seconds (300 m at the equator) [32]. By combining multiple remote sensing products with ground-truth observations, the ESA CCI-LC maps describe terrestrial surface characteristics through 37 different land cover classes. Six of these classes are cropland or mosaic cropland. We identified abandoned cropland by tracking grid cells transitioning from cropland in 1992 to any non-cropland (and non-urban) class in 2015. In other words, abandoned cropland includes all grid cells that were registered as cropland in 1992 and not in 2015. The cropland grid cells that transitioned to urban land are excluded and not considered as available for renewable energy production, as this is a non-reversible transition.

2.2. Primary bioenergy potential

The bioenergy crops considered here are three promising perennial grasses: switchgrass (*Panicum virgatum*), miscanthus (*Miscanthus x giganteus*), and reed canary grass (*Phalaris arundinacea*). They were selected because they have proven to thrive well on marginal lands due to their suitability to a variety of soil and climate conditions as well as their relatively high yields, low cost and various environmental co-benefits [44–46]. Switchgrass has a C_4 photosynthetic pathway for carbon fixation and can survive in a variety of environmental conditions [47–49]. Switchgrass is native to North America [45,50], but has been introduced in China [46,51,52], Europe [44,48], and many other regions. It is highly adaptive to soil with less fertile, erosive, or acidic conditions, as it has a well-developed root system [46]. However, the species does not cope well under drought conditions [53,54]. The harvesting of switchgrass typically happens throughout autumn [47]. Miscanthus also has a C_4 photosynthetic pathway [47,48]. Miscanthus originated in South-East Asia, but has been introduced in many other regions because of its suitability for establishment in a wide climatic range [49]. Today, miscanthus is present in Europe [48,55], the UK [56], China [52], Turkey [45], among many other regions. Usually, harvesting of miscanthus occurs in late winter or early spring [57,58]. Reed canary grass has a C_3 photosynthetic pathway. It is especially suitable in temperate climates with cool and humid conditions [57,59]. Reed canary grass is currently mainly established in Europe where the species originated [48]. Even in extreme climatic conditions such as floods and droughts, reed canary grass can survive due to its well-adaptive water regime [60]. Similar to miscanthus, the harvest of reed canary grass occurs in late winter or early spring [57,58].

We applied the parameterized crop yield model Global Agro-Ecological Zones 3.0 (GAEZ) to model local yields of bioenergy crops at five arc minutes resolution [61]. GAEZ was developed by the Food and Agriculture Organization (FAO) of the United Nations in collaboration with the International Institute for Applied Systems Analysis (IIASA). GAEZ models dry mass yields based on a variety of crop-specific parameters related to crop characteristics, local soil quality and terrain, agricultural management practices, and site-specific climatic conditions (e.g., radiation, precipitation, and temperature) [33]. It considers the response in crop productivity to yearly variability in soil moisture, pests, frosts and constraints to soil workability. Furthermore, it models the effects of fertilizer use, pesticides, and agricultural conservation measures. Additionally, GAEZ quantify crop water balances, water deficits, and evapotranspiration using the optimal crop growth calendar at rainfed conditions. Based on this, it also models irrigated crop yields by assuming no water deficits throughout the crop growth cycle (i.e. water losses by evapotranspiration do not exceed water absorption at any point). We quantify bioenergy yields for a modern, mechanized and market oriented agricultural management system, with

high yielding varieties, and optimal fertilizer and pesticide use. Maximum attainable dry mass yields for switchgrass, miscanthus, and reed canary grass were computed for both rain-fed and irrigated conditions.

We considered a mixed water supply system with rain-fed water supply in areas threatened by physical water scarcity and irrigation elsewhere. The Aquamaps database [62] provides datasets on physical water scarcity (i.e., when the water demands of the available renewable water resources is not met [63]) at a river basin level. While multiple methods exist to assess water scarcity, the physical water scarcity indicator is especially suitable to address local potentials of new water infrastructure development and measures to increase water use efficiency [64,65]. Additional water withdrawals in areas threatened by water scarcity have higher risks of causing sustainability trade-offs on water depletion. Areas with annual agricultural water use as <10%, 10–20% and >20% of renewable water resources are classified as low, moderate and high physical water scarce, respectively [66]. As an upper irrigation potential, we constrained irrigation deployment to low water scarce areas only.

Applying lower heating values of 17.82 MJ kg^{-1} for switchgrass, 18.55 MJ kg^{-1} for miscanthus, and 18.06 MJ kg^{-1} for reed canary grass [67], we convert dry mass yields to bioenergy yields. By performing an energy-based optimization of the global crop distribution with mixed water supply, each grid is assigned the bioenergy crop with the largest potential. This approach allows to maximize bioenergy yields locally with reduced risks of additional water depletion in water scarce areas.

2.3. Solar photovoltaic primary energy potential

Local PV potentials depend on climatic conditions and nominal installed PV capacity [68]. The incoming solar radiation is the most significant factor for determining the site-specific PV potential [12,69]. Other studies have included additional meteorological conditions such as humidity [70–73], diffuse radiation [74,75], or cloud-cover [76]. The effects of ambient temperature and wind speed are also important for a proper quantification of PV potentials [77,78]. Some previous studies have estimated PV potentials on abandoned cropland at the local and national scale [14,30], but the global PV potential on abandoned cropland is still unclear.

We used the climate data from the Centro Euro-Mediterraneo sui Cambiamenti Climatici Climate Model (CMCC-CM) atmosphere-ocean general circulation model to assess local PV potentials on abandoned cropland [34]. In CMCC-CM, the global circulation is represented by coupling the atmospheric model ECHAM5 [79] and the ocean model OPA8.2 [80], with a resolution of 0.75° and 2°, respectively. Interface between the atmospheric and ocean components is performed by the Ocean Atmosphere Sea Ice Soil version 3 (OASIS3) [81], with a coupling period of 160 min for all parameters. Previous applications of CMCC-CM include assessments of precipitation and cyclones [82], extreme weather [83], vegetation response to climate change [84], and variability of wave power [85]. Spatially explicit climate data on surface downwelling shortwave radiation (RSDS), near-surface air temperature (TAS), and near-surface wind speed (sfcWind) is obtained from the "Atmos" collection of CMCC-CM. Climate model output for the stabilization scenario for Representative Concentration Pathway of 4.5 Wm^{-2} radiative forcing (RCP4.5), with monthly ensemble means from 2010 to 2040 which were aggregated to yearly means served as an estimate for the current climatic conditions. While nominal installed PV capacity is typically provided at standardized conditions (i.e. at a PV cell temperature (T_{cell}) of 25 °C, and RSDS of 1000 Wm^{-2}), the efficiency of PV cells changes with T_{cell} based on local climatic conditions. We apply a parameterized approach to quantify the primary energy potential of a PV deployment on abandoned cropland [35]. The method is widely used and validated through a range of applications [68,86–89].

$$T_{cell}(i,j) = c_1 + c_2 \cdot TAS(i,j) + c_3 + c_4 \cdot sfcWind(i,j) \quad (1)$$

$$PR(i,j) = 1 + \gamma[T_{cell}(i,j) - T_{std}] \quad (2)$$

$$PV_{pot}(i,j) = PR(i,j) \cdot \frac{RSDS(i,j)}{RSDS_{stc}} \quad (3)$$

$$PV_{pri}(i,j) = PV_{pot}(i,j) \cdot P_N \cdot c_{area} \cdot 8760 \quad (4)$$

The site-specific PV potential (PV_{pot}) calculated through Equations (1)–(3) accounts for the ambient effects on T_{cell} of *RSDS*, *TAS*, *sfcWind*, and a set of additional coefficients (Table 1). Further, to obtain the annual primary energy that PV will produce (PV_{pri}) the dimensionless magnitude of PV_{pot} is multiplied with nominal installed power (P_N), the share of solar cells cover of the total land available (c_{area}), and the number of hours in a year (8760) (Equation (4)).

2.4. Development Potential Index for the renewable energy options

Optimal distribution of bioenergy or solar PV on the identified abandoned cropland areas is not only dependent on the primary energy potential, but also on many other factors including biophysical aspects, local land-use or administrative contexts and socio-economic feasibility constraints associated with the intended renewable energy option [9,10,94]. For example, evaluation of local soil characteristics, topography of the landscape and the prevailing climate, as well as grid-specific accessibility to infrastructure, markets, and other socio-economic conditions, are key factors that affect priorities among different renewable energy options [11].

In order to take these aspects into account, Oakleaf et al. [36] introduced the Development Potential Index (DPI), which incorporates site-specific development constraints and criteria when determining the land suitability for development of the given renewable energy option. Spatially explicit DPIs are available for 13 renewable energy sources, including bioenergy and PV. By applying a multi-criteria decision analysis technique integrated with geographic information systems [93], site-specific suitability is mapped globally with a 1 km resolution. DPIs include various development constraints associated with the specific resource, land-use and biophysical criteria, technical yields, feasibility criteria (e.g., major roads, electrical grid, and demand centers), and feasibility measures (e.g., logistics), which differ by location and type of renewable energy option considered. All these factors are integrated in terms of relative importance through an analytic hierarchy process [95] combined with a weighted linear combination method [93], so that the computed normalized spatial DPI values range between 0 and 1. For PV, energy yields and distance to electrical grids contribute the most to DPI values (weighted 0.447 and 0.228, respectively). Landcover characteristics (0.115), distance to urban areas (0.069), and distance to railways and ports (0.026) are also included in the parameterization. Bioenergy DPIs are quantified based on bioenergy crop yields (0.493), market accessibility (0.311) and land supply elasticity (0.196) [36].

We overlapped the DPIs for bioenergy and PV based on Oakleaf et al. [36] with our identified maps of abandoned cropland to quantify their development potentials. We used ESRI ArcGIS Desktop 10.8 [96] to remap DPI data from the Mollweide coordinates system to the WGS 1984 coordinate system. It was possible to directly assign DPI values for bioenergy and PV to

Table 1
Parameters for estimating spatially explicit PV primary energy potential.

Notation	Value	Unit	Description	Reference
c_1	4.3	$°C$	Response coefficient accounting for climate effects	[68,90]
c_2	0.943	-	Response coefficient accounting for climate effects	[68,90]
c_3	0.028	$°Cm^2W^{-1}$	Response coefficient accounting for climate effects	[68,90]
c_4	−1.528	$°Csm^{-1}$	Response coefficient accounting for climate effects	[68,90]
γ	−0.005	$°C^{-1}$	Maximum power thermal coefficient	[35,68,91]
T_{std}	25	$°C$	Standard test conditions of PV cell temperature	[68,90]
$RSDS_{stc}$	1000	Wm^{-2}	Standard test conditions of *RSDS*	[68,90]
P_N	110	W_pm^{-2}	Nominal power (or Watt peak)	[27,28,92,93]
c_{area}	0.33	-	PV coverage of total land available	[27–29]

47 Mha and 56 Mha of abandoned cropland, respectively, and there were 40 Mha of abandoned cropland for which it was possible to assign DPI values for both renewable energy sources. For some areas of abandoned cropland, it was thus not possible to assign a given DPI value owing to missing entries in the original DPI dataset, e.g., for latitudes 60–90 °N. We applied a data filling method to quantify DPI values of these abandoned cropland areas by taking the moving mean of surrounding grid cells for a range of different window sizes (from 3 × 3 to 31 × 31 cell windows). With a window size of 3 × 3 cells that only considers the nearest neighbor cells, the extent of abandoned cropland with DPI values for bioenergy and PV increases from 40 Mha to 67 Mha. Across all assessed window sizes, we obtain DPI values for both bioenergy and PV for an additional 27–40 Mha of abandoned cropland. This increases total DPI coverage up to 67–80 Mha. Supplementary Fig. 1 shows that while there are rapid gains in abandoned cropland with DPI values at smaller window sizes, the curve quickly starts to converge towards 80 Mha. The remaining 3 Mha of abandoned cropland are located within larger clusters of missing values such as seen in parts of northern Africa and eastern Asia. We have thus identified the 11 × 11 cell window (about 1 ° × 1 °) as the best option to balance trade-offs between lower areas with DPI coverage and increased uncertainties related to data filling by taking DPI values from far areas within larger clusters. This choice results in 78 Mha (out of the 83 Mha identified globally) of abandoned cropland with assigned DPI values for both bioenergy and PV.

By comparing the spatially explicit DPIs for bioenergy and PV on abandoned cropland, the optimal combination for renewable energy production on abandoned cropland is determined. The energy potentials described in section 2.2 and 2.3 are applied to each given grid cell so that the bioenergy potential is computed for areas where the bioenergy DPI is higher than the DPI for PV, and the PV potential for areas where DPI for PV is higher than bioenergy DPI. Further, a sensitivity analysis explores the land requirements and energy potentials across different DPI thresholds (i.e., deploying energy production on all areas with DPI values above a given threshold), and the effect of the data filling method on the global potentials. The DPI-optimized land allocation to bioenergy and PV, the corresponding mean energy yields, and total energy potentials on abandoned cropland is therefore computed for a range of window sizes between 3 × 3 and 31 × 31 cells.

3. Results and discussion

3.1. Abandoned cropland

A total of 83 Mha of abandoned cropland globally can be identified from the ESA CCI-LC land cover maps between 1992 and 2015 (Fig. 1). Most of these areas are located in Asia (30%), followed by Americas (28%), Africa (22%), Europe (20%), and, lastly, Oceania (5%). Drivers behind abandonment of agricultural land are many and include environmental, socio-economic and political factors [97,98]. Natural geophysical constraints, such as a decline in soil quality and land degradation, may motivate the cropland abandonment [15,98] as well as topography (e.g., mountain regions and dry areas) [99]. Nevertheless, socio-economic drivers are of larger importance. Lack of availability of critical infrastructure (such as roads) and missing subsidies for farming may force landowners to give up the land [98]. Abandonment of cropland may also result from changes in internal or external politics (e.g., migration of land-use activities to less developed countries [100]), and the shift towards market-driven economies (e.g., the dissolution of the Soviet Union) [99].

In Asia, we find intensive cropland abandonment in Southeast regions close to the equator (e.g., Malaysia and Indonesia). Smaller fractions of abandoned cropland are found in North and Central America, and along the coast of South America. In Africa, regions just south of the equator, such as Congo, Angola, and Tanzania, have large areas of abandoned cropland. In Europe, large areas of abandoned cropland are found in the former Soviet Union (e.g., Russia, Ukraine, and Kazakhstan) and eastern parts of Europe. Also, abandonment of farming occurs in Oceania, mainly along the coastlines of Australia and New Zealand.

3.2. Primary energy potential of bioenergy and PV

Annually, global bioenergy potentials on abandoned cropland are estimated to be 35 EJ (Fig. 2a), assuming modern agricultural practices and irrigation in areas with no physical water scarcity. This means that in water scarcity areas where the abandoned cropland is not suitable to rain-fed bioenergy crops (about 5 Mha), there is no bioenergy potential. On the other hand, PV farms on

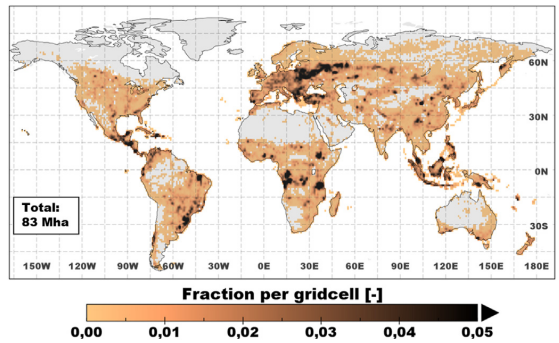

Fig. 1. Globally identified abandoned cropland between 1992 and 2015. The color bar shows the grid cell fraction at 1° resolution (aggregated from the resolution of the original dataset for visualization purposes). (For interpretation of the references to color in this figure legend, the reader is referred to the Web version of this article.)

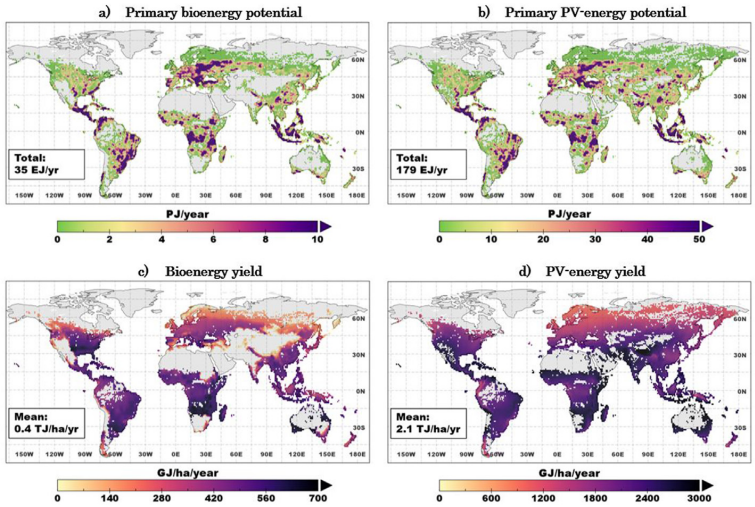

Fig. 2. Primary energy potentials on abandoned cropland for bioenergy (a) and PV-energy (b), in PJ year^{-1} and energy yield (i.e., energy output per hectare of land) for bioenergy (c) and PV-energy (d) in GJ ha^{-1} year^{-1}. Note that scales of the color bars are different for each panel. (For interpretation of the references to color in this figure legend, the reader is referred to the Web version of this article.)

abandoned cropland can produce 179 EJ year^{-1} (Fig. 2b), which is more than five times higher than the bioenergy potential. The mean primary energy yield of bioenergy is 0.4 TJ ha^{-1} year^{-1} (Fig. 2c) and for PV 2.1 TJ ha^{-1} year^{-1} (Fig. 2d).

For all locations of abandoned cropland, the potential primary energy output is higher for PV compared to bioenergy; however, the magnitude by which PV performs better than bioenergy differs regionally. A clear latitudinal trend can be identified: bioenergy performs better in the tropics (where yields are high) compared to higher latitudes, even though it does not out-compete PV. The highest bioenergy yields are located in the west coast of South America, Africa, and Southeast Asia. However, a significant bioenergy potential is also found in eastern parts of Europe and some locations in Central America. Areas with high PV potential are widely scattered. The main productive regions include the east coast of South America, Central America, parts of Africa, mid-Europe and South East Asia. The lowest PV yields are found in Scandinavia and North America.

3.3. Development Potential Index for bioenergy and PV

We mapped Development Indices (DPIs), a measure of technical and socioeconomic feasibility, of bioenergy and PV from Oakleaf et al. [36] on the identified areas of abandoned cropland (Fig. 3). Average DPI for bioenergy across abandoned cropland is found to be 0.53 (Fig. 3a), while it is 0.58 for solar PV (Fig. 3b). This result indicates that globally the development of solar PV farms on abandoned cropland has a slightly higher development potential compared to bioenergy. However, bioenergy is more suitable compared to PV in some areas due to several local biophysical and socio-economic feasibility factors considered in the DPI. In general, the highest DPI for bioenergy on abandoned cropland are located in tropical and mild temperate regions, while the development potential for PV is higher in dryer climatic conditions. By investigating the differences between DPI for PV and DPI for bioenergy on abandoned cropland per grid cell (Fig. 3c) we find a mean global difference of 0.05. The difference in DPI per grid cell is closer to zero around the equator (mainly in Africa and South America) and in Central-Europe, among other regions (light blue and yellow color in Fig. 3c). The DPI of PV is higher than the DPI of bioenergy in large parts of sub-Saharan Africa, North America, the eastern Part of South America, Central Asia and the eastern parts of Australia (red color in Fig. 3c). In contrast, the DPI of bioenergy is higher than the DPI of PV for areas such as the western and middle parts of South America, South-East Asia, and some clusters in Europe, Africa and Australia (dark blue color in Fig. 3c).

3.4. Optimal deployment of bioenergy and PV based on DPIs

By comparing the site-specific DPIs, an optimal distribution of bioenergy and PV deployment for renewable energy production is determined (Fig. 4) for 78 Mha of the initial 83 Mha abandoned cropland. The remaining 5 Mha has no DPI due to the selected size of the window for the data filling methods. The influence of alternative window sizes is explored in a sensitivity analysis. The results show that 68% (53 Mha) of the abandoned cropland have higher suitability for establishment of PV infrastructure, while the other 32% (25 Mha) is more suitable for bioenergy deployment (Fig. 4a). An optimal DPI-based deployment of these two renewable energy options has a primary energy potential of 125 EJ year^{-1} at a global level, of which 114 EJ year^{-1} are from PV and 11 EJ year^{-1} from bioenergy. Therefore, a significantly higher share of the total energy generated will come from PV deployment (91%) compared to bioenergy (9%). We find that the optimal land management of abandoned cropland combining PV and bioenergy will have DPI values greater than 0.1 for all locations (Fig. 4b and c). However, most of the primary energy potential is associated with land areas with a DPI ranging from 0.4 to 0.8, and only a tiny fraction of the land will have a DPI close to 1 (i.e., maximum development potential).

While the overall optimal deployment for PV and bioenergy is quite fragmented (Fig. 4a), some trends can be observed. North America and a large part of Central and South America have a higher development potential for PV compared to bioenergy. In Europe, the Mediterranean countries are more suitable for PV than bioenergy deployment. In contrast, bioenergy has larger DPI values in Great Britain, Ireland, Poland, and the former Soviet states except

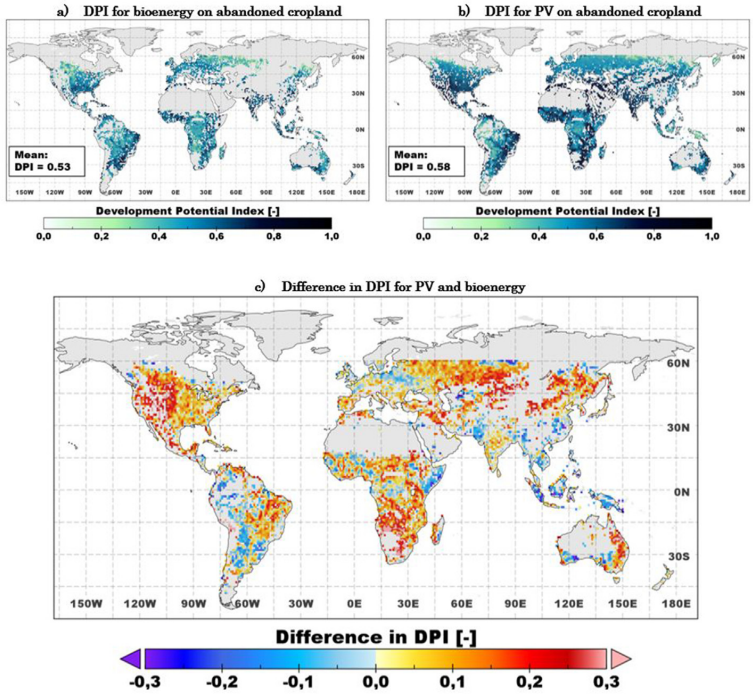

Fig. 3. Development Potential Index (DPI) on abandoned cropland for bioenergy (a), PV-energy (b) and (c) difference between DPI for PV and DPI for bioenergy on (cells of) abandoned cropland. Range for DPI is between 0 and 1, where 1 represent maximum development potential. DPIs are based on Oakleaf et al. [36] and applied to the identified abandoned cropland areas. The difference in DPI is calculated as DPI of PV minus the DPI of bioenergy per grid cell. This means that if a grid cell has a value greater than zero it has a higher DPI for PV than for bioenergy.

for Russia. In the African continent, bioenergy is a better option in the eastern part of the Horn of Africa, western and central Africa, while PV is the preferred option under the equator. Large parts of Asia have a higher development potential for PV, but some exceptions are in Pakistan, China, and Southeastern Asia. Further, we find that the eastern states of Australia and New Zealand have a higher potential for PV. Along a latitudinal gradient, the areas between 30 and 60°N have a higher PV potential while most of the tropical areas situated around the equator have a higher bioenergy potential. In total, 125 EJ year^{-1} of primary energy can be generated, at a global mean primary energy potential of 1.6 TJ ha^{-1} year^{-1} for an optimal deployment of abandoned cropland areas (Fig. 4d and e). This potential is produced with an average DPI of 0.61 (Fig. 4f). This value is higher than the mean DPI when only deployment of bioenergy (mean DPI 0.53) or PV (mean DPI 0.58) is considered (see Fig. 3a and b), meaning that an optimal allocation of renewable energy production to abandoned cropland on the basis of the DPI offers higher potentials of development.

This primary energy potential from abandoned cropland can be compared to the expected renewable energy deployment in future climate change mitigation scenarios. The projected median renewable primary energy needed to limit global warming to 1.5 °C across different SSPs in 2100 is 224–412 EJ year^{-1} from biomass and 54–243 EJ year^{-1} from solar energy [5,6]. Comparing these estimates to our result of bioenergy (11 EJ year^{-1} under DPI-based optimal land allocation), it is clear that limiting bioenergy production to abandoned cropland is not sufficient. More resources from forest residues, waste products, or bioenergy crops produced on current cropland or pastureland are needed to reach the projections across all SSPs. However, deployment of perennial grasses on abandoned cropland is a promising near-term option that can facilitate a gradual upscale of bioenergy production from second generation feedstocks. On the other hand, our estimate of 114 EJ year^{-1} for PV represents a large share of the expected PV demand, and in one scenario (SSP4) it can cover all the projected solar energy demand. It also covers large parts of the 2100 demand in SSP1 and SSP2 (83% and 78%, respectively), and 47% of the demand in the energy intensive SSP5 scenario where a delayed energy transition leads to an extensive deployment of renewable energy sources in the second half of the century [6].

3.5. Development Potential Index thresholds and land-energy interactions

There are non-linear relationships between DPI-thresholds, land availability and energy potentials (Fig. 5). Half of the abandoned cropland is located in areas where DPI is higher than 0.53 and 0.60 for bioenergy (Fig. 5a) and PV (Fig. 5b), respectively. With DPI optimized land management, there is relatively higher land availability for energy production at a given DPI threshold (Fig. 5c). Half of the abandoned cropland can be utilized at a DPI threshold of 0.63, with 13 Mha and 26 Mha allocated to bioenergy and PV, respectively. Abandoned cropland with DPI above 0.8 is limited for both bioenergy and PV (2.4 Mha and 1.7 Mha, respectively). Even in the DPI optimized scenario, only 3.8 Mha of the abandoned cropland has DPI above 0.8 (2.3 Mha and 1.5 Mha allocated to bioenergy and PV, respectively). At the same time, 85%, and 95% of abandoned cropland has DPI above 0.4 for bioenergy and PV, respectively. The

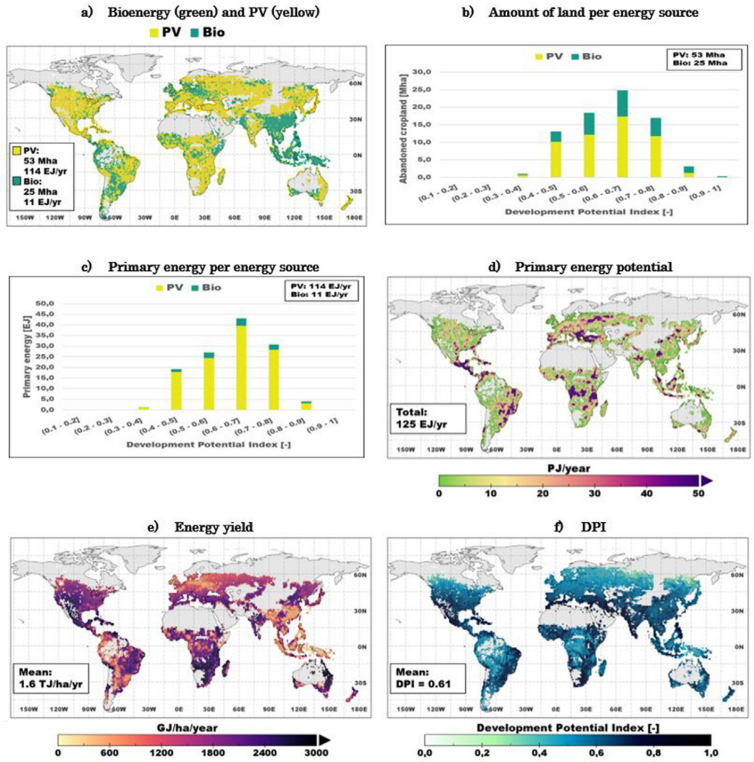

Fig. 4. Optimal allocation to abandoned cropland of PV and bioenergy based on the Development Potential Index (DPI). Areas identified with higher DPI for PV in yellow and bioenergy in green (a). Amount of hectares of land (b) and primary energy production (c) for the optimal management of PV (yellow) and bioenergy (green) by ranges of DPIs. Primary energy potential per year (in PJ year^{-1}) (d) and energy yield (in GJ ha^{-1} year^{-1}) (e) for optimal management of abandoned cropland. (f) Development Potential Index (DPI) for optimal land management on abandoned cropland for renewable energy production by bioenergy and PV. (For interpretation of the references to color in this figure legend, the reader is referred to the Web version of this article.)

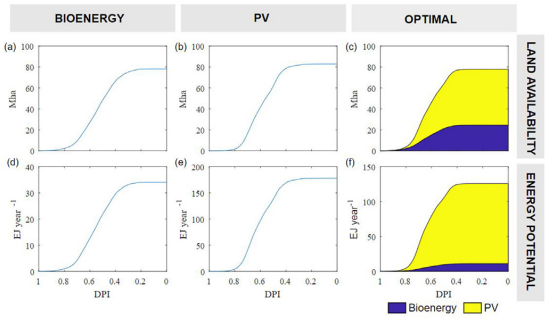

Fig. 5. Relationship between DPI levels, land availability and achievable primary energy potentials assuming all abandoned cropland above a given DPI is utilized for energy production. Land availability [Mha] are shown for (a) bioenergy, (b) PV, and (c) for the DPI optimized allocation of bioenergy and PV on abandoned cropland. Maximum land availability differs slightly between scenarios due to variations in DPI data availability. Energy potentials [EJ year^{-1}] are shown for (d) bioenergy, (e) PV, and (f) the DPI optimized allocation of bioenergy and PV on abandoned cropland. Note different scales on y-axis for energy potentials in (d), (e) and (f).

optimized land management make use of 99% of abandoned cropland above a 0.4 DPI threshold, with 24 Mha and 53 Mha allocated to bioenergy and PV, respectively.

Reaching half of the bioenergy potential requires a DPI threshold of 0.55 and 37 Mha of abandoned cropland, with a mean bioenergy yield of 460 GJ ha^{-1} year^{-1} (Fig. 5d). Half the PV potential is achievable with a DPI threshold of 0.61 by utilizing 39 Mha of abandoned cropland, and a mean PV energy yield of 2349 GJ ha^{-1} year^{-1} (Fig. 5e). With optimal land management, half of the energy potential is reached at a higher DPI threshold of 0.64 (Fig. 5f). This requires 12 Mha and 25 Mha to produce 5.8 EJ year^{-1} and 59.5 EJ year^{-1} for bioenergy and PV, respectively. Mean energy yields increase slightly at a 0.64 DPI threshold to 467 GJ ha^{-1} year^{-1} and 2380 GJ ha^{-1} for PV and bioenergy, respectively.

The top 10 percentiles of the energy potentials are achievable at DPI thresholds of 0.71, 0.74 and 0.76, with land requirements of 8.1 Mha, 7.5 Mha and 9.5 Mha to produce 3.6 EJ year^{-1}, 19 EJ year^{-1} and 13 EJ year^{-1} for bioenergy, PV and optimal land management, respectively. In the optimal land management scenario, 1.7 EJ year^{-1} and 11 EJ year^{-1} is produced with mean energy yields of 439 GJ ha^{-1} year^{-1} and 2481 GJ ha^{-1} year^{-1} for bioenergy and PV, respectively. On the other hand, 90% of the total potential is reachable with DPI threshold of 0.38, 0.44 and 0.47, thereby producing 30 EJ year, 161 EJ year^{-1} and 114 EJ year^{-1} with land requirements of 69 Mha, 74 Mha and 70 Mha for bioenergy, PV and optimal land management, respectively. With optimal land management, 10 EJ year^{-1} and 103 EJ year^{-1} is produced, with mean energy yields of 454 GJ ha^{-1} year^{-1} and 2196 GJ ha^{-1} year^{-1} for

bioenergy and PV, respectively.

While PV energy yields peak at a 0.96 DPI threshold for the optimal land management scenario (2825 GJ ha^{-1} year^{-1}), we find that mean bioenergy yields peak at a DPI threshold of 0.63 (466 GJ ha^{-1} year^{-1}). This indicates that market accessibility or land supply elasticity (i.e. the relationship between land use change, and land and crop prices) might be a constraint in some of the highest yielding areas for bioenergy production. Furthermore, we deploy irrigated bioenergy production in areas that are not threatened by water scarcity, which is not directly reflected by the DPI values.

3.6. Uncertainty and limitations

We performed a sensitivity analyses to assess the effects of the DPI data filling method on areas of abandoned cropland with an assigned DPI value and the resulting primary energy potentials. Supplementary Table 1 shows how results vary according to different sizes of the moving window (between 3 × 3 to 31 × 31 cell windows). Across all the window sizes considered, we obtained DPI values for an additional 27–40 Mha. Including these additional cells brings total abandoned cropland with both bioenergy and PV DPIs to 67–80 Mha, with optimal energy potentials ranging between 107 and 129 EJ year^{-1}. While a larger window size increases both the considered land availability and energy potentials, it does not affect the share of land distributed between bioenergy and PV. Allocated shares of abandoned cropland to bioenergy and PV are 31–32% and 68–69% across all considered window sizes, respectively. This indicates an even spread of missing values across the abandoned cropland grids. Likewise, mean bioenergy and PV energy yields show small variations (454–457 GJ ha^{-1} and 2130–2153 GJ ha^{-1}, respectively). Contributions to optimal total energy production stay at 9% and 91% for bioenergy and PV, respectively.

The recently released ESA CCI-LC products aim to give a more realistic representation of land cover dynamics compared to former datasets by resolving some of their limitations [101,102]. Several previous studies validated the accuracy of the ESA CCI-LC dataset. The global overall accuracy is 71% [103], but with some regional differences. Overall accuracies are 72% in China [104], 62% in Africa [105], 70% in South America [105], 62% in the Arctic [106] and 84% in coastal Eurasia [107]. Cropland classes have the highest global accuracy. Median global user and producer accuracies of cropland classes are 89% and 80%, respectively [103]. The ESA CCI-LC dataset is also found to be broadly consistent with other cropland identification approaches [105,108]. This makes the ESA CCI-LC especially useful for cropland monitoring, with both a relatively high precision in total cropland extent, and a high spatial cropland match. Moreover, the estimates of a detected change in terrestrial surface are based on changes registered over a two year period, so that temporary changes (e.g., a short period of extreme events such as draughts) will not affect the data, and this is considered a strength of the CCI-LC database. An increasing number of studies rely on the ESA CCI-LC products for analysis of effects of land cover changes. Examples include effects of recent land-use and land-cover changes on the terrestrial carbon stocks [102,109], air temperature and humidity effects [110], surface energy budget [109], assessments of global cropland sparing potentials [111], global urban expansion [112], and land cover changes within biodiversity hotspots [113].

The GAEZ model relies on complex databases to provide spatial agro-climatic yields, and both the databases and the assumptions in the model itself have intrinsic uncertainties [33]. Despite this, the GAEZ model is widely tested, validated and used in multiple applications [114–118]. In order to estimate the bioenergy potential on abandoned cropland, the energy-based optimal solution for perennial grasses allocation in combination with high agricultural management levels and mixed water supply system is utilized. Bioenergy potentials are lower if a low or medium agriculture management intensity is considered (e.g., lower inputs of nutrients, lower mechanization of field work, etc.), but higher if irrigation is deployed on all abandoned cropland. More refined estimates of bioenergy potentials can be achieved with regional analysis that considers local trade-offs with economic and environmental factors to identify the best management practice.

Meteorological data from CMCC-CM rely on the atmospheric model ECHAM5 [79] and the ocean model OPA8.2 [80] coupled by the OASIS3 interface [81]. As each of the models are combined to create the CMCC-CM, the datasets from CMCC-CM include the intrinsic uncertainties related to each model and those from their combination [82]. The primary energy potential for PV is estimated based on two main assumptions that are subject to uncertainties: the nominal installed power [27,28,92,119] and the amount of area covered by solar panels [27–29]. These parameters can be adjusted to represent advancements in technologies or by accounting for site-specific conditions. The primary energy potential of PV also depends on solar radiation, ambient temperature, cell temperature, and wind speed, and future changes in background climatic conditions can influence productivity of PV. Nominal installed production, area covered with solar cells and technical parameters like orientation, tilt, and incline of the PV modules also affect estimates of potentials [120]. Typically, PV systems using a tracking system that follow the sun path compared to fixed orientation can gain higher efficiency [121].

Regarding the DPI data, the uncertainty of model outputs as well as the sensitivity to model inputs have been investigated in the original study that produced the DPI dataset [36]. The study also validated the DPIs by investigating recent or planned developments by using more than 6000 data-points and 200,000 km^2 of mapped locations. A Monte Carlo approach determined the uncertainty, and the mean coefficient of variation for bioenergy DPI (0.137) is higher compared to the mean coefficient of variation for PV DPI (0.048). In general, lower uncertainty is found for higher DPI areas. For PV, high uncertainty is typically associated with areas in remote regions that lacked supporting infrastructure or market access but had higher than average resource potential (i.e., yield criteria in all DPIs). For bioenergy, the highest uncertainty values mainly occurred in regions with lower yields and longer distances to markets or infrastructure.

Additional work can explore the optimal DPI land management on abandoned cropland under the changing climate niche [122]. As energy yield is the most important parameter in the DPI methodology for PV and bioenergy [36], and are depending on climate conditions, future climate changes will likely affect the optimal land allocation and energy potentials. Bioenergy dry mass yields are projected to decrease globally in the 21st century for rain-fed bioenergy crops in RCP4.5 and RCP8.5, with the magnitude of change being almost double in RCP8.5 relative to RCP4.5 [123]. The largest declines are projected in the tropics and subtropics, but there are also increasing yields projected at higher latitudes in parts of the northern hemisphere. Global crop yield losses can to some extents be mitigated through irrigation deployment and genetic modifications [123–125]. For PVs, cell efficiency decreases with increased cell temperatures and cloud cover but increase with increased incoming solar radiation [126]. Global PV energy yields are expected to decrease globally as a response to climate change [69]. For example, mean PV potentials are projected to decrease towards 2100 in RCP8.5 with −10% and −4% in Europe [68] and Africa [89], respectively.

Although our analysis only focused on renewable energy potentials, there are multiple local environmental effects associated with bioenergy or solar PV deployment that are important to

consider, and that can differ significantly between the two options. There are several environmental benefits that can be obtained by introducing dedicated bioenergy crops on former cropland. For example, lower nutrient and soil losses [50], and supporting several ecosystem services [44]. On the other hand, producing solar energy with photovoltaic panels on open land is sometimes heavily contested because of nature protection, accessibility, and cultural heritage [42].

Deployment strategies for renewable energy options are highly influenced by political and economic factors [16]. Local, national or international laws, regulations, and subsidies can either promote or inhibit renewable energy deployment. The integration of ESA CCI-LC and DPIs allows assessing opportunity costs and the potential of a land-use conversion from abandoned cropland to energy production. The results of our spatially explicit analysis offer the opportunity to zoom into different local and regional contexts. As the DPI methodology is especially suitable to identify priority regions for new deployment of renewable energy infrastructure [36], our findings show the potential hidden at low risks for rising competition for land and provide a preliminary screening of the key regions with extensive cropland abandonment that can be prioritized for bioenergy or PV deployment. Implementation of these solutions should consider the specific local factors for sustainable land management and energy planning at the local level, and involve environmental and socio-economic indicators other than those included in the analysis (e.g., resource availability, material requirements, biodiversity, social factors, political factors, energy system characteristics or property rights). For example, bioenergy crops are found to improve many indicators of ecosystem services relative to cropland (including biodiversity), whereas PV panels would have a likely more detrimental effects on terrestrial ecosystems on which they are established. Further, the inclusion of other renewable energy sources in the analysis may change the optimal allocation of renewable energy options to specific grid cells, and likely lead to overall increased DPI values on abandoned cropland. For example, abandoned cropland may be more suitable for wind energy production [14], or could contribute to the deployment of new hydropower reservoirs [127].

4. Concluding remarks

This study provided a detailed analysis of the optimal land management on abandoned cropland for renewable energy production considering bioenergy or solar PV deployment. By only considering the potential primary energy output of each renewable energy option, the PV potential far outcompetes the one of bioenergy crops at a global level. However, the consideration of different biophysical and socio-economic factors provides a more realistic comparison and deployment potential. Considering site-specific DPIs, a mix of bioenergy and PV is found to be the best solution for renewable energy production on abandoned cropland. About 68% of the total area of abandoned cropland favors the deployment of solar PV farms, and the rest (32%) favors the establishment of bioenergy. In total, the optimal land management on abandoned cropland can potentially produce 125 EJ primary energy per year, where 91% (114 EJ year^{-1}) is from PV and 9% (11 EJ year $^{-1}$) from bioenergy. Further, an optimal allocation of renewable energy production to abandoned cropland on the basis of the DPI offers higher potentials of development than considering the deployment of an individual option (either PV or bioenergy). Overall, the estimated bioenergy potentials under this optimal management of abandoned cropland are not sufficient to meet a large share of the expected bioenergy demand from long-term projections in 1.5 °C future scenarios. On the other hand, the estimates of PV potentials cover almost all the 2100 PV demand in SSP1-1.9 and makes a substantial contribution even in the energy intensive SSP5-1.9 scenario (47%).

To meet the Paris Agreement's goals and, at the same time, provide a significant energy supply for a sustainable future, renewable energy production from large-scale deployment of both bioenergy from perennial grasses and PV technologies is a critical factor. Bioenergy and PV have non-negligible potentials for primary energy production on abandoned cropland, which can be used to guide an early phase deployment of large-scale renewable energy production at lower risks of competition with environmental protection and food security. We show that there is an optimal mix for the implementation of these two options at a global level under a range of biophysical and socio-economic indicators. Targeted measures can stimulate the production of renewable energy, taking into consideration the local context for implementing the most suitable options in each specific region. Site-specific analyses considering sustainability indicators, regional conditions, and the international political arena are instrumental for determining tailor-made implementation practices for renewable energy productions. Future research integrating aspects of land use sciences, energy sciences, and social sciences connected to different renewable energy options and local contexts are necessary for promoting more assertive sustainable land management strategies for the energy transition required to meet the most ambitious targets for renewable energy production and GHG emission reduction.

CRediT authorship contribution statement

Malene Eldegard Leirpoll: Writing - original draft, Writing - review & editing. **Jan Sandstad Næss:** Writing - review & editing. **Otavio Cavalett:** Validation, Writing - review & editing. **Martin Dorber:** Resources. **Xiangping Hu:** Resources. **Francesco Cherubini:** Supervision, Funding acquisition, Writing - review & editing.

Declaration of competing interest

The authors declare that they have no known competing financial interests or personal relationships that could have appeared to influence the work reported in this paper.

Acknowledgments

We acknowledge the support of the Norwegian Research Council through the projects BioPath (no. 294534), Bio4Fuels (no. 257622), and MitiStress (no. 286773). We gratefully acknowledge the provision of spatial land-cover data by the ESA-CCI Land Cover project, bioenergy yield data from GAEZ, climate data from CMCC-CM, and DPI data from Oakleaf et al.

Appendix A. Supplementary data

Supplementary data to this article can be found online at https://doi.org/10.1016/j.renene.2020.11.159.

References

[1] V. Masson-Delmotte, P. Zhai, H.O. Pörtner, D. Roberts, J. Skea, P.R. Shukla, A. Pirani, W. Moufouma-Okia, C. Péan, R. Pidcock, S. Connors, J.B. Matthews, Y. Chen, X. Zhou, M.I. Gomis, E. Lonnoy, T. Maycock, M. Tignor, T. Waterfield, Summary for policymakers, in: Global Warming of 1.5°C. An IPCC Special Report on the Impacts of Global Warming of 1.5°C above Pre-industrial Levels and Related Global Greenhouse Gas Emission Pathways, in the Context of Strengthening the Global Response to, 2018. https://report.ipcc.ch/sr15/pdf/sr15_spm_final.pdf%0Ahttp://www.ipcc.ch/report/sr15/.

[2] IEA 2020, Global Energy Review 2019, Iea, 2019. https://www.iea.org/reports/global-energy-review-2019.

[3] IRENA, Global energy transformation: a roadmap to 2050. http://irena.org/publications/2018/Apr/Global-Energy-Transition-A-Roadmap-to-2050%0Awww.irena.org, 2019.

[4] A. Popp, K. Calvin, S. Fujimori, P. Havlik, F. Humpenöder, E. Stehfest, B.L. Bodirsky, J.P. Dietrich, J.C. Doelmann, M. Gusti, T. Hasegawa, P. Kyle, M. Obersteiner, A. Tabeau, K. Takahashi, H. Valin, S. Waldhoff, I. Weindl, M. Wise, E. Kriegler, H. Lotze-Campen, O. Fricko, K. Riahi, D.P. va Vuuren, Land-use futures in the shared socio-economic pathways, Global Environ. Change 42 (2017) 331–345, https://doi.org/10.1016/j.gloenvcha.2016.10.002.

[5] K. Riahi, D.P. van Vuuren, E. Kriegler, J. Edmonds, B.C. O'Neill, S. Fujimori, N. Bauer, K. Calvin, R. Dellink, O. Fricko, W. Lutz, A. Popp, J.C. Cuaresma, S. KC, M. Leimbach, L. Jiang, T. Kram, S. Rao, J. Emmerling, K. Ebi, T. Hasegawa, P. Havlik, F. Humpenöder, L.A. Da Silva, S. Smith, E. Stehfest, V. Bosetti, J. Eom, D. Gernaat, T. Masui, J. Rogelj, J. Strefler, L. Drouet, V. Krey, G. Luderer, M. Harmsen, K. Takahashi, L. Baumstark, J.C. Doelman, M. Kainuma, Z. Klimont, G. Marangoni, H. Lotze-Campen, M. Obersteiner, A. Tabeau, M. Tavoni, B.C. O'Neill, S. Fujimori, N. Bauer, K. Calvin, R. Dellink, O. Fricko, W. Lutz, A. Popp, J.C. Cuaresma, S. KC, M. Leimbach, L. Jiang, T. Kram, S. Rao, J. Emmerling, K. Ebi, T. Hasegawa, P. Havlik, F. Humpenöder, L.A. Da Silva, S. Smith, E. Stehfest, V. Bosetti, J. Eom, D. Gernaat, T. Masui, J. Rogelj, J. Strefler, L. Drouet, V. Krey, G. Luderer, M. Harmsen, K. Takahashi, L. Baumstark, J.C. Doelman, M. Kainuma, Z. Klimont, G. Marangoni, H. Lotze-Campen, M. Obersteiner, A. Tabeau, M. Tavoni, The Shared Socioeconomic Pathways and their energy, land use, and greenhouse gas emissions implications: an overview, Global Environ. Change 42 (2017) 153–168, https://doi.org/10.1016/j.gloenvcha.2016.05.009.

[6] J. Rogelj, A. Popp, K.V. Calvin, G. Luderer, J. Emmerling, D. Gernaat, S. Fujimori, J. Strefler, T. Hasegawa, G. Marangoni, V. Krey, E. Kriegler, K. Riahi, D.P. Van Vuuren, J. Doelman, L. Drouet, J. Edmonds, O. Fricko, M. Harmsen, P. Havlík, F. Humpenöder, E. Stehfest, M. Tavoni, Scenarios towards limiting global mean temperature increase below 1.5 °c, Nat. Clim. Change 8 (2018) 325–332, https://doi.org/10.1038/s41558-018-0091-3.

[7] P. Smith, K. Calvin, J. Nkem, D. Campbell, F. Cherubini, G. Grassi, V. Korotkov, A. Le Hoang, S. Lwasa, P. McElwee, E. Nkonya, N. Saigusa, J.F. Soussana, M.A. Taboada, F.C. Manning, D. Nampanzira, C. Arias-Navarro, M. Vizzarri, J. House, S. Roe, A. Cowie, M. Rounsevell, A. Arneth, Which practices co-deliver food security, climate change mitigation and adaptation, and combat land degradation and desertification? Global Change Biol. 26 (2020) 1532–1575, https://doi.org/10.1111/gcb.14878.

[8] L.R. Boysen, W. Lucht, D. Gerten, Trade-offs for food production, nature conservation and climate limit the terrestrial carbon dioxide removal potential, Global Change Biol. 23 (2017) 4303–4317, https://doi.org/10.1111/gcb.13745.

[9] R. Thomas, M. Reed, K. Clifton, N. Appadurai, A. Mills, C. Zucca, E. Kodsi, J. Sircely, F. Haddad, C. Hagen, E. Mapedza, K. Woldearegay, K. Shalander, M. Bellon, Q. Le, S. Mabikke, S. Alexander, S. Leu, S. Schlingloff, T. Lala-Pritchard, V. Mares, R. Quiroz, A framework for scaling sustainable land management options, Land Degrad. Dev. 29 (2018) 3272–3284, https://doi.org/10.1002/ldr.3080.

[10] F. Poggi, A. Firmino, M. Amado, Planning renewable energy in rural areas: impacts on occupation and land use, Energy 155 (2018) 630–640, https://doi.org/10.1016/j.energy.2018.05.009.

[11] J. Malczewski, GIS-based land-use suitability analysis: a critical overview, Prog. Plann. 62 (2004) 3–65, https://doi.org/10.1016/j.progress.2003.09.002.

[12] Y. Choi, J. Suh, S.-M. Kim, GIS-based solar radiation mapping, site evaluation, and potential assessment: a review, Appl. Sci. 9 (2019), https://doi.org/10.3390/app9091960.

[13] C.B. Field, J.E. Campbell, D.B. Lobell, Biomass energy: the scale of the potential resource, Trends Ecol. Evol. 23 (2008) 65, https://doi.org/10.1016/j.tree.2007.12.001.

[14] A.R. Milbrandt, D.M. Heimiller, A.D. Perry, C.B. Field, Renewable energy potential on marginal lands in the United States, Renew. Sustain. Energy Rev. 29 (2014) 473–481, https://doi.org/10.1016/j.rser.2013.08.079.

[15] A. Zumkehr, J.E. Campbell, Historical U.S. cropland areas and the potential for bioenergy production on abandoned croplands, Environ. Sci. Technol. 47 (2013) 3840–3847, https://doi.org/10.1021/es3033132.

[16] G.P.P. Robertson, S.K.S.K. Hamilton, B.L.B.L. Barham, B.E.B.E. Dale, R.C.C. Izaurralde, R.D.R.D. Jackson, D.A.D.A. Landis, S.M.S.M. Swinton, K.D.K.D. Thelen, J.M. Tiedje, Cellulosic biofuel contributions to a sustainable energy future: choices and outcomes, Science (80-.) (2017) 356, https://doi.org/10.1126/science.aal2324.

[17] V. Daioglou, J.C. Doelman, B. Wicke, A. Faaij, D.P. van Vuuren, Integrated assessment of biomass supply and demand in climate change mitigation scenarios, Global Environ. Change 54 (2019) 88–101, https://doi.org/10.1016/j.gloenvcha.2018.11.012.

[18] J.L. Field, T.L. Richard, E.A.H. Smithwick, H. Cai, M.S. Laser, D.S. LeBauer, S.P. Long, K. Paustian, Z. Qin, J.J. Sheehan, P. Smith, M.Q. Wang, L.R. Lynd, Robust paths to net greenhouse gas mitigation and negative emissions via advanced biofuels, Proc. Natl. Acad. Sci. U. S. A 117 (2020) 21968–21977, https://doi.org/10.1073/pnas.1920877117.

[19] Y. Yang, D. Tilman, C. Lehman, J.J. Trost, Sustainable intensification of high-diversity biomass production for optimal biofuel benefits, Nat. Sustain. 1 (2018) 686–692, https://doi.org/10.1038/s41893-018-0166-1.

[20] B.P. Werling, T.L. Dickson, R. Isaacs, H. Gaines, C. Gratton, K.L. Gross, H. Liere, C.M. Malmstrom, T.D. Meehan, L. Ruan, B.A. Robertson, G.P. Robertson, T.M. Schmidt, A.C. Schrotenboer, T.K. Teal, J.K. Wilson, D.A. Landis, Perennial grasslands enhance biodiversity and multiple ecosystem services in bioenergy landscapes, Proc. Natl. Acad. Sci. U. S. A 111 (2014) 1652–1657, https://doi.org/10.1073/pnas.1309492111.

[21] L. Lai, C. Oh Hong, S. Kumar, S.L. Osborne, R.M. Lehman, V.N. Owens, Soil nitrogen dynamics in switchgrass seeded to a marginal cropland in South Dakota, GCB Bioenergy 10 (2018) 28–38, https://doi.org/10.1111/gcbb.12475.

[22] K.J. Harding, T.E. Twine, A. VanLoocke, J.E. Bagley, J. Hill, Impacts of second-generation biofuel feedstock production in the central U.S. on the hydrologic cycle and global warming mitigation potential, Geophys. Res. Lett. 43 (2016) 10,773–10,781, https://doi.org/10.1002/2016GL069981.

[23] P. Zhu, Q. Zhuang, J. Eva, C. Bernacchi, Importance of biophysical effects on climate warming mitigation potential of biofuel crops over the conterminous United States, GCB Bioenergy 9 (2017) 577–590, https://doi.org/10.1111/gcbb.12370.

[24] Y. Yang, S.E. Hobbie, R.R. Hernandez, J. Fargione, S.M. Grodsky, D. Tilman, Y.-G. Zhu, Y. Luo, T.M. Smith, J.M. Jungers, M. Yang, W.-Q. Chen, Restoring abandoned farmland to mitigate climate change on a full earth, One Earth 3 (2020) 176–186, https://doi.org/10.1016/j.oneear.2020.07.019.

[25] A. Goodrich, T. James, M. Woodhouse, Residential, commercial, and utility scale photovoltaic (PV) System prices in the United States: current drivers and cost-reduction opportunities, Photovolt. Costs U.S. Anal. Prices Trends. (2012) 1–58.

[26] International Renewable Energy Agency IRENA, Future of solar photovoltaic: deployment, investment, technology, grid integration and socio-economic aspects. https://www.irena.org/-/media/Files/IRENA/Agency/Publication/2019/Oct/IRENA_Future_of_wind_2019.pdf, 2019.

[27] T.J. Dijkman, R.M.J. Benders, Comparison of renewable fuels based on their land use using energy densities, Renew. Sustain. Energy Rev. 14 (2010) 3148–3155, https://doi.org/10.1016/j.rser.2010.07.029.

[28] B. Pillot, N. Al-Kurdi, C. Gervet, L. Linguet, An integrated GIS and robust optimization framework for solar PV plant planning scenarios at utility scale, Appl. Energy 260 (2020), 114257, https://doi.org/10.1016/j.apenergy.2019.114257.

[29] E.G. Hertwich, T. Gibon, E.A. Bouman, A. Arvesen, S. Suh, G.A. Heath, J.D. Bergesen, A. Ramirez, M.I. Vega, L. Shi, Integrated life-cycle assessment of electricity-supply scenarios confirms global environmental benefit of low-carbon technologies, Proc. Natl. Acad. Sci. U. S. A 112 (2015) 6277–6282, https://doi.org/10.1073/pnas.1312753111.

[30] K. Calvert, W. Mabee, More solar farms or more bioenergy crops? Mapping and assessing potential land-use conflicts among renewable energy technologies in eastern Ontario, Canada, Appl. Geogr. 56 (2015) 209–221, https://doi.org/10.1016/j.apgeog.2014.11.028.

[31] C. Breyer, D. Bogdanov, A. Gulagi1, A. Aghahosseini, L.S.N.S. Barbosa, O. Koskinen, M. Barasa, U. Caldera, S. Afanasyeva, M. Child, J. Farfan1, P. Vainikka, On the role of solar photovoltaics in global energy transition scenarios, IEEE Trans. Fuzzy Syst. 20 (2017) 727–745, https://doi.org/10.1002/pip.

[32] S. Bontemps, P. Defourny, J. Radoux, E. Van Bogaert, C. Lamarche, F. Achard, P. Mayaux, M. Boettcher, C. Brockmann, G. Kirches, M. Zülkhe, V. Kalogirou, O. Arino, Consistent global land cover maps for climate modeling communities: current achievements of the ESA's land cover CCI, in: ESA Living Planet Symp. 2013, 2013, pp. 9–13. https://ftp.space.dtu.dk/pub/loana/papers/s274_2bont.pdf.

[33] G. Fischer, F.O. Nachtergaele, S. Prieler, E. Teixeira, G. Toth, H. van Velthuizen, L. Verelst, D. Wiberg, Global Agro-Ecological Zones (GAEZ): Model Documentation, 2012, pp. 1–179.

[34] E. Scoccimarro, S. Gualdi, A. Bellucci, A. Sanna, P.G. Fogli, E. Manzini, M. Vichi, P. Oddo, A. Navarra, Effects of tropical cyclones on ocean heat transport in a high-resolution coupled general circulation model, J. Clim. 24 (2011) 4368–4384, https://doi.org/10.1175/2011JCLI4104.1.

[35] F. Mavromatakis, G. Makrides, G. Georghiou, A. Pothrakis, Y. Franghiadakis, E. Drakakis, E. Koudoumas, Modeling the photovoltaic potential of a site, Renew. Energy 35 (2010) 1387–1390, https://doi.org/10.1016/j.renene.2009.11.010.

[36] J.R. Oakleaf, C.M. Kennedy, S. Baruch-Mordo, J.S. Gerber, P.C. West, J.A. Johnson, J. Kiesecker, Global development potential indicies for renewable energy, fossil fuels, mining and agriculture sectors, figshare, Sci. Data 6 (2019) 101, https://doi.org/10.1038/s41597-019-0084-8.

[37] J.E. Campbell, D.B. Lobell, R.C. Genova, C.B. Field, The global potential of bioenergy on abandoned agriculture lands, Environ. Sci. Technol. 42 (2008) 5791–5794, https://doi.org/10.1021/es800052w.

[38] X. Cai, X. Zhang, D. Wang, Land availability for biofuel production, Environ. Sci. Technol. 45 (2011) 334, https://doi.org/10.1021/es103338e.

[39] R. Slade, A. Bauen, R. Gross, Global bioenergy resources, Nat. Clim. Change 4 (2014) 99–105, https://doi.org/10.1038/nclimate2097.

[40] T. Beringer, W. Lucht, S. Schaphoff, Bioenergy production potential of global biomass plantations under environmental and agricultural constraints, GCB Bioenergy 3 (2011) 299–312, https://doi.org/10.1111/j.1757-1707.2010.01088.x.

[41] Y. Charabi, A. Gastli, PV site suitability analysis using GIS-based spatial fuzzy multi-criteria evaluation, Renew. Energy 36 (2011) 2554–2561, https://doi.org/10.1016/j.renene.2010.10.037.

[42] F. Kienast, N. Huber, R. Hergert, J. Bolliger, L.S.L.S. Moran, A.M.A.M. Hersperger, Conflicts between decentralized renewable electricity production and landscape services – a spatially-explicit quantitative assessment for Switzerland, Renew. Sustain. Energy Rev. 67 (2017) 397–407, https://doi.org/10.1016/j.rser.2016.09.045.
[43] D. Lingfors, J. Widén, J. Marklund, M. Boork, D. Larsson, Photovoltaics in Swedish agriculture: technical potential, grid integration and profitability, in: ISES Sol. World Congr. 2015, Conf. Proc., 2015, pp. 259–267, https://doi.org/10.18086/swc.2015.07.14.
[44] D. Scordia, S.L. Cosentino, Perennial energy grasses: resilient crops in a changing european agriculture, Agric. For. 9 (2019), https://doi.org/10.3390/agriculture9080169.
[45] R.I. Nazli, V. Tansi, H.H. Öztürk, A. Kusvuran, Miscanthus, switchgrass, giant reed, and bulbous canary grass as potential bioenergy crops in a semi-arid Mediterranean environment, Ind. Crop. Prod. 125 (2018) 9–23, https://doi.org/10.1016/j.indcrop.2018.08.090.
[46] A. Ameen, L. Han, G.H. Xie, Dynamics of soil moisture, pH, organic carbon, and nitrogen under switchgrass cropping in a semiarid sandy wasteland, Commun. Soil Sci. Plant Anal. 50 (2019) 922–933, https://doi.org/10.1080/00103624.2019.1594883.
[47] D. Cooney, H. Kim, L. Quinn, M.S. Lee, J. Guo, S. lin Chen, B. cheng Xu, D.K. Lee, Switchgrass as a bioenergy crop in the Loess Plateau, China: potential lignocellulosic feedstock production and environmental conservation, J. Integr. Agric. 16 (2017) 1211–1226, https://doi.org/10.1016/S2095-3119(16)61587-3.
[48] I. Lewandowski, J.M.O. Scurlock, E. Lindvall, M. Christou, The development and current status of perennial rhizomatous grasses as energy crops in the US and Europe, Biomass Bioenergy 25 (2003) 335–361, https://doi.org/10.1016/S0961-9534(03)00030-8.
[49] I. Lewandowski, J.C. Clifton-Brown, J.M.O. Scurlock, W. Huisman, Miscanthus, European experience with a novel energy crop, Biomass Bioenergy 19 (2000) 209–227, https://doi.org/10.1016/S0961-9534(00)00032-5.
[50] G. Siri-Prieto, M. Bustamante, V. Picasso, O. Ernst, Impact of nitrogen and phosphorous on biomass yield, nitrogen efficiency, and nutrient removal of perennial grasses for bioenergy, Biomass Bioenergy 136 (2020), 105526, https://doi.org/10.1016/j.biombioe.2020.105526.
[51] A. Ameen, J. Liu, L. Han, G.H. Xie, Effects of nitrogen rate and harvest time on biomass yield and nutrient cycling of switchgrass and soil nitrogen balance in a semiarid sandy wasteland, Ind. Crop. Prod. 136 (2019) 1–10, https://doi.org/10.1016/j.indcrop.2019.04.066.
[52] B. Zhang, A. Hastings, J.C. Clifton-Brown, D. Jiang, A.P.C. Faaij, Modeled spatial assessment of biomass productivity and technical potential of Miscanthus × giganteus, Panicum virgatum L., and Jatropha on marginal land in China, GCB Bioenergy 12 (2020) 328–345, https://doi.org/10.1111/gcbb.12673.
[53] D. Hui, C.L. Yu, Q. Deng, E. Kudjo Dzantor, S. Zhou, S. Dennis, R. Sauve, T.L. Johnson, P.A. Fay, W. Shen, Y. Luo, Effects of precipitation changes on switchgrass photosynthesis, growth, and biomass: a mesocosm experiment, PLoS One 13 (2018) 1–18, https://doi.org/10.1371/journal.pone.0192555.
[54] Q. Deng, S. Aras, C.L. Yu, E.K. Dzantor, P.A. Fay, Y. Luo, W. Shen, D. Hui, Effects of precipitation changes on aboveground net primary production and soil respiration in a switchgrass field, Agric. Ecosyst. Environ. 248 (2017) 29–37, https://doi.org/10.1016/j.agee.2017.07.023.
[55] N. Ben Fradj, S. Rozakis, M. Borzęcka, M. Matyka, Miscanthus in the European bio-economy: a network analysis, Ind. Crop. Prod. 148 (2020), https://doi.org/10.1016/j.indcrop.2020.112281.
[56] R. Smith, F.M. Slater, The effects of organic and inorganic fertilizer applications to Miscanthus×giganteus, Arundo donax and Phalaris arundinacea, when grown as energy crops in Wales, UK, GCB Bioenergy (2010), https://doi.org/10.1111/j.1757-1707.2010.01051.x no-no.
[57] S. Usťak, J. Šinko, J. Muñoz, Reed canary grass (Phalaris arundinacea l.) as a promising energy crop, J. Cent. Eur. Agric. 20 (2019) 1143–1168, https://doi.org/10.5513/JCEA01/20.4.2267.
[58] R. Dopazo, D. Vega-Nieva, L. Ortiz, Herbaceous energy crops: reviewing their productivity for bioenergy production, Publ. Internet Http//…. https://www.researchgate.net/publication/228481008%0Ahttp://193.146.36.56/ence/publicaciones/Valencia_OC7.3.pdf, 2010, 1-3
[59] A. Laurent, E. Pelzer, C. Loyce, D. Makowski, Ranking yields of energy crops: a meta-analysis using direct and indirect comparisons, Renew. Sustain. Energy Rev. 46 (2015) 41–50, https://doi.org/10.1016/j.rser.2015.02.023.
[60] R.C. Miller, J.B. Zedler, Responses of native and invasive wetland plants to hydroperiod and water depth, Plant Ecol. 167 (2003) 57–69, https://doi.org/10.1023/A:1023918619073.
[61] G. Fischer, H. Van Velthuizen, M. Shah, F. Nachtergaele, Global agro-ecological assessment for agriculture in the 21st Century : methodology and results, analysis, RR-02-02, http://www.iiasa.ac.at/Admin/PUB/Documents/RR-02-002.pdf, 2002, 119.
[62] FAO, Aquamaps. Global spatial database on water and agriculture. http://www.fao.org/nr/water/aquamaps/, 2010.
[63] F.R. Rijsberman, Water scarcity: fact or fiction? Agric. Water Manag. 80 (2006) 5–22, https://doi.org/10.1016/j.agwat.2005.07.001.
[64] J. Liu, H. Yang, S.N. Gosling, M. Kummu, M. Flörke, S. Pfister, N. Hanasaki, Y. Wada, X. Zhang, C. Zheng, J. Alcamo, T. Oki, Water scarcity assessments in the past, present, and future, Earth's Futur. 5 (2017) 545–559, https://doi.org/10.1002/2016EF000518.
[65] A. Brown, M.D. Matlock, A Review of Water Scarcity Indices and Methodologies, 2011. White Pap.
[66] FAO, The State of the World's Land and Water Resources for Food and Agriculture: Managing Systems at Risk, Food and Agriculture Organization of the United Nations, Rome Earthscan, London, 2011.
[67] ECN.TNO., Phyllis2, Database for Biomass and Waste, 2019.
[68] S. Jerez, I. Tobin, R. Vautard, J.P. Montávez, J.M. López-Romero, F. Thais, B. Bartok, O.B. Christensen, A. Colette, M. Déqué, G. Nikulin, S. Kotlarski, E. Van Meijgaard, C. Teichmann, M. Wild, The impact of climate change on photovoltaic power generation in Europe, Nat. Commun. 6 (2015), https://doi.org/10.1038/ncomms10014.
[69] M. Wild, D. Folini, F. Henschel, N. Fischer, B. Müller, Projections of long-term changes in solar radiation based on CMIP5 climate models and their influence on energy yields of photovoltaic systems, Sol. Energy 116 (2015) 12–24, https://doi.org/10.1016/j.solener.2015.03.039.
[70] W. Sawadogo, B.J. Abiodun, E.C. Okogbue, Impacts of global warming on photovoltaic power generation over West Africa, Renew. Energy 151 (2020) 263–277, https://doi.org/10.1016/j.renene.2019.11.032.
[71] H.A. Kazem, M.T. Chaichan, I.M. Al-shezawi, H.S. Al-saidi, H.S. Al-rubkhi, K. Al-sinani, A.H.A. Al-waeli, Effect of humidity on the PV performance in Oman, Asian Trans. Eng. 2 (2014) 29–32.
[72] T. Bhattacharya, A.K. Chakraborty, K. Pal, Effects of ambient temperature and wind speed on performance of monocrystalline solar photovoltaic module in Tripura, India, J. Sol. Energy. 2014 (2014) 1–5, https://doi.org/10.1155/2014/817078.
[73] S. Mekhilef, R. Saidur, M. Kamalisarvestani, Effect of dust, humidity and air velocity on efficiency of photovoltaic cells, Renew. Sustain. Energy Rev. 16 (2012) 2920–2925, https://doi.org/10.1016/j.rser.2012.02.012.
[74] S. Pfenninger, I. Staffell, Long-term patterns of European PV output using 30 years of validated hourly reanalysis and satellite data, Energy 114 (2016) 1251–1265, https://doi.org/10.1016/j.energy.2016.08.060.
[75] J. Müller, D. Folini, M. Wild, S. Pfenninger, CMIP-5 models project photovoltaics are a no-regrets investment in Europe irrespective of climate change, Energy 171 (2019) 135–148, https://doi.org/10.1016/j.energy.2018.12.139.
[76] J.A. Crook, L.A. Jones, P.M. Forster, R. Crook, Climate change impacts on future photovoltaic and concentrated solar power energy output, Energy Environ. Sci. 4 (2011) 3101–3109, https://doi.org/10.1039/c1ee01495a.
[77] D. Thevenard, S. Pelland, Estimating the uncertainty in long-term photovoltaic yield predictions, Sol. Energy 91 (2013) 432–445, https://doi.org/10.1016/j.solener.2011.05.006.
[78] N.H. Reich, B. Mueller, A. Armbruster, W.G.J.H.M. van Sark, K. Kiefer, C. Reise, Performance ratio revisited: is PR>90% realistic? Prog. Photovoltaics Res. Appl. 20 (2012) 1114–1129, https://doi.org/10.1002/pip.
[79] E. Roeckner, G. Bauml, L. Bonaventura, R. Brokopf, M. Esch, M. Giorgetta, S. Hagemann, I. Kirchner, L. Kornblueh, E. Manzini, A. Rhodin, U. Schlese, U. Schulzweida, A. Tompkins, The atmospheric general circulation model ECHAM5 model description, J. Geophys. Res. Atmos. 1 (2003), https://doi.org/10.1029/2010JD014036.
[80] G. Madec, P. Delecluse, Institut pierre simon laplace ocean general circulation model reference manual, Tech. Rep. (1998).
[81] S. Valcke, The OASIS3 coupler: a European climate modelling community software, Geosci, Model Dev 6 (2013) 373–388, https://doi.org/10.5194/gmd-6-373-2013.
[82] A. Sanna, P. Lionello, S. Gualdi, Coupled atmosphere ocean climate model simulations in the Mediterranean region: effect of a high-resolution marine model on cyclones and precipitation, Nat. Hazards Earth Syst. Sci. 13 (2013) 1567–1577, https://doi.org/10.5194/nhess-13-1567-2013.
[83] E. Bucchignani, A.L. Zollo, L. Cattaneo, M. Montesarchio, P. Mercogliano, Extreme weather events over China: assessment of COSMO-CLM simulations and future scenarios, Int. J. Climatol. 37 (2017) 1578–1594, https://doi.org/10.1002/joc.4798.
[84] Y. Zheng, J. Han, Y. Huang, S.R. Fassnacht, S. Xie, E. Lv, M. Chen, Vegetation response to climate conditions based on NDVI simulations using stepwise cluster analysis for the Three-River Headwaters region of China, Ecol. Indicat. 92 (2018) 18–29, https://doi.org/10.1016/j.ecolind.2017.06.040.
[85] M.J. Alizadeh, T. Alinejad-Tabrizi, M.R. Kavianpour, S. Shamshirband, Projection of spatiotemporal variability of wave power in the Persian Gulf by the end of 21st century: GCM and CORDEX ensemble, J. Clean. Prod. 256 (2020), https://doi.org/10.1016/j.jclepro.2020.120400.
[86] I.F. Abdin, Y.P. Fang, E. Zio, A modeling and optimization framework for power systems design with operational flexibility and resilience against extreme heat waves and drought events, Renew. Sustain. Energy Rev. 112 (2019) 706–719, https://doi.org/10.1016/j.rser.2019.06.006.
[87] J.C. Pérez, A. González, J.P. Díaz, F.J. Expósito, J. Felipe, Climate change impact on future photovoltaic resource potential in an orographically complex archipelago, the Canary Islands, Renew. Energy 133 (2019) 749–759, https://doi.org/10.1016/j.renene.2018.10.077.
[88] B. François, B. Hingray, M. Borga, D. Zoccatelli, C. Brown, J.D. Creutin, Impact of climate change on combined solar and run-of-river power in Northern Italy, Energies 11 (2018) 1–22, https://doi.org/10.3390/en11020290.
[89] A. Bichet, B. Hingray, G. Evin, A. Diedhiou, C.M.F. Kebe, S. Anquetin, Potential impact of climate change on solar resource in Africa for photovoltaic energy: analyses from CORDEX-Africa climate experiments, Environ. Res. Lett. 14 (2019), https://doi.org/10.1088/1748-9326/ab500a.
[90] R. Chenni, M. Makhlouf, T. Kerbache, A. Bouzid, A detailed modeling method

for photovoltaic cells, Energy 32 (2007) 1724–1730, https://doi.org/10.1016/j.energy.2006.12.006.
[91] J.K. Tonui, Y. Tripanagnostopoulos, Performance improvement of PV/T solar collectors with natural air flow operation, Sol. Energy 82 (2008) 1–12, https://doi.org/10.1016/j.solener.2007.06.004.
[92] P. Ruiz, W. Nijs, D. Tarvydas, A. Sgobbi, A. Zucker, R. Pilli, R. Jonsson, A. Camia, C. Thiel, C. Hoyer-Klick, F. Dalla Longa, T. Kober, J. Badger, P. Volker, B.S. Elbersen, A. Brosowski, D. Thrän, ENSPRESO - an open, EU-28 wide, transparent and coherent database of wind, solar and biomass energy potentials, Energy Strateg. Rev. 26 (2019), 100379, https://doi.org/10.1016/j.esr.2019.100379.
[93] J. Malczewski, C. Rinner, Multicriteria decision analysis in geographic information science. https://doi.org/10.1007/978-3-540-74757-4, 2015.
[94] S. Dunnett, A. Sorichetta, G. Taylor, F. Eigenbrod, Harmonised global datasets of wind and solar farm locations and power, Sci. Data 7 (2020) 1–12, https://doi.org/10.1038/s41597-020-0469-8.
[95] T.L. Saaty, How to make a decision: the analytic hierarchy process, Eur. J. Oper. Res. 48 (1990) 9–26, https://doi.org/10.1016/0377-2217(90)90057-I.
[96] ESRi, ArcGIS Desktop 10.7: ArcMap Functionality Matrix, 2019.
[97] H. Yin, A. B Jr., J. Buchner, D. Helmers, B.G. Iuliano, N.E. Kimambo, K.E. Lewińska, E. Razenkova, A. Rizayeva, N. Rogova, S.A. Spawn, Y.H. Xie, V.R. C, Monitoring cropland abandonment with Landsat time series, in review, Remote Sens. Environ. 246 (2020), https://doi.org/10.1016/j.rse.2020.111873.
[98] G.I. Díaz, L. Nahuelhual, C. Echeverría, S. Marín, Drivers of land abandonment in Southern Chile and implications for landscape planning, Landsc. Urban Plann. 99 (2011) 207–217, https://doi.org/10.1016/j.landurbplan.2010.11.005.
[99] P. Meyfroidt, F. Schierhorn, A.V. Prishchepov, D. Müller, T. Kuemmerle, Drivers, constraints and trade-offs associated with recultivating abandoned cropland in Russia, Ukraine and Kazakhstan, Global Environ. Change 37 (2016) 1–15, https://doi.org/10.1016/j.gloenvcha.2016.01.003.
[100] J. Kamp, A. Reinhard, M. Frenzel, S. Kämpfer, J. Trappe, N. Hölzel, Farmland bird responses to land abandonment in Western Siberia, Agric. Ecosyst. Environ. 268 (2018) 61–69, https://doi.org/10.1016/j.agee.2018.09.009.
[101] C. Quéré, R. Andrew, P. Friedlingstein, S. Sitch, J. Hauck, J. Pongratz, P. Pickers, J. Ivar Korsbakken, G. Peters, J. Canadell, A. Arneth, V. Arora, L. Barbero, A. Bastos, L. Bopp, P. Ciais, L. Chini, P. Ciais, S. Doney, T. Gkritzalis, D. Goll, I. Harris, V. Haverd, F. Hoffman, M. Hoppema, R. Houghton, G. Hurtt, T. Ilyina, A. Jain, T. Johannessen, C. Jones, E. Kato, R. Keeling, K. Klein Goldewijk, P. Landschützer, N. Lefèvre, S. Lienert, Z. Liu, D. Lombardozzi, N. Metzl, D. Munro, J. Nabel, S.I. Nakaoka, C. Neill, A. Olsen, T. Ono, P. Patra, A. Peregon, W. Peters, P. Peylin, B. Pfeil, D. Pierrot, B. Poulter, G. Rehder, L. Resplandy, E. Robertson, M. Rocher, C. Rödenbeck, U. Schuster, I. Skjelvan, R. Séférian, I. Skjelvan, T. Steinhoff, A. Sutton, P. Tans, H. Tian, B. Tilbrook, F. Tubiello, I. Van Der Laan-Luijkx, G. Van Der Werf, N. Viovy, A. Walker, A. Wiltshire, R. Wright, S. Zaehle, B. Zheng, Global carbon budget 2018, Earth Syst. Sci. Data 10 (2018), https://doi.org/10.5194/essd-10-2141-2018.
[102] S.A. Spawn, C.C. Sullivan, T.J. Lark, H.K. Gibbs, Harmonized global maps of above and belowground biomass carbon density in the year 2010, Sci. Data 7 (2020) 1–22, https://doi.org/10.1038/s41597-020-0444-4.
[103] ESA, Land cover CCI: product user guide version 2.0 [Online], https://maps.elie.ucl.ac.be/CCI/viewer/download/ESACCI-LC-Ph2-PUGv2_2.0.pdf, 2017.
[104] Y. Yang, P. Xiao, X. Feng, H. Li, Accuracy assessment of seven global land cover datasets over China, ISPRS J. Photogrammetry Remote Sens. 125 (2017) 156–173, https://doi.org/10.1016/j.isprsjprs.2017.01.016.
[105] A. Pérez-Hoyos, F. Rembold, H. Kerdiles, J. Gallego, Comparison of global land cover datasets for cropland monitoring, Rem. Sens. 9 (2017), https://doi.org/10.3390/rs9111118.
[106] L. Liang, Q. Liu, G. Liu, H. Li, C. Huang, Accuracy evaluation and consistency analysis of four global land cover products in the arctic region, Rem. Sens. 11 (2019), https://doi.org/10.3390/rs11121396.
[107] W. Hou, X. Hou, Data fusion and accuracy analysis of multi-source land use/land cover datasets along coastal areas of the Maritime Silk Road, ISPRS Int. J. Geo-Inf. 8 (2019), https://doi.org/10.3390/ijgi8120557.
[108] X. Liu, L. Yu, W. Li, D. Peng, L. Zhong, L. Li, Q. Xin, H. Lu, C. Yu, P. Gong, Comparison of country-level cropland areas between ESA-CCI land cover maps and FAOSTAT data, Int. J. Rem. Sens. 39 (2018) 6631–6645, https://doi.org/10.1080/01431161.2018.1465613.
[109] G. Duveiller, J. Hooker, A. Cescatti, The mark of vegetation change on Earth's surface energy balance, Nat. Commun. 9 (2018), https://doi.org/10.1038/s41467-017-02810-8.
[110] B. Huang, X. Hu, G.A. Fuglstad, X. Zhou, W. Zhao, F. Cherubini, Predominant regional biophysical cooling from recent land cover changes in Europe, Nat. Commun. 11 (2020) 1–13, https://doi.org/10.1038/s41467-020-14890-0.
[111] C. Folberth, N. Khabarov, J. Balkovič, R. Skalský, P. Visconti, P. Ciais, I.A. Janssens, J. Peñuelas, M. Obersteiner, The global cropland-sparing potential of high-yield farming, Nat. Sustain. 3 (2020) 281–289, https://doi.org/10.1038/s41893-020-0505-x.
[112] J. van Vliet, Direct and indirect loss of natural area from urban expansion, Nat. Sustain. 2 (2019) 755–763, https://doi.org/10.1038/s41893-019-0340-0.
[113] X. Hu, B. Huang, F. Verones, O. Cavalett, F. Cherubini, Overview of recent land cover changes in the biodiversity hotspots. https://doi.org/10.31223/osf.io/4rwda, 2020, 1-7.
[114] S. Kang, S. Selosse, N. Maïzi, Contribution of global GHG reduction pledges to bioenergy expansion, Biomass Bioenergy 111 (2018) 142–153, https://doi.org/10.1016/j.biombioe.2017.05.017.
[115] M.D. Staples, R. Malina, P. Suresh, J.I. Hileman, S.R.H. Barrett, Aviation CO2 emissions reductions from the use of alternative jet fuels, Energy Pol. 114 (2018) 342–354, https://doi.org/10.1016/j.enpol.2017.12.007.
[116] N. Deng, P. Grassini, H. Yang, J. Huang, K.G. Cassman, S. Peng, Closing yield gaps for rice self-sufficiency in China, Nat. Commun. 10 (2019) 1–9, https://doi.org/10.1038/s41467-019-09447-9.
[117] K.F. Davis, M.C. Rulli, A. Seveso, P. D'Odorico, Increased food production and reduced water use through optimized crop distribution, Nat. Geosci. 10 (2017) 919–924, https://doi.org/10.1038/s41561-017-0004-5.
[118] M.D. Staples, H. Olcay, R. Malina, P. Trivedi, M.N. Pearlson, K. Strzepek, S.V. Paltsev, C. Wollersheim, S.R.H. Barrett, Water consumption footprint and land requirements of large-scale alternative diesel and jet fuel production, Environ. Sci. Technol. 47 (2013) 12557–12565, https://doi.org/10.1021/es4030782.
[119] M.Z. Jacobson, Review of solutions to global warming, air pollution, and energy security, Energy Environ. Sci. 2 (2009) 148–173, https://doi.org/10.1039/b809990c.
[120] V.V. Tyagi, N.A.A. Rahim, N.A.A. Rahim, J.A.L. Selvaraj, Progress in solar PV technology: research and achievement, Renew. Sustain. Energy Rev. 20 (2013) 443–461, https://doi.org/10.1016/j.rser.2012.09.028.
[121] U. Desideri, F. Zepparelli, V. Morettini, E. Garroni, Comparative analysis of concentrating solar power and photovoltaic technologies: technical and environmental evaluations, Appl. Energy 102 (2013) 765–784, https://doi.org/10.1016/j.apenergy.2012.08.033.
[122] C. Xu, T.A. Kohler, T.M. Lenton, J.C. Svenning, M. Scheffer, Future of the human climate niche, Proc. Natl. Acad. Sci. U. S. A 117 (2020), https://doi.org/10.1073/pnas.1910114117.
[123] S. Levis, A. Badger, B. Drewniak, C. Nevison, X. Ren, CLMcrop yields and water requirements: avoided impacts by choosing RCP 4.5 over 8.5, Climatic Change 146 (2018) 501–515, https://doi.org/10.1007/s10584-016-1654-9.
[124] T.J. Troy, C. Kipgen, I. Pal, The impact of climate extremes and irrigation on US crop yields, Environ. Res. Lett. 10 (2015), https://doi.org/10.1088/1748-9326/10/5/054013.
[125] B. Schauberger, S. Archontoulis, A. Arneth, J. Balkovic, P. Ciais, D. Deryng, J. Elliott, C. Folberth, N. Khabarov, C. Müller, T.A.M. Pugh, S. Rolinski, S. Schaphoff, E. Schmid, X. Wang, W. Schlenker, K. Frieler, Consistent negative response of US crops to high temperatures in observations and crop models, Nat. Commun. 8 (2017), https://doi.org/10.1038/ncomms13931.
[126] E.H. Adeh, S.P. Good, M. Calaf, C.W. Higgins, Solar PV power potential is greatest over croplands, Sci. Rep. 9 (2019) 1–6, https://doi.org/10.1038/s41598-019-47803-3.
[127] D.E.H.J. Gernaat, P.W. Bogaart, D.P.V. Vuuren, H. Biemans, R. Niessink, High-resolution assessment of global technical and economic hydropower potential, Nat. Energy 2 (2017) 821–828, https://doi.org/10.1038/s41560-017-0006-y.

Chapter 4: Energy potentials and water requirements from perennial grasses on abandoned land in the former Soviet Union

Material from: Næss, J. S., Iordan, C. M., Muri, H. & Cherubini, F. Energy potentials and water requirements from perennial grasses on abandoned land in the former Soviet Union. Environ. Res. Lett. 17, 45017 (2022).
https://doi.org/10.1088/1748-9326/ac5e67

Energy potentials and water requirements from perennial grasses on abandoned land in the former Soviet Union

ENVIRONMENTAL RESEARCH
LETTERS

LETTER

Energy potentials and water requirements from perennial grasses on abandoned land in the former Soviet Union

Jan Sandstad Næss*, Cristina Maria Iordan, Helene Muri and Francesco Cherubini

Industrial Ecology Programme, Department of Energy and Process Engineering, Norwegian University of Science and Technology, Trondheim, Norway

* Author to whom any correspondence should be addressed.

E-mail: jan.s.nass@ntnu.no

Keywords: bioenergy, abandoned land, land–energy–water nexus, irrigation

Supplementary material for this article is available online

OPEN ACCESS

RECEIVED
15 October 2021

REVISED
7 March 2022

ACCEPTED FOR PUBLICATION
16 March 2022

PUBLISHED
29 March 2022

Abstract

A ramp-up of bioenergy supply is vital in most climate change mitigation scenarios. Using abandoned land to produce perennial grasses is a promising option for near-term bioenergy deployment with minimal trade-offs to food production and the environment. The former Soviet Union (fSU) experienced substantial agricultural abandonment following its dissolution, but bioenergy potentials on these areas and their water requirements are still unclear. We integrate a regional land cover dataset tailored towards cropland abandonment, an agro-ecological crop yield model, and a dataset of sustainable agricultural irrigation expansion potentials to quantify bioenergy potentials and water requirements on abandoned land in the fSU. Rain-fed bioenergy potentials are 3.5 EJ yr^{-1} from 25 Mha of abandoned land, with land-sparing measures for nature conservation. Irrigation can be sustainably deployed on 7–18 Mha of abandoned land depending on water reservoir size, thereby increasing bioenergy potentials with rain-fed production elsewhere to 5.2–7.1 EJ yr^{-1}. This requires recultivating 29–33 Mha combined with 30–63 billion m^3 yr^{-1} of blue water withdrawals. Rain-fed productive abandoned land equals 26%–61% of the projected regional fSU land use for dedicated bioenergy crops in 2050 for 2 °C future scenarios. Sustainable irrigation can bring productive areas up to 30%–80% of the projected fSU land requirements. Unraveling the complex interactions between land availability for bioenergy and water use at local levels is instrumental to ensure a sustainable bioenergy deployment.

1. Introduction

Stringent climate change mitigation pathways typically rely on large-scale bioenergy deployment [1]. Median projected land requirements for bioenergy crops in 2100 in 1.5 °C scenarios are in the range of 430–760 million hectares (Mha) [2]. The need to dedicate large areas to bioenergy production for climate change mitigation in such scenarios raises concerns of increasing competition for land resources, deployment feasibility, and potential adverse effects on food security, water scarcity and biodiversity [3–5].

Competition for land with food production and nature conservation limits the land availability for bioenergy. Irrigation of bioenergy crops can ramp up bioenergy supply with reduced land requirements but may pose increased risks of water scarcity [6–8]. Water availability for irrigated bioenergy production is limited by competition for water with irrigated food production, urban water usage, and environmental flow protection [9, 10]. Nexus approaches integrating the interactions between bioenergy potentials, land use, and irrigation water use are key to assess environmental benefits and sustainability trade-offs of bioenergy production [11–13].

Abandoned land has emerged as a crucial option for early bioenergy deployment with reduced trade-offs on the environment and food security relative to targeting areas with primary vegetation or productive croplands [12, 14, 15]. Abandoned land is typically already affected by human activities and located near existing infrastructure as it was previously used for food production. The former Soviet Union (fSU) has experienced major historical land abandonment

over the last 30 years, mainly due to a restructuring of the economy, rural-to-urban migration, decreasing agricultural investments, and access to open markets [16–19]. A recultivation of abandoned land across the fSU may offer an opportunity to ramp-up biomass production [12, 20]. Recent research with a global perspective highlighted the substantial bioenergy potentials for the fSU and relatively high marginal energy gains from irrigation [12, 21]. The fSU also show large expansion opportunities for sustainably deployed agricultural irrigation [22].

Previous land–energy–water nexus assessments of irrigated bioenergy production on abandoned land did not consider if or where the remaining renewable water budget can sustain different levels of new irrigated agricultural activities [12]. It is unclear how sustainable irrigation strategies aiming to protect key environmental water flows can affect bioenergy production potentials. Identifying abandoned land where smaller irrigation infrastructure such as check dams can provide sufficient blue water resources to increase bioenergy productivity may be environmentally preferable to a build-up of larger irrigation infrastructure. There is also a need to investigate green water (i.e. rainfall water in soils available for plant growth) use by bioenergy crops, which is typically underrepresented in the bioenergy scenario literature [23] despite its importance in sustainable water resource management [24, 25].

Studies of bioenergy potentials on abandoned land have so far mainly taken a global scale perspective [12, 21, 26, 27]. They rely on global land cover datasets that typically lack spatially differentiated validation of cropland classes and land use transitions. Regional land cover datasets that are extensively validated and have higher accuracy than global products represents opportunities for refined bioenergy estimates. So far, area-limited studies applying regional land cover datasets are few and have been limited to the United States [28–30]. A regional land cover dataset tailored towards abandoned land has been made available for the fSU [16]. The dataset is validated both at the regional and country level against 5972 datapoints and achieves abandoned land user and producer accuracies of 31% and 62%, respectively. It is therefore an attractive dataset for refined regional assessments.

In this work, we perform a land–energy–water nexus analysis of bioenergy potentials from abandoned land by integrating specific datasets for each of the nexus elements: a recently developed and extensively validated land dataset [16] (land), an agro-ecological crop yield model (global agro-ecological zones (GAEZ) v3.0) [31] (energy), and newly developed spatial datasets of sustainable agricultural irrigation expansion [22] (water). Bioenergy potentials are quantified for two types of perennial grasses, reed canary grass and switchgrass, at rainfed and irrigated conditions and two management intensities (medium and high management intensities). In addition to fully rainfed and irrigated conditions, we consider three different sustainable irrigation management strategies and quantify their effects on bioenergy potentials and water use. Using country specific confusion matrices describing land cover dataset accuracy for correction [16], we quantify total potentials, and associated land and water use from abandoned land for each country in the fSU.

2. Methods

2.1. Land availability

We used the land cover map from Lesiv *et al* [16, 32] of arable and abandoned land across the fSU, here referred to as the hybrid map. The abandoned land class (59 Mha) from the hybrid map serves as a basis for land availability. Abandoned land is defined as land previously cultivated before 2010 that is unutilized for more than 5 years. The hybrid map was produced by combining multiple input data sets, including specialized land abandonment data from remote sensing [33–36], series of annual land cover maps [37, 38], and static land cover maps and cropland maps [39, 40]. A Bayesian network was applied to fuse them into one product at 10 arcseconds resolution [16].

Parts of the abandoned land (10%) is located within biodiversity hotspots [41] and protected areas [42] where habitat restoration can be especially beneficial for biodiversity [43, 44] (supplementary text 1 and supplementary figure 1 available online at stacks.iop.org/ERL/17/045017/mmedia). We excluded abandoned land within these areas from the main analysis using masks of biodiversity hotspots [45] and protected areas [31, 42].

For comparisons, we used country masks [46] to filter out future projections of fSU bioenergy land use in 2 °C scenarios from a gridded land cover dataset at 0.05° resolution [47] produced by the global change assessment model [48, 49] and the land use downscaling model DEMETER [50, 51]. These projections cover a comprehensive set of shared socio-economic pathways [52] (SSPs) and representative concentration pathways [53] (RCPs). We considered the harmonized future land use projections for all SSPs with RCP2.6 [54] in 2050 where the temperature target [55] is achieved (all but SSP3).

2.2. Water availability

Bioenergy potentials and water requirements are estimated according to different water supply regimes: rainfed conditions, unconstrained irrigation, and three different strategies for sustainable irrigation. The sustainable irrigation strategies are based on a state-of-the-art dataset of candidate areas for sustainable agricultural irrigation expansion from Rosa *et al* [22] that is available at 5 arcmin resolution [56]. We integrated the irrigation expansion dataset

with the hybrid map to identify abandoned land within candidate areas for sustainable agricultural irrigation. Based on the irrigation budgets from the irrigation expansion dataset, we calculated gridded fractions of abandoned land that can be irrigated.

The irrigation expansion dataset identifies irrigation practices as sustainable if their water use does not exceed local renewable water availability of surface and ground water and does not deplete environmental flows or freshwater stocks. It is based on a hydrological analysis done at a grid cell level using historical observational data (1996–2005) of precipitation, water runoff and evaporation [22]. A minimum monthly threshold of 60% of water runoff was allocated to environmental flows, thereby limiting trade-offs on freshwater ecosystems [57, 58]. Cells are classified as candidate areas for irrigation expansion if the remaining renewable water resources can meet total irrigation water requirements from the agricultural sector. It provides spatial recommendations of three irrigation strategies based on a priority list. First, a soft-path scenario with small monthly water storages meeting the necessary irrigation water requirements to avoid all crop water deficits. This is a decentralized approach with small and modular infrastructure that allows productivity benefits whilst minimizing adverse environmental impacts of large irrigation infrastructure. Second, a soft-path deficit irrigation deployment with small monthly storages where only 80% of the irrigation water requirements needed to avoid crop water deficits can be met. Third, hard-path irrigation with large annual storages transferring water both between months and from wet to dry seasons, thereby meeting all irrigation water requirements. Hard-path irrigation requires larger investments to construct large-scale water reservoirs and substantial additional infrastructure, and reservoir storage capacity needs to be larger than dry-season water withdrawals. Grids where none of the irrigation strategies can meet irrigation water requirements are classified as primarily rain-fed.

2.3. Bioenergy crop productivity

We consider two perennial grasses switchgrass and reed canary grass (supplementary text 2). Bioenergy crop yields (dry mass) and crop evapotranspiration (water evaporated and transpired from soil and plants to the atmosphere) on abandoned land were quantified at 5 arcmin resolution using data from the parameterized crop model GAEZ v3.0 [31] (supplementary text 3). We consider two different agricultural management intensities with both rain-fed and irrigated water supply. Medium agricultural management intensity refers to cultivation with a partly mechanized system and some fertilizer and pesticide use, and is closer to the dominant practice across the fSU today [12]. High agricultural management intensity represents a modern system with closed yield gaps, full mechanization, improved varieties, and optimal use of fertilizer and pesticides. For irrigated conditions, we quantified irrigation water requirements needed to avoid water deficits during the crop growth cycle with GAEZ data. Sustainable irrigation strategies (soft-path, soft-path with deficit, and hard-path) considers a mix of rain-fed and irrigated yields, which we allocated spatially based on the irrigation expansion dataset. For soft-path deficit irrigation, we assumed a linear increase in yields with partially added irrigation from fully rain-fed to irrigated conditions [59]. This means that the 80% deficit irrigation provides an 80% increase from rain-fed to fully irrigated yields. We used GAEZ data considering climatic conditions centered around the 2020s (2010–2040) from the Hadley Centre coupled model v3 [60] in the main analysis to remain comparable with previous studies [12, 21]. Additionally, we repeated the analysis considering a measurement based climate input from the Climate Research Unit [61, 62] (1960–1990) to assess how the driving climate data considered by GAEZ affects results. Dry mass crop yields are converted to bioenergy yields using lower heating values of 17.82 MJ kg^{-1} for switchgrass and 18.06 MJ kg^{-1} for reed canary grass [63].

We compared predicted switchgrass yields from GAEZ with those from a machine learning dataset [64] and from the global hydrological model H08 (v.bio1) [65] (supplementary figure 2 and supplementary text 4). Pixel-based estimates of both reed canary grass and switchgrass yields were additionally compared with observational data found in literature, both at a site-specific and an aggregated country level (supplementary figure 3 and supplementary text 5). Gathered observational data for reed canary grass and switchgrass is shown in supplementary tables 1 and 2, respectively (partly taken from [66]). We also processed yield data of willow, poplar, and eucalypt from the machine learning dataset [64] to assess the potentials of woody bioenergy crops (supplementary figure 4 and supplementary text 6), as they could be an alternative to perennial grasses.

2.4. Land–energy–water nexus

Irrigation expansion datasets are integrated with quantified bioenergy yields and land availability maps to assess the effects of different irrigation management strategies on the land–energy–water nexus. We optimized the bioenergy crop distribution for maximum primary energy production per grid cell. In total, we considered 180 different variants of land and water-dependent bioenergy potentials (supplementary table 3). Results in the main text are mainly shown for medium agricultural management intensity, and with land use constraints limited to abandoned land outside protected areas and biodiversity hotspots. Other results are available in the supplementary information.

We quantified mean bioenergy yields and evapotranspiration rates at the country level using country

masks [46]. Based on country-specific confusion matrices from the hybrid map [16, 67], we produced adjusted estimates of total bioenergy potentials, productive areas, and water use across the fSU that consider abandoned land dataset accuracy. We partition between green and blue water use. Green water is water stored locally in the soil recharged by precipitation and available for plant growth, while blue water is water withdrawn for irrigation from lakes, rivers, groundwater or artificially created infrastructure such as reservoirs [24, 68].

The land–energy–water nexus is unraveled by assessing key indicators related to bioenergy yields and land and water use. We map water use efficiency (GJ mm^{-1} ha^{-1}) given as the relationship between bioenergy potentials, crop water evapotranspiration (green and blue water), and land requirements, thereby incorporating all the dimensions of the land–energy–water nexus. Similarly, we assess marginal energy gains of irrigation (GJ mm^{-1} ha^{-1}), as the relationship between total energy gains of irrigation, irrigated land use, and irrigated blue water use. This indicator includes energy gains from changes in the optimal crop calendar allowed by irrigated water supply and is not directly comparable to water use efficiency. Finally, we show green and blue water footprints (m^3 GJ^{-1}), assessing trade-offs between water depletion and increased bioenergy production.

3. Results

3.1. Bioenergy potentials, productive land, and water use

Depending on water supply system, the total bioenergy potential from abandoned land range between 3.5 and 16 exajoules (EJ) yr^{-1}, assuming optimal crop mix, medium agricultural management intensity, and sparing of protected areas and biodiversity hotspots for nature conservation (figure 1(a)). The associated productive land requirements are 25–53 Mha (figure 1(b)). Green and blue water requirements are 98–192 billion m^3 and 0–223 billion m^3, respectively (figure 1(c)).

The rain-fed bioenergy potential is 3.5 EJ yr^{-1}. The corresponding green water use is 108 billion m^3 yr^{-1}, with 19 and 6.3 Mha of land allocated to reed canary grass and switchgrass, respectively. In general, high bioenergy potentials heavily rely on irrigation deployment, which boosts yields and increases productive area extent through increased water use. We find that 18 Mha of the 53 Mha of abandoned land outside biodiversity hotspots and protected areas can be irrigated without breaching grid-box specific water budgets, based on local renewable freshwater availability and environmental flow protection (supplementary figure 5). Implementing sustainable irrigation strategies can double bioenergy potentials relative to rain-fed conditions (figure 1(a)). Introducing soft-path irrigation with small monthly water storages on 7.8 Mha by applying 30 billion m^3 yr^{-1} of blue water withdrawals allows adding another 4.4 Mha (or +8%) into production, thereby increasing the bioenergy potential by 1.7 EJ yr^{-1} (or +49%). Additional soft-path irrigation with water deficits on 2.5 Mha of land increases potentials with another 0.6 EJ yr^{-1} and blue water use with another 10 billion m^3 yr^{-1}. Adding hard path irrigation management with large annual water storage deployed on 7.9 Mha further ramps-up bioenergy potentials with 1.3 EJ yr^{-1} and blue water requirements with 22 billion m^3 yr^{-1}, respectively. With complete irrigation, a maximum potential of 16 EJ yr^{-1} is achievable with 223 billion m^3 yr^{-1} of blue water withdrawals. However, this involves using 160 billion m^3 of blue water for irrigation where it is classified as unsustainable.

Compared to the land area in the fSU set aside for bioenergy in 2050 across different SSPs for 2 °C scenarios, our estimates of rain-fed productive abandoned land are equal to 26%–61% (figure 1(d)). The inclusion of different sustainable irrigation strategies can bring productive areas up to 30%–80% of it. The highest projected fSU land demand for bioenergy crops is found in SSP5-2.6 with 97 Mha, and productive rain-fed abandoned land equals 26% of it. Different irrigation management strategies increase productive land area to 30%–34% of SSP5-2.6 land requirements, respectively.

With improved agricultural management to close yield gaps (high agricultural management intensity), bioenergy potentials are 3.9–21 EJ yr^{-1}, or 12%–31% higher than those at medium management intensity across the different water supply systems (supplementary figure 6). The three considered sustainable irrigation strategies achieve potentials between 6.1 and 8.6 EJ yr^{-1}, with 32–67 billion m^3 yr^{-1} of blue water withdrawals and 6.6–16.3 Mha of irrigated areas. Whilst total blue water withdrawals for irrigation increase (+7% for all) to meet rising rain-fed crop water deficits per hectare, the total irrigated area extent decreases (−6% to −7%) across irrigation strategies. This is due to blue water budget constraints that limits further water withdrawals to remain sustainable in some locations (supplementary figure 7).

3.2. Bioenergy productivity across water management strategies

With rain-fed water supply at medium agricultural management intensity, reed canary grass is the dominant crop (figure 2). Reed canary grass and switchgrass yields at rain-fed conditions range between 50–200 GJ ha^{-1} yr^{-1} and 150–250 GJ ha^{-1} yr^{-1}, respectively. Crop water deficits are a major constraint to bioenergy productivity across the fSU. With irrigation, nearly all abandoned lands are productive, and switchgrass becomes the highest yielding crop in most locations. Irrigated bioenergy yields mainly range between 150–200 GJ ha^{-1} yr^{-1}

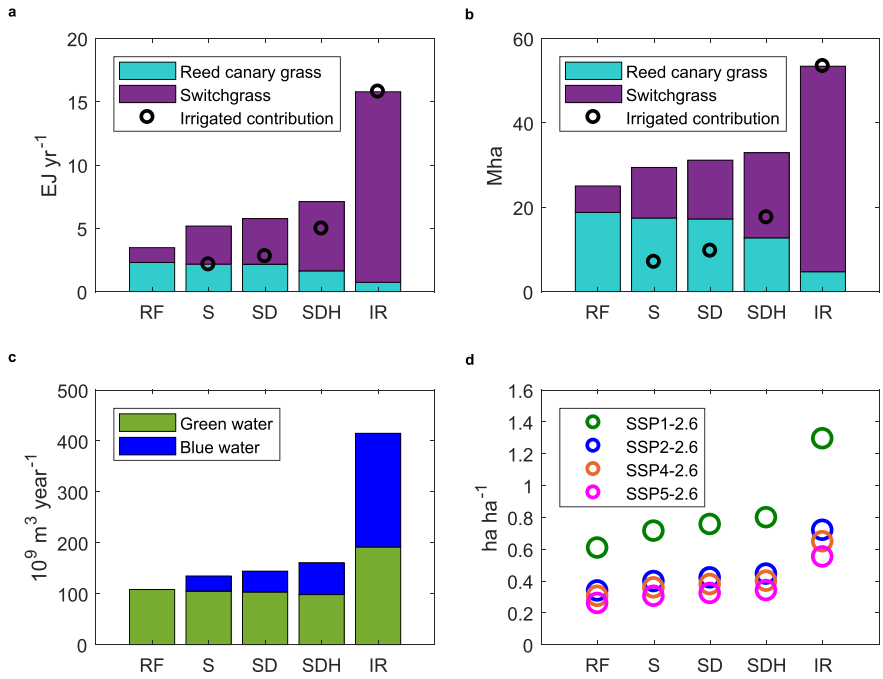

Figure 1. Bioenergy potentials and their land and water use requirements across water supply systems. (a) Bioenergy potentials (EJ yr^{-1}). (b) Productive abandoned land (Mha). (c) Crop water use (10^9 m^3 yr^{-1}) originating from green and blue water sources (local precipitation and irrigated water withdrawals, respectively). (d) Total productive abandoned land found here divided by projected SSPx-2.6 fSU bioenergy land use in 2050 (ha/ha). All shown values are adjusted for country-specific land cover dataset confusion matrices. Medium agricultural management intensity is considered. Water supply systems are rain-fed (RF), soft-path irrigation with monthly water storage (S), soft-path irrigation with crop water deficit (D), hard-path irrigation with annual water storage (H), and complete irrigation (IR). Water supply systems applying combinations of S, D, and H considers rain-fed supply on the remaining non-irrigated land. Land use considered refer to abandoned land outside biodiversity hotspots and protected areas. Irrigated part of productive lands and bioenergy potentials are shown in (a) and (b) with an empty black circle.

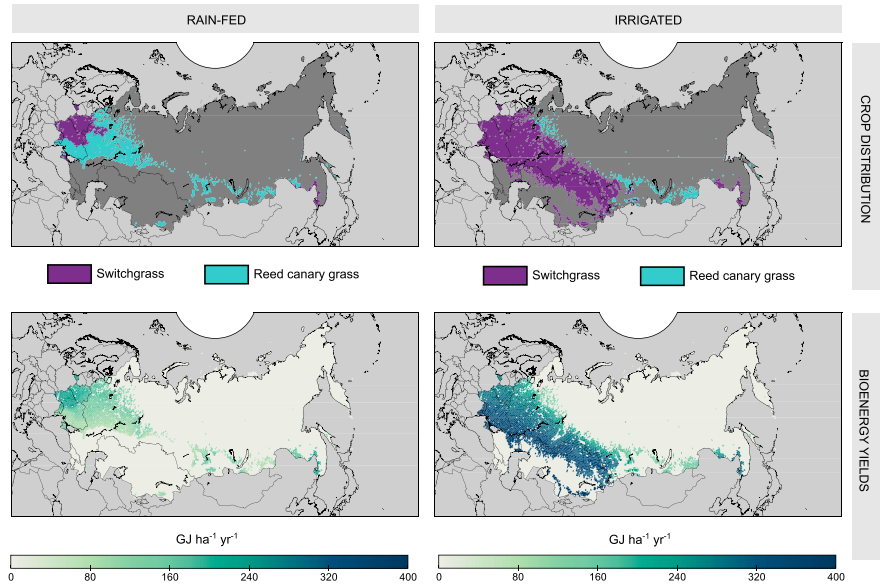

Figure 2. Irrigation effects on spatially optimal crop allocation and bioenergy yields at medium agricultural management intensity. Results are shown for rain-fed and irrigated water supply in left and right columns, respectively.

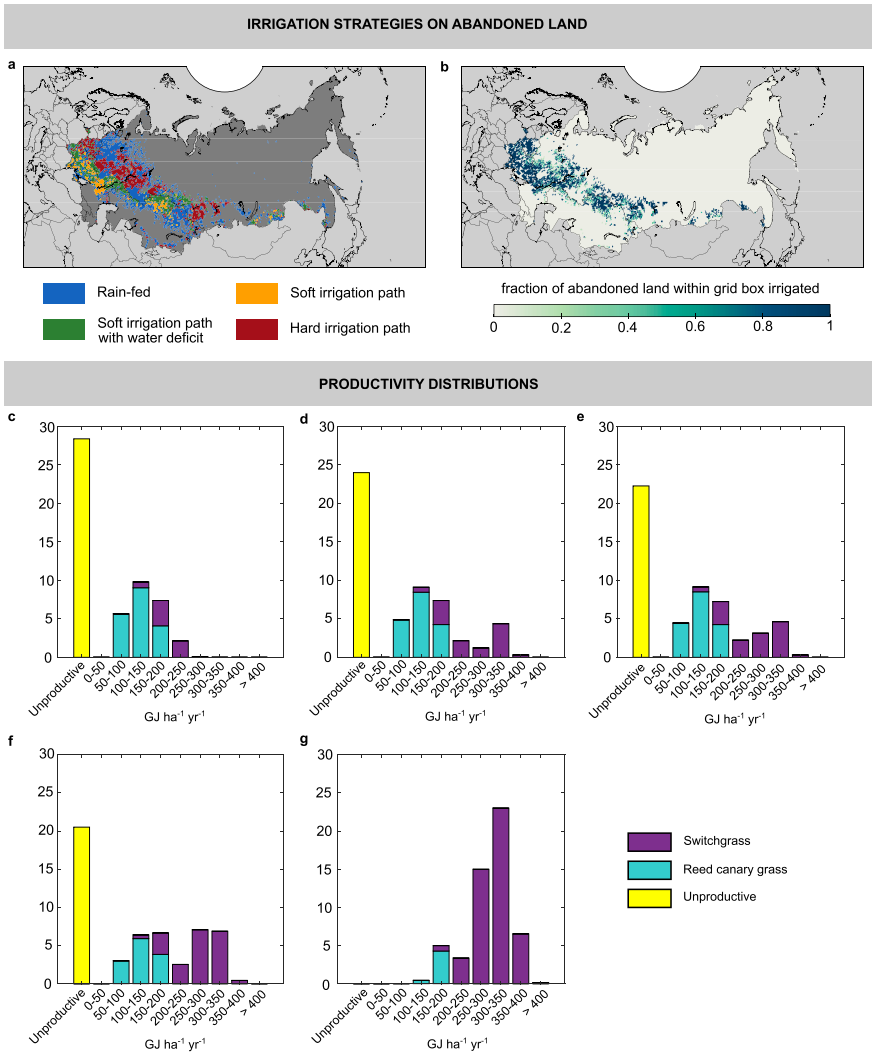

Figure 3. Spatial distribution and productivity histograms of candidate irrigation strategies on abandoned land. (a) Spatial locations of abandoned land under different candidate areas for sustainable irrigation expansion. Irrigation strategies are soft-path, soft-path with water deficit, hard-path and areas which should be primarily rain-fed as they are not suitable for sustainable irrigation. (b) Fraction of abandoned land within each grid box that can be sustainably irrigated whilst sustaining environmental flows. Productivity histograms (c)–(g) refers to (c) no irrigation with fully rain-fed conditions, (d) soft-path irrigation and rain-fed conditions elsewhere, (e) soft-path and soft-path with water deficit irrigation and rain-fed conditions elsewhere, (f) soft-path, soft-path with water deficit, and hard-path irrigation and rain-fed conditions elsewhere, and (g) complete irrigation (including unsustainable areas). Medium agricultural management intensity is considered. The maps in (a) and (b) are harmonized with the histogram in (f).

and 200–400 GJ ha^{-1} yr^{-1} for reed canary grass and switchgrass, respectively.

In addition to the full irrigation, bioenergy potentials are also explored according to the deployment of three intermediate sustainable irrigation strategies (following [22]) (figure 3 and supplementary figure 8). Considering soft-path and soft-path deficit irrigation approaches with small monthly water storages, we find suitable areas mainly north of the Black Sea, Northern Kazakhstan, in addition to some smaller clusters in Eastern Russia (figure 3(a)). A hard irrigation path with large annual storages can be considered around the middle and upper Volga region and in parts of Belarus.

At rain-fed conditions the mean bioenergy yield is 139 GJ ha^{-1} yr^{-1} with 28 Mha left unproductive (figure 3(c)). Reed canary grass and switchgrass have mean bioenergy yields of 122 and 187 GJ ha^{-1} yr^{-1}, respectively. Soft-path irrigation (figure 3(d)) increases the mean bioenergy yield to

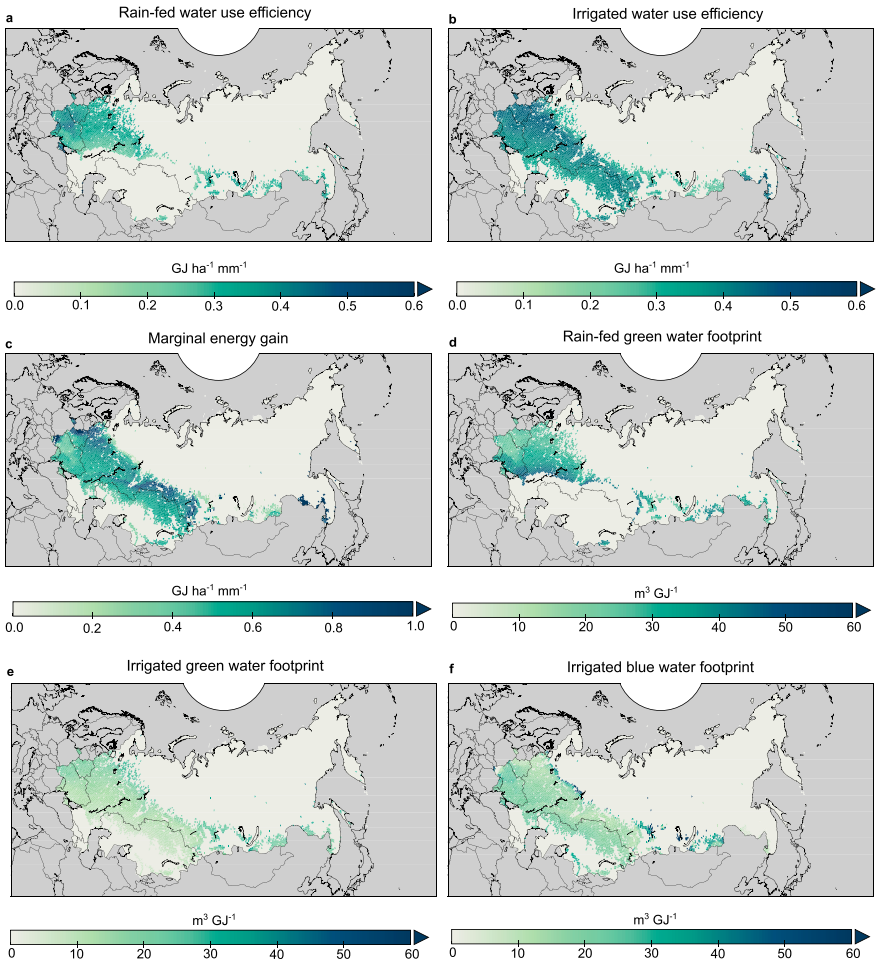

Figure 4. Land–energy–water interactions of deploying bioenergy with optimal crop allocation and medium management intensity. (a) Water use efficiency at rain-fed conditions. (b) Water use efficiency at irrigated conditions. (c) Marginal energy gain of irrigation deployment. (d) Green water footprint at rain-fed conditions. (e) Green water footprint at irrigated conditions. (f) Blue water footprint at irrigated conditions. The blue water footprint is given here as the blue water use per unit energy gained at irrigated conditions relative to at rain-fed conditions.

176 GJ ha^{-1} yr^{-1}, while additionally considering soft-path deficit irrigation (figure 3(e)) and hard-path irrigation (figure 3(f)) increases means to 185 and 216 GJ ha^{-1} yr^{-1}, respectively. Deploying all three paths reduces unproductive areas to 21 Mha (−25%). Mean switchgrass yields increase more than reed canary grass yields relative to rain-fed conditions (to 271 and 128 GJ ha^{-1} yr^{-1} (or +45% and +5%), respectively). With complete irrigation (figure 3(g)) mean bioenergy yields are 296 GJ ha^{-1} yr^{-1}, but it implies irrigating areas where blue water withdrawals are unsustainable or where blue water might not be locally available.

Large productive areas with rain-fed water supply are found in Russia (21 Mha) and Ukraine (2.9 Mha), with bioenergy potentials of 2.8 and 0.5 EJ yr^{-1}, and mean bioenergy yields of 133 and 164 GJ ha^{-1} yr^{-1} (supplementary table 4). Kazakhstan has limited productive areas at rain-fed conditions (0.3 Mha), and different sustainable irrigation management strategies can substantially favor bioenergy productivity (up to 3.6 Mha of land can become productive with a potential of 1.0 EJ yr^{-1}).

3.3. Spatial land–energy–water interactions

Water use efficiencies range between 0.2 and 0.5 GJ ha^{-1} mm^{-1} at rain-fed conditions and medium management intensity (figure 4(a)). Water use efficiencies are typically higher with switchgrass than reed canary grass. With irrigation, the combined use of green and blue water increases water use efficiencies to above 0.3 GJ ha^{-1} mm^{-1} everywhere with a fSU mean of 0.38 GJ ha^{-1} mm^{-1} (figure 4(b)). This

is due to more land being allocated to switchgrass and to changing crop calendars.

Marginal energy gains of irrigation mainly range between 0.3 and 1 GJ ha^{-1} mm^{-1} (figure 4(c)). Marginal energy gains are especially high in the very western part of the fSU, in Eastern Russia and in Russia–Kazakhstan border areas. Lower marginal energy gains below 0.5 GJ ha^{-1} mm^{-1} are found in Siberia, and southern parts of Kazakhstan.

Blue water withdrawals for irrigation also affect green water use as it can allow for a crop change or make new areas cultivable. At rain-fed conditions, green water footprints are primarily between 20 and 50 m^3 GJ^{-1}, with a mean of 31 m^3 GJ^{-1} (figure 4(d)). Spatially, the green water footprint is higher in areas allocated to reed canary grass than to switchgrass. We find decreasing green water footprint with irrigation across the fSU to 0–30 m^3 GJ^{-1} with a mean of 12 m^3 GJ^{-1} (figure 4(e)). Green water footprints are above 20 m^3 GJ^{-1} only at high latitudes and in the Eastern parts of Russia. In areas with relatively low green water footprint the crop water use is dominated by irrigated blue water, such as in large parts of Kazakhstan. Blue water footprints are between 10 and 40 m^3 GJ^{-1}, with a fSU mean of 18 m^3 GJ^{-1} (figure 4(f)). The highest blue water footprints are found in Siberia. Of the three sustainable irrigation strategies, soft path deficit irrigation has the highest blue water footprint with 20 m^3 GJ^{-1}, while soft and hard-path irrigation have means of 17 and 16 m^3 GJ^{-1}, respectively (caused by the differences in spatial distribution of the irrigation strategies).

Irrigation can be an especially attractive option where smaller water reservoirs can provide enough blue water for (deficit) irrigation and where bioenergy yield gains per unit of supplied water is relatively high. Clusters with both marginal energy gains of irrigation in the top quartile and soft-path or soft-path with deficit irrigation opportunities are found in Russia–Kazakhstan border areas, in the far west of Ukraine, and in Eastern Russia.

4. Discussion and conclusions

Our study finds higher bioenergy potentials (3.5–23 EJ yr^{-1} across 180 scenarios) from abandoned lands in the fSU than in previous studies (0.7–3.8 EJ yr^{-1}) [12, 21] that used a global land cover product to identify abandoned cropland (supplementary table 5). To isolate the role of the land cover dataset, we used the same yield model and considered the same climatic conditions and agricultural management intensities as in those previous studies. The increase in potential found here is attributable to the use of a validated regional land cover dataset tailored for land abandonment monitoring, which is a clear advance relative to global land cover datasets [16, 67].

There are still a variety of uncertainties and limitations that can affect our findings (supplementary text 7). For example, the irrigation expansion dataset is based on historical data [22], while bioenergy potentials are quantified here for a 30 years average climate centered around the 2020s. We also considered a measurement based climate input to the yield model (supplementary figure 9). This led to highly comparable results in terms of sustainable potentials for rain-fed production and with small monthly water storages (−1.5% to +2.9% change, medium agricultural management). They differed somewhat more with the additional introduction of larger hard-path annual water storages (−6.7% change). It also led to increasing productive area extent (up to 4.4%), increases in green water use (up to 10%), and decreases in blue water use (down to −13%) for these scenarios. More research is needed to assess how bioenergy potentials are affected by changing crop productivity, water use, and irrigation opportunities under future climatic conditions.

The climate change mitigation benefits of bioenergy production on abandoned land will depend on the degree of natural regrowth since abandonment and bioenergy conversion technology [69]. Most of the abandoned land in the fSU has been under natural regrowth for nearly three decades with shrubs and young forests appearing in many locations [16, 70]. In general, the carbon accumulation has been slow in the fSU with few areas exceeding 5 Mg C ha^{-1} and with the highest standing carbon stocks in the western parts of the region [70]. Bioenergy deployment should aim to target areas where bioenergy crop productivity and the climate benefits of fossil fuel substitution outperforms natural based solutions.

Deploying bioenergy crops on fSU abandoned land can contribute to close regional ambition gaps to meet the National Declared Contributions to the Paris Agreement [71], especially when bioenergy production is coupled with carbon capture and storage (BECCS) [14, 69, 72]. Perennial grasses can serve as an input to BECCS in thermal power plants or in biorefineries, as the biomass conversion processes involved produce exhaust CO_2 streams targetable for carbon capture [69, 72, 73]. Comparing our findings with future fSU land use projections in 2050 for 2 °C scenarios shows that rain-fed productive abandoned lands can meet 26%–61% of bioenergy land requirements across the SSPs (or 30%–80% with sustainable irrigation). A further deployment of bioenergy crops would require targeting present day cropland, pastures, or areas with primary vegetation. Future agricultural intensification or a reduction in land-based feed and food products through dietary changes would be needed to free lands for additional bioenergy production [2, 74].

While the hard-path irrigation strategy is sustainable in the sense that it accounts for environmental

flow protection [22], it also involves high capital costs and the construction of large water reservoir infrastructure that can be unsustainable by impacting habitats, displacing humans or altering hydrological regimes [75]. These factors must be accounted for in irrigation planning, and the smaller dams needed in the soft-path strategy have relatively lower risks of causing sustainability trade-offs. Any large-scale deployment of irrigation infrastructure would likely require policy support and incentives and should be accompanied by legislations aiming to ensure their sustainability.

Management of land and water resources stands at the heart of sustainable bioenergy deployment strategies. While irrigated bioenergy deployment increases bioenergy potentials with reduced land requirements, uncontrolled irrigation expansion risks causing water stress [7]. Our findings suggests that irrigation can be sustainably considered in up to 18 Mha of abandoned land. This can double bioenergy potentials relative to rain-fed conditions from 3.5 to 7.1 EJ yr^{-1}, but involves using a large share of the remaining sustainably available blue water budget in the fSU (supplementary figure 10), thereby limiting the opportunity for new irrigated food production.

As recultivation is currently gaining momentum in the fSU [20, 76], the joint consideration of potential environmental and socio-economic co-benefits or trade-offs of land sparing and rain-fed or irrigated recultivation for food and bioenergy production is important to identify optimal land and water management practices at the local level. Assessments should determine how global challenges can be better addressed from the given local context. Using abandoned land to grow bioenergy crops is a favorable way of increasing bioenergy supply with reduced risks to food security and the environment. Nexus approaches integrating the multiple complex interactions between bioenergy potentials, and land and water use contributes to improved understanding of resource management and to shaping sustainable bioenergy deployment strategies.

Data availability statements

The data that support the findings of this study are available upon reasonable request from the authors.

Acknowledgments

We gratefully acknowledge the provision of GAEZ data by IIASA, GPWv4 data by NASA, lower heating values by Phyllis2, fSU land cover data [16, 32], sustainable irrigation expansion data [22, 56], GCAM-DEMETER land use projections [47], lignocellulosic bioenergy crop yields data [64, 66], and biodiversity hotspots data [45]. We thank Zhipin Ai for providing H08 yield data for switchgrass. H M was funded by Research council of Norway project Bio4-7Seas (Project No. 302276) and the European Union's Horizon 2020 research and innovation programme under Grant Agreement No 869357, Project OceanNETs. Computations were performed on resources provided by Sigma2—the National Infrastructure for High Performance Computing and Data Storage in Norway (Account nn9518k).

Conflict of interest

The authors declare no conflict of interest.

ORCID iDs

Jan Sandstad Næss https://orcid.org/0000-0003-3166-913X
Cristina Maria Iordan https://orcid.org/0000-0001-9975-2656
Helene Muri https://orcid.org/0000-0003-4738-493X
Francesco Cherubini https://orcid.org/0000-0002-7147-4292

References

[1] Rogelj J *et al* 2018 Scenarios towards limiting global mean temperature increase below 1.5 °C *Nat. Clim. Change* **8** 325–32
[2] IPCC 2019 Summary for policymakers *Climate Change and Land: An IPCC Special Report on Climate Change, Desertification, Land Degradation, Sustainable Land Management, Food Security, and Greenhouse Gas Fluxes in Terrestrial Ecosystems*
[3] Vaughan N E and Gough C 2016 Expert assessment concludes negative emissions scenarios may not deliver *Environ. Res. Lett.* **11** 95003
[4] Forster J, Vaughan N E, Gough C, Lorenzoni I and Chilvers J 2020 Mapping feasibilities of greenhouse gas removal: key issues, gaps and opening up assessments *Glob. Environ. Change* **63** 102073
[5] Anderson K and Peters G 2016 The trouble with negative emissions *Science* **354** 182 LP—183
[6] Jans Y, Berndes G, Heinke J, Lucht W and Gerten D 2018 Biomass production in plantations: land constraints increase dependency on irrigation water *GCB Bioenergy* **10** 628–44
[7] Stenzel F, Greve P, Lucht W, Tramberend S, Wada Y and Gerten D 2021 Irrigation of biomass plantations may globally increase water stress more than climate change *Nat. Commun.* **12** 1512
[8] Stenzel F, Gerten D, Werner C and Jägermeyr J 2019 Freshwater requirements of large-scale bioenergy plantations for limiting global warming to 1.5 °C *Environ. Res. Lett.* **14** 84001
[9] D'Odorico P *et al* 2018 The global food-energy-water nexus *Rev. Geophys.* **56** 456–531
[10] Ai Z, Hanasaki N, Heck V, Hasegawa T and Fujimori S 2021 Global bioenergy with carbon capture and storage potential is largely constrained by sustainable irrigation *Nat. Sustain.* **4** 884–91
[11] Liu J *et al* 2018 Nexus approaches to global sustainable development *Nat. Sustain.* **1** 466–76
[12] Næss J S, Cavalett O and Cherubini F 2021 The land–energy–water nexus of global bioenergy potentials from abandoned cropland *Nat. Sustain.* **4** 525–36

[13] Johnson N et al 2019 Integrated solutions for the water-energy-land nexus: are global models rising to the challenge? Water 11 2223
[14] Muri H 2018 The role of large-scale BECCS in the pursuit of the 1.5 °C target: an Earth system model perspective Environ. Res. Lett. 13 44010
[15] Daioglou V, Doelman J C, Wicke B, Faaij A and van Vuuren D P 2019 Integrated assessment of biomass supply and demand in climate change mitigation scenarios Glob. Environ. Change 54 88–101
[16] Lesiv M et al 2018 Spatial distribution of arable and abandoned land across former Soviet Union countries Sci. Data 5 180056
[17] Lasanta T, Arnáez J, Pascual N, Ruiz-Flaño P, Errea M P and Lana-Renault N 2017 Space–time process and drivers of land abandonment in Europe CATENA 149 810–23
[18] Baumann M, Kuemmerle T, Elbakidze M, Ozdogan M, Radeloff V C, Keuler N S, Prishchepov A V, Kruhlov I and Hostert P 2011 Patterns and drivers of post-socialist farmland abandonment in Western Ukraine Land Use Policy 28 552–62
[19] Li S and Li X 2017 Global understanding of farmland abandonment: a review and prospects J. Geogr. Sci. 27 1123–50
[20] Prishchepov A V, Ponkina E V, Sun Z, Bavorova M and Yekimovskaja O A 2021 Revealing the intentions of farmers to recultivate abandoned farmland: a case study of the Buryat Republic in Russia Land Use Policy 107 105513
[21] Leirpoll M E, Næss J S, Cavalett O, Dorber M, Hu X and Cherubini F 2021 Optimal combination of bioenergy and solar photovoltaic for renewable energy production on abandoned cropland Renew. Energy 168 45–56
[22] Rosa L, Chiarelli D D, Sangiorgio M, Beltran-Peña A A, Rulli M C, D'Odorico P and Fung I 2020 Potential for sustainable irrigation expansion in a 3 °C warmer climate Proc. Natl Acad. Sci. 117 29526 LP–29534
[23] Stenzel F, Gerten D and Hanasaki N 2021 Global scenarios of irrigation water abstractions for bioenergy production: a systematic review Hydrol. Earth Syst. Sci. 25 1711–26
[24] Rockström J, Falkenmark M, Karlberg L, Hoff H, Rost S and Gerten D 2009 Future water availability for global food production: the potential of green water for increasing resilience to global change Water Resour. Res. 45 W00A12
[25] Velpuri N M and Senay G B 2017 Partitioning evapotranspiration into green and blue water sources in the conterminous United States Sci. Rep. 7 6191
[26] Campbell J E, Lobell D B, Genova R C and Field C B 2008 The global potential of bioenergy on abandonded agricultural lands Environ. Sci. Technol. 42 5791–4
[27] Cai X, Zhang X and Wang D 2011 Land availability analysis for biofuel production Environ. Sci. Technol. 45 334–9
[28] Baxter R E and Calvert K E 2017 Estimating available abandoned cropland in the United States: possibilities for energy crop production Ann. Am. Assoc. Geogr. 107 1162–78
[29] Zumkehr A and Campbell J E 2013 Historical US cropland areas and the potential for bioenergy production on abandoned croplands Environ. Sci. Technol. 47 3840–7
[30] Lark T J, Meghan Salmon J and Gibbs H K 2015 Cropland expansion outpaces agricultural and biofuel policies in the United States Environ. Res. Lett. 10 44003
[31] Fischer G et al 2012 Global agro-ecological zones (GAEZ v3. 0)-model documentation
[32] Lesiv M et al 2017 Spatial distribution of abandoned arable land in former Soviet Union countries, link to map in GeoTIFF format. In supplement to: Lesiv M et al 2018 Spatial distribution of arable and abandoned land across former Soviet Union countries Sci. Data 5 180056
[33] Alcantara C et al 2013 Mapping the extent of abandoned farmland in Central and Eastern Europe using MODIS time series satellite data Environ. Res. Lett. 8 35035
[34] Estel S, Kuemmerle T, Alcántara C, Levers C, Prishchepov A and Hostert P 2015 Mapping farmland abandonment and recultivation across Europe using MODIS NDVI time series Remote Sens. Environ. 163 312–25
[35] Schierhorn F, Müller D, Beringer T, Prishchepov A V, Kuemmerle T and Balmann A 2013 Post-Soviet cropland abandonment and carbon sequestration in European Russia, Ukraine, and Belarus Glob. Biogeochem. Cycles 27 1175–85
[36] Prishchepov A V, Radeloff V C, Baumann M, Kuemmerle T and Müller D 2012 Effects of institutional changes on land use: agricultural land abandonment during the transition from state-command to market-driven economies in post-Soviet Eastern Europe Environ. Res. Lett. 7 24021
[37] Defourny P et al 2017 Land cover CCI product user guide version 2.0
[38] Friedl M A, Sulla-Menashe D, Tan B, Schneider A, Ramankutty N, Sibley A and Huang X 2010 Remote sensing of environment MODIS collection 5 global land cover : algorithm refinements and characterization of new datasets Remote Sens. Environ. 114 168–82
[39] Kraemer R, Prishchepov A V, Müller D, Kuemmerle T, Radeloff V C, Dara A, Terekhov A and Frühauf M 2015 Long-term agricultural land-cover change and potential for cropland expansion in the former Virgin Lands area of Kazakhstan Environ. Res. Lett. 10 54012
[40] Jun C, Ban Y and Li S 2014 Open access to Earth land-cover map Nature 514 434
[41] Myers N, Mittermeier R A, Mittermeier C G, Fonseca G A B and Kent J 2000 Biodiversity hotspots for conservation priorities Nature 403 853–8
[42] WDPA 2009 World database of protected areas (Annual Release)
[43] Folberth C, Khabarov N, Balkovič J, Skalský R, Visconti P, Ciais P, Janssens I A, Peñuelas J and Obersteiner M 2020 The global cropland-sparing potential of high-yield farming Nat. Sustain. 3 281–9
[44] Hu X, Huang B, Verones F, Cavalett O and Cherubini F 2020 Overview of recent land-cover changes in biodiversity hotspots Front. Ecol. Environ. 19 91–97
[45] Hoffman M, Koenig K, Bunting G, Costanza J and Williams K J 2016 Biodiversity hotspots (version 2016.1) (https://doi.org/10.5281/zenodo.3261807)
[46] Center for International Earth Science Information Network—CIESIN and Columbia University & Centro Internacional de Agricultura Tropical—CIAT Gridded population of the World, version 4 (GPWv4): national identifier grid (https://doi.org/10.7927/H4TD9VDP)
[47] Chen M, Vernon C R, Graham N T, Hejazi M, Huang M, Cheng Y and Calvin K 2020 Global land use for 2015–2100 at 0.05° resolution under diverse socioeconomic and climate scenarios Sci. Data 7 320
[48] Calvin K et al 2019 GCAM v5.1: representing the linkages between energy, water, land, climate, and economic systems Geosci. Model Dev. 12 677–98
[49] Wise M, Calvin K, Kyle P, Luckow P and Edmonds J A E 2014 Economic and physical modeling of land use in GCAM 3.0 and an application to agricultural productivity, land, and terrestrial carbon Clim. Change Econ. 05 1450003
[50] Chen M, Vernon C R, Huang M, Calvin K V and Kraucunas I P 2019 Calibration and analysis of the uncertainty in downscaling global land use and land cover projections from GCAM using Demeter (v1.0.0) Geosci. Model Dev. 12 1753–64
[51] Vernon C R, Le Page Y, Chen M, Huang M, Calvin K V, Kraucunas I P and Braun C J 2018 Demeter—a land use and land cover change disaggregation model J. Open Res. Softw. 6
[52] Riahi K et al 2017 The shared socioeconomic pathways and their energy, land use, and greenhouse gas emissions implications: an overview Glob. Environ. Change 42 153–68
[53] van Vuuren D P et al 2011 The representative concentration pathways: an overview Clim. Change 109 5

[54] van Vuuren D P et al 2011 RCP2. 6: exploring the possibility to keep global mean temperature increase below 2 °C *Clim. Change* **109** 95–116
[55] Chen M et al 2020 Global land use for 2015–2100 at 0.05° resolution under diverse socioeconomic and climate scenarios (Pacific Northwest National Laboratory) 2; PNNL (https://doi.org/10.25584/data.2020-07.1357/1644253)
[56] Rosa L et al 2020 *Potential for sustainable irrigation expansion in a 3C warmer climate [Data set] Zenodo* (https://doi.org/10.5281/zenodo.3995044)
[57] Jägermeyr J, Pastor A, Biemans H and Gerten D 2017 Reconciling irrigated food production with environmental flows for sustainable development goals implementation *Nat. Commun.* **8** 15900
[58] Pastor A V, Ludwig F, Biemans H, Hoff H and Kabat P 2014 Accounting for environmental flow requirements in global water assessments *Hydrol. Earth Syst. Sci.* **18** 5041–59
[59] Rosa L, Chiarelli D D, Rulli M C, Dell'Angelo J and D'Odorico P 2020 Global agricultural economic water scarcity *Sci. Adv.* **6** eaaz6031
[60] Cox P M, Betts R A, Bunton C B, Essery R L H, Rowntree P R and Smith J 1999 The impact of new land surface physics on the GCM simulation of climate and climate sensitivity *Clim. Dyn.* **15** 183–203
[61] New M, Lister D, Hulme M and Makin I 2002 A high-resolution data set of surface climate over global land areas *Clim. Res.* **21** 1–25
[62] Mitchell T D and Jones P D 2005 An improved method of constructing a database of monthly climate observations and associated high-resolution grids *Int. J. Climatol.* **25** 693–712
[63] ECN.TNO 2019 Phyllis2, database for (treated) biomass, algae, feedstocks for biogas production and biochar (available at: https://phyllis.nl/)
[64] Li W et al 2020 Mapping the yields of lignocellulosic bioenergy crops from observations at the global scale *Earth Syst. Sci. Data* **12** 789–804
[65] Ai Z, Hanasaki N, Heck V, Hasegawa T and Fujimori S 2020 Simulating second-generation herbaceous bioenergy crop yield using the global hydrological model H08 (v.bio1) *Geosci. Model Dev.* **13** 6077–92
[66] Li W, Ciais P, Makowski D and Peng S 2018 A global yield dataset for major lignocellulosic bioenergy crops based on field measurements *Sci. Data* **5** 180169
[67] Olofsson P, Foody G M, Herold M, Stehman S V, Woodcock C E and Wulder M A 2014 Good practices for estimating area and assessing accuracy of land change *Remote Sens. Environ.* **148** 42–57
[68] Liu J et al 2017 Water scarcity assessments in the past, present, and future *Earth's Future* **5** 545–59
[69] Field J L et al 2020 Robust paths to net greenhouse gas mitigation and negative emissions via advanced biofuels *Proc. Natl Acad. Sci.* **117** 21968 LP–77
[70] Meyfroidt P, Schierhorn F, Prishchepov A V, Müller D and Kuemmerle T 2016 Drivers, constraints and trade-offs associated with recultivating abandoned cropland in Russia, Ukraine and Kazakhstan *Glob. Environ. Change* **37** 1–15
[71] Roelfsema M et al 2020 Taking stock of national climate policies to evaluate implementation of the Paris Agreement *Nat. Commun.* **11** 2096
[72] Hanssen S V, Daioglou V, Steinmann Z J N, Doelman J C, van Vuuren D P and Huijbregts M A J 2020 The climate change mitigation potential of bioenergy with carbon capture and storage *Nat. Clim. Change* **10** 1023–9
[73] Liu G, Larson E D, Williams R H, Kreutz T G and Guo X 2011 Making Fischer−Tropsch fuels and electricity from coal and biomass: performance and cost analysis *Energy Fuels* **25** 415–37
[74] van Vuuren D P, Bijl D L, Bogaart P, Stehfest E, Biemans H, Dekker S C, Doelman J C, Gernaat D E H J and Harmsen M 2019 Integrated scenarios to support analysis of the food–energy–water nexus *Nat. Sustain.* **2** 1132–41
[75] Gleick P H 2003 Global freshwater resources: soft-path solutions for the 21st century *Science* **302** 1524–8
[76] Kamp J 2014 Weighing up reuse of Soviet croplands *Nature* **505** 483

Chapter 5: Negative emission potentials of biofuels produced from perennial crops and nature-based solutions on abandoned and degraded cropland in Nordic countries

Material from: Næss, J. S., Hu, X., Gvein, M. H., Iordan, C., Cavalett, O., Dorber, M., & Cherubini, F. (Under review). Negative emission potentials of biofuels produced from perennial crops and nature-based solutions on abandoned and degraded cropland in Nordic countries

Under review in Journal of Environmental Management. Submitted December 23rd.

This paper is awaiting publication and is not included in NTNU Open

Chapter 6: Synthesis

In this section I summarize the main findings from my work. Furthermore, I discuss the policy implications of the work, limitations, and provide concluding remarks.

6.1 Main findings in relation to research questions

As established in Chapter 1.5, I considered four main research questions which are discussed below.

Research question 1: Where can bioenergy plantations be deployed in the near-term to increase sustainable bioenergy supply, what is the extent of suitable areas, and what are the energy potentials?

Among the land management strategies for deployment of bioenergy plantations, the consideration of areas where competition with food production and environmental impacts are limited, or where a switch to bioenergy crops can provide significant environmental co-benefits and mitigate land degradation processes are often discussed. Two promising options are abandoned cropland which lays unproductive and without primary vegetation, and cropland threatened by soil erosion where perennial crops can reduce soil erosion rates. The results presented here suggest that there is an untapped potential to target these areas for bioenergy production. The work advances the existing literature by providing the first high-resolution and spatially explicit global assessment of abandoned cropland extent and associated management and water supply dependent bioenergy potentials.

More specifically, 83 Mha of abandoned cropland was identified globally over the period between 1992 and 2015 using a global land cover dataset. Abandonment is widespread, and key regions with intensive land abandonment are Eastern Europe, Southeast Asia, Central Africa, Central America, and the Southeastern parts of South America. Achievable global bioenergy potentials are between 6 to 39 EJ $year^{-1}$ from deploying three perennial grasses (miscanthus, switchgrass and reed canary grass) on abandoned croplands, equal to 11 to 68% of the current global bioenergy demand.

Whilst global land cover products are useful to identify the key regions with abandonment and their suitability for bioenergy crops, global analysis should be followed up with regional and local assessments. The availability of a regional land cover dataset with high abandonment accuracy covering the former Soviet Union offered an opportunity to refine estimates. Refined bioenergy potentials are found to be 3.5 to 23 EJ on abandoned land in the former Soviet Union alone. Targeting abandoned land in this region can substantially ramp-up bioenergy supply and contribute to climate change mitigation in line with the regional projections from economic models.

In a Nordic case study, I investigated the opportunities to deploy perennial bioenergy crops on croplands threatened by soil erosion. Croplands moderately or highly susceptible to wind erosion which can be targeted for bioenergy production was found to be 0.9 Mha, mainly in Denmark and the southern parts of Norway and Sweden. Croplands under unsustainable levels of soil erosion by water was 0.1 Mha, mainly found in coastal and mountainous areas of Norway. The Nordic primary energy potential of deploying willow windbreaks on croplands threatened from soil erosion by wind and deploying perennial bioenergy crops on croplands threatened from soil erosion by water for bioenergy production is quantified to 105 PJ $year^{-1}$.

Research question 2: How can the nexus between sustainable bioenergy potentials and their land and water requirements be unraveled, and what is the importance of the following factors: agricultural management, climatic conditions, resource constraints arising from water scarcity for irrigation, and potential land-sparing strategies for nature conservation?

I addressed this question by quantifying bioenergy potentials of perennial grasses deployed on abandoned cropland considering different agricultural management, climatic conditions and constraints to land and water resource availability (Chapters 2 and 4). I find that:

- Unravelling the spatial complexity of land-energy-water interactions requires the use of indicators suitable to link resource dependencies with potentials, and to assess sustainability trade-offs and co-benefits. Indicators should incapsulate all the dimensions of the land-energy-water nexus for quantitative assessments. In combination with considerations of site-specific trade-offs on nature conservation and

water scarcity, they allow for identifying priority regions for rain-fed and irrigated bioenergy deployment.

- Irrigation can increase bioenergy potentials on abandoned cropland with 52 to 58% relative to rain-fed conditions depending on agricultural management (upper extreme) and requires infrastructure development for water withdrawals and availability of blue water resources. The overlap between abandoned cropland and physical water scarce areas is limited to 16% and there is a potential to increase bioenergy production through irrigation in key areas with limited trade-offs on water depletion.

- Land sparing for nature conservation can significantly limit bioenergy potentials as 40% of abandoned cropland is in the biodiversity hotspots (mainly in tropical regions). This reduces bioenergy potentials by 42 to 51% depending on agricultural management and water supply system compared to a complete bioenergy deployment.

- The combined effect of sparing abandoned cropland in biodiversity hotspots for continued regrowth and irrigating only areas that are not physically water scarce was found to give a global potential with high management intensity of 20 EJ $year^{-1}$, or a 25% decrease relative to rain-fed conditions and complete land availability.

- Different agricultural management resulted in global bioenergy potentials on abandoned cropland between 12-25 EJ $year^{-1}$ at rain-fed conditions. Management is thus a vital part of achieving better crop productivity in bioenergy plantations. Closing yield gaps globally requires mechanization, improved varieties, and increased fertilizer and pesticide use.

- Global warming is expected to decrease bioenergy potentials on abandoned cropland at lower latitudes and increase them at higher latitudes, with a net global loss of potentials (up to -17% in RCP8.5 by 2080 relative to present day). In subarctic and continental climates, currently unsuitable areas can become productive with increased warming. Productivity losses from climate change in the tropics can to some extent be mitigated through irrigation if water resources are available.

- The former Soviet Union is an example of a region with intensive abandonment where marginal energy gains of irrigation are high, blue water resources are (partially) available considering environmental flow protection, and sustainable irrigation is key to achieve increased bioenergy potentials. Nature conservation policies are relatively less important in this region as there is little overlap with biodiversity hotspots and protected areas.

Research question 3: Where does bioenergy show both high energy potentials and high development potentials, and how does bioenergy spatially compare against solar photovoltaics?

Chapter 3 addressed the development potential of bioenergy on abandoned cropland. The Development Potential Index (DPI) served as a measure to consider the technical and socioeconomic feasibility to deploy bioenergy crops on abandoned cropland.
Abandoned cropland with DPI within the top quartile are mainly found in Central America, southeastern parts of South America, Southeast Asia and in the southern part of North America. These areas generally overlap both with intensive historical cropland abandonment and relatively high total bioenergy potentials.

Additionally, the DPI for bioenergy on abandoned cropland was compared to solar photovoltaics as another option for renewable energy production on abandoned cropland, thereby aiming to gain further insights on potential land use competition and optimal land use allocation. Bioenergy shows higher DPI than photovoltaics in several clusters with high bioenergy potentials, such as in South America, Southeast Asia, and parts of Central America. Bioenergy also has higher DPI than photovoltaics in the western parts of the former Soviet states.

Research question 4: What is the climate change mitigation potential of liquid biofuel production with and without CCS, and how does the achieved mitigation spatially compare to negative emissions from natural regrowth?

The potential climate change mitigation of liquid biofuel production from dedicated bioenergy crops depends on many factors, including previous land use characteristics, bioenergy productivity, biorefinery technology, soil carbon dynamics, and integration with

CCS technologies. I investigated the mitigation performance of liquid biofuels produced from abandoned cropland and from cropland threatened by soil erosion by wind and water in the Nordic region (Chapter 5). The work provides the first bottom-up and spatially explicit comparison of achievable climate benefits from biofuel production and natural regrowth on abandoned and degraded cropland.

The average net annual climate change mitigation over the first fifteen years of producing liquid biofuels with the best energy yielding crop on Nordic abandoned cropland is -9.0 ± 5.9 $tCO_2eq\ ha^{-1}\ year^{-1}$, considering a commercially available biorefinery technology without CCS (ranges refer to one standard deviation of spatial variability). Future refinery technology with improved energy conversion efficiency increases average net annual mitigation to -16 ± 6.0 tCO_2eq, whilst energy conversion efficiency gains in combination with introduction of CCS technologies can achieve an average climate change mitigation of -26 ± 7.9 $tCO_2eq\ ha^{-1}\ year^{-1}$. Continued natural regrowth on abandoned cropland can bring average annual carbon sequestration of -6.1 ± 4.6 tCO2eq $ha^{-1}\ year^{-1}$ over the same period. Biofuels produced with the current biorefinery technologies provides higher cumulative mitigation than continued natural regrowth on 60% of abandoned cropland over the first fifteen years. With the future biorefinery technologies and CCS technologies, liquid biofuel production is preferable on nearly all the abandoned croplands.

For Nordic croplands threatened by soil erosion, average annual mitigation over the first fifteen years is -6.1 ± 3.4, 9.2 ± 3.6 and -15 ± 4.1 $tCO_2eq\ ha^{-1}\ year^{-1}$ for the current, future and BECCS biorefineries respectively. For comparison, average annual carbon sequestration from natural regrowth on croplands threatened by soil erosion is -9.0 ± 3.8 $tCO_2eq\ ha^{-1}\ year^{-1}$. Biofuels performs better than natural regrowth on 17%, 68%, and 95% of the land over the period with the current, future, and BECCS biorefineries, respectively. In general, natural regrowth is more competitive on areas threatened by soil erosion by wind, primarily because of a forced crop allocation of willow to a windbreak system. As willow yields are lower than perennial grasses, it leads to lower potential climate change mitigation. Gains in biorefinery energy conversion efficiency and CCS is necessary to ensure higher mitigation through willow windbreak deployment than natural regrowth on Nordic croplands threatened by soil erosion by wind.

As an upper potential, the deployment of bioenergy crops for liquid biofuel production on Nordic abandoned cropland and croplands threatened by soil erosion could provide an annual climate change mitigation equal to 17-42% of the current Nordic annual road transport emissions, depending on biorefinery energy efficiency and the availability of CCS. Crop yields and the energy conversion efficiency achievable by available biorefinery technology are both important to achieve higher mitigation through liquid biofuel production compared to natural regrowth.

6.2 Policy implications

This work identified a substantial potential to produce bioenergy from areas where land use change will have limited societal and environmental trade-offs, and where a switch to bioenergy crops may even provide additional benefits through reduced land degradation processes. I have also shown the physical potential to increase bioenergy crop productivity through irrigation in key regions of the world and identified suitable land that is not currently threatened by physical water scarcity and overlaps with available blue water resources. The integrated management of land and water resources is vital for a sustainable bioenergy deployment. Bioenergy land and water use must be governed such that it is kept within sustainable limits to avoid environmental trade-offs.

Land management strategies should aim to identify the best use of land from the given local context, considering current land use, ongoing land degradation processes and potential environmental benefits and trade-offs of different land use strategies. Targeting abandoned cropland for bioenergy deployment can contribute to increase bioenergy supply and decarbonize the energy sector, whilst avoiding many of the trade-offs typically associated with land use change such as competition with food production or loss of primary vegetation. Further deployment should happen where bioenergy crops can be a win-win strategy co-delivering energy and environmental benefits, such as exemplified here by targeting croplands threatened by soil erosion.

Water management strategies for irrigated bioenergy production needs to account for available renewable water resources, potential yield gains of irrigation, and potential trade-offs on water depletion. Irrigation should be avoided in water scarce areas where further blue

water withdrawals can make it challenging to meet societal water demands or where it has adverse environmental impacts. The identification of areas where renewable blue water resources are available and bioenergy crop growth can benefit from irrigation means that there is an untapped opportunity to ramp-up production either through complete irrigation or deficit irrigation.

Large-scale bioenergy deployment is a necessity in most climate change mitigation scenarios. Rain-fed bioenergy production from abandoned cropland has an upper potential to supply 10-30% of the global bioenergy demand in 2050 for 1.5°C scenarios across the different SSPs. Sustainable irrigation strategies or the consideration of degraded lands increases these potentials further. There is thus a near-term opportunity to increase bioenergy supply with relatively low environmental and societal trade-offs, but institutional support will be a necessity.

Countries aiming to increase bioenergy supply for climate change mitigation should consider implementing incentives to accelerate the sustainable deployment of bioenergy plantations. Historically, the most likely outcome of land abandonment in recent decades is unmanaged regrowth of secondary vegetation[1]. The recultivation of abandoned areas requires the presence of a young and motivated work force, in addition to political and institutional support[2]. Subsidies can contribute to overcome the initial cost of recultivation[1,2]. Campaigns aiming to spread information of the potential benefits of recultivation and highlighting the societal issues connected to land abandonment may also help nudge landowners towards a potential recultivation[1]. Likewise, the conversion of croplands threatened by soil erosion to bioenergy crop cultivation will require institutional support. Irrigation deployment aiming to increase crop productivity typically requires the construction of reservoirs to store and transfer water from wetter periods to dryer periods[3,4]. Policies incentivizing irrigation infrastructure development can speed up deployment.

Restrictive regulations and improved sustainability certification schemes will also be needed to make sure that bioenergy plantations do not expand uncontrolled into primary vegetation to limit trade-offs on natural ecosystems and to protect aboveground carbon stocks. Conversion of cropland to bioenergy crops should also be carefully monitored to make sure food security is not compromised. Regulations are also necessary to avoid unsustainable blue

water withdrawals for irrigation in areas under physical water scarcity, and to make sure sustainable renewable water budgets are not exceeded.

In some cases, nature based solutions outperform bioenergy production for climate change mitigation. For example, continued regrowth on abandoned cropland may be preferable if aboveground carbon stocks have become substantial and land-clearance would induce a major initial carbon penalty, or if regrowth can deliver considerable benefits to biodiversity and natural ecosystems. Therefore, site-specific evaluations are necessary to evaluate the best mitigation option locally, considering local context and polices, different future land use trajectories, natural regrowth rates, bioenergy yields of considered crops, achievable agricultural management performance, possibilities to enhance yields through irrigation, biorefinery technology and CCS availability.

Implementation of BECCS is necessary to achieve the highest possible mitigation, but barriers still remain due to costs and lack of social acceptance, political priority, and policy incentives, including carbon pricing[5]. Immediate political and economic incentives are necessary for a quick BECCS introduction[6]. The polluter pays principle is commonly applied to price GHG emissions through a tax or emission system. BECCS offer negative emissions as a common benefit, and turned around, the beneficiary pays principle leads to the idea that the state (or taxpayers) should provide guarantees to buy carbon removal by BECCS over a certain time[7]. Other potential models to incentivize BECCS include quota obligations where carbon emitters are forced to pay for carbon removal, introducing BECCS credits in international carbon markets, including BECCS credits in voluntary carbon offset markets, and inter-state trades of BECCS outcomes to meet National Determined Contributions to the Paris Agreement[7,8].

6.3 Limitations and uncertainties

I integrated different models, datasets, and methods in this work to provide new insights on bioenergy land and water use, and sustainable deployment potentials. I highlight three key limitations from the work presented here, one from each of the dimensions of the land-energy-water nexus. For more detailed discussions on the limitations and uncertainties of other individual components, see the different thesis subchapters.

For example, uncertainties arise from land cover dataset accuracy. Currently, there are two main barriers limiting more accurate estimates of global cropland abandonment. The first is the lack of agricultural censuses in large parts of the world, mainly in developing countries[9]. This has led to attempts to quantify cropland abandonment through satellite data (such as applied here). The second barrier is the lack of global sample-based validation datasets of land use change that can improve evaluations of total area extent of land cover and land use changes[10]. Such datasets are mainly available with regional coverage such as for the former Soviet Union[11], where I applied a regional land cover dataset to refine bioenergy estimates. It is vital that future research targets developing a high-resolution validation dataset to assess global cropland abandonment and improve our understanding of spatial and temporal accuracy. Crowd-sourced efforts may offer opportunities for cost-efficient development. Combined with continuous technological improvements of remote sensing techniques, it should make it possible to improve the detection of future abandonment patterns.

Second, crop yield models are subject to different limitations. The agro-ecological parameterized crop yield model GAEZ[12,13] was used to assess perennial grasses and a dataset based on machine learning techniques[14] to assess willow. Furthermore, comparisons were made with a global machine-learning dataset of bioenergy yields[15] and data from the hydrological model H08[16]. The underlying assumptions of the different models leads to a range of quantified bioenergy potentials, something that is also previously seen in larger intercomparison projects of food crop models[17,18]. Efforts to also intercompare bioenergy crop yield models under consistent scenario assumptions are underway[19]. This will help reveal the importance of model choice on quantified sustainable bioenergy and climate change mitigation potentials.

Third, this work applies the physical water scarcity indicator and datasets of potential irrigation expansion which are based on historical data[3,12] to identify opportunities for irrigation with reduced trade-offs on water depletion. Renewable water resources will change with climate change[3] and the effect of global warming on sustainably irrigated bioenergy potentials is still uncertain. Whilst some important advances have been made recently discussing the limits to future irrigated bioenergy production[20,21], additional work is needed to include sustainable land use opportunities in sophisticated hydrological assessments of bioenergy water use. Historically abandoned areas more frequently overlap with blue water

availability such as in the former Soviet Union, and there is a need to specifically assess how climate change will affect sustainably irrigated bioenergy potentials in these areas.

6.4 Concluding remarks

Bioenergy plays a vital role in climate change mitigation scenarios limiting global warming to below 2°C by the end of the century[22,23]. It is a flexible energy carrier important for energy system decarbonization, which can also provide carbon dioxide removal when linked to CCS[24]. The massive deployment of bioenergy plantations seen in climate change mitigation scenarios has led to a debate discussing the feasible scale of bioenergy plantations and how environmental and societal trade-offs related to their land and water use can be avoided[24–28]. Land and water are both limited resources, and their management should reflect how global challenges can be better addressed whilst co-delivering environmental and societal benefits and minimizing associated trade-offs.

I conclude that there is a physical global potential to recultivate abandoned cropland for bioenergy production at a large enough scale that it can make a meaningful contribution to mitigation pathways. Abandoned areas frequently overlap with sustainable irrigation expansion opportunities, and blue water withdrawals for bioenergy crop irrigation can contribute to increase bioenergy productivity and alleviate pressure on land resources. Bioenergy deployment can further target cropland threatened from soil erosion by wind and water, with associated co-benefits through reduced soil erosion rates. Deployment beyond what is considered here can aim to target other degraded areas where a switch to bioenergy crops can co-deliver many environmental co-benefits. Reducing land-based food and feed demand or future productivity gains may also help free agricultural land for bioenergy production.

The simultaneous consideration of land and water use sustainability, deployment feasibility, and achievable bioenergy potentials makes it possible to guide improved sustainable bioenergy deployment strategies. Lack of proper governance can lead to increased land use competition, trade-offs on food security, loss of primary vegetation, and increased water stress. With proper governance, bioenergy and BECCS will contribute to decarbonize the energy sector, mitigate climate change, and additionally co-deliver multiple environmental benefits and enhance ecosystem services. The findings presented here helps shed light on the

importance of sustainable land and water management in bioenergy production systems, which ultimately can help to achieve global sustainability targets.

6.5 References

1. Fayet, C. M. J., Reilly, K. H., Van Ham, C. & Verburg, P. H. What is the future of abandoned agricultural lands? A systematic review of alternative trajectories in Europe. *Land use policy* **112**, 105833 (2022).
2. Prishchepov, A. V, Ponkina, E. V, Sun, Z., Bavorova, M. & Yekimovskaja, O. A. Revealing the intentions of farmers to recultivate abandoned farmland: A case study of the Buryat Republic in Russia. *Land use policy* **107**, 105513 (2021).
3. Rosa, L. *et al.* Potential for sustainable irrigation expansion in a 3 °C warmer climate. *Proc. Natl. Acad. Sci.* **117**, 29526 LP – 29534 (2020).
4. D'Odorico, P. *et al.* The Global Food-Energy-Water Nexus. *Rev. Geophys.* **56**, 456–531 (2018).
5. Fridahl, M. & Lehtveer, M. Bioenergy with carbon capture and storage (BECCS): Global potential, investment preferences, and deployment barriers. *Energy Res. Soc. Sci.* **42**, 155–165 (2018).
6. Fuss, S. & Johnsson, F. The BECCS Implementation Gap–A Swedish Case Study. *Frontiers in Energy Research* **8**, 385 (2021).
7. Zetterberg, L., Johnsson, F. & Möllersten, K. Incentivizing BECCS—A Swedish Case Study. *Frontiers in Climate* **3**, 99 (2021).
8. Roelfsema, M. *et al.* Taking stock of national climate policies to evaluate implementation of the Paris Agreement. *Nat. Commun.* **11**, 2096 (2020).
9. Gennari, P., Rosero-Moncayo, J. & Tubiello, F. N. The FAO contribution to monitoring SDGs for food and agriculture. *Nat. Plants* **5**, 1196–1197 (2019).
10. Olofsson, P. *et al.* Good practices for estimating area and assessing accuracy of land change. *Remote Sens. Environ.* **148**, 42–57 (2014).
11. Lesiv, M. *et al.* Spatial distribution of arable and abandoned land across former Soviet Union countries. *Sci. Data* **5**, 180056 (2018).
12. Fischer, G. *et al.* Global Agro-ecological Zones (GAEZ v3. 0)-Model Documentation.

(2012).

13. Fischer, G. *et al. Global Agro-Ecological Zones v4–Model documentation*. (Food & Agriculture Org., 2021). doi:https://doi.org/10.4060/cb4744en
14. Mola-Yudego, B., Rahlf, J., Astrup, R. & Dimitriou, I. Spatial yield estimates of fast-growing willow plantations for energy based on climatic variables in northern Europe. *GCB Bioenergy* **8**, 1093–1105 (2016).
15. Li, W. *et al.* Mapping the yields of lignocellulosic bioenergy crops from observations at the global scale. *Earth Syst. Sci. Data* **12**, 789–804 (2020).
16. Ai, Z., Hanasaki, N., Heck, V., Hasegawa, T. & Fujimori, S. Simulating second-generation herbaceous bioenergy crop yield using the global hydrological model H08 (v.bio1). *Geosci. Model Dev.* **13**, 6077–6092 (2020).
17. Müller, C. *et al.* The Global Gridded Crop Model Intercomparison phase 1 simulation dataset. *Sci. Data* **6**, 50 (2019).
18. Rosenzweig, C. *et al.* Assessing agricultural risks of climate change in the 21st century in a global gridded crop model intercomparison. *Proc. Natl. Acad. Sci.* **111**, 4–9 (2014).
19. AgMIP. Bioenergy-Crop Model Initiative. (2019). Available at: https://agmip.org/bioenergy-crop-model-initiative/.
20. Stenzel, F. *et al.* Irrigation of biomass plantations may globally increase water stress more than climate change. *Nat. Commun.* **12**, 1512 (2021).
21. Ai, Z., Hanasaki, N., Heck, V., Hasegawa, T. & Fujimori, S. Global bioenergy with carbon capture and storage potential is largely constrained by sustainable irrigation. *Nat. Sustain.* (2021). doi:10.1038/s41893-021-00740-4
22. Rogelj, J. *et al.* Scenarios towards limiting global mean temperature increase below 1.5 °C. *Nat. Clim. Chang.* **8**, 325–332 (2018).
23. Rogelj, J. *et al.* Chapter 2: Mitigation pathways compatible with 1.5°C in the context of sustainable development. in *Global Warming of 1.5 °C an IPCC special report on the impacts of global warming of 1.5 °C above pre-industrial levels and related global greenhouse gas emission pathways, in the context of strengthening the global response to the threat of climate change* (Intergovernmental Panel on Climate Change, 2018).
24. Calvin, K. *et al.* Bioenergy for climate change mitigation: scale and sustainability. *GCB Bioenergy* **n/a**, (2021).

25. Vaughan, N. E. & Gough, C. Expert assessment concludes negative emissions scenarios may not deliver. *Environ. Res. Lett.* **11**, 95003 (2016).
26. Forster, J., Vaughan, N. E., Gough, C., Lorenzoni, I. & Chilvers, J. Mapping feasibilities of greenhouse gas removal: Key issues, gaps and opening up assessments. *Glob. Environ. Chang.* **63**, 102073 (2020).
27. Anderson, K. & Peters, G. The trouble with negative emissions. *Science (80-.).* **354**, 182 LP – 183 (2016).
28. IPCC. Summary for Policymakers. in *Climate Change and Land: an IPCC Special Report on climate change, desertification, land degradation, sustainable land management, food security, and greenhouse gas fluxes in terrestrial ecosystems* (2019).

Appendix

This section contains supplementary information to the individual thesis articles:

A.1 Supplementary Information – The land-energy-water nexus of global bioenergy potentials from abandoned cropland

A.2 Supplementary Information – Optimal combination of bioenergy and solar photovoltaic for renewable energy production on abandoned cropland

A.3 Supplementary Information – Energy potentials and water requirements from perennial grasses on abandoned land in the former Soviet Union

A.4 Supplementary Information – Negative emission potentials of biofuels produced from perennial crops and nature-based solutions on abandoned and degraded cropland in Nordic countries

nature research

https://doi.org/10.1038/s41893-020-00680-5

Supplementary information

The land–energy–water nexus of global bioenergy potentials from abandoned cropland

In the format provided by the authors and unedited

The land-energy-water nexus of global bioenergy potentials from abandoned cropland

Supplementary Information

Jan Sandstad Næss[1,*], Otavio Cavalett[1] and Francesco Cherubini[1].

[1]*Industrial Ecology Programme, Department of Energy and Process Engineering, Norwegian University of Science and Technology (NTNU), Trondheim, Norway.*

[*]*Corresponding author. Email: jan.s.nass@ntnu.no*

Table of Contents

Supplementary Figures

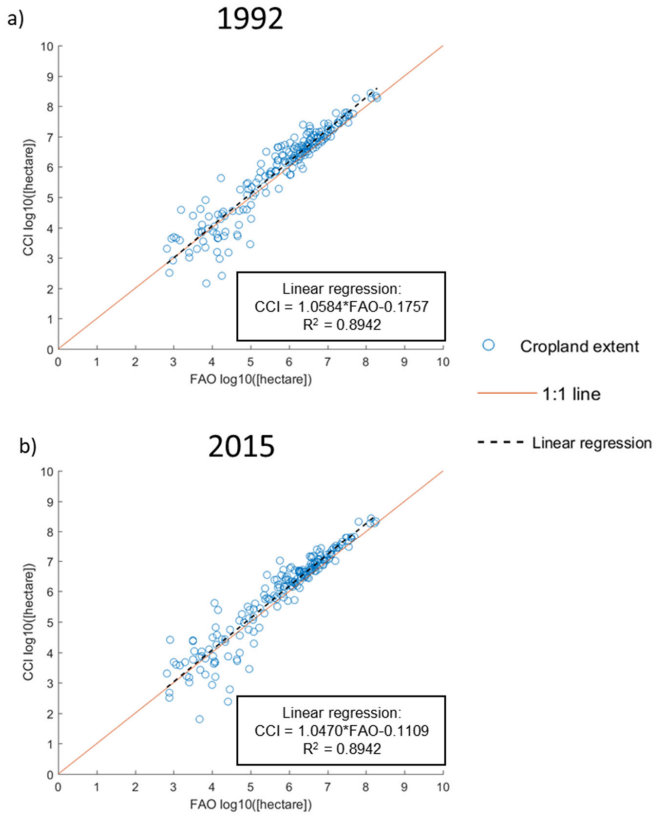

Supplementary Fig. 1 | Comparison of country level cropland extent (hectares) from FAO statistics[1] with cropland extent quantified here using the ESA CCI-LC product for 1992 (a) and 2015 (b). Each blue dot represents a single country's cropland extent, the orange line represents the 1:1 ratio, and the black dotted line represents the linear regression.

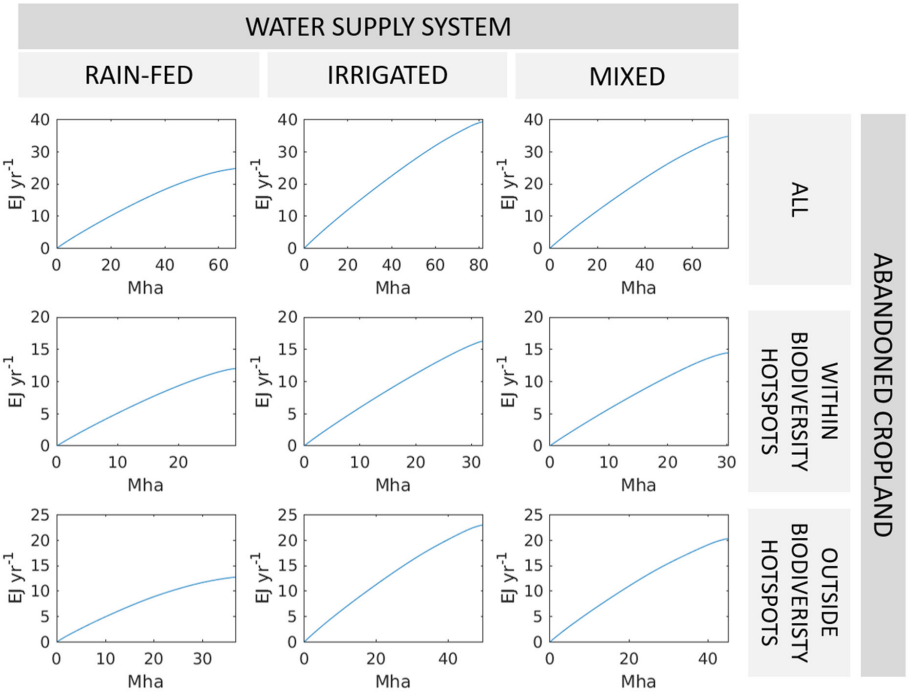

Supplementary Fig. 2 | Relationship between bioenergy potentials (EJ year^{-1}) and land requirements, assuming optimally located bioenergy deployment on abandoned cropland. Results are shown for three water supply systems (rain-fed, irrigated, and mixed), three land availability constraints (abandoned cropland, abandoned cropland in biodiversity hotspots, and abandoned cropland outside biodiversity hotspots), and high agricultural management intensity. Optimal energy-based crop allocation per grid cell. Note different scales on axis.

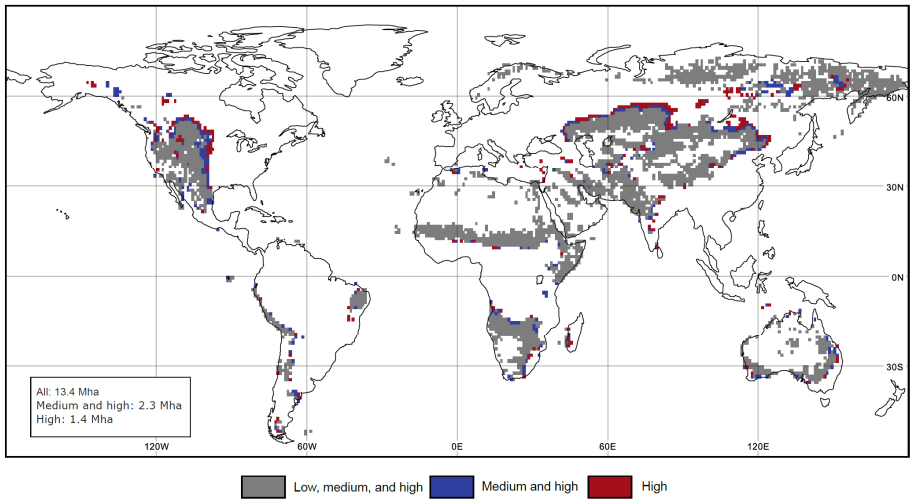

Supplementary Fig. 3 | Unproductive locations of abandoned cropland areas at rain-fed conditions and present day climate across different agricultural management intensities. Results are shown for only high, medium and high, and all (low, medium and high) management intensities. Map is shown at one-degree resolution (aggregated for visualization purposes).

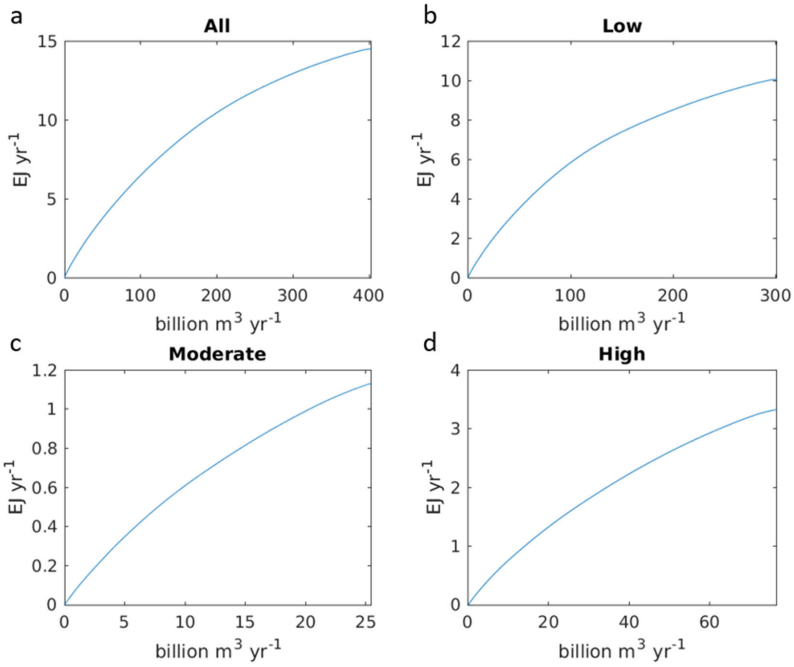

Supplementary Fig. 4 | Relationship between gains in bioenergy potentials of irrigated bioenergy production relative to rain-fed water supply (EJ year^{-1}), and the minimized required water withdrawals (m^3 year^{-1}) assuming optimally located irrigation deployment on abandoned cropland at different physical water scarcity levels (all (a), low (b), moderate (c), and high (d)). Results are shown for present day, optimal crop allocation, no nature conservation measures, and high agricultural management intensity. Note different scales on axis.

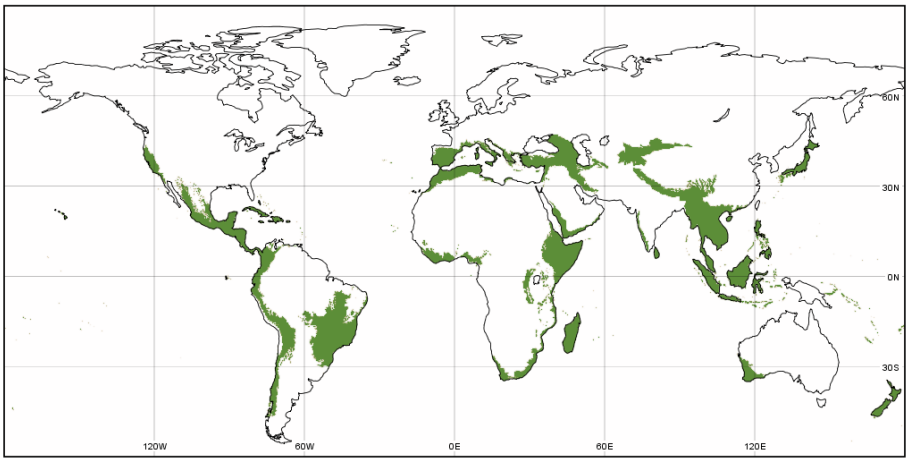

Supplementary Fig. 5 | Map of biodiversity hotspots.

Supplementary Tables

Supplementary Table 1 | Review of previous estimates of abandoned cropland. Note that time periods, resolutions, land classification methods and abandonment criteria vary between studies. See Supplementary Text 1 for a discussion considering previous estimates relative to our work.

Assessed area	Time period	Years	Abandoned cropland (Mha)	Reference
Global	300 years	1700 – 2000	385 - 472	[2]
Global	300 years	1700 - 2000	386	[3]
Global	142 years	1850 - 1992	207	[4]
Europe	11 years	2001 - 2012	7.6	[5]
Europe	N/A	Until 2012	46	[5]
Central and Eastern Europe	N/A	Until 2005	52	[6]
Eastern Europe	19 years	1990 - 2009	31	[7]
Brazil	31 years	1975 – 2006	11	[8]
China	15 years	1990 – 2005	9.8	[9]
Mexico	13 years	2001 - 2014	1.5	[10]
Angola (Huambo)	29 years	1990 – 2009	0.35	[11]
USA	34 years	1978 - 2012	15	[12]
USA	5 years	2007 – 2012	4.9	[12]
USA	4 years	2008 - 2012	1.8	[13]
USA	65 years	1945 – 2000	43	[14]
Western Siberia (Tyumen)	25 years	1990 - 2015	0.14	[15]
Puerto Rico	9 years	1991 – 2000	0.031	[16]
Indonesia (Lombok Island)	20 years	1990 – 2010	0.010	[17]

Supplementary Table 2 | Present day bioenergy potentials on abandoned cropland with optimal crop allocation across different land availability, agricultural management intensities and water supply systems. Land availability is constrained by abandoned cropland (AC) or abandoned cropland outside biodiversity hotspots (ACOBH). Agricultural management intensities are low, medium, high, or mixed (i.e., management intensity based on today's yield gaps). Water supply systems are rain-fed (RF), irrigated (IR), or mixed (i.e. irrigation deployed only in areas under medium and high management intensity that are not threatened by water scarcity).

Land availability	Agricultural management intensity	Water supply	Bioenergy potential (EJ yr-1)	Average bioenergy yield on all areas (GJ ha^{-1} yr^{-1})	Productive area (Mha)	Average bioenergy yield on productive areas (GJ ha^{-1} yr^{-1})
AC	Low	RF	11	130	70	155
AC	Medium	RF	20	239	68	294
AC	High	RF	25	298	66	374
AC	Medium	IR	30	365	82	372
AC	High	IR	39	472	82	481
AC	Medium	Mixed	27	325	76	357
AC	High	Mixed	35	418	75	461
AC	Mixed	RF	20	236	67	291
AC	Mixed	Mixed	25	306	74	346
ACOBH	Low	RF	5.5	109	39	140
ACOBH	Medium	RF	10	199	38	268
ACOBH	High	RF	13	249	36	345
ACOBH	Medium	IR	17	346	49	354
ACOBH	High	IR	23	452	49	463
ACOBH	Medium	Mixed	15	306	45	345
ACOBH	High	Mixed	20	399	45	450
ACOBH	Mixed	RF	9.6	189	38	255
ACOBH	Mixed	Mixed	14	273	43	321

Supplementary Table 3 | Comparison of historical abandoned cropland (1992-2015) and median projected land requirements for bioenergy crop production in 2050 for 1.5°C scenarios across different SSPs in top-down Integrated Assessment Models[18]. SSP3 and SSP4 are not shown as models either could not achieve the climate target (SSP3-1.9), or the climate target was achieved by one model but no land data was provided (SSP4-1.9).

Shared Socio-economic Pathway	**Median projected land requirement for bioenergy crops in 2050 for 1.5°C scenarios[18]**	**Abandoned cropland (83 Mha) as share of 2050 land requirement**	**Abandoned cropland outside biodiversity hotspots (50 Mha) as share of 2050 land requirement**
SSP1-1.9	210 Mha	40%	24%
SSP2-1.9	450 Mha	19%	11%
SSP5-1.9	670 Mha	12%	8%

Supplementary Table 4 | Accuracy estimates found in the literature comparing the ESA CCI-LC product against validated ground points. Producer and user accuracies refers to how often certain ground points are correctly classified in the dataset, or how often dataset pixel classification match certain ground points, respectively. Classes with high producer and high user accuracies have both high spatial match and high precision in total area extent compared with ground truth. In combination, lower producer and higher user accuracies of classes indicates an under-mapping, while higher producer and lower user accuracies indicates an over-mapping.

Assessed area	Overall accuracy all land cover	Producer accuracy of cropland classes	User accuracy of cropland classes	Total validation points	Cropland validation points	Reference
Global	71.5 %	79 %	89 %	2329	574	[19]
Global (only heterogeneous points)	75.4 %	79 %	83-92 %	1499	383	[19]
Global	71.1 %	79-92 %	85-94 %	1353	235	[20]
Global	70.8 %	78.5 %	79.2 %	3857	1146	[21]
Global	80.4 %	66.4 %	94.2 %	525	122	[22]
Africa	55.5 %	79.2 %	-	3887	-	[23]
Africa	62 %	-	-	5058	1052	[24]
South America	70 %	-	-	587	98	[24]
Southeast Asia	59 %	-	-	1688	439	[24]
North Korea	70 %	92 %	55 %	36	13	[24]
Arctic region	62.2 %	15.4 %	100 %	940	26	[25]
China	72 %	87 %	68 %	1063	203	[26]
Coastal areas in Eurasia	84.4 %	83%	62%	5896	-	[27]
India	59.6 %	74.9 %	90.2 %	-	-	[28]
Finland	63.8 %	62.6 %	65.3 %	-	-	[29]
Portugal (Coimbra)	68.3 %	-	-	-	-	[30]
Portugal (forested area)	83.9 %	-	-	-	-	[30]

Supplementary Text

Supplementary Text 1 | Comparison of abandoned cropland estimates

At a global level, a direct comparison of our findings with other studies is not possible because previous estimates (207-472 Mha) considered much longer time periods (e.g. 300 years), datasets had much coarser resolution, and/or applied different criteria for the identification of cropland abandonment[2–4]. However, more detailed comparisons are possible for specific regions. In general, the main abandonment patterns identified here are consistent with the findings reported in the literature, such as the intensive cropland abandonment in parts of Eastern Europe, South America, Central America, Central Africa and Eastern Asia. Discrepancies across estimates can be explained by a number of factors, including unharmonized land cover classification systems, spatial and temporal resolutions of the different land cover products[24].

More specifically, previous studies found that 11 Mha of farmland contraction occurred in the coastal part of Brazil between 1975 and 2006 (mainly due to agricultural intensification)[8], 1.5 Mha in Mexico between 2001 and 2014 (largely caused by rural-urban migration and drug-related violence)[10], 9.8 Mha in China between 1990 and 2005 (mainly driven by market integration, agricultural intensification, migration to urban areas, and policy efforts to reduce soil erosion)[31–33], 0.031 Mha in Puerto Rico between 1990 and 2000 (due to rural-urban migration)[16], 0.14 Mha in Western Siberia (Tyumen province) between 1990 and 2015 (driven by a sudden access to open markets)[15], 0.010 Mha in Indonesia (Lombok Island) between 1990 and 2010[17], and 0.35 Mha in Angola (Huambo province) between 1990 and 2009 (primarily driven by armed conflicts)[11]. For comparison, we found 7.9 Mha of cropland abandonment in Brazil, 2.3 Mha in Mexico, 6.2 Mha in China, 0.067 Mha in Puerto Rico, 0.089 Mha in Western Siberia (Tyumen province), 0.021 Mha in Indonesia (Lombok Island) and 0.21 Mha in Angola (Huambo province) between 1992 and 2015.

We identified 16 Mha of cropland abandonment in Europe between 1992 and 2015. Previous assessments have shown cropland abandonment across European regions in the range of 7.6-52 Mha[5–7], with high range estimates including areas which already had successional vegetation cover in the early 1990s during the dissolution of the Soviet Union[5,6], or applying a modelling approach to estimate abandonment[7]. The lowest estimate (7.6 Mha) covered a

shorter time period of 11 years between 2001 and 2012[5], and did not capture the wide-spread cropland abandonment shown in Eastern Europe during the 1990s.

In USA, we find 3.5 Mha of abandoned cropland between 1992 and 2015. Previous estimates range from 1.8-43 Mha based on different methodological choices and time periods. The highest estimate (43 Mha) covers a 65 year period after the end of the Second World War (1945-2000), is dependent on spatial overlays of static remote sensing data with survey data, and includes land transitioning from cropland to pastures[14]. Another study estimated cropland abandonment at the county level in the USA, and found 15 Mha and 4.9 Mha over a 34 year (1978-2012) and a 5 year (2007-2012) period, respectively[12]. The study relied on survey data, and did no attempts at local level spatial differentiation[12]. The smallest USA estimate (1.8 Mha) which assessed a 4 year period between 2008 and 2012 also aggregated classes of pasture/grass, pasture/hay, and other hay/non-alfa as not croplands[13], leading to higher cropland abandonment rates than with the classification methodologies applied here.

Supplementary Text 2 | Global bioenergy potentials under climate change

Bioenergy potentials on abandoned cropland will be affected by climate change, here exemplified by using future projections consistent with RCP4.5 and RCP8.5 (Extended Data Fig. 2). Crop productivity response is stronger in RCP8.5 than in RCP4.5, where differences in temperature and precipitation relative to present conditions are stronger. Global bioenergy potentials (rain-fed water supply, high agricultural management intensity, optimal crop allocation, no nature conservation measures) decrease by -0.6 EJ $year^{-1}$ or -1.6 EJ $year^{-1}$ by 2050 under RCP4.5 or RCP8.5, respectively. In 2080, potentials further decrease by -1.2 EJ $year^{-1}$ under RCP4.5 and by -4.2 EJ $year^{-1}$ under RCP8.5. In relative terms, global bioenergy potentials decrease by -2% in 2050 and -5% in 2080 for RCP4.5, and -6% in 2050 and -17% in 2080 for RCP8.5.

There are clear regional patterns for the response of bioenergy potentials to future changes in climatic conditions. In general, bioenergy potentials decrease at lower latitudes and increase at higher latitudes. In today's subarctic and continental climates, significant gains in bioenergy potentials are expected for both future climate projections. Areas that are currently unsuitable for bioenergy production will become productive at milder temperatures (up to about 3 Mha), primarily in RCP8.5. In temperate climates, a loss of bioenergy potential is observed in some locations (up to -20%), but many other places also show net energy gains (up to 20%), such as in parts of oceanic climate zones. In the tropics, bioenergy potentials consistently decrease in South America, Central America, Southeast Asia and Central Africa. In general, a decrease in bioenergy potentials is estimated at rain-fed conditions in areas affected by physical water scarcity for both RCP4.5 and RCP8.5, apart from Central Asia.

Temperature and precipitation changes will impact our estimates of optimal crop allocation across the globe. For example, miscanthus, reed canary grass and switchgrass are allocated 43 Mha, 7.6 Mha and 16 Mha of abandoned cropland, respectively, at present day (rain-fed, high agricultural management intensity, no nature conservation). This optimal crop distribution will change to 39 Mha, 4.5 Mha and 18 Mha, respectively in 2080 under RCP8.5. As the Northern Hemisphere at higher latitudes becomes warmer and wetter, improved rain-fed growth conditions increases bioenergy potentials. Reed canary grass domain will expand northwards into subarctic areas previously unsuitable for crops. Switchgrass will outcompete reed canary grass in the southern parts of the present-day reed canary grass domain. Similarly, the miscanthus domain will further expand northwards, and starts

outcompeting switchgrass in the southern parts of the present-day switchgrass domain. Increased precipitation in tropical zones in Africa and Southeast Asia will not improve bioenergy potentials as water deficit is not a major limitation in these regions. The projected warming will rather cause a slight decline in miscanthus bioenergy yields. Regional drying is expected to decrease bioenergy potentials in Central America, around the Mediterranean, and in the Amazon as rain-fed renewable water availability for miscanthus decreases. Large areas become unsuitable for miscanthus production without irrigation around present day semi-arid and arid climatic regions as water deficits increase. In total, the amount of abandoned cropland without bioenergy potential at these conditions increase from 17 Mha to 22 Mha.

Supplementary Text 3 | Interdependency of bioenergy estimates on local conditions

Extended Data Fig. 3 shows how bioenergy potentials simultaneously change across different climate projections, agricultural management intensity, water supply, and whether nature conservation measures are considered in the biodiversity hotspots. The decline in global bioenergy potentials in RCP8.5 can partially be reduced through large-scale irrigation. Full irrigation deployment with high agricultural management intensity and no nature conservation measures will lead to a potential of 38 EJ $year^{-1}$ in 2080, limiting the relative decline to -4% compared to present-day conditions. A partial deployment of irrigation on areas that are not threatened by water scarcity can provide a potential of 34 EJ $year^{-1}$. These two irrigation options will bring under production 21 Mha and 15 Mha of abandoned cropland, respectively. On the other hand, water scarcity projections are sensitive to climate change patterns, and new regions can become subject to water scarcity, as drying effects will threat water resources. These factors could limit future water availability for irrigation deployment and associated bioenergy potentials.

Future bioenergy potentials are heavily dependent on the spatially projected temperature and precipitation changes, which are sensitive to the type of climate model used. However, we can expect that the use of different climate projections would affect the absolute changes of bioenergy potentials, but not the direction of their trends.

Supplementary References:

1. FAO. FAOSTAT database. (2020). Available at: http://www.fao.org/faostat/en.

2. Campbell, J. E., Lobell, D. B., Genova, R. C. & Field, C. B. The global potential of bioenergy on abandonded agricultural lands. *Environ. Sci. Technol.* **42**, 5791–5794 (2008).

3. Field, C. B., Campbell, J. E. & Lobell, D. B. Biomass energy: the scale of the potential resource. *Trends Ecol. Evol.* 65–72 (2008). doi:10.1016/j.tree.2007.12.001

4. Ramankutty, N. & Foley, J. A. Estimating historical changes in global land cover: Croplands from 1700 to 1992. *Global Biogeochem. Cycles* **13**, 997–1027 (1999).

5. Estel, S. *et al.* Mapping farmland abandonment and recultivation across Europe using MODIS NDVI time series. *Remote Sens. Environ.* **163**, 312–325 (2015).

6. Alcantara, C. *et al.* Mapping the extent of abandoned farmland in Central and Eastern Europe using MODIS time series satellite data. *Environ. Res. Lett.* **8**, 35035 (2013).

7. Schierhorn, F. *et al.* Post-Soviet cropland abandonment and carbon sequestration in European Russia, Ukraine, and Belarus. *Global Biogeochem. Cycles* **27**, 1175–1185 (2013).

8. Barretto, A. G. O. P., Berndes, G., Sparovek, G. & Wirsenius, S. Agricultural intensification in Brazil and its effects on land-use patterns: an analysis of the 1975–2006 period. *Glob. Chang. Biol.* **19**, 1804–1815 (2013).

9. Li, S. *et al.* An estimation of the extent of cropland abandonment in mountainous regions of China. *L. Degrad. Dev.* **29**, 1327–1342 (2018).

10. Bonilla-Moheno, M. & Aide, T. M. Beyond deforestation: Land cover transitions in Mexico. *Agric. Syst.* **178**, 102734 (2020).

11. Cabral, A. I. R., Vasconcelos, M. J., Oom, D. & Sardinha, R. Spatial dynamics and quantification of deforestation in the central-plateau woodlands of Angola (1990–2009). *Appl. Geogr.* **31**, 1185–1193 (2011).

12. Baxter, R. E. & Calvert, K. E. Estimating Available Abandoned Cropland in the United States: Possibilities for Energy Crop Production. *Ann. Am. Assoc. Geogr.* **107**, 1162–1178 (2017).

13. Lark, T. J., Meghan Salmon, J. & Gibbs, H. K. Cropland expansion outpaces agricultural and biofuel policies in the United States. *Environ. Res. Lett.* **10**, 44003 (2015).

14. Zumkehr, A. & Campbell, J. E. Historical U.S. Cropland Areas and the Potential for Bioenergy Production on Abandoned Croplands. *Environ. Sci. Technol.* **47**, 3840–3847 (2013).

15. Nguyen, H., Hölzel, N., Völker, A. & Kamp, J. Patterns and Determinants of Post-Soviet Cropland Abandonment in the Western Siberian Grain Belt. *Remote Sensing* **10**, (2018).

16. Parés-Ramos, I. K., Gould, W. A. & Aide, T. M. Agricultural abandonment, suburban growth, and forest expansion in Puerto Rico between 1991 and 2000. *Ecol. Soc.* **13**, (2008).

17. Kim, C. Land use classification and land use change analysis using satellite images in Lombok Island, Indonesia. *Forest Sci. Technol.* **12**, 183–191 (2016).

18. IPCC. Summary for Policymakers. in *Climate Change and Land: an IPCC Special Report on climate change, desertification, land degradation, sustainable land management, food security, and greenhouse gas fluxes in terrestrial ecosystems* (2019).

19. Defourny, P. *et al. Land Cover CCI product user guide version 2.0.* (2017).

20. UCLouvain. *Product Quality Assessment Report IDCR Land Cover 2016 and 2017.* (2019).

21. Tsendbazar, N. E., de Bruin, S., Mora, B., Schouten, L. & Herold, M. Comparative assessment of thematic accuracy of GLC maps for specific applications using existing reference data. *Int. J. Appl. Earth Obs. Geoinf.* **44**, 124–135 (2016).

22. Liu, H. *et al.* Annual dynamics of global land cover and its long-term changes from 1982 to 2015. *Earth Syst. Sci. Data* **12**, 1217–1243 (2020).

23. Tsendbazar, N.-E., De Bruin, S., Fritz, S. & Herold, M. Spatial accuracy assessment and integration of global land cover datasets. *Remote Sens.* **7**, 15804–15821 (2015).

24. Pérez-Hoyos, A., Rembold, F., Kerdiles, H. & Gallego, J. Comparison of global land cover datasets for cropland monitoring. *Remote Sens.* **9**, 1118 (2017).

25. Liang, L., Liu, Q., Liu, G., Li, H. & Huang, C. Accuracy Evaluation and Consistency Analysis of Four Global Land Cover Products in the Arctic Region. *Remote Sens.* **11**, 1396 (2019).

26. Yang, Y., Xiao, P., Feng, X. & Li, H. Accuracy assessment of seven global land cover datasets over China. *ISPRS J. Photogramm. Remote Sens.* **125**, 156–173 (2017).

27. Hou, W. & Hou, X. Data Fusion and Accuracy Analysis of Multi-Source Land Use/Land Cover Datasets along Coastal Areas of the Maritime Silk Road. *ISPRS Int. J. Geo-Information* **8**, 557 (2019).

28. Madhusoodhanan, C. G., Sreeja, K. G. & Eldho, T. I. Assessment of uncertainties in global land cover products for hydro□climate modeling in India. *Water Resour. Res.* **53**, 1713–1734 (2017).

29. Karvonen, V., Ribard, C., Sädekoski, N., Tyystjärvi, V. & Muukkonen, P. Comparing ESA land cover data with higher resolution national datasets. *Creat. Manag. Anal. geospatial data databases Geogr. themes* 26–45 (2018).

30. Fonte, C. C., See, L., Lesiv, M. & Fritz, S. A preliminary quality analysis of the climate change initiative land cover products for continental Portugal. in *ISPRS - International Archives of the Photogrammetry, Remote Sensing and Spatial Information Sciences* **42**, 1213–1220 (ISPRS, 2019).

31. Liu, Y., Fu, B., Lü, Y., Wang, Z. & Gao, G. Hydrological responses and soil erosion potential of abandoned cropland in the Loess Plateau, China. *Geomorphology* **138**, 404–414 (2012).

32. Jiao, J. *et al.* Can the study of natural vegetation succession assist in the control of soil erosion on abandoned croplands on the Loess Plateau, China? *Restor. Ecol.* **15**, 391–399 (2007).

33. Dong, J., Liu, J., Yan, H., Tao, F. & Kuang, W. Spatio-temporal pattern and rationality

of land reclamation and cropland abandonment in mid-eastern Inner Mongolia of China in 1990–2005. *Environ. Monit. Assess.* **179**, 137–153 (2011).

Optimal combination of bioenergy and solar photovoltaic for renewable energy production on abandoned cropland

Malene Eldegard Leirpoll *[1], Jan Sandstad Næss[1], Otavio Cavalett[1], Martin Dorber[1], Xiangping Hu[1], Francesco Cherubini[1]

*Corresponding author malene@villenergi.no

Table of Contents

Supplementary figures

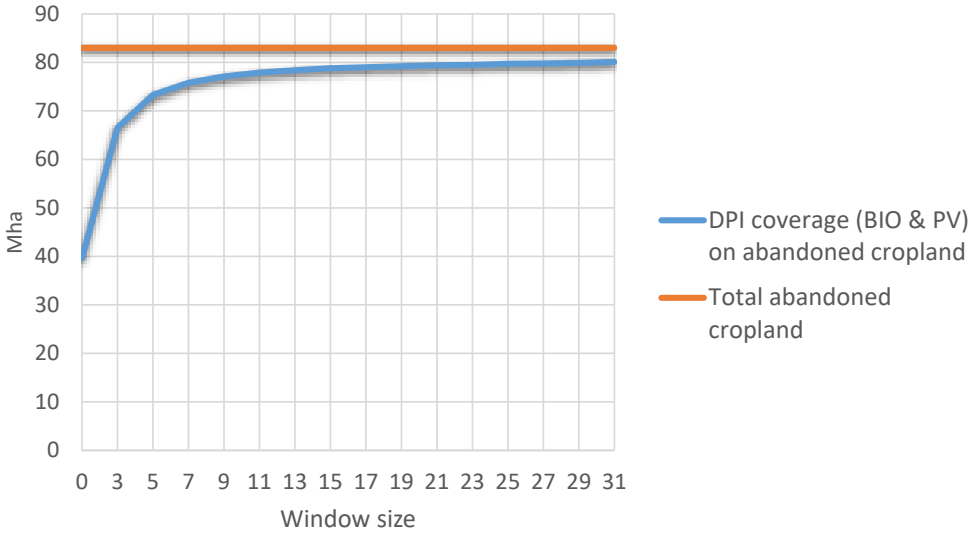

Supplementary Figure 2: *Abandoned cropland with DPI coverage for both BIO and PV as a function of different moving mean window sizes.*

Supplementary tables

Supplementary Table 2: *Sensitivity of optimal BIO and PV allocation and associated energy potentials on abandoned cropland (AC) to DPI data filling method by moving mean window size.*

Moving mean window size [cells]	AC assigned to DPI values [Mha]	AC optimally allocated to BIO [Mha]	AC optimally allocated to PV [Mha]	Total energy potential [EJ yr^{-1}]	Total BIO potential on AC [EJ yr^{-1}]	Total PV potential on AC [EJ yr^{-1}]	Mean bioenergy yield [GJ ha^{-1} yr^{-1}]	Mean PV energy yield [GJ ha^{-1} yr^{-1}]
None	39.6	12.7	26.9	63.1	5.8	57.3	457	2130
3	66.5	21.3	45.2	106.6	9.7	96.9	455	2144
5	73.3	23.4	49.9	117.8	10.7	107	457	2144
7	75.8	24.1	51.7	122.1	11	111.1	456	2149
9	77.1	24.4	52.7	124.3	11.1	113.2	455	2148
11	77.9	24.6	53.2	125.7	11.2	114.5	455	2152
13	78.4	24.7	53.6	126.6	11.2	115.4	453	2153
15	78.8	24.8	54	127.4	11.3	116.1	456	2150
17	79	24.9	54.2	127.9	11.3	116.6	454	2151
19	79.2	25	54.2	128	11.4	116.7	456	2153
21	79.4	25.1	54.3	128.3	11.4	116.9	454	2153
23	79.5	25.1	54.4	128.5	11.4	117.1	454	2153
25	79.7	25.2	54.5	128.8	11.4	117.4	452	2154
27	79.8	25.3	54.5	128.9	11.4	117.4	451	2154
29	79.9	25.3	54.6	129.1	11.5	117.6	455	2154
31	80.1	25.4	54.7	129.2	11.5	117.8	453	2154

Energy potentials and water requirements from perennial grasses on abandoned land in the former Soviet Union

Supplementary Information

Jan Sandstad Næss[1*], Cristina Maria Iordan[1], Helene Muri[1], and Francesco Cherubini[1].

[1] Industrial Ecology Programme, Department of Energy and Process Engineering, Norwegian University of Science and Technology, Trondheim, Norway.

* Corresponding author. Email: jan.s.nass@ntnu.no

Table of Contents

Supplementary Figures

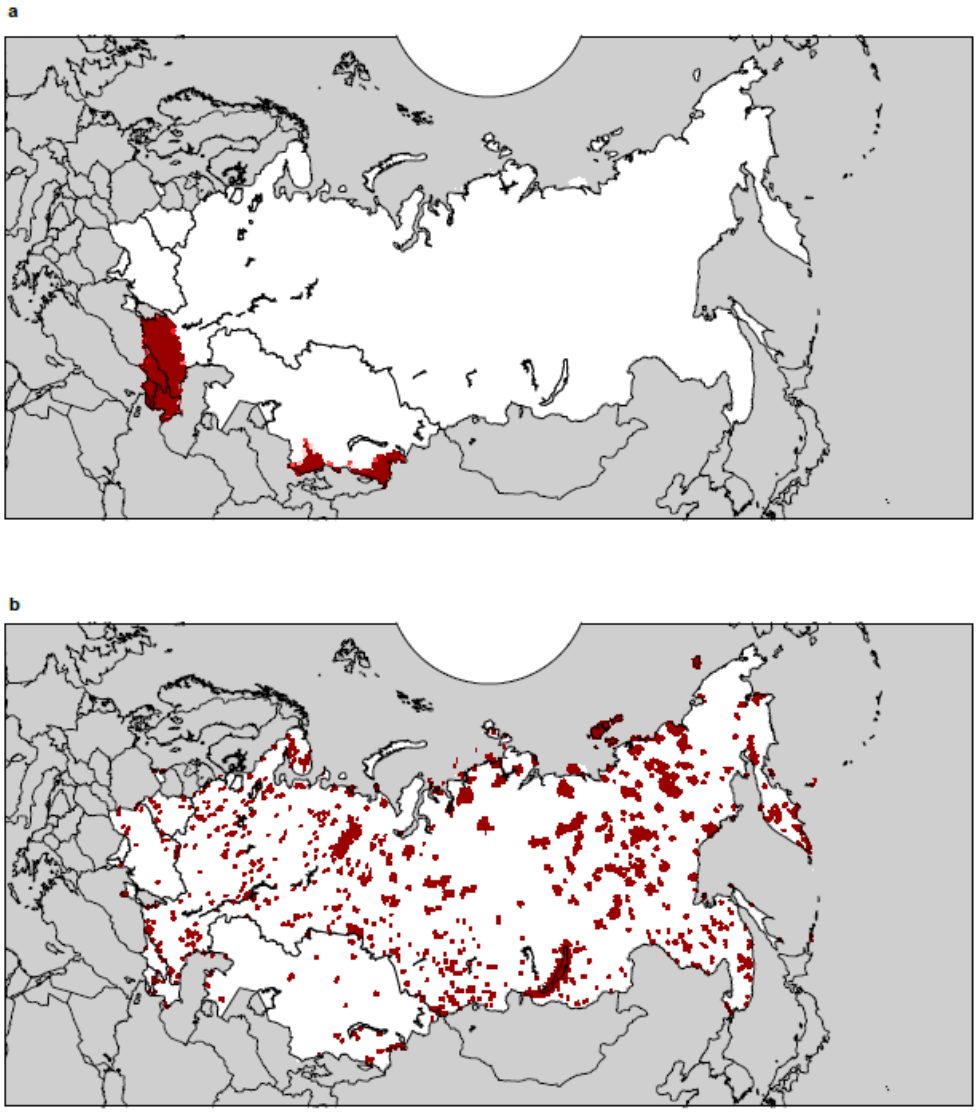

Supplementary Figure 1: Maps of biodiversity hotspots (a) and considered protected areas (b) in the fSU.

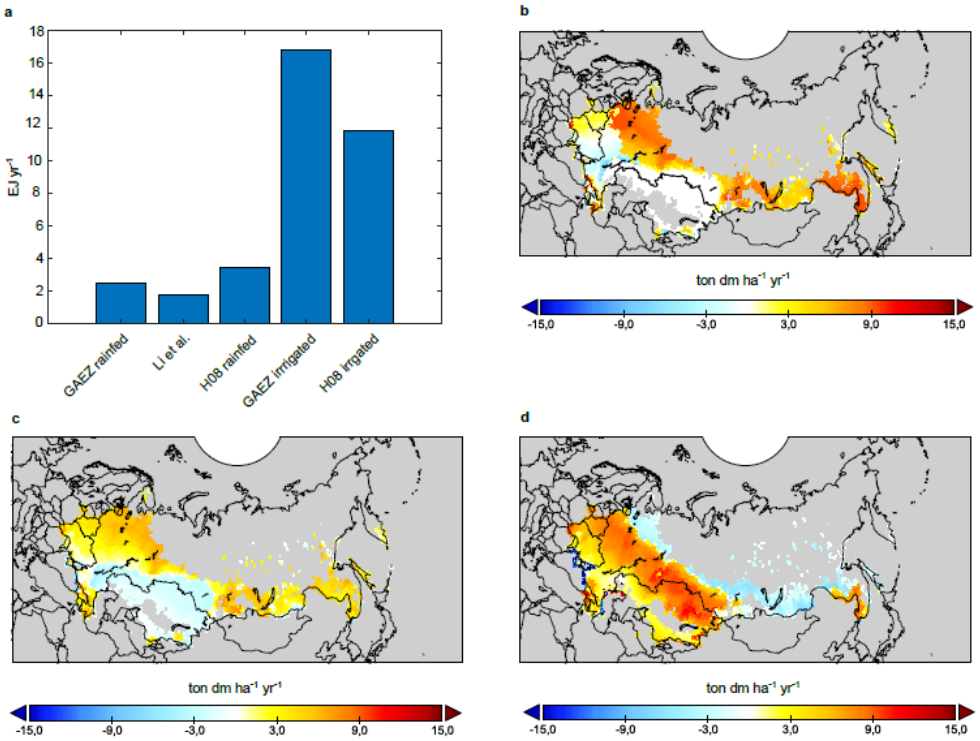

Supplementary Figure 2: Cross-model comparison of switchgrass productivity and bioenergy potentials on fSU abandoned land. *(a) Switchgrass fSU bioenergy potentials quantified using GAEZ (medium agricultural management intensity at rain-fed and irrigated conditions), the random-forest yield dataset from Li et al (rainfed, ref. [1]), and H08 (rainfed and irrigated conditions, ref. [2]). (b-c) Comparisons of the rainfed switchgrass yield difference of GAEZ minus Li et al (b), the rainfed switchgrass yield difference of GAEZ minus H08 (c), and the irrigated switchgrass yield difference of GAEZ minus H08 (d).*

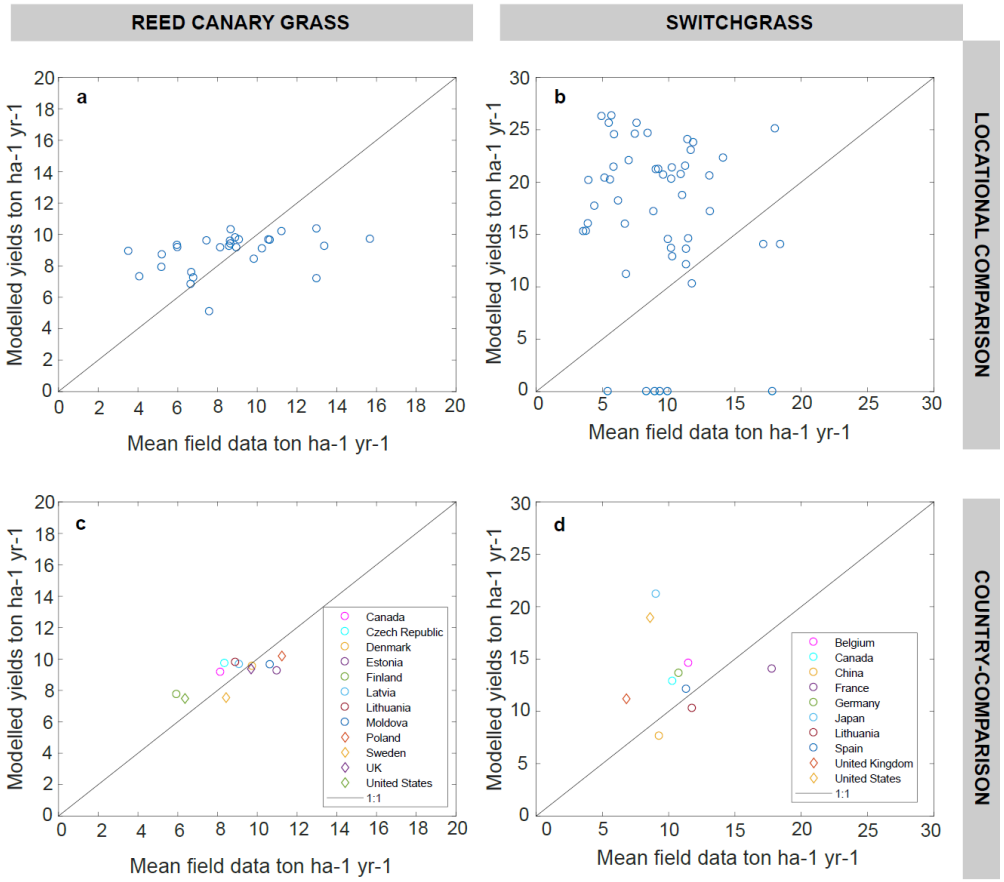

Supplementary Figure 3: Comparison of GAEZ reed canary grass and switchgrass rain-fed yields at medium management intensity with observational field data from Li et al. (ref. [3]). *Location based comparisons of mean reported yields across years vs GAEZ pixel estimate for (a) reed canary grass and (b) switchgrass. Country means from observations across all datapoints vs GAEZ means based on the same pixels are shown for (c) reed canary grass and (d) switchgrass.*

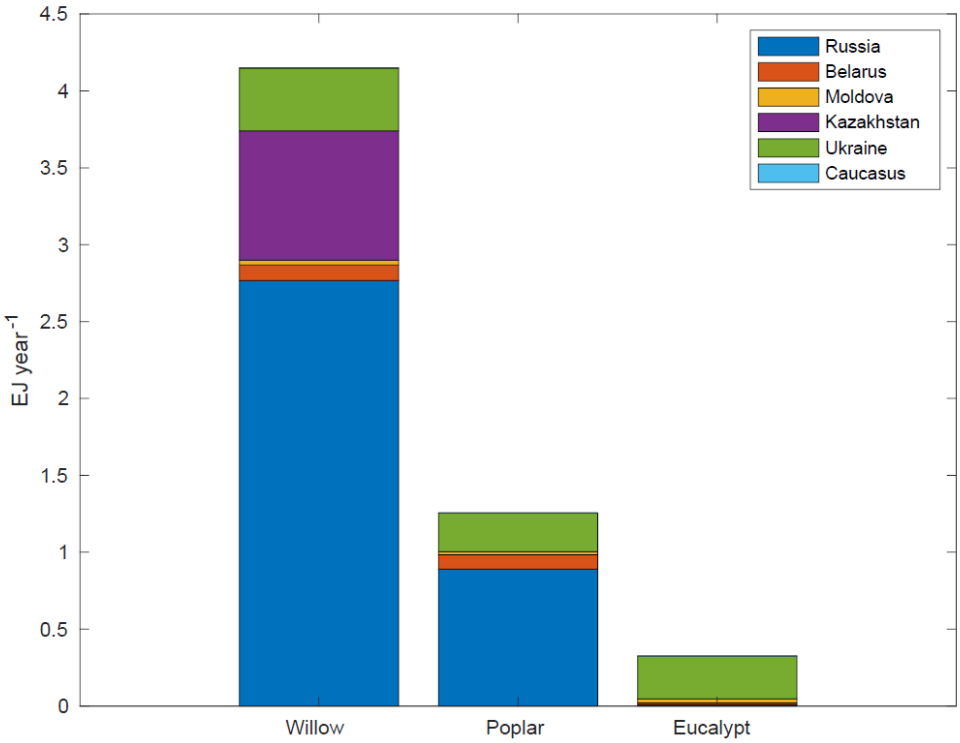

***Supplementary Figure 4*: Bioenergy potentials of woody bioenergy crops.** *Bioenergy potentials on abandoned land across the fSU of deploying woody bioenergy crops found by integrating our land availability estimates with data from the random-forest yield dataset from Li et al (rainfed, ref. [1]). This yield dataset is based on historical measurements and is produced through machine-learning techniques. Considered woody crops here are willow, poplar, and eucalypt. Land availability is constrained to abandoned land outside biodiversity hotspots and protected areas.*

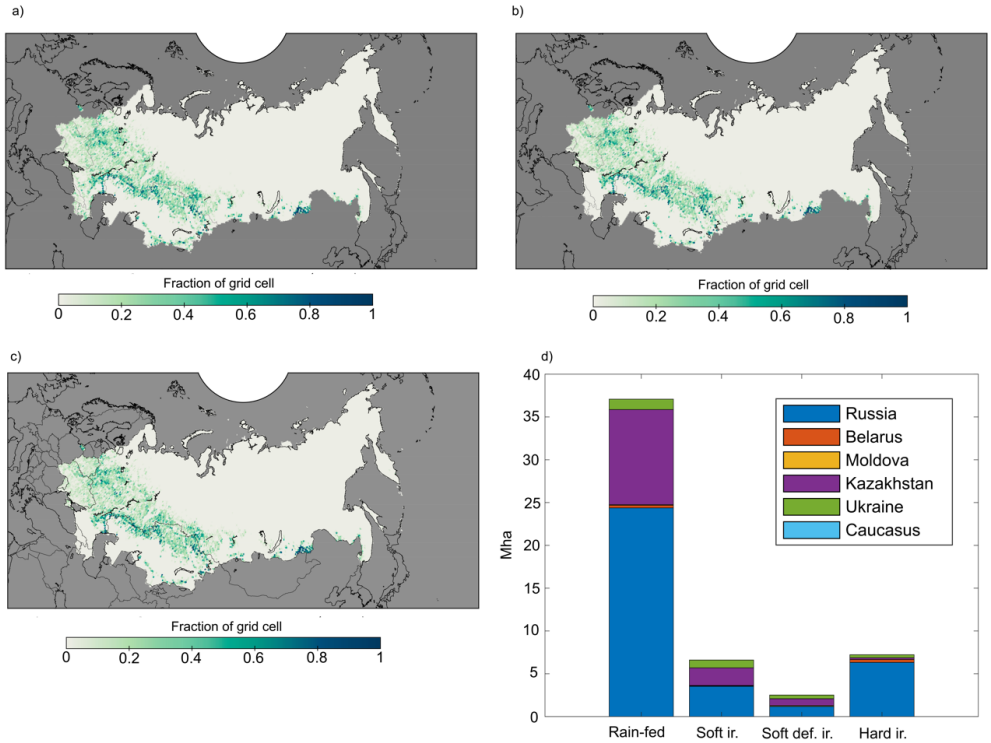

Supplementary Figure 5: Abandoned land and candidate irrigation areas. *Maps of (a) abandoned land (upscaled from ref. [4]), (b) abandoned land outside biodiversity hotspots, and (c) abandoned land outside biodiversity hotspots and protected areas are shown as fraction of grid cell. (d) Abandoned land outside biodiversity hotspots and protected areas adjusted for country level land cover dataset confusion matrices and distributed across water supply systems and countries. All maps are shown at 5 arcminutes.*

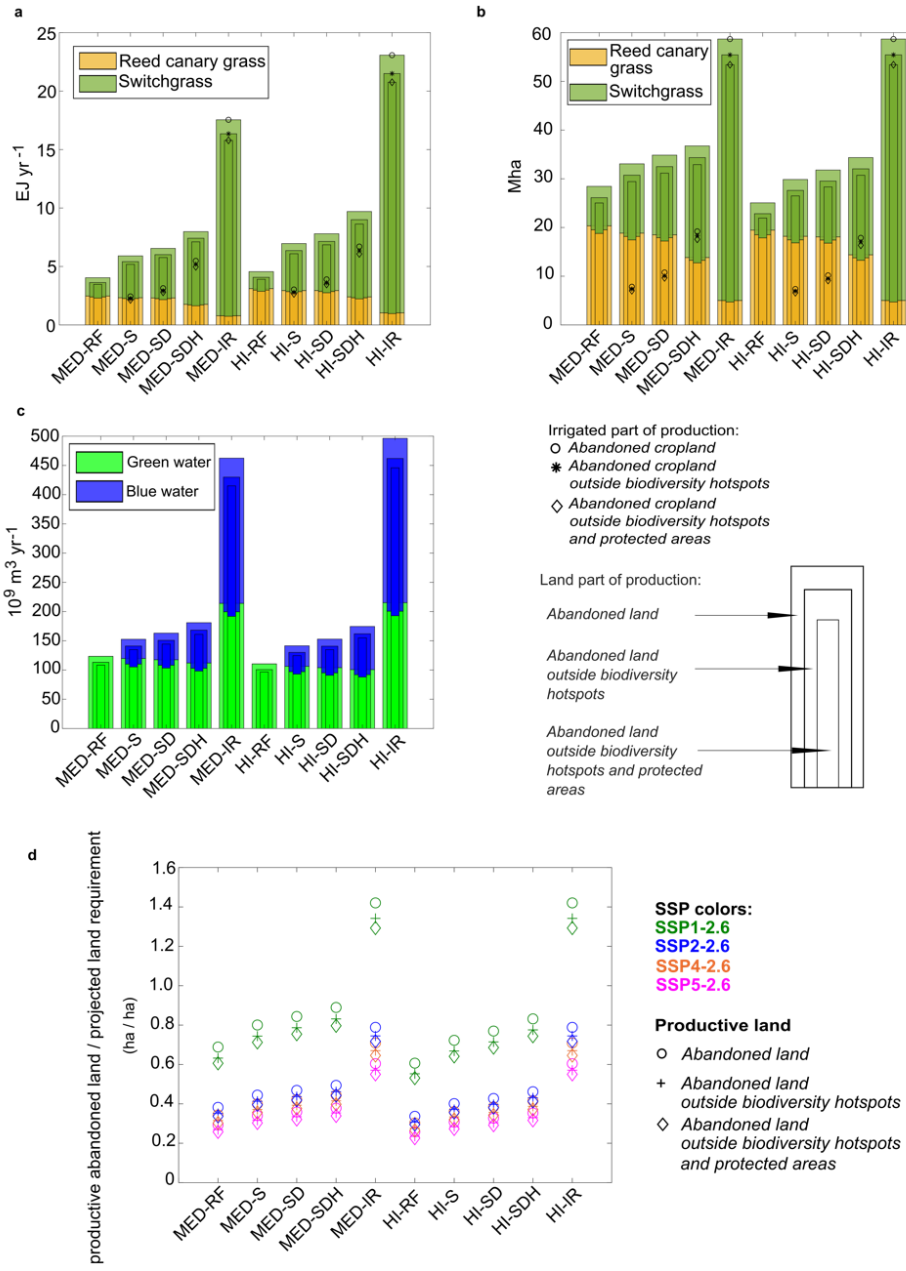

Supplementary Figure 6: Bioenergy potentials and their land and water use requirements across management intensities, land availability and water supply systems. *(a) Bioenergy potentials (EJ year^{-1}). (b) Productive abandoned land (Mha). (c) Crop water use (10^9 m^3 year^{-1}) originating from green and blue water sources (local precipitation and irrigated water withdrawals, respectively). (d) Comparison of productive abandoned land across management intensities, land availability and water supply systems with the projected fSU bioenergy land requirements to meet bioenergy demand for 2°C scenarios in 2050 across the different SSPs obtained by processing GCAM data (ha/ha). All shown values are adjusted for country-specific land cover dataset confusion matrices. X-axis notations describes agricultural management intensities and water supply. Management intensities are medium (MED) and high (HI). Water supply systems are rain-fed (RF), soft-path irrigation with monthly water storage (S), soft-path irrigation with crop water deficit (D), hard-path irrigation with annual water storage (H), and complete irrigation (IR). Water supply systems applying combinations of S, D, and H*

considers rain-fed supply on the remaining non-irrigated land. Land use in (a-c) refer to abandoned land (thick bars), abandoned land outside biodiversity hotspots (middle bars), and abandoned land outside biodiversity hotspots and protected areas (thin bars). Irrigated part of productive lands and bioenergy potentials are shown in (a) and (b) as scattered datapoints.

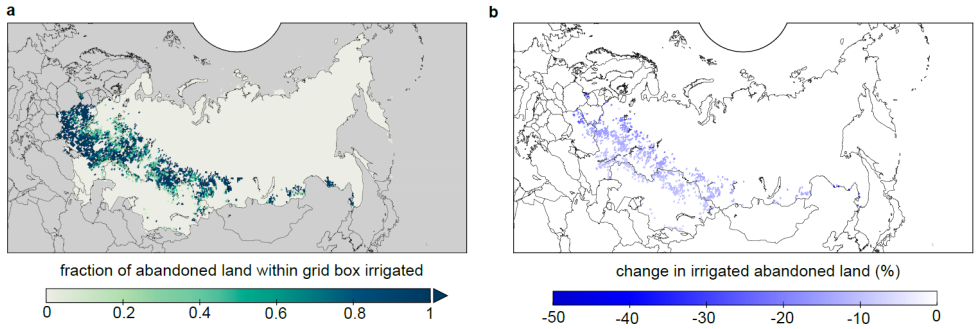

Supplementary Figure 7: Irrigated areas at high agricultural management intensity. *(a) Fraction of abandoned land within grid box irrigated. (b) Change in irrigated abandoned land (%) with high management intensity relative to medium management intensity. Both maps are consistent with deploying irrigation in line with all three irrigation management strategies (soft, soft deficit, and hard irrigation combined).*

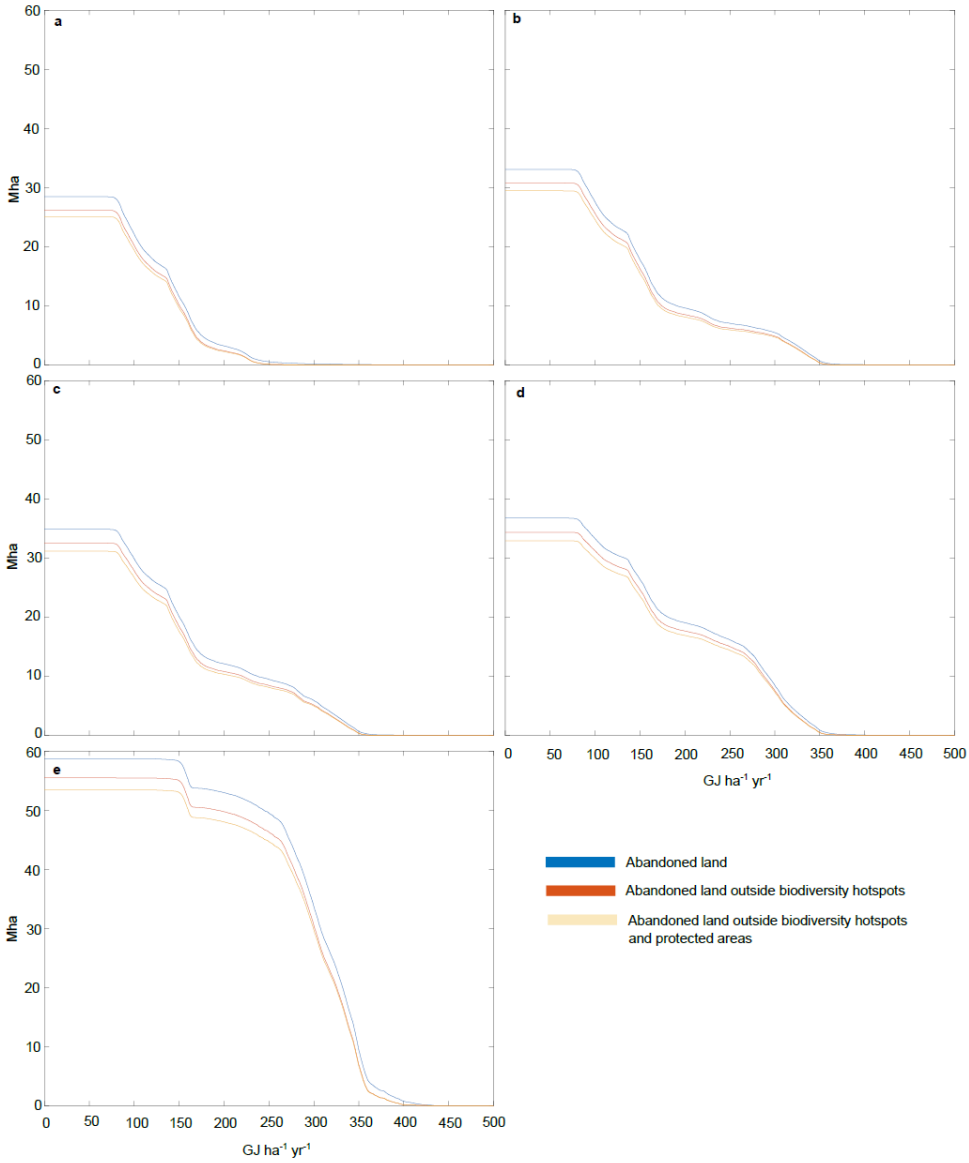

Supplementary Figure 8: Productivity curves with optimal crop allocation at medium management intensity. *Results describe total abandoned land which have higher bioenergy yields than different yield thresholds. Sub-figures refer to (a) rain-fed water supply, (b) soft-path irrigation and rain-fed elsewhere, (c) soft-path and soft-path irrigation with water deficits and rain-fed elsewhere, (d) soft-path, soft-path with deficit and hard-path irrigation and rain-fed elsewhere, and (e) fully irrigated water supply. Results are show for three different land availabilities (abandoned land, abandoned land outside biodiversity hotspots, and abandoned land outside biodiversity hotspots and protected areas).*

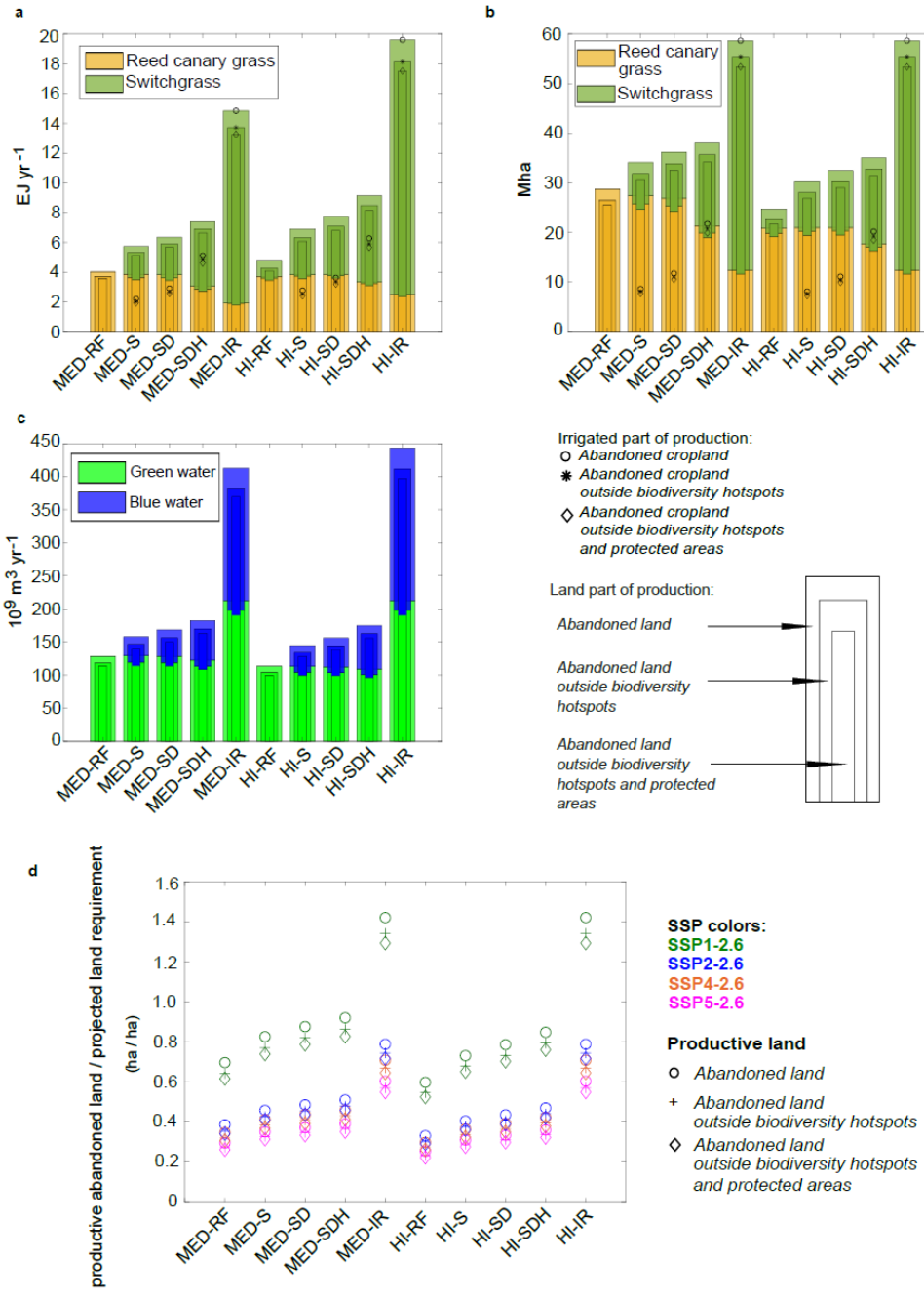

Supplementary Figure 9: Bioenergy potentials and their land and water use requirements across management intensities, land availability and water supply systems obtained by considering a measurement based climate input from CRU[5,6] (1960-1990) to GAEZ[7] instead of a HadCM3[8] 2020s climate (2010-2040). *(a) Bioenergy potentials (EJ year^{-1}). (b) Productive abandoned land (Mha). (c) Crop water use (10^9 m^3 year^{-1}) originating from green and blue water sources (local precipitation and irrigated water withdrawals, respectively). (d) Comparison of productive abandoned land across management intensities, land availability and water supply systems with the projected fSU bioenergy land requirements to meet bioenergy demand for 2°C scenarios in 2050 across the different SSPs obtained by processing GCAM data (ha/ha). All*

shown values are adjusted for country-specific land cover dataset confusion matrices. X-axis notations describes agricultural management intensities and water supply. Management intensities are medium (MED) and high (HI). Water supply systems are rain-fed (RF), soft-path irrigation with monthly water storage (S), soft-path irrigation with crop water deficit (D), hard-path irrigation with annual water storage (H), and complete irrigation (IR). Water supply systems applying combinations of S, D, and H considers rain-fed supply on the remaining non-irrigated land. Land use in (a-c) refer to abandoned land (thick bars), abandoned land outside biodiversity hotspots (middle bars), and abandoned land outside biodiversity hotspots and protected areas (thin bars). Irrigated part of productive lands and bioenergy potentials are shown in (a) and (b) as scattered datapoints.

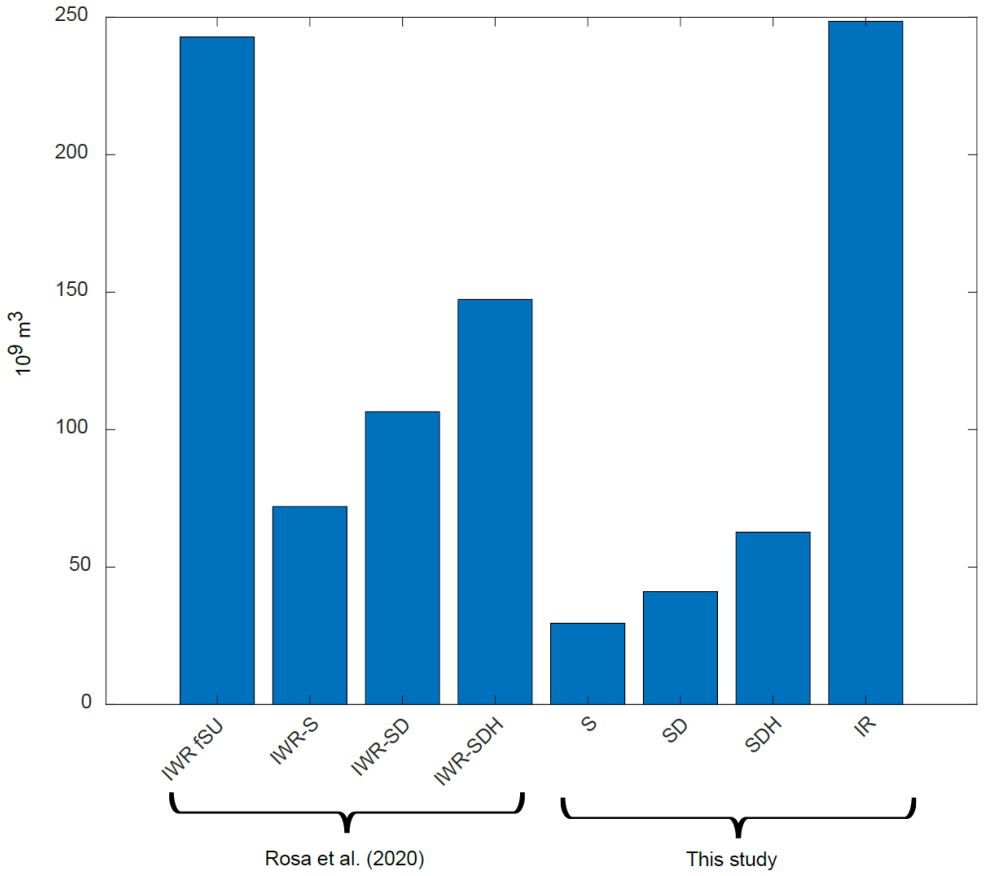

Supplementary Figure 10: Comparison of modelled irrigation requirements by Rosa et al. (2020)[9] and quantified irrigation blue water use at medium management intensity from this study*. Land availability is constrained to only abandoned land outside biodiversity hotspots and protected areas. X-axis notations describe soft irrigation with monthly water storage (S), soft irrigation with crop water deficit (D), hard irrigation with annual water storage (H), and complete irrigation (IR)). Results on the left hand side of the figure describe total irrigation water requirements (IWR) for the present day agricultural sector found by processing data from Rosa et al. (2020). Totals from Rosa et al. (2020) are given for the whole fSU (IWR-fSU) and with spatial constraints corresponding to the specific cells where irrigated water withdrawals are deployed here to supply bioenergy crops for the different irrigation strategies (IWR-S, IWR-SD, IWR-SDH). Right hand side results describe irrigation water requirements of bioenergy crops from this study.*

Supplementary Tables

Supplementary Table 1: Field observations of reed canary grass yields. *Observed mean yields of fertilized and rainfed reed canary grass from multiple year field experiments at different locations found in literature. We removed any datapoints without fertilizer application and any datapoints with irrigation before calculating mean yields for different locations.*

Country	Spatial coordinates [lat, lon]	Mean reported dry mass yield [ton ha^{-1} yr^{1}]	References
Canada	(46.5, -71.1)	8.2	[10]
Czech Republic	(50.0, 14.3)	8.7	[11]
	(49.4, 15.0)	8.7	[11]
	(49.1, 16.4)	8.7	[11]
	(50.3, 13.2)	7.5	[11]
Denmark	(49.0, 14.4)	13.0	[12]
	(56.2, 9.0)	10.3	[12]
	(56.4, 9.7)	6.0	[13]
Estonia	(58.6, 24.4)	8.6	[14]
	(58.3, 24.2)	13.4	[15,16]
Finland	(62.5, 31.2)	5.2	[17]
	(64.7, 25.3)	6.7	[18]
Latvia	(56.4, 25.1)	9.1	[17]
Lithuania	(55.2, 23.5)	8.9	[19]
Moldova	(56.4, 28.5)	10.7	[20]
Poland	(50.4, 22.2)	11.2	[21]
Sweden	(63.8, 20.2)	4.1	[22]
			[22]
	(63.2, 14.3)	13.0	[23]
			[23]
	(56.4, 15.6)	9.9	
	(63.8, 20.1)	6.8	
United Kingdom	(52.0, 0.4)	3.5	[24]
	(51.5, -0.5)	9.0	[25]
			[26]
	(52.1, -2.5)	15.7	[26]
	(52.1, -2.4)	10.6	
United States	(42.5, -97.2)	7.6	[27]

(44.35, -97.0)	6.7	[27]
(46.65, -76.79)	6.0	[28]
(47.0, -73.4)	5.2	[28]

Supplementary Table 2: Field observations of switchgrass yields. *Observed mean yields of fertilized and rainfed switchgrass from multiple year field experiments at different locations found in literature. We removed any datapoints without fertilizer application and any datapoints with irrigation before calculating mean yields for different locations.*

Country	Spatial coordinates [lat, lon]	Mean reported dry mass yield [ton ha^{-1} yr^{1}]	References
Belgium	(51.0, 3.5)	11.5	[29]
Canada	(45.5, -73.8)	10.3	[30,31]
China	(39.6, 116.5)	17.8	[32]
	(37.5, 118.5)	3.9	[33]
	(40.2, 116.1)	5.4	[34]
	(36.9, 109.3)	10.0	[35]
France	(49.9, 3.0)	18.4	[36]
	(49.8, 3.0)	17.2	[37]
Germany	(48.7, 8.9)	11.3	[38]
	(48.8, 8.9)	10.2	[39]
Lithuania	(54.5, 24.5)	11.8	[40]
Japan	(35.7, 139.5)	9.1	[41]
Spain	(43.4, 5.5)	11.3	[42]
United Kingdom	(51.8, -0.4)	6.8	[43]
United States	(41.9, -88.9)	9.2	[44,45]
	(40.1, -88.2)	14.1	[44,45]
	(37.5, -88.7)	11.3	[44,45]
	(30.3, -89.9)	9.9	[46]
	(39.8, -90.8)	10.3	[46]
	(38.4, -88.4)	13.1	[46]
	(39.0, -89.0)	10.9	[46]
	(32.4, -85.9)	11.7	[47,48]
	(32.8, -85.7)	5.5	[47]
	(47.0, -97.0)	9.0	[27]
	(46.7, -97.2)	9.4	[27]
	(32.2, -98.2)	13.1	[49]
	(28.5, -97.7)	8.3	[49]
	(38.2, -78.0)	11.9	[50]
	(37.9, -78.0)	11.4	[50]
	(36.9, -78.2)	7.5	[50]

(42.5, -76.5)	6.7	[51]
(42.9, -77.0)	4.4	[51]
(44.4, -73.4)	3.8	[51]
(42.5, -76.4)	3.6	[51]
(35.9, -84.0)	18.0	[52]
(32.2, -98.2)	8.9	[53]
(40.0, -96.8)	6.2	[53]
(42.0, -93.8)	9.6	[54]
(41.0, -93.4)	10.2	[54]
(33.9, -87.9)	8.4	[55]
(32.8, -85.7)	7.6	[55]
(34.3, -86.0)	5.9	[55]
(32.0, -87.3)	5.9	[55]
(41.5, -83.1)	5.6	[56,57]
(41.4, -83.1)	5.2	[57]
(41.4, -82.8)	4.0	[57]
(36.1, -97.1)	11.0	[58]
(39.9, -75.4)	7.0	[59]
(35.3, -77.5)	5.7	[60]
(34.8, -76.7)	5.0	[60]

Supplementary Table 3: An overview of all considered variants of land availability, crop allocation, agricultural management intensities and water supply systems for estimating bioenergy potentials from abandoned land in the fSU. *Results in the main text are mostly shown for the following combination: abandoned land outside biodiversity hotspots and protected areas, optimal energy-based crop allocation, medium agricultural management intensity, climatic conditions centered around the 2020s, and all the different water supply systems. Other results are found in the Supplementary Information (this document). Climatic conditions refer to the background climate considered by the yield model.*

Land availability	**Perennial grass**	**Agricultural management intensity**	**Water supply**	**Climatic conditions**
Abandoned land outside biodiversity hotspots and protected areas	Optimal energy-based crop allocation	Medium	Rain-fed	Centered around the 2020s (HadCM3[8], 2010-2040)
Abandoned land outside biodiversity hotspots	Reed canary grass	High	Soft-path irrigation and rain-fed elsewhere	Measurement based (CRU[5,6], 1960-1990)
Abandoned land	Switchgrass		Soft-path and soft-path with deficit irrigation, rain-fed elsewhere	
			Soft-path, soft-path with deficit and hard-path irrigation, rain-fed elsewhere	
			Complete irrigation	

Supplementary Table 4: Country specific productive area, mean bioenergy yields on productive abandoned land and bioenergy potentials across different water supply systems. *Results refer to medium agricultural management intensity with nature conservation policies that exclude all areas in protected areas and biodiversity hotspots.*

Country	Water supply system	Productive area [Mha]	Mean bioenergy yield on productive land [GJ ha^{-1} yr^{1}]	Bioenergy potential [EJ yr^{-1}]
Russia	Rainfed	21	133	2.8
Russia	Irrigated	35	275	9.8
Russia	Soft path	23	156	3.7
Russia	Soft path w/deficit	24	162	3.9
Russia	Hard path	26	200	5.1
Belarus	Rainfed	0.69	199	0.14
Belarus	Irrigated	0.69	282	0.19
Belarus	Soft path	0.69	206	0.14
Belarus	Soft path w/deficit	0.69	206	0.14
Belarus	Hard path	0.69	245	0.17
Moldova	Rainfed	0.22	185	0.041
Moldova	Irrigated	0.22	346	0.077
Moldova	Soft path	0.22	215	0.048
Moldova	Soft path w/deficit	0.22	267	0.059
Moldova	Hard path	0.22	273	0.060
Kazakhstan	Rainfed	0.31	108	0.033
Kazakhstan	Irrigated	14	341	4.8
Kazakhstan	Soft path	2.5	299	0.75
Kazakhstan	Soft path w/deficit	3.4	290	0.98
Kazakhstan	Hard path	3.6	294	1.0
Ukraine	Rainfed	2.9	164	0.48
Ukraine	Irrigated	2.9	318	0.92
Ukraine	Soft path	2.9	217	0.63

Ukraine	Soft path w/deficit	2.9	239	0.70
Ukraine	Hard path	2.9	250	0.73

Supplementary Table 5: Comparison of fSU bioenergy potentials, productive abandoned land and blue water withdrawals found here with previous global studies. *Global data was obtained from the respective previous studies and processed to provide results for the fSU region.*

Study	Bioenergy potential [EJ yr-1]	Productive abandoned land [Mha]	Blue water withdrawals [10^9 m^3 yr^{-1}]
Leirpoll et al. (2021) (ref. [61])	3.5	9.9	Not provided.
Næss et al. (2021) (ref. [62])	0.7-3.8	7.6-10	0-34
This study (All land availabilities, water supply systems, and management intensities)	3.5-23	25-58	0-281
This study (Nature conservation, rain-fed water supply, medium management)	3.5	25	0
This study (Nature conservation, sustainable irrigation strategies, medium management)	5.2-7.1	29-33	30-63

Supplementary Texts

Supplementary Text 1 | Protected areas and biodiversity hotspots

Biodiversity hotspots are defined as areas containing a minimum of 1500 endemic vascular plants that have lost more than 70% of the natural vegetation[63]. Sparing abandoned land in biodiversity hotspots for habitat restoration can be especially beneficial for conservation of vascular plants[64,65]. We filtered out and excluded abandoned land within biodiversity hotspots using masks at 10 arcseconds (Supplementary Figure 1a).

Likewise, abandoned land in selected protected areas were identified based on the World Database of Protected Areas[66] using a mask[7] at 5 arcminutes and excluded (Supplementary Figure 1b). Protected areas considered include National Parks, Forest Reserves, Zapovednik (specific Russian protected areas), Wildlife Management Areas, Nature Parks, Resource Reserves, Nature Reserves and Game Reserves[66].

Supplementary Text 2 | Bioenergy crops

We consider two bioenergy crops for the analysis: switchgrass and reed canary grass. Switchgrass (*Panicum virgatum)* is a C4 grass originally growing in North America from Mexico in the south and up to 55°N[67]. Switchgrass photosynthetic rates peak between 25°C and 30°C[68]. It is vulnerable to severe draughts and potential yield losses can be mitigated through irrigation during draughts[69–71]. Switchgrass is typically harvested during autumn[72]. Reed canary grass is a C3 grass native to Eurasia and North America, growing in temperate climates under cool and moist conditions[73,74]. It has an optimal growth rate between 20°C and 25°C[75] and is able to grow under a range of water regimes[74,76]. Typically, reed canary grass harvest happens during late winter or early spring[73].

Supplementary Text 3 | GAEZ model

Global Agro-Ecological Zones v3.0 is a parameterized crop yield model which has been widely used to quantify agricultural productivity and water implications of crops[7]. GAEZ considers a range of crop-specific parameters describing crop characteristics, different agricultural management, irrigation practices and site-specific parameters such as climatic conditions (radiation, precipitation, and temperature), soil quality and terrain to estimate crop yields. Yearly variability of soil moisture, yield losses due to pests, soil workability constraints and frosts is also accounted for. It uses the optimal crop growth calendar to quantify crop water balances, water deficits and evapotranspiration at rain-fed conditions. GAEZ also models irrigated crop yields by assuming no crop water deficits over the growth period. We used GAEZ data to quantify rain-fed and irrigated crop yields on abandoned land of reed canary grass and switchgrass at two agricultural management intensities. Medium agricultural management intensity is both subsistence and commercially based with some mechanization, soil conservation measures and fertilizer and pesticide use[7]. High management intensity refers to a future potential agricultural system with closed yield gaps which is highly mechanized and market oriented, using optimal application of fertilizers and pesticides, and high yielding varieties. GAEZ was also used to quantify green and blue crop water used. For a detailed model description, see ref. [7].

Supplementary Text 4 | Comparing switchgrass bioenergy potentials and productivity across three models

We compared switchgrass yields and switchgrass bioenergy potentials across the fSU using three different models as an additional test (Supplementary Figure 2). At rainfed conditions, total bioenergy potentials on all abandoned land from the study area are 2.4 EJ yr-1, 1.8 EJ yr^{-1} and 3.4 EJ yr^{-1} using GAEZ with medium management intensity[7], the random forest (RF) dataset[1] and H08[2], respectively (Supplementary Figure 2a). With a completely irrigated water supply, GAEZ shows a switchgrass bioenergy potential of 17 EJ yr^{-1}, while H08 gives a lower potential of 12 EJ yr^{-1}. We find that switchgrass crop yields differ spatially between models. GAEZ produces higher rainfed switchgrass yields than the RF dataset in northern and eastern Russia and southern Caucasus, while the RF dataset show higher yields north of the Black Sea (Supplementary Figure 2b). In Kazakhstan, most areas are unproductive with both GAEZ and the RF dataset. With H08 Kazakhstan is productive and showing higher yields than GAEZ, while GAEZ produce higher yields in most other areas (Supplementary Figure 2c). With irrigation, GAEZ produces higher switchgrass yields than H08 in most of the fSU, except in northern Russia and Siberia where H08 yields are higher (Supplementary Figure 2d).

Supplementary Text 5 | Comparing predicted reed canary grass and switchgrass yields with observations

We gathered observational data to compare with GAEZ modelled reed canary grass and switchgrass yields at medium management intensity and rainfed conditions. A large share of observational data was collected directly from the Li et al. (2018)[3] database of field trial yields. In total, we obtained field data from 28 different locations across 19 individual studies for reed canary grass (Supplementary Table 1) and from 50 different locations across 32 individual studies for switchgrass (Supplementary Table 2). All datapoints without fertilizer application or with any use of irrigation was removed.

We calculated location specific mean yields over all reported years, thereby removing some of the inter-annual variability and allowing for a better comparison with GAEZ yields (30 years modelled average). Mean observations and pixel based yield estimates were compared for each location. Consistent with the methodology applied in this paper, we also aggregated observed yields to the country level and compare with the corresponding aggregated GAEZ modelled mean yields based on the same locations. While no field data was obtainable from the fSU, this validation exercise still provides valuable insights into general GAEZ model performance at the country level.

For reed canary grass, the pixel-based locational comparison shows a coefficient of determination (R^2) between predictions and observations of 0.15 (Supplementary Figure 3a). However, there is a moderate goodness of fit with observed yields at the country level (Supplementary Figure 3c). A R^2 of 0.52 was obtained, indicating that about half of the variance in modelled yields can be explained by the GAEZ model. Datapoints mainly follow the 1:1 line, but with some outliers on both sides (no clear bias from GAEZ emerged) and a root mean square error of 1.1. For example, in Finland modelled mean yields are 7.7 ton ha^{-1} yr^{-1}, while mean observed yields are 6.0 ton ha^{-1} yr^{-1}. The closest match between modelled and observed mean yields are found in Denmark, with 9.8 and 10.0 ton ha^{-1} yr^{-1}, respectively.

For rain-fed switchgrass, GAEZ generally produces higher locational yields at medium management intensity than seen in field observations (Supplementary Figure 3b). Especially for switchgrass, improved agricultural management may thus be needed to achieve predicted rain-fed yields. The pixels that are overestimated the most are mainly located in USA and Japan, and not in Europe (Supplementary Figure 3d). This gives some support to that predicted switchgrass yields may be closer to observed yields in the fSU than the global average. Most of the data gathered is from field trials in North America (74%), while the rest is from Eurasia (26%). In mainland Eurasia, we find a country-level R^2 of 0.15 with a root mean square error of 2.8 when comparing switchgrass observations and predictions. A lower share of the variance in modelled yields is thus explainable by the model for switchgrass than reed canary grass.

Discrepancies between modelled and observed yields are explainable by a variety of factors such as agricultural management, previous land use and annual variations in meteorological conditions. Field studies typically apply varying levels of fertilizers and pesticides which are not standardized to meet the GAEZ management intensities[7]. Fertilizer application rates were often found to vary across different sub-fields and years even within the same study and at the same location[3]. Furthermore, the number of years considered varied across studies, and especially dry, wet, warm, or cold years might lead to the observed yields deviating from the long-term mean. Some field-trials also go several decades back in time and others are more recent, which also leads to additional

uncertainties of actual agricultural management as practices has changed over time. All these factors contribute to make crop yield validation efforts challenging. It was not possible to compare irrigated yield estimates to observations due to a lack of sufficient field data for the given crops with reported irrigation[3]. Further field studies of irrigated bioenergy crop production are needed to allow comparisons of predicted and observed yields.

Supplementary Text 6 | Bioenergy potentials of woody bioenergy crops

We processed yield data of willow, poplar and eucalypt[1] to estimate their potential across the fSU (Supplementary Figure 4). Bioenergy potentials on abandoned land with biodiversity hotspots and protected areas excluded are 4.1, 1.3, and 0.3 EJ $year^{-1}$ for willow, poplar, and eucalypt, respectively. Our findings indicate that willow may be a robust alternative to perennial grasses, especially in Kazakhstan where willow produced a higher potential (0.8 EJ $year^{-1}$) than what was found here for rain-fed perennial grasses (0.3 EJ $year^{-1}$). More work is needed to unravel the land-energy-water interactions of woody bioenergy crop deployment on abandoned land.

Supplementary Text 7 | Study limitations and uncertainties

A key strength of the fSU abandoned land dataset relative to global land cover datasets is the extensive validation efforts previously performed at a country level[4]. Yet, the spatial accuracy within each country may still vary between regions. Our results are corrected for country level accuracies, which means that we rely on the spatial abandonment pattern within each country to calculate mean bioenergy yields, and water evapotranspiration rates from GAEZ.

Any map derived from remote sensing practices can be expected to contain errors and uncertainties. Good practices for estimation of the total extent of land use change involves validation against observational ground-truth reference datasets[77]. This allows adjusting pixel-based estimates of total land use change found with the land cover dataset based on the reference observational dataset which has better accuracy. Previous efforts from the developers of the hybrid fSU land cover map (Lesiv et al. 2018)[4] have invested major efforts into developing a reference dataset to compare against and to estimate accuracies. The abandoned land class in the fSU hybrid map achieves user and producer accuracies of 31% and 62%, respectively. The abandoned land class covers 91 Mha in the raw data of the hybrid map but is adjusted to 59 Mha after a series of mathematical operations (see ref. [77] for further description of good practice methods). We make use of this at a country level to also adjust bioenergy potentials and water requirements.

GAEZ is widely used to model bioenergy crops[61,62,78–82], but also relies on different limitations and uncertainties such as crop mortality due to frosts and pests, growth response to fertilizer use, or yield losses caused by water deficits[7]. To assess the model-specific dependency of our results we processed switchgrass yield data from two other models (Li et al. (ref. [1]) and H08[2]). Results are shown in Supplementary Figure 2 and discussed in Supplementary Text 4. Similarly, a further cross-model comparisons of modeled crop water use can help reveal how different model assumption affects the crop water budget.

We used a dataset of sustainable irrigation expansion areas[9] which is designed for the agricultural sector to obtain insights into the potential for irrigated recultivation for bioenergy. While we have made sure that annual blue water budgets are not exceeded, further work is needed to refine irrigation expansion potentials specifically for bioenergy crops as crop water use may temporally differ during the growth season from food crops. If the small monthly water storages used in the soft-path and soft-path with deficit irrigation pathways cannot deliver sufficient blue water in some months at some locations, this would imply increasing use of deficit irrigation or hard-path larger annual storages. On the other hand, it could also mean that there is excess water in other locations or months that is not accounted for which could allow further soft irrigation expansion. More refined estimates of soft-path irrigation expansion potentials for bioenergy crops should assess water availability and crop water use at a higher temporal frequency.

There is also a need to address potential benefits and trade-offs in the nexus between new sustainably irrigated bioenergy and food production, and to identify optimal management strategies considering both irrigated recultivation and new irrigation deployment on in-use arable land. Irrigated recultivation for bioenergy taps into the sustainable irrigation budget, thereby decreasing the room for new irrigated food production. Additional insights into the economic feasibility of large-scale reservoir construction can also help identify how targeted policies can contribute to their deployment (especially large annual storages).

Future climatic changes will affect bioenergy productivity, water use, and water availability. Future yields are projected to increase in subarctic and continental climates with higher levels of global

warming due to changing temperature and precipitation patterns and the carbon dioxide (CO_2) fertilization effect[62,83]. The available future renewable freshwater budget for agricultural irrigation will depend on future climatic conditions and future anthropogenic activities[9]. Higher levels of global warming is expected to reduce the expansion potential of soft-path irrigation in Eastern Europe and Central Asia[84]. This can to some extent be compensated by increased deployment of large annual water storages (hard-path)[84]. More work is needed to unravel bioenergy potentials and water requirements from fSU abandoned land under different levels of global warming. Our work also used input from a single climate model (HadCM3[8]), and further work should compare the effect of using data from multiple climate models as inputs on estimated bioenergy potentials.

Biophysical effects of changing land surface characteristics will affect local land-atmosphere interactions[85]. For example, a potential shift from food crops to bioenergy crops has been associated with a regional cooling effect in the US[86–88]. We show that a large-scale bioenergy deployment on abandoned land across the fSU would affect evapotranspiration rates and freshwater availability depending on land availability, agricultural management, and water supply systems. Irrigation deployment can lead to changing local precipitation patterns[89] and have remote effects through atmospheric moisture recycling[90]. Future research should address how biophysical effects from deploying bioenergy crops across the fSU affects the regional climate, and how this in turn again affects both crop yields and the available freshwater budget for irrigation.

Other land management options than bioenergy crops such as nature restoration[91] or recultivation for food production[92,93] may be preferable in parts of the abandoned land. We excluded protected areas and biodiversity hotspots from the main part of the analysis. While a larger share of abandoned land is located within biodiversity hotspots at the global scale (about 40%)[62], we find that only 7% of the abandoned land in the fSU is in a biodiversity hotspot and 3% in protected areas. A full deployment including these areas would marginally increase bioenergy potentials by 11% at rain-fed conditions. Current nature conservation policies are thus not the major limitation for deploying bioenergy crops on abandoned land across the fSU. However, the sparing of additional abandoned land for continued rewilding beyond what is considered here can contribute to connect protected areas and key habitats such as the Eurasian Steppe[91], with potential benefits to biodiversity through reduced habitat fragmentation[94]. Switchgrass is a crop native to North America[67,72]. Further work is needed to assess the potential impacts of species invasiveness on the local biodiversity, and to identify management strategies to prevent invasive spread.

Other key gaps in knowledge that is not addressed here, but that should be targeted to get a better understanding of how bioenergy can contribute to climate change mitigation include taking system approaches to assess how different feedstocks can affect biofuel and bioelectricity production and BECCS potentials. Further work should also assess how the energy consumption needed by irrigation systems affect net energy gains of pursuing bioenergy production. There is also a need for a cost-benefit analysis comparing required investments costs with potential gains from deploying bioenergy. Likewise, there is a need to investigate how abandoned land can be recultivated for bioenergy production at a national scale as each nation in the fSU have independent regulations and priorities. This social side of bioenergy deployment also needs to be explored.

Supplementary References

1. Li, W. *et al.* Mapping the yields of lignocellulosic bioenergy crops from observations at the global scale. *Earth Syst. Sci. Data* **12**, 789–804 (2020).
2. Ai, Z., Hanasaki, N., Heck, V., Hasegawa, T. & Fujimori, S. Simulating second-generation herbaceous bioenergy crop yield using the global hydrological model H08 (v.bio1). *Geosci. Model Dev.* **13**, 6077–6092 (2020).
3. Li, W., Ciais, P., Makowski, D. & Peng, S. A global yield dataset for major lignocellulosic bioenergy crops based on field measurements. *Sci. Data* **5**, 180169 (2018).
4. Lesiv, M. *et al.* Spatial distribution of arable and abandoned land across former Soviet Union countries. *Sci. Data* **5**, 180056 (2018).
5. New, M., Lister, D., Hulme, M. & Makin, I. A high-resolution data set of surface climate over global land areas. *Clim. Res.* **21**, 1–25 (2002).
6. Mitchell, T. D. & Jones, P. D. An improved method of constructing a database of monthly climate observations and associated high-resolution grids. *Int. J. Climatol.* **25**, 693–712 (2005).
7. Fischer, G. *et al.* Global Agro-ecological Zones (GAEZ v3. 0)-Model Documentation. (2012).
8. Cox, P. M. *et al.* The impact of new land surface physics on the GCM simulation of climate and climate sensitivity. *Clim. Dyn.* **15**, 183–203 (1999).
9. Rosa, L. *et al.* Potential for sustainable irrigation expansion in a 3 °C warmer climate. *Proc. Natl. Acad. Sci.* **117**, 29526 LP – 29534 (2020).
10. Massé, D. *et al.* Methane yield from switchgrass and reed canarygrass grown in Eastern Canada. *Bioresour. Technol.* **102**, 10286–10292 (2011).
11. Strašil, Z. Evaluation of reed canary grass (Phalaris arundinacea L.) grown for energy use. *Res. Agric. Eng.* **58**, 119–130 (2012).
12. Kandel, T. P., Elsgaard, L., Karki, S. & Lærke, P. E. Biomass Yield and Greenhouse Gas Emissions from a Drained Fen Peatland Cultivated with Reed Canary Grass under Different Harvest and Fertilizer Regimes. *BioEnergy Res.* **6**, 883–895 (2013).
13. Karki, S., Elsgaard, L., Audet, J. & Lærke, P. E. Mitigation of greenhouse gas emissions from reed canary grass in paludiculture: effect of groundwater level. *Plant Soil* **383**, 217–230 (2014).
14. Heinsoo, K., Hein, K., Melts, I., Holm, B. & Ivask, M. Reed canary grass yield and fuel quality in Estonian farmers' fields. *Biomass and Bioenergy* **35**, 617–625 (2011).
15. Järveoja, J. *et al.* Mitigation of greenhouse gas emissions from an abandoned Baltic peat extraction area by growing reed canary grass: life-cycle assessment. *Reg. Environ. Chang.* **13**, 781–795 (2013).
16. Mander, Ü. *et al.* Reed canary grass cultivation mitigates greenhouse gas emissions from abandoned peat extraction areas. *GCB Bioenergy* **4**, 462–474 (2012).
17. Laasasenaho, K. *et al.* Biogas and combustion potential of fresh reed canary grass grown on cutover peatland. (2020).

18. Lindh, T. *et al.* Production of reed canary grass and straw as blended fuel in Finland. *VTT Process.* 4–5 (2005).

19. Pocienė, L., Šarūnaitė, L., Tilvikienė, V., Šlepetys, J. & Kadžiulienė, Ž. The yield and composition of reed canary grass biomass as raw material for combustion. *Biologija* **59**, (2013).

20. Ţîţei, V. *et al.* The green mass and silage quality of reed canary grass, Phalaris arundinacea under the conditions of Moldova. (2020).

21. Kołodziej, B., Stachyra, M., Antonkiewicz, J., Bielińska, E. & Wiśniewski, J. The effect of harvest frequency on yielding and quality of energy raw material of reed canary grass grown on municipal sewage sludge. *Biomass and Bioenergy* **85**, 363–370 (2016).

22. Lindvall, E., Gustavsson, A.-M. & Palmborg, C. Establishment of reed canary grass with perennial legumes or barley and different fertilization treatments: effects on yield, botanical composition and nitrogen fixation. *GCB Bioenergy* **4**, 661–670 (2012).

23. Palmborg, C., Lindvall, E. & Gustavsson, A. M. Demand for K and P in reed canary grass (Phalaris arundinacea) during the harvest years. *Futur. Eur. Grasslands* 498 (2014).

24. Shield, I. F., Barraclough, T. J. P., Riche, A. B. & Yates, N. E. The yield response of the energy crops switchgrass and reed canary grass to fertiliser applications when grown on a low productivity sandy soil. *Biomass and Bioenergy* **42**, 86–96 (2012).

25. Christian, D. G., Yates, N. E. & Riche, A. B. The effect of harvest date on the yield and mineral content of Phalaris arundinacea L. (reed canary grass) genotypes screened for their potential as energy crops in southern England. *J. Sci. Food Agric.* **86**, 1181–1188 (2006).

26. Semere, T. & Slater, F. M. Ground flora, small mammal and bird species diversity in miscanthus (Miscanthus×giganteus) and reed canary-grass (Phalaris arundinacea) fields. *Biomass and Bioenergy* **31**, 20–29 (2007).

27. Meyer, D. W., Norby, W. E., Erickson, D. O. & Johnson, R. G. *Evaluation of herbacceous biomass crops in the northern Great Plains. Final report*. (Oak Ridge National Lab., TN (United States), 1994).

28. Pfeier, R. A., Fick, G. W., Lahwell, D. J. & Maybee, C. *Screening and Selection of Herbaceous Species for Biomass Production in the Midwest/Lake States: Final Report 1985-1989. Biomass Feed. Dev. Program, Oak Ridge Natl. Lab. Oak Ridge, Tennessee (1990).* (1990).

29. Muylle, H. *et al.* Yield and energy balance of annual and perennial lignocellulosic crops for bio-refinery use: A 4-year field experiment in Belgium. *Eur. J. Agron.* **63**, 62–70 (2015).

30. Madakadze, I. C. *et al.* Light interception, use-efficiency and energy yield of switchgrass (Panicum virgatum L.) grown in a short season area. *Biomass and Bioenergy* **15**, 475–482 (1998).

31. Madakadze, I. C. *et al.* Leaf Area Development, Light Interception, and Yield among Switchgrass Populations in a Short-Season Area. *Crop Sci.* **38**, cropsci1998.0011183X003800030035x (1998).

32. Fan, X. *et al.* Dynamic change of biomass and quality of switchgrass in different growing seasons. *Prataculture Sci.* (2014).

33. Gao, L., Liu, J., Deng, B., Yang, F. & Zhang, Y. Effects of nitrogen level and harvest time on biomass yield and energy characteristics of switchgrass. *Prataculture Sci.* (2016).

34. Hou, X., Fan, X., Zuo, H., Wu, J. & Li, Z. Effect of nitrogen fertilizer on the growth characteristics and biomass yield of bioenergy grasses on abandoned sand excavation lands. *Acta Agrestia Sin.* **18**, 268–279 (2010).

35. Xu, B. C., Li, F. M. & Shan, L. Switchgrass and milkvetch intercropping under 2:1 row-replacement in semiarid region, northwest China: Aboveground biomass and water use efficiency. *Eur. J. Agron.* **28**, 485–492 (2008).

36. Cadoux, S. *et al.* Implications of productivity and nutrient requirements on greenhouse gas balance of annual and perennial bioenergy crops. *GCB Bioenergy* **6**, 425–438 (2014).

37. El Akkari, M. *et al.* Using a Crop Model to Benchmark Miscanthus and Switchgrass. *Energies* **13**, (2020).

38. Boehmel, C., Lewandowski, I. & Claupein, W. Comparing annual and perennial energy cropping systems with different management intensities. *Agric. Syst.* **96**, 224–236 (2008).

39. Iqbal, Y., Gauder, M., Claupein, W., Graeff-Hönninger, S. & Lewandowski, I. Yield and quality development comparison between miscanthus and switchgrass over a period of 10 years. *Energy* **89**, 268–276 (2015).

40. Jurgutis, L., Šlepetienė, A., Amalevičiūtė-Volungė, K., Volungevičius, J. & Šlepetys, J. The effect of digestate fertilisation on grass biogas yield and soil properties in field-biomass-biogas-field renewable energy production approach in Lithuania. *Biomass and Bioenergy* **153**, 106211 (2021).

41. Ra, K., Shiotsu, F., Abe, J. & Morita, S. Biomass yield and nitrogen use efficiency of cellulosic energy crops for ethanol production. *Biomass and Bioenergy* **37**, 330–334 (2012).

42. Oliveira, J. A., West, C. P., Afif, E. & Palencia, P. Comparison of Miscanthus and Switchgrass Cultivars for Biomass Yield, Soil Nutrients, and Nutrient Removal in Northwest Spain. *Agron. J.* **109**, 122–130 (2017).

43. Christian, D. G., Riche, A. B. & Yates, N. E. The yield and composition of switchgrass and coastal panic grass grown as a biofuel in Southern England. *Bioresour. Technol.* **83**, 115–124 (2002).

44. Arundale, R. A. *et al.* Yields of Miscanthus × giganteus and Panicum virgatum decline with stand age in the Midwestern USA. *GCB Bioenergy* **6**, 1–13 (2014).

45. HEATON, E. A., DOHLEMAN, F. G. & LONG, S. P. Meeting US biofuel goals with less land: the potential of Miscanthus. *Glob. Chang. Biol.* **14**, 2000–2014 (2008).

46. Arundale, R. A., Dohleman, F. G., Voigt, T. B. & Long, S. P. Nitrogen Fertilization Does Significantly Increase Yields of Stands of Miscanthus × giganteus and Panicum virgatum in Multiyear Trials in Illinois. *BioEnergy Res.* **7**, 408–416 (2014).

47. Ma, Z., Wood, C. W. & Bransby, D. I. Impact of row spacing, nitrogen rate, and time on carbon partitioning of switchgrass. *Biomass and Bioenergy* **20**, 413–419 (2001).

48. Sladden, S. E., Bransby, D. I. & Aiken, G. E. Biomass yield, composition and production costs for eight switchgrass varieties in Alabama. *Biomass and Bioenergy* **1**, 119–122 (1991).

49. Muir, J. P., Sanderson, M. A., Ocumpaugh, W. R., Jones, R. M. & Reed, R. L. Biomass Production of 'Alamo' Switchgrass in Response to Nitrogen, Phosphorus, and Row Spacing. *Agron. J.* **93**, 896–901 (2001).

50. Parrish, D. J., Wolf, D. D., Daniels, W. L., Vaughn, D. H. & Cundiff, J. S. *Perennial species for*

optimum production of herbaceous biomass in the Piedmont. (Oak Ridge National Lab., TN (USA); Virginia Polytechnic Inst. and State Univ …, 1990).

51. Pfeifer, R. A., Fick, G. W., Lathwell, D. J. & Maybee, C. Screening and Selection of Herbaceous Species for Biomass Production in the Midwest/Lake States: Final Report 1985-1989. *ORNL/Sub/85-27410/5, Submitt. to Biomass Feed. Dev. Program, Oak Ridge Natl. Lab. Oak Ridge, Tennessee* (1990).

52. Reynolds, J. H., Walker, C. L. & Kirchner, M. J. Nitrogen removal in switchgrass biomass under two harvest systems. *Biomass and Bioenergy* **19**, 281–286 (2000).

53. Sanderson, M. A., Read, J. C. & Reed, R. L. Harvest Management of Switchgrass for Biomass Feedstock and Forage Production. *Agron. J.* **91**, 5–10 (1999).

54. Anderson, I. C., Buxton, D. R. & Hallam, J. A. *Selection of herbaceous energy crops for the western corn belt*. (Oak Ridge National Lab., TN (United States), 1994).

55. Bransby, D. I., Sladden, S. E. & Kee, D. D. Selection and Improvement of Herbaceous Energy Crops for the Southeastern USA, Final Report in a Field and Laboratory Research Program for the period March 15, 1985 to March 19, 1990. *ORNL/Sub//85-27409/5, Oak Ridge Natl. Lab. Biomass/Feedstock Dev. Program, Oak Ridge, TN* (1990).

56. Wright, L. & Turhollow, A. Switchgrass selection as a "model" bioenergy crop: A history of the process. *Biomass and Bioenergy* **34**, 851–868 (2010).

57. Wright, N. A. Screening of herbaceous species for energy crops on wet soils in Ohio. in *Advances in new crops. Proceedings of the first national symposium'New crops: research, development, economics', Indianapolis, Indiana, USA, 23-26 October 1988.* 263–267 (Timber Press, 1990).

58. Aravindhakshan, S. C., Epplin, F. M. & Taliaferro, C. M. Switchgrass, Bermudagrass, Flaccidgrass, and Lovegrass biomass yield response to nitrogen for single and double harvest. *Biomass and Bioenergy* **35**, 308–319 (2011).

59. Stout, W. L., Jung, G. A. & Shaffer, J. A. Effects of Soil and Nitrogen on Water Use Efficiency of Tall Fescue and Switchgrass Under Humid Conditions. *Soil Sci. Soc. Am. J.* **52**, 429–434 (1988).

60. Tian, S. *et al.* Switchgrass growth and pine–switchgrass interactions in established intercropping systems. *GCB Bioenergy* **9**, 845–857 (2017).

61. Leirpoll, M. E. *et al.* Optimal combination of bioenergy and solar photovoltaic for renewable energy production on abandoned cropland. *Renew. Energy* **168**, 45–56 (2021).

62. Næss, J. S., Cavalett, O. & Cherubini, F. The land–energy–water nexus of global bioenergy potentials from abandoned cropland. *Nat. Sustain.* **4**, 525–536 (2021).

63. Myers, N., Mittermeier, R. A., Mittermeier, C. G., Fonseca, G. A. B. & Kent, J. Biodiversity hotspots for conservation priorities. *Nature* **403**, 853–858 (2000).

64. Folberth, C. *et al.* The global cropland-sparing potential of high-yield farming. *Nat. Sustain.* **3**, 281–289 (2020).

65. Hu, X., Huang, B., Verones, F., Cavalett, O. & Cherubini, F. Overview of recent land-cover changes in biodiversity hotspots. *Front. Ecol. Environ.* (2020). doi:10.1002/fee.2276

66. WDPA. World Database of Protected Areas, Annual Release 2009.

67. Lewandowski, I., Scurlock, J. M. O., Lindvall, E. & Christou, M. The development and current

status of perennial rhizomatous grasses as energy crops in the US and Europe. *Biomass and Bioenergy* **25**, 335–361 (2003).

68. Casler, M. D., Mitchell, R. B. & Vogel, K. P. Switchgrass. in *Handbook of Bioenergy Crop Plants.* 563–590 (2012).

69. Barney, J. N. & DiTomaso, J. M. Bioclimatic predictions of habitat suitability for the biofuel switchgrass in North America under current and future climate scenarios. *Biomass and Bioenergy* **34**, 124–133 (2010).

70. Hui, D. *et al.* Effects of precipitation changes on switchgrass photosynthesis, growth, and biomass: A mesocosm experiment. *PLoS One* **13**, e0192555–e0192555 (2018).

71. Deng, Q. *et al.* Effects of precipitation changes on aboveground net primary production and soil respiration in a switchgrass field. *Agric. Ecosyst. Environ.* **248**, 29–37 (2017).

72. Cooney, D. *et al.* Switchgrass as a bioenergy crop in the Loess Plateau, China: Potential lignocellulosic feedstock production and environmental conservation. *J. Integr. Agric.* **16**, 1211–1226 (2017).

73. Usťak, S., Šinko, J. & Muňoz, J. Reed canary grass (Phalaris arundinacea L.) as a promising energy crop. *J. Cent. Eur. Agric.* **20**, 1143–1168 (2019).

74. Laurent, A., Pelzer, E., Loyce, C. & Makowski, D. Ranking yields of energy crops: A meta-analysis using direct and indirect comparisons. *Renew. Sustain. Energy Rev.* **46**, 41–50 (2015).

75. Ge, Z. M. *et al.* Acclimation of photosynthesis in a boreal grass (Phalaris arundinacea L.) under different temperature, CO2, and soil water regimes. *Photosynthetica* **50**, 141–151 (2012).

76. Miller, R. C. & Zedler, J. B. Responses of native and invasive wetland plants to hydroperiod and water depth. *Plant Ecol.* **167**, 57–69 (2003).

77. Olofsson, P. *et al.* Good practices for estimating area and assessing accuracy of land change. *Remote Sens. Environ.* **148**, 42–57 (2014).

78. Trivedi, P. *et al.* Energy return on investment for alternative jet fuels. *Appl. Energy* **141**, 167–174 (2015).

79. Staples, M. D., Malina, R., Suresh, P., Hileman, J. I. & Barrett, S. R. H. Aviation CO2 emissions reductions from the use of alternative jet fuels. *Energy Policy* **114**, 342–354 (2018).

80. Staples, M. D., Malina, R. & Barrett, S. R. H. The limits of bioenergy for mitigating global life-cycle greenhouse gas emissions from fossil fuels. *Nat. Energy* **2**, 16202 (2017).

81. Staples, M. D. *et al.* Water Consumption Footprint and Land Requirements of Large-Scale Alternative Diesel and Jet Fuel Production. *Environ. Sci. Technol.* **47**, 12557–12565 (2013).

82. Zhang, B., Hastings, A., Clifton-Brown, J. C., Jiang, D. & Faaij, A. P. C. Modeled spatial assessment of biomass productivity and technical potential of Miscanthus × giganteus, Panicum virgatum L., and Jatropha on marginal land in China. *GCB Bioenergy* **12**, 328–345 (2020).

83. Rosenzweig, C. *et al.* Assessing agricultural risks of climate change in the 21st century in a global gridded crop model intercomparison. *Proc. Natl. Acad. Sci.* **111**, 4–9 (2014).

84. Rosa, L. *et al.* Potential for sustainable irrigation expansion in a 3C warmer climate [Data set]. (2020). doi:10.5281/zenodo.3995044

85. Huang, B. *et al.* Predominant regional biophysical cooling from recent land cover changes in

Europe. *Nat. Commun.* **11**, 1066 (2020).

86. Harding, K. J., Twine, T. E., VanLoocke, A., Bagley, J. E. & Hill, J. Impacts of second-generation biofuel feedstock production in the central U.S. on the hydrologic cycle and global warming mitigation potential. *Geophys. Res. Lett.* **43**, 10,710-773,781 (2016).

87. Georgescu, M., Lobell, D. B. & Field, C. B. Direct climate effects of perennial bioenergy crops in the United States. *Proc. Natl. Acad. Sci.* **108**, 4307–4312 (2011).

88. Wang, M. *et al.* On the Long-Term Hydroclimatic Sustainability of Perennial Bioenergy Crop Expansion over the United States. *J. Clim.* **30**, 2535–2557 (2016).

89. Alter, R. E., Im, E.-S. & Eltahir, E. A. B. Rainfall consistently enhanced around the Gezira Scheme in East Africa due to irrigation. *Nat. Geosci.* **8**, 763–767 (2015).

90. Harding, K. J. & Snyder, P. K. Modeling the atmospheric response to irrigation in the Great Plains. Part II: The precipitation of irrigated water and changes in precipitation recycling. *J. Hydrometeorol.* **13**, 1687–1703 (2012).

91. Baumann, M. *et al.* Declining human pressure and opportunities for rewilding in the steppes of Eurasia. *Divers. Distrib.* **26**, 1058–1070 (2020).

92. Prishchepov, A. V, Ponkina, E. V, Sun, Z., Bavorova, M. & Yekimovskaja, O. A. Revealing the intentions of farmers to recultivate abandoned farmland: A case study of the Buryat Republic in Russia. *Land use policy* **107**, 105513 (2021).

93. Swinnen, J., Burkitbayeva, S., Schierhorn, F., Prishchepov, A. V & Müller, D. Production potential in the “bread baskets” of Eastern Europe and Central Asia. *Glob. Food Sec.* **14**, 38–53 (2017).

94. Kuipers, K. J. J., May, R. F., Graae, B. J. & Verones, F. Reviewing the potential for including habitat fragmentation to improve life cycle impact assessments for land use impacts on biodiversity. *Int. J. Life Cycle Assess.* **24**, 2206–2219 (2019).

Negative emission potentials of biofuels produced from perennial crops and nature-based solutions on abandoned and degraded cropland in Nordic countries

Supplementary Information

Table of Contents